Passivity based methods in Real-time Hybrid Testing

Peiris, Hashan

Award date:
2020

Awarding institution:
University of Bath

Passivity based methods in Real-time Hybrid Testing

Submitted by

Lokukankanamge Dushyantha Hashan Peiris

for the degree of Doctor of Philosophy

of the

University of Bath

Department of Mechanical Engineering

September 2019

Signature of Author . . . . . .

Hashan Peiris

Abstract

Real-time hybrid testing allows engineering systems to be tested using a combination of modelling and experimental methods. By separating the system into numerical and physical substructures the scheme enables the benefits of both schemes to be attained such as low cost due to minimal component requirements and the ability to test complex systems that cannot be simulated. The numerical and physical substructures of the hybrid test are coupled and run together using actuators and force sensors to transfer data at the interface in real-time. However, actuator dynamics lead to poor stability and tracking errors which undermine the reliability of hybrid tests. Existing techniques to mitigate actuator dynamics are largely based on linear models of actuation hardware and are thus less effective in the face of nonlinearity. Moreover, such schemes require information of actuator dynamics to be known prior to testing.

This thesis explores the application of several passivity controllers in real-time hybrid testing to improve stability and performance. The work here covers the first applications of passivity control in hybrid tests and uses a combination of modelling and experimental techniques to validate the effectiveness of the schemes proposed. Performance of the compensated hybrid tests are assessed in comparison to a simulation of the true system to be emulated. The preliminary passivity controller designed is based on damping the numerical substructure using measurements of energy flowing in the system and was found to restore unstable systems with phase margins of up to -21^0. Performance of the scheme with state-of-the-art model-based lag compensators were found to further improve performance allowing targeted improvements in tracking to be achieved with improved stability. Experimental results show the effectiveness of passivity control and 2^{nd} order transfer function based lag compensation in mitigating phase lags of up to 22^0 from a closed loop hybrid test.

However, high dependency on the magnitude of energy flow required considerable tuning of the passivity controller when operating conditions shifted. Thus, a modified passivity control scheme acting on a normalised power flow measurement was designed which alleviates this limitation whilst still allowing stability gains to be achieved. Unlike its predecessor, the modified scheme was seen to enable identical performance for a range of excitation amplitudes resulting in the same system natural frequency, damping ratio and response distortion for step excitations of magnitudes 0.5mm up to 500mm.

Besides linear hybrid tests, this thesis also focusses strongly on nonlinear systems and all schemes presented require no information of actuator dynamics to function. Nonlinearities tested in the numerical and physical substructures include stiffening behaviour and discontinuity whilst nonlinearity in the actuator in the form of nonlinear friction has also been tested. In all cases, the passivity controller was seen to improve the response by stabilizing diverging systems and eliminating oscillation caused by periodic instability in the actuator due to friction.

A limitation of passivity control used by itself however is its inability to eliminate the phase lag in the actuator. Thus, the use of passivity control together with a novel adaptive feedforward filter to mitigate actuator phase lag was analysed. The two schemes were found to complement each other with passivity control allowing stability to be maintained in otherwise unstable tests while adaptive filtering converged the substructure position error towards zero overtime. Finally, to end with, a passivity based adaptive delay compensation scheme was designed which measures the energy flow in the hybrid test to quantify the actuator delay. This scheme was seen to enable phase lags of up to 36^0 in the actuator to be cancelled.

This thesis is written in the alterative format, with each passivity controller presented in a research paper. Each paper precedes a context section which outlines the motivation and purpose and the chapter ends with a summary linking the main findings to the overall research question. The work in this thesis comprises of a conference paper, four journal papers and a technical article.

Acknowledgements

This PhD has been a tremendous journey for me which I am very thankful to have been fortunate to experience. The past four years of intensive thinking, reading, simulations, experiments and analysis have been a challenging yet extremely rewarding life changing experience which has enabled me to grow as a researcher and discover my strengths and overcome many of my weaknesses. There are several individuals whom I wish to thank for supporting me throughout this journey which enabled me to reach the end of my research and submit my thesis.

First and foremost, I would like to extend a huge thank you to my supervisors Dr. Jonathan du Bois and Prof. Andrew Plummer, whose advice and guidance have been instrumental in enabling me to complete my research. I thank them for their endless patience with me over the past four years. I very deeply appreciate them meeting me once every week throughout the first 3 years of my PhD despite their busy schedules. It is at these meetings where I was given the opportunity to discuss my research with them and they not only gave me invaluable advice but also fuelled my ideas and taught me to think like a researcher. Moreover, they always monitored my performance and mindset, greatly helping me withstand the immense workload and pressure whilst at the same time, never failed to point out the areas where I could improve. They also took the time and effort to read and review all research papers of this thesis giving me valuable feedback which has greatly improved the quality of each paper. My development as a researcher was significantly attributed to the efforts of these two amazing academics whom I have over the years come to feel as part of my family.

I would also like to thank the technical staff of the Department of Mechanical Engineering at the University of Bath. Particularly, Mr. Steve Coombes for providing the load cell for my experiments, Mr. Robin Harris for helping me configure my actuator for initial use and Mr. Guy Brace for manufacturing the bespoke parts needed for my test rig. I am also grateful to Mr. David Ramos of the IT support team for the setup of my Simulink Real-time Target controller. I wish to express my gratitude to the Department of Mechanical Engineering for my PhD scholarship. This scholarship covered my tuition fee and provided the funds required to manufacture bespoke components required for my research. I also express my appreciation to the Engineering and Physical Sciences Research Council for funding the equipment needed for my experiments, grant reference EP/N032829/1. I would also like to thank my colleague Dr. Andreas Bartl who was on placement at the University of Bath during his PhD. I had the privilege of doing many experiments with Dr. Bartl which manifested as two research papers in this thesis. It was an absolute pleasure working with him and seeing the complementation of both our PhD projects in real-time hybrid testing.

Further, I wish to thank my dad Dr. Jagath Peiris who gave me valuable advice which helped me stay focussed on my research. I also thank him for the tips on writing my thesis and the experiences he shared from during his PhD which certainly helped me through mine. He was one of the main figures that first inspired me to think about pursuing a PhD, which was one of the best decisions I made. My dad is my strength, and I can always rely on him for help and support. Finally, I wish to thank my mum Mrs. Fawzan Peiris, without her support, I would not have been able to finish my PhD. Through all the times of stress and anxiety, she was always my main solace, and I have no words to describe how much her moral support means to me. The number of times she has calmed me down and helped me recollect my thoughts are countless, and her benevolence and patience with me through these times were incredible. She accompanied me to the UK to support me on my higher studies which immensely helped me throughout my course. I greatly appreciate her and thank her from the bottom of my heart for everything.

Contents

Chapter 1

Introduction

1.1 Real-time Hybrid Dynamic Systems

Experimental testing has long since been an invaluable tool for validating systems in all disciplines of engineering owing to its superlative reliability, whilst computational models are widely adopted due to its unparalleled ease of use and excellent versatility. These methods are undoubtedly powerful tools for scientists and engineers in the advent of innovative products and novel systems. However, there is a multitude of physical systems that suffer from the disadvantages associated with each of these prime techniques. For example, there are many systems which are too large or costly to test experimentally and too complex to model numerically. Air-to-air refuelling systems, wave energy conversion devices, aircraft stability control systems and building structures are a few such systems which have called for the introduction of a synergetic method known as Hybrid Testing. This method is also referred to as Structural Hardware-in-the-loop Testing, Model-in-the-loop Testing and Real-time Dynamic Substructuring by some authors.

Hybrid testing aims to provide the excellent reliability of experimental techniques as well as the convenience and high efficiency of numerical simulation [1]. The complete system is split into two parts to be tested using different methods in synchronisation; the most complex or critical component of the system is setup in an experimental test rig often referred to as the physical substructure by many authors, whilst the remainder of the system is modelled numerically in a computer simulation. These two substructures are then coupled via an interface or Transfer System (often comprising of actuation hardware and physical state sensors) and are run together. As such, a real-time hybrid test forms a closed loop system. In conventional hybrid systems, the numerical model computes the dynamic response of the system and feeds the required displacements to the physical substructure though the actuators, whilst the physical sensors feedback information about the state of the experimental system to the numerical model.

Originally, hybrid systems were run at slow rates on an extended timescale (referred to as Pseudo-dynamic (PsD) Testing) and were therefore incompatible with rate dependant components. Real-time Hybrid Testing (RtHT), a variation of PsD, alleviates this limitation as it allows displacements to be applied in real-time. The advent of this technique enabled the testing of a large class of structural components to do with vibration control including active, semi-active and passive control devices [2]. This major milestone in Hybrid Testing only recently became realisable with advancements in high speed computing technology. Besides serving as a means of testing dynamic systems, RtHT also enables systems to be implemented and executed without the need to build all components involved.

However, the need to run in real-time significantly increases the efficiency required in the Transfer System, as real-time operation would require commands to be executed rapidly (often in less than 10ms) [2]. This is an ongoing challenge in the industry as several factors such as processing delays, actuator dynamics and model complexity all undermine the rate of execution of RtHT systems. The conventional methods used to mitigate the problems associated with real-time operation of hybrid systems, are often difficult to implement in the face of nonlinearity, due to the additional problems of actuator saturation, backlash and discontinuous behaviour which leads to unpredictability and/or stability issues. Therefore, although RtHT has been a tremendous

breakthrough in the domain of validating systems, there is much work to be done in order to utilize this method to its full potential.

1.2 Background to Real-time Hybrid Testing

In order to accurately replicate the behaviour of the true or emulated system through a hybrid test, high fidelity data transfer is required at the interface between numerical and physical substructures [2]. Although sensing delays from most load cells used for force measurement are relatively trivial, the delay or lag in the actuators used to transfer displacement data is often problematic in hybrid testing, as command displacements from the numerical substructure cannot physically be applied instantaneously. Delays and lags manifest as time shifts in the demand signal and increase the amount of phase lag in the system. This can lead to tracking errors between the numerical and physical substructure displacements or in worse cases, instability of the hybrid test. It is therefore essential to mitigate the actuator dynamics in the transfer system to ensure that the hybrid test is a true representation of the emulated system. Thus, control schemes that can adequately compensate for delays and lags in the actuator response are imperative in many applications of hybrid testing.

Conventional transfer dynamics mitigation methods are largely based on model-based feedforward control schemes which predict the actuator response ahead of the delay or lag. One such control technique is delay compensation where the actuator is modelled as a time delay and a forward predictive algorithm is used to augment the input to the actuator such that the desired displacements are achieved despite the delay. This method is widely used in real-time hybrid testing and many authors have developed several forward predictive algorithms, each with various merits and limitations which will be investigated in the literature review presented in chapter 2. Another common feedforward control scheme is lag compensation. In this method, a linear transfer function is fit to the actuator response using system identification procedures and the identification is subsequently inverted and added in the loop of the hybrid test. The convolution of the actuator dynamics and inverted transfer function is expected to mitigate any lag the actuator imposes on the demand so that the command displacement is correctly applied to the physical substructure as required. However, these schemes rely on the actuator behaviour being predictable ahead of the response. Although this is achievable to a reasonable extent in linear systems, transfer dynamics cannot as readily be predicted in the presence of nonlinearity. In most cases, the dynamics of the actuator are reliant on the physical substructure it acts against. It is not reasonable to expect the lag of the actuator to always be constant and independent of the hybrid system it acts in. Often, the lag of the actuator varies with parameters of the physical substructure such as inertia, stiffness and damping. Moreover, the dynamics of the actuator itself may not be linear. Factors such as Coulomb friction and Stiction may give rise to different actuator performance depending on the significance of frictional forces in comparison to the driving forces. Further, even in linear systems where model based compensatory action succeeds in mitigating actuator lag, there is often a need for very high accelerations to achieve this, and this may trigger various saturation limits in the system which undermine performance. Although some schemes of circumventing said saturation limits have been investigated by various authors as detailed in chapter 2, there is a clear need for a novel means of addressing transfer dynamics in the face of nonlinearity without reliance on the test system.

1.3 Novel Research Contributions

The work presented in this thesis aims to introduce new methods of alleviating instability and tracking errors in RtHT which unlike the conventional schemes mentioned in section 1.2, make no assumptions about linearity. Methods that require no information of system dynamics are investigated such that modular application to a range of systems regardless of linearity can be easily achieved. The methods explored are based on controlling the flow of energy and power through the hybrid test. This technique of control is known as Passivity Control.

The work presented in this thesis explores the first applications of passivity control in real-time hybrid testing. A preliminary passivity control scheme is developed and assessed in terms of its advantages and drawbacks as opposed to conventional transfer dynamics control schemes. The controller design is subsequently revised to further enhance its usability whilst mitigating some of the limitations of its parent design. Scope for using passivity controllers in hybrid tests alongside other conventional schemes and other novel developments in the field are also assessed. A novel passivity based adaptive delay compensation scheme specifically designed to cancel actuator delay in real-time hybrid tests is also introduced.

1.4 Scope of Thesis

This thesis conforms to the alternative format based on research papers. Each research paper presented herewith investigates the design and functionality of a new passivity-based control scheme for hybrid tests which improves upon its preceding design. Each publication is presented in a chapter and each chapter begins with a context section and ends with a summary section. The context section outlines the motivation and work covered in the paper. The summary highlights the key advantages and limitations of the proposed method and relates the findings to the research question, with implications to the big picture. Limitations of each new scheme form the basis of the improved design discussed in the following publication. This thesis comprises of a conference paper, 4 journal papers and a technical article, each presented in a separate chapter. Preceding each research paper, is a form that describes the contributions of the authors and other individuals towards the work, and states within brackets the percentage contribution of the candidate.

Chapter 2 provides an in-depth review of salient literature in the fields of hybrid testing and passivity control. An overview of real-time hybrid testing and its advantages over alternative testing schemes together with a discussion of its limitations are available with an appraisal of the ground-breaking research done in this field. The application of hybrid testing in various sectors of engineering are also highlighted to illustrate the importance of the technique in modern day testing and existing methods of addressing actuator dynamics are discussed in terms of their repeatability, advantages and limitations. A review of the state-of-the-art passivity control techniques is also presented and its application in various engineering systems is discussed.

Chapter 3 presents a conference paper which introduces the first passivity controller design for real-time hybrid tests. The scheme measures the flow of energy between the transfer system and the numerical and physical substructures of the hybrid test as an indicator of system stability. A variable rate virtual damper acting on the numerical substructure is proposed to dissipate the excess energy added to the hybrid test from the transfer system, so that closed loop system stability can be maintained. The merit of the novel control scheme is validated in simulation results which were used to highlight its key advantages over conventional transfer dynamics

mitigation schemes, whilst addressing limitations in its design. The actuator of the hybrid test simulation was modelled as a pure delay.

Chapter 4 presents a journal paper which explores the first experimental application of the methods introduced in the conference paper of chapter 3. The simple delay model used in the conference paper was replaced by a real electromagnetic actuator with a more sophisticated control scheme and nonlinear friction. The physical substructure modelled earlier was now replaced by springs setup to create stiffening behaviour with respect to actuator displacement. The results of this publication validated those found in the simulations of the conference paper in terms of the effectiveness of passivity control in maintaining stability in real-time hybrid tests. Moreover, the passivity controller was used alongside a state-of-the-art model-based compensation scheme which resulted in further improvements in performance thus highlighting how passivity control and other actuator compensation schemes can complement each other.

The journal paper in chapter 5 addresses the limitations of the abovementioned passivity controller by proposing an improved passivity controller design. A major limitation of the preceding passivity control scheme was the dependence of its performance on the excitation signal which induced significant tuning requirements by the user. This limitation was caused by the dependence of the virtual damper rate on the absolute value of the net transfer system power flow. Thus, by using a normalised power flow variable to quantify stability, the new controller enabled uniform performance to be obtained regardless of the excitation signal. Moreover, by using filtered measurements of power flow, the new controller was found to be less sensitive to the history of the system response than its predecessor which damps the system even when the closed loop system is adequately stable.

The journal paper in chapter 6 applies the normalised passivity controller with a novel adaptive feed-forward filtering scheme which is designed to synchronise substructure displacements in hybrid tests. The biggest selling point of passivity control is its effectiveness in maintaining stability whilst the main selling point of adaptive feed-forward filtering is its ability to synchronise substructure displacements in stable hybrid test applications. With both methods being completely independent to the test system, when used together it was envisaged and then found that both schemes complemented each other to stabilize an otherwise unstable hybrid test and subsequently synchronise substructure displacements. The use of both methods together, was found to stabilize the test and eliminate tracking errors without any information of the transfer system or any assumptions about linearity.

In chapter 7, the use of passivity control in improving the stability of adaptive feed-forward controllers is examined. Adaptive feed-forward filters are known to destabilize hybrid tests in the presence of unsuitable tuning configurations. Much like the initial passivity controller design presented in this thesis, the optimal tuning of parameters depends on the excitation signal and the operating regime. Therefore, in the publication presented in this chapter, the effectiveness of passivity control in altering the adaption gain of the adaptive feed-forward filter is assessed. The net substructure power error in the hybrid test is used as an indicator of stability as earlier, and when stability is seen to deplete, the adaption gain of the feed-forward controller is stepped down until the power surge is adequately suppressed to prevent instability of the closed loop system.

The final paper presented in chapter 8 is a technical note which proposes a novel energy based adaptive delay compensation scheme for real-time hybrid testing, which aims to simultaneously improve both stability and tracking in real-time hybrid tests. The performance of the scheme is

experimentally verified and compared against a state-of-the-art adaptive delay compensation scheme. Although similar performance between schemes were found, the novel passivity control scheme provides a unique advantage that it does not rely on zero crossings for compensation to activate unlike the state-of-the-art scheme. This makes the passivity-based solution more readily applicable to certain tests as discussed further in the article.

To finish with, chapter 9 highlights the main conclusions of this thesis describing the main benefits of the research to the field and describes the future aspirations of passivity control in real-time hybrid testing in terms of further research and applications.

Chapter 2

Literature Review

This chapter provides an in-depth discussion of real-time hybrid testing and its application in engineering systems. An appraisal of its benefits over conventional testing schemes is described to highlight the reasons for its popularity in several fields of engineering in section 2.1. The limitations of hybrid testing are also discussed and conventional methods of addressing these limitations are introduced and evaluated qualitatively in sections 2.2 and 2.3. The advantages offered by the application of passivity-based techniques are described in section 2.4 with examples of its successful application in other types of engineering systems.

2.1 Development of Real-time Hybrid Testing

The theoretical framework describing the underlying concepts of RtHT will be examined in this section and applications of hybrid test methods in different fields of Engineering will be analysed in tandem. Variations in hybrid testing adapted to suit different applications will be discussed as well.

An example of the predecessor to RtHT, pseudo-dynamic testing, can be seen in the work of Bolien et al. [3], where a Robotic Pseudodynamic Test (RPsDT) method is proposed, to model the contact impact scenario of an air to air refuelling drogue. As the drogue makes contact, a discontinuity is encountered which constitutes a problem that cannot be rectified using conventional delay and lag compensation techniques as future responses of the system cannot be readily predicted. The proposed RPsDT method allows hybrid testing of highly nonlinear scenarios. However, due to the nature of the test method, rate dependencies could not be modelled, and satisfactory response speeds could not be attained. That being mentioned, the authors argue that real-time techniques could not be applied to the aforementioned robots due to restricted access to the axis controller [3]. However, it is likely that the use of faster robots with less significant transfer dynamics and more customisable control systems will enable future developments in air-to-air refuelling to make use of RtHT.

As detailed in [4], advancements in numerical methods over the years have led to the realisation of a multitude of benefits to engineers such as cost savings, reduced product development times, higher reliability and low risk testing capabilities. However, many systems still require experimentation due to their complexity and demanding real world interactions [4]. The attractiveness of real-time hybrid testing largely stems from its ability to merge the convenience of computational simulation with the realism of experimental test procedures. Hybrid testing expands on the possibilities of experimentation by coupling a physical component setup with realistic conditions on a test rig, to a real-time numerical model [4]. With elements of both conventional rig based testing and numerical simulation, it inherits a vast number of benefits of both traditional schemes making it a very attractive solution for many applications. This technique has seen popularity in many industrial developments, and commercial products for real-time simulation are readily available on the market to enable solutions for off-the-shelf physical test components without the need for specialist knowledge in programming or hardware architecture [4].

Some of the benefits offered by real-time hybrid testing are described in [4]. Advancements in computational technology progressively reduces the implementation costs of real-time simulation

making real-time hybrid testing an economically viable solution for many applications. It also enables lower product development time with greater certainty whilst allowing components to be tested prior to the availability of prototypes. The virtual prototypes offered by real-time hybrid testing enable several engineers to work on a single subcomponent unlike with physical systems that can only accommodate a limited number of engineers at a time. Real-time hybrid testing not only offers the cost effectiveness of numerical simulation but also its repeatability with precisely applied boundary conditions. Moreover, dangerous or destructive events can also be tested without incurring damage to components. Parameters that are difficult to maintain in a laboratory environment can also be simulated greatly increasing the ease of testing for the engineer. Further, parameters of the numerical model can be easily adjusted in contrast to the requirement of changing parameters of an experimental system. Components of the numerical substructure can also be substituted with ease [4]. Further advantages of real-time hybrid testing detailed in Fathy et al. [5] are the reduction in hardware apparatus required compared to experimentation, higher execution speeds compared to pure simulations and its suitability for training human operators (eg: pilots) in safe environments.

In [5], the key enablers of RtHT and the advancement of RtHT in the field of automotive engineering is surveyed. The authors describe hybrid testing as a control system in which the numerical model commands the physical substructure to track a specified reference system. The authors also identify that a significant proportion of literature on the topic focusses on the advent of fast and unobtrusive actuators and sensors which have minimal effect on the underlying dynamic system. The key enablers of hybrid testing as proposed in this literature are

- Unobtrusiveness and fidelity of actuators and sensors
- Advancements in digital signal processing and signal conditioning
- Advent of rapid processors, real-time operating systems and fixed step integration schemes
- Development of more informative sensors and high quality actuators
- Development of advanced simulation methods and real-time control algorithms
- Multi-rate integration schemes and multithreading processors which allow components of the numerical substructure with different stiffnesses to be processed at different speeds
- High bandwidth networking; the distribution of components of a hybrid test increases simulation capabilities whilst eliminating the need for all hardware to be collocated and mobile as is the case with conventional offline processors. Furthermore, the authors argue that the prime benefit of online RtHT is the empowerment of modular hybrid test design where the control systems for different components of the test can be designed independently and combined to produce the full system.
- Improved hardware/software integration for effective data transmission at the interface between the numerical and physical substructures.

The work goes on to describe some applications of RtHT in the automotive industry such as active/passive car suspensions where a hybrid test setup is used to validate and optimize the suspension before installation in a vehicle. Furthermore, the development of microprocessor technology is described to have instigated the advent of Engine Control units (ECUs) which benefit from RtHT for calibration, testing and validation. The authors further develop the work on ECUs via experimentation on a diesel engine coupled to a vehicle model through a real-time driver in a hybrid test. The test method proposed is described to accurately emulate the behaviour of the powertrain in a vehicle and is therefore characterised as an optimal solution for measuring transient emissions, fuel economy and powertrain performance. One limitation in this publication is that the results of the RtHT system i.e. engine speed, emissions and fuel efficiency of the diesel

engine, have not been validated against drive cycle results of a vehicle fitted with the same powertrain. Close correlation with drive cycle results would further consolidate the effectiveness of RtHT methods in powertrain testing.

In Plummer [6], RtHT is explained to have evolved from the concept of controlling actuated plants using simulated control systems. The modern manifestation of RtHT is described to differ in the sense that it has become an integral part of the entire mechanical system and not simply an element of the control system [6]. The author describes that the numerical substructure of the hybrid test interfaces with the rest of the system through actuators and sensors that are not a part of the true system to be tested. Thus, the characteristics of the actuators and sensors are said to detract from the realism of the response of the complete system. More advantages of hybrid testing are detailed in this literature such as the ability to test systems prior to realisation of all parts and the possibility of emulating via simulation, realistic test conditions that cannot be replicated in a laboratory.

Due to the advantages it offers, real-time hybrid testing is rapidly gaining recognition in a number of sectors. As such, it is referred to using a number of different terms in different fields of engineering. In Civil Engineering, it is often known as Real-time Dynamic Substructuring. Some applications in this sector include seismic testing of buildings [7], analysis of vibration isolators [8], integrity testing of composite structures [9] and the testing of vehicle bridge interaction during earthquakes [10]. Due to the low frequency seismic excitations seen by building structures, a non-real-time application of hybrid testing, i.e. pseudodynamic testing, can often be employed. As this technique involves running the hybrid test over an extended time-scale, it is highly suitable for systems that do not incur rapid changes over a single test. The work of Qi et al. [11] is a recent example of the application of pseudo-dynamic testing to assess the structural fidelity of steel frame structures whilst Yadav et al. [12] utilize the method to assess the earthquake response of a concrete filled steel tube. More examples of peudodynamic testing outside the field of civil engineering are also widespread with the work of Melo et al. [13] which investigates the deformation of an automotive air spring suspension.

A good example of the application of Nonlinear RtHT in the Civil Engineering field is seen in the work of Reinhorn et al. [14] where an earthquake scenario is simulated using shake tables actuated by hydraulic actuators subject to fluid compressibility and nonlinear servo valves. This research addresses a problem inherent to all mechanical RtHT systems which is discussed in further detail in section 2.2. The authors assess two methods of compensating for actuator dynamics based on Force Control strategies. The first approach is referred to as the Convolution method in which the frequency response of the system is inverted and used to alter the force input to the actuation system [14]. However, the authors recognize that this method requires precise system identification and an offline computation which is not realisable in real-time. It is also stated that force control requires a mechanically compliant (low impedance) system [14], which is difficult to achieve with hydraulic actuation owing to high actuator stiffnesses. Therefore, in the alternative approach, velocity feedback as described by Dimig [15], was included in the controller making the system more compatible with force control, and a spring was installed in series with the actuator to increase mechanical compliance [14]. The authors also acknowledge that impedance control strategies can be used as an alternative to using a spring, in order to control the behaviour of the actuator at its interface with the surrounding system. By adding a PID displacement controller to the system with the embedded spring, the actuator is made to control force using displacement feedback. Upon testing the force control strategies, the authors deduce that the actuator can be modelled as a pure delay over the range of interest and proceed to apply

a delay compensation scheme based on forward prediction to account for this. The proposed methods have been shown to be sufficiently accurate for the earthquake scenario tested. This publication illustrates a useful result which may be extended across hybrid testing for all disciplines; by using a spring in series with velocity feedback and PID displacement control for a nonlinear hydraulic actuator, the transfer dynamics can be reduced to a pure delay over a certain frequency range.

In the electrical and electronic engineering sectors, real-time hybrid testing is widely known as hardware-in-the-loop testing. Marks et al. [16] analyse the stability of a power hardware in the loop system based on an ideal transformer with a voltage source converter for power amplification. The transfer system of the hybrid test consists of power amplifiers which facilitate the power interface between the numerical and physical substructures, which contrasts with most mechanical and civil engineering applications which utilize actuators. Another application is seen in the work of Thönnessen et al. [17] where hardware in the loop testing is employed to compare the actual behaviour of a programmable logic controller with its desired behaviour. In the power distribution sector, the growth of power electronics devices due to increasing integration with renewable energy sources is becoming a challenge for distribution grids [18]. Carne et al. [18] utilize power hardware in the loop testing to analyse a smart transformer system which aims to provide a solution to this problem. Further advantages of hybrid testing in the energy distribution sector can be seen in the work of Kotsampopoulos et al. [19] which proposes a hardware in the loop system to test the integration of distributed energy resources into state-of-the-art and future power grids.

Hybrid testing is increasingly being implemented in the aerospace industry as well. A good example illustrating the application of Hardware-in-the-loop systems in this industry is seen in Yoo et al [20], where the actuators of a smart UAV (Unmanned Aerial Vehicle) is tested in a hybrid system. The actuation system of this UAV is required to enable the aircraft to switch between helicopter and airplane modes of operation thereby requiring a sophisticated control system which was designed and tested in a hardware-in-the-loop experiment. The numerical substructure modelled the flight dynamics whilst flaperon, elevator, rotor and nacelle tilt actuators were mounted on the air vehicle in an experimental setup [20]. The numerical substructure of this system is clearly nonlinear due to the nature of the aerodynamic forces, and the authors do not indicate the scope for this system to be tested in real-time. No significant nonlinearity in the actuation systems are described, and a time delay is said to exist in the flaperon system [20]. Although pseudo-dynamic testing will produce a reliable indication of the performance of the control system, it would be preferable to run such tests in real-time as this would allow rate dependant effects to be studied and entire flight simulations to be performed as well. It is likely that nonlinearities in the experimental substructure and/or actuation system, could potentially be addressed by high fidelity control systems, whilst real-time operation may be enabled with the use of a high power computing system as demonstrated by the more recent work of Montazeri-Gh et al. [21] described below.

Montazeri-Gh et al. [21] illustrate a structural hardware-in-the-loop application in the aerospace industry, where a jet engine Fuel Control Unit (FCU) is tested in a hybrid system. The FCU is setup experimentally as the physical substructure whilst the numerical substructure models the aerodynamics. An electric motor is employed to power the fuel pump whilst an electrohydraulic actuation system is used to apply loads on the FCU. Unlike the system of Yoo et al. [20], this aerospace application is described to consist of significant nonlinearities stemming from servo valve port shapes and control valve saturation [21]. The authors state that the hybrid system is

capable of running in real-time which further increases aspirations for Hardware-in-the-loop tests to be implemented in the aerospace industry. The authors elaborate that in order to achieve real-time operation, a host-target architecture was implemented over an Ethernet connection, as done in this PhD, whilst a high speed industrial computer was used to run the numerical model [21].

Hybrid Testing is also rapidly gaining recognition in wave energy conversion systems. Börner and Alam [22] explain the difficulty in accurately modelling ocean wave energy converters due to the complications in the fluid domain arising from reciprocating excitation forces [22]. The authors explain that pure simulation is very demanding computationally whilst pure experimentation is ruled out due to scaling difficulties and high implementation costs, thereby inducing the need for alternative, hybrid methods. The authors model a wave energy conversion device known as the 'Wave Carpet' in a hybrid test where the wave is modelled as the physical component and the power take-off system is modelled numerically. Force transducers were used to measure wave forces whilst the effect of the pumps on the device was emulated using actuators [22]. The authors describe the interaction between wave forces and the device to be highly nonlinear. The virtual power take-off system was programmed in LabVIEW and it was found that the simulation time was more than 3 times higher when nonlinear as opposed to linear damping was assumed [22]. The authors conclude that real-time application of hybrid testing in wave energy conversion systems is difficult albeit on the verge of being realisable with the rapid advancements in numerical and experimental techniques. This research illustrates yet another field where fully developed nonlinear RtHT systems will flourish.

2.2 Transfer Dynamics Mitigation Schemes

The transfer system, or interface between the numerical and experimental substructures of a hybrid test, has been identified as a subsystem of paramount importance. For a generic hybrid test of a mechanical system, position or velocity demand signals calculated in the numerical model are applied to the physical substructure through an actuator whilst force measurements from the physical substructure is fed back to the numerical model through a load cell. In this simplest of configurations, there are two fundamental control loops governing the operation of the hybrid system; the integrated control system melds the two substructures through the interface whilst the actuator control system nested within the integrated system governs the motion of the actuator. This is illustrated in figure 1. Real-time operation will therefore rely on the design of these fundamental control loops to yield a fast and efficient transfer system able to minimize effects of lags, delays and saturation. Existing methods to compensate for these effects are reviewed in this section.

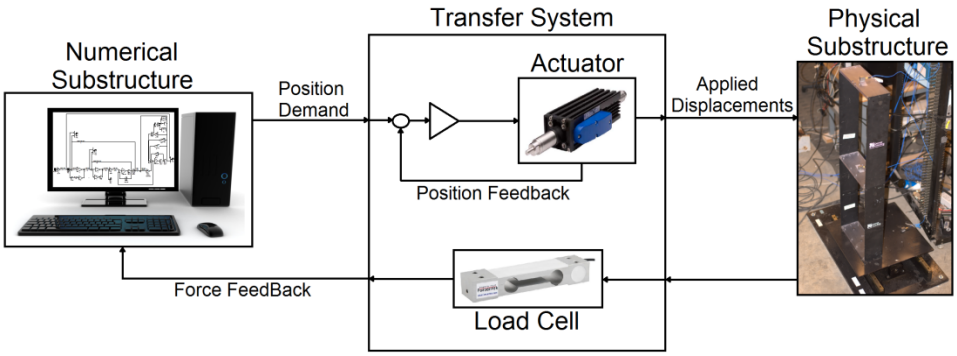

Figure 1: Key elements in a generic RtHT system [23]–[27]

Wallace et al. [28] propose modelling the actuation delay using a delay differential equation (DDE) which is used to analyse the effect of the delay on the system. An adaptive delay compensation method based on a polynomial forward prediction scheme (as described in another publication by Wallace et al. [29]) is applied and has been shown to be successful in stabilizing a linear mass-spring system [28]. The method used is based on a least squares approximation to fit an Nth order polynomial through the data points at previous time steps in order to extrapolate forward the expected output at a future time so as to compensate for the delay using the forward stepping algorithm [28]. Second and fourth order forward prediction schemes have been applied to stabilize the system, with the latter yielding higher accuracy. The proposed technique is described in the literature, to be suited for civil engineering structures which are often of high stiffness or low damping. The authors also illustrate a number of methods to identify the 'critical delay' where the system is at the brink of instability.

In another study by Wallace et al. [30], RTHT methods are applied to a rotor blade system in which a nonlinear lag damper is setup as the physical component. Robust system design is applied following the methodology of Gawthrop et al. [31] in order to cancel transfer system dynamics using a feed forward controller. The transfer system dynamics are modelled as a first order system and the transfer function obtained via system identification is then inverted and programmed into the feed-forward controller in order to compensate for the lag of the interface system [30]. Although the nature of this approach is sound, 1st order transfer functions are sometimes unable to accurately model the dynamics of actuation hardware. Hence, 1st order transfer function inversions may not adequately cancel transfer system dynamics. In many cases,

higher order transfer functions may be required to more accurately identify transfer dynamics. Unfortunately, higher order transfer functions cannot readily be inverted due to causality issues, as it becomes increasingly difficult to accurately describe higher order derivatives. Hence additional procedures such as pole placement will be required to realize higher order model inversions.

In du Bois et al. [32] the superiority of higher order compensators are elucidated and the use of process models, i.e. transfer function models coupled with delays, as opposed to pure transfer function models are shown to improve transfer dynamics cancellation. In this research, the use of open loop linear controllers is proposed to complement the corrective action of the actuator control systems. With a hybrid test of a two mass system setup with a damper as the physical substructure, the authors identify 1st and 2nd order transfer function models and process models (i.e with delay) to represent the transfer system dynamics. The second order transfer function model was found to be more effective than the first order transfer function in reproducing the actuator response whilst the process models with delay further improved the correlation significantly. These process models were inverted using the forward predictive methods of Wallace et al. [30], and applied to the hybrid test as open loop controllers. Results illustrated the superiority of higher order process models over higher order transfer function models in cancelling transfer dynamics by yielding lower overall substructure tracking error [32]. However, the research identifies that nonlinearities and discontinuities in the actuator stroke lead to tracking errors. Moreover, higher order model inversions introduce lead terms which are not causal, thus inducing the need for additional pole placement procedures which may alter the dynamics of the system. Hence there is a trade-off between accuracy and ease of implementation which poses restrictions on the highest order of models that may be used for a given system.

Ou et al. [33] state that stability in RtHT systems are substantially affected by the phase lags associated with the dynamics of the system. The authors argue that the nature of communication between the numerical and physical substructures at the interface causes delays in force measurement which undermine the performance and stability of the system even when no other delays or phase lags are present. The research puts forward a modified Runge-Kutta algorithm to compensate for such delays in RtHT systems. The proposed method calculates a pseudo response using the delayed force measurements and uses this response to identify the force that must be fed back in the next step [33]. The authors illustrate that the proposed scheme is robust in the presence of uncertainty and up to 40% modelling error in lightly damped systems, whilst remaining accurate and stable for a range of time steps. The hybrid test of this research was performed on a moment resisting frame. The issue of force measurement delays at the interface system between the numerical and physical substructures is an interesting phenomenon; much research in transfer dynamics mitigation is focussed on actuator dynamics compensation, with little emphasis on force feedback delays. In this sense, this research adds unique value to the field of hybrid testing.

An innovative method of addressing actuator dynamics which differs from the work of most other authors can be seen in Nikzad et al. [34] where a novel compensation scheme based on a multilayer feed-forward neurocontroller is used to mitigate computational time delays and actuator transfer dynamics. A two degree-of-freedom actuation-mass system has been used to illustrate the superiority of a neurocontroller in mitigating transfer system dynamics compared with that of a conventional feed-forward controller. The authors conclude that the enhanced performance of the neurocontroller is attributed to its superior delay compensation and high frequency noise cancelling qualities. The proposed method has the advantage of compensating

for actuator delay and lag simultaneously using a single algorithm, unlike conventional forward stepping algorithms which only cancel actuator delay [34]. However, the results presented in this research have not been obtained from a hybrid test; the neurocontroller has been tested purely in simulation. Adapting this solution to complex RtHT systems may potentially be problematic since the neurocontroller also relies on inverting a transfer function model much like the solution proposed by Wallace et al. [30]. Although this may suffice for lower order systems, implementing this with higher order transfer functions may cause several problems as described above. Therefore, for hybrid testing, the neurocontroller solution is likely to only be feasible for systems in which the actuator dynamics can be approximated to low order models with enough accuracy.

A publication by Ou et al. [35] illustrates the use of a Robust Integrated Actuator Control strategy to yield a flexible, robust system with high demand tracking accuracy [35]. The proposed control system comprises of $H\infty$ optimization, Linear Quadratic Estimation for noise cancellation and a feedforward controller for actuator lag and delay compensation. A hybrid test consisting of a MR damper in a 3 degree of freedom building frame as the experimental substructure is used to illustrate the effectiveness of the integrated control system in minimizing effects of noise and uncertainty whilst enabling good tracking. Results have also been validated experimentally. However, the proposed system is based on the assumption that the actuator model and its PID loop, is a linear time invariant system [35] thereby relying on linear quadratic regulation for noise cancellation. Unfortunately, inevitable friction in actuation hardware introduces nonlinearities which often cannot be neglected.

A Hardware-in-the-loop simulation for a simple nonlinear system is implemented in El-Nagar and El-Bardini [36] – an inverted pendulum controlled by a PIC microcontroller running an interval type 2 fuzzy proportional-derivative controller is modelled in simulation as a nonlinear system. Time domain results illustrate the resiliency of the system to a 20N force disturbance and structural uncertainty [36]. However, the idealized nonlinear model of the pendulum compromises the scope of the proposed method to be applicable to RtHT systems; the authors state that it is assumed that no friction exists between pendulum or the cart it is mounted on nor between the cart and its rolling surface [36]. This may explain the adequacy of a PD type controller in stabilizing the system; when friction is taken into account, it may be found that steady state errors may become more prominent requiring integral control action as well. Extension of these principles to a RtHT with an experimentally set up inverted pendulum system may therefore require more advanced control architectures. Furthermore, the authors state that serial communication was used for data transmission between the controller and the programming environment [36]. However, for RtHT systems which require rapid data transmission between numerical and physical substructures, serial communication may cause bottlenecks in execution speed thereby inducing the need for faster data transmission tools and a more sophisticated real-time target controller to replace the PIC microcontroller used in this research.

Another nonlinear control strategy is applied in Hunnekens et al. [37], where a phase-based variable gain control approach is utilized to achieve a time-domain performance specification which cannot be attained using conventional LTI controllers. The gain of the Variable Gain Controller (VGC) is allowed to change with the error signal and its derivative, in contrast to standard linear controllers which utilize fixed gains. Simulation results illustrate a noticeable improvement in the time-domain response of a linear plant through the use of the VGC, with an approximate 50% reduction in settling time compared with the response obtained with a linear fixed gain controller. Significant reductions in overshoot and oscillation are also evident. However,

it must be noted that the nonlinear methodology proposed has only been tested against a linear plant model in this research. It will be interesting to see the effectiveness of the proposed controller applied to nonlinear systems. The proposed solution is likely to be viable for nonlinear systems with varying mechanical properties so long as saturation does not inhibit the performance of the VGC.

In an early example of Hybrid Testing from 1999 by Darby et al. [38], a simple Hybrid test of an actuated mass was conducted with a PID controlled hydraulic actuator and a load cell forming the transfer system [38]. A lag between the demand and output positions of the actuator was identified thereby introducing the problem of transfer dynamics. The dynamics were modelled as a delay which was compensated for using a polynomial based forward prediction algorithm. The authors note that instability is likely if the delay exceeds the size of the time step used in the delay compensation integration scheme [38]. The proposed method relies on the assumption that the transfer dynamics can be accurately modelled as a delay which is often not the case. Regardless, this research in comparison with more modern work reviewed above, illustrates the significant developments in Hybrid Testing since the 20th century; from simple delay compensation schemes to newer more sophisticated lag compensators, it is clear that the field is rapidly evolving as new control technology and more powerful hardware and computational tools emerge.

Having reviewed some of the most widely used transfer dynamics mitigation schemes as well as new developments in this regard, it is evident that most schemes rely on linear techniques, or some form of linearization to capture actuator behaviour. The effectiveness of the methods presented by Wallace et al. [30], du Bois et al. [32], Ou et al. [35] and Darby et al. [38], all depend on how accurately the actuator can be characterized by a linear model. In the presence of a physical substructure which affects actuator behaviour, or in the presence of inherent nonlinearities such as stiction, the accuracy of these linear model-based methods in describing transfer dynamics will be compromised. Thus, there reflects a need for a method of addressing the problems of transfer dynamics that does not depend on the characterisation of the actuator. A single control scheme whose performance is independent to the nature of the actuator behaviour will enable a modular solution applicable to a wide range of systems. Such solutions are explored through this PhD.

2.3 Actuator Saturation Mitigation

Compensating for transfer dynamics often requires actuation hardware to perform near its design limits to maximize lag cancellation whilst responding rapidly to disturbances and changes in demand. However, it is imperative that saturation limits are not violated during operation in order to maintain high performance and avert the onset of nonlinearity. This section briefly overviews some of the different controller synthesis techniques proposed to overcome saturation in mechatronic systems.

Hu and Lin [39] present an analysis of saturation effects in actuation hardware. The authors argue that saturation mitigation techniques can be broadly categorized into 2 main strategies. The first of these strategies relies on neglecting saturation in the primary stage of controller design and implementing problem-specific methods to overcome the problems caused by saturation. Such methods are widely referred to as anti-windup schemes. Anti-windup schemes serve to stop the integrators in the system from integrating as long as the actuator control input is saturated. The second strategy involves including the saturation limits in the initial stages of controller design

and the closed loop system under saturation is analysed allowing the controller to be redesigned with the objective of enhancing performance whilst maintaining stability, or vice versa [39].

Visioli [40] presents an overview of windup and two widely used anti-windup schemes. The author describes windup as a phenomenon that takes place when a saturated signal is passed through an integrator; as the error signal of the system decreases at a slower pace due to saturation, the integral of the error becomes large thereby causing the system to exhibit significant overshoot and poor settling time [40]. Conditional Integration, also known as Clamping, is the first anti-windup scheme described, and involves restricting integral action to take place only when the system error is smaller than a specified value. Therefore, as saturation takes place causing the total error to grow, integral action is stopped [40]. The literature also describes a variation of this technique known as preloading in which a constant value is given to the integrator upon saturation. The other anti-windup scheme described is Back Calculation – in this method, the difference between the saturated and unsaturated error signals are scaled by the reciprocal of a specified tracking time constant and fed back to the integrator input. The tracking time constant determines the rate at which the integral term is reset [40]. The author also presents an evaluation of the effectiveness of both methods in compensating delayed 1^{st} order plants – Conditional Integration was shown to provide better performance than Back Calculation when the plant delay was small, although significant increases in settling time were seen when a large delay was used. Back Calculation was shown to provide a more consistent response for both plants compared with that of Conditional Integration.

Model Predictive Control (MPC) is a technique that has been shown to circumvent the effects of actuator saturation in real-time hybrid testing. MPC uses a process model to predict future outputs in order to optimize the control signals [41], [42]. Li et al. [43] demonstrate the effectiveness of a traditional online MPC strategy to mitigate actuator slew rate and magnitude saturation in a multivariable hybrid test of a quasi-motorcycle (QM) system. In order to run the tests in real-time despite the high computational power requirements of MPC, the authors implemented a modified hybrid test which utilized a reduced order observer. The substructuring errors of the QM system were shown to be reduced from ±0.002m to ±0.001m. Two main optimization cost functions were tested in this research; one which only compensated for actuator magnitude saturation, and the other which compensated for both magnitude and slew rate saturation. It was found that the computation time of the MPC strategy was notably higher when the optimization cost function which mitigated both slew rate and magnitude saturation was used. The proposed method runs in real-time for the tested system and inspires aspirations for future work to further extend the applicability of MPC in RtHT. However, the tested QM system is linear and can be represented by a reduced order observer. Higher order systems may not be readily compatible with reduced order observers whilst the behaviour of nonlinear systems is even more difficult to predict. Furthermore, since MPC is very computationally intensive, real-time operation for nonlinear systems may be difficult to achieve.

Li et al. [44] describe the prime drawback of using MPC, as the sample rate limitation due to its computational burden. They propose using a Back Calculation anti-windup scheme applied through a $H\infty$ Robust Disturbance Rejection controller to address the problem of actuator saturation. The authors utilize weighting functions to reduce the input to a nonlinear saturation operator in order to prevent saturation from taking place [44]. Results illustrate an approximate 50% reduction in the substructuring error when the anti-windup scheme is included in the $H\infty$ controlled system. The growth of the substructuring error with time is also seen to have been limited by this scheme.

It is evident that each existing saturation mitigation strategy offers unique advantages although there are difficulties in terms of program execution speeds and elimination of substructuring errors. Selection of the most appropriate technique will therefore rely heavily on the nature of the plant being controlled.

2.4 Passivity Control

The concept of Passivity [45] is a valuable means of describing the energy and power properties of systems and is widely used in analysing the stability of complex systems consisting of several substructures [46]. Passivity control schemes are widely used in the teleoperation industry to ensure stability between master and slave operators. The master and slave operators in such systems are analogous to the numerical and physical substructures of the hybrid test, as the interface between these two subcomponents is where the problems of instability arise due to actuator dynamics. Some applications of passivity control in maintaining stability in teleoperation systems will be discussed. In Chen et al. [46], a passive system is defined as one which either stores or dissipates the power supplied to it. For a system to remain passive, the energy supplied to it must always be greater than its energy output. Instability is a form of active behaviour when the energy output of a system or subcomponent grows exponentially with respect to its supplied energy. As such, a passive system is always stable.

In [47], passivity is described as an adequate condition for stability. Further, the authors highlight the following features of passivity making it a highly attractive solution for all its applications.

- The utilization of energy concepts is intuitive. Passivity can be easily identified by ensuring that energy inflow exceeds the energy outflow.
- Enables the stability of the entire system to be achieved by maintaining the passivity of all its individual subcomponents.
- Can be applied to linear as well as nonlinear systems

In Chen et al. [46], a multi-lateral teleoperation system with *n* masters and *n* slaves is tested with delayed communication channels. Power based passivity control is utilized to achieve passivity of the complete system in the presence of the time delays with weighting coefficients used to perform the weighted effects of the different master or slave manipulators. The power flow in the system is calculated by taking the product of the force and velocity of each master and slave. Through their results, the authors illustrate the effectiveness of the scheme in maintaining stability of the master-slave system. Acceptable tracking is seen in the face of slow inputs although, the authors acknowledge the inability of the proposed passivity control scheme to guarantee good tracking performance.

An energy based passivity controller is utilized in the work of Hannaford and Ryu [47] to ensure a haptic interface system is kept stable under a range of operating conditions. A passivity observer is designed to measure the real-time energy inflow and outflow with respect to individual subsystems whilst the passivity controller is designed as an adaptive dissipative element to absorb the net energy measured by the passivity observer. The authors illustrate the effectiveness of the proposed scheme in achieving stable operation in the presence of stiffnesses greater than 100N/mm with time delays as large as 15ms. The authors highlight that the key advantages of the proposed method are the low computational power requirements and the fact that a dynamic model of the system does not need to be identified.

In the work of Ryu et al. [48], the robustness of passivity control is highlighted. Simulation results on a single link flexible manipulator are used to illustrate resiliency under a wide variety of operating conditions with no model information. An uncertain plant is used with a wide range of admittance or impedance from zero to infinite. Results indicate totally stable behaviour of the manipulator in the presence of passivity control whilst unstable behaviour was seen without passivity control. The authors emphasize that the power of passivity control lies in its simplicity and ease of application for a wide range of systems.

An application of passivity control in electronics is seen in the work of Dissanayake et al. [49]. The authors design a passivity based nonlinear adaptive controller to regulate the output voltage of a power electronic converter. Unlike conventional adaptive controllers which require the input voltage of the controller to be known, the proposed method needs no information of input voltage or output resistance. Results illustrate good voltage regulation upon start up, under a demand voltage change and under a load disturbance. The authors further elaborate that the proposed adaptive controller can be applied to control any other DC-DC converter without loss of generality. This work elaborates the independence of the functionality of passivity control to the system it acts on, a key factor motivating its application to hybrid testing.

In the work of Henze et al. [50], we see the application of passivity control in humanoid robots. The authors propose a robust and reliable passivity based balancing controller for humanoid robots on different ground surfaces. The passivity considerations utilized by the author cover not only the robot but also the ground surface to ensure acceptable performance even in the presence of unsteady ground behaviour.

An application of passivity control in the energy distribution sector can be seen by the work of Gui et al. [51]. A novel passivity-based control system is proposed for an islanded AC microgrid consisting of renewable energy sources and energy storage systems. The energy stores support the voltage of the microgrid and in normal operation, the renewable energy sources inject maximum power to the microgrid. The passivity principle is used to guarantee the asymptotical stability of the whole microgrid. The authors describe that the main advantage of the passivity-based energy regulation scheme is that it alleviates the need for a phase locked loop system thereby enhancing the plug and play capabilities of the renewable energy sources.

In the work of Zhang et al. [52], passivity control is applied for the first time to solve the kinematic control problem of redundant manipulators. Redundancy of manipulators occurs when its number of degrees of freedom is greater than that required to perform a given task. Manipulator redundancy is highly appealing as it enables secondary tasks such as avoiding joint limits when performing primary tasks [52]. Conventional means of addressing this kinematic control problem generally do not consider joint velocity limits and this may allow damage to actuators. The authors propose a passivity-based method for the kinematic control of redundant manipulators which also takes into account joint velocity limits.

Kim et al. [53] propose the use of a passivity-based admittance controller for a powered upper-limb exoskeleton robot governed by a nonlinear equation of motion. The motivation for the use of passivity was to enable the use of a human operator and environmental interaction in the control loop. The authors validate the proposed scheme on a single degree of freedom testbench where the exoskeleton was used to lift and manoeuvre an unknown payload. The passivity-based nonlinear admittance controller which is made up of a feedback interconnection of passive subsystems, fully captures the nonlinear dynamics of the robot. With the passivity controller,

stable human-in-the-loop operation with unknown environmental interaction was achieved. Performance improvements with respect to control gain was seen to obey a linear trend [53].

As such, it is evident that passivity control has been successful in maintaining stable operation in several systems across a wide range of engineering disciplines. In all above cases, the operations of the passivity controllers are insensitive to the nature of the test system. This is a significant advantage particularly useful for real-time hybrid testing, where conventional transfer dynamics mitigation schemes are reliant on accurately characterising the coupled dynamics of the actuator and physical substructure. With passivity control, there is no such requirement thus enabling compensation for hybrid tests with uncharacterizable transfer systems. The motivation for using passivity control in real-time hybrid testing stems from the hypothesis that ensuring the passivity of the actuator, passivity and therefore stability of the entire hybrid test can be guaranteed. This is analogous to the fact presented in [54] that passivity of the complete system can be achieved by ensuring the passivity of its individual components.

Chapter 3

Preliminary Analysis of Passivity Control in Real-time Hybrid Tests

3.1 Context

As discussed in the literature review in chapter 2, the lag of actuators in hybrid tests has induced the need for a novel transfer dynamics mitigation scheme that does not rely on a linear model of actuation hardware. The concept of using energy-based passivity control was investigated via simulation in the publication presented in this chapter.

A hybrid test was simulated with a single degree of freedom linear numerical substructure and an actuator modelled as a pure delay. The physical substructure was modelled as a stiffness of linear and nonlinear nature and the publication presents the effectiveness of the energy-based passivity control scheme in each hybrid test simulation. Performance improvements in terms of tracking and stability were assessed in the time and frequency domains.

The concept of the passivity-based control scheme stems from the need to maintain stability in the system through the regulation of the energy flow. Instability caused by actuator delay is always accompanied by a growth in the energy flow of the system with time as vibration amplitudes grow exponentially. This reflects that measurement of the energy flow can be used as an indicator of system stability, and a means of rejecting excess energy introduced by the actuator will enable the stability of a system to be maintained. Energy rejection is achieved by a variable rate virtual damper acting on the numerical substructure of the hybrid test. Thus, the scheme is designed to control the stability of the system regardless of the nature of the transfer system or hybrid test substructures. This is envisaged to be widely applicable to many hybrid tests whilst enabling easy implementation of the modular subsystem consisting of the passivity controller and the virtual damping element to dissipate excess energy in the system.

This declaration concerns the article entitled:									
Passivity Control in Real-time Hybrid Testing									
Publication status (tick one)									
Draft manuscript		**Submitted**		**In review**		**Accepted**		**Published**	✓
Publication details (reference)	L. D. H. Peiris, A. R. Plummer, and J. L. Du Bois, "Passivity Control in Real-Time Hybrid Testing," in *UKACC 12th International Conference on Control (CONTROL),* 2018, pp. 317–322.								
Copyright status (tick the appropriate statement)									
I hold the copyright for this material	✓	Copyright is retained by the publisher, but I have been given permission to replicate the material here							
Candidate's contribution to the paper (provide details, and also indicate as a percentage)	**The candidate contributed to / considerably contributed to / predominantly executed the…** **Formulation of ideas:** Concept of using passivity damping to stabilize hybrid tests based on discussions with supervisors Dr. Jonathan du Bois and Prof. Andrew Plummer. Candidate's contribution (50%). **Design of methodology:** Methodology designed with supervisors Dr. Jonathan du Bois and Prof. Andrew Plummer. Candidate's contribution (65%). **Experimental work:** Selection of tests with supervisors Dr. Jonathan du Bois and Prof. Andrew Plummer. Candidate's contribution (70%). Running of tests, solely by the candidate (100%). **Presentation of data in journal format:** Paper to follow layout and structure of conference proceedings. Paper written by candidate, reviewed and corrected by supervisors Prof. Andrew Plummer and Dr. Jonathan du Bois. Overall contribution of candidate (75%).								
Statement from Candidate	This paper reports on original research I conducted during the period of my Higher Degree by Research candidature.								
Signed	L DH Peiris					**Date**	24/09/2019		

Passivity Control in Real-time Hybrid Testing

L. D. Hashan Peiris
Department of Mechanical Engineering, University of Bath, Bath, United Kingdom
ldhp20@bath.ac.uk

Andrew R. Plummer
Department of Mechanical Engineering, University of Bath, Bath, United Kingdom

Jonathan L. du Bois
Department of Mechanical Engineering, University of Bath, Bath, United Kingdom

***Abstract*—This paper details the application of passivity control in stabilizing real-time hybrid test (RtHT) systems with linear and nonlinear physical substructures. The effectiveness of this novel application in hybrid systems is assessed in the time and frequency domains with special attention given to improvements in stability and tracking performance. A 1 degree-of-freedom system is chosen as a test case with transfer dynamics modelled as a pure delay. The application of passivity control widely used in the teleoperation industry has been found to stabilize the hybrid test system under a wide range of operating conditions whilst resulting in tracking improvements as well. Unlike conventional model based compensation schemes, the application of passivity control does not require any information about the transfer system and/or physical substructure making this technique practical and effective in compensating complex hybrid tests where accurate linear models are unavailable.**

Keywords—passivity; hybrid test; transfer system; substructure;

NOMENCLATURE

ΔE = Net energy added at the transfer system
P_P = Physical substructure power
P_N = Numerical substructure power
F_P = Physical substructure force
V_P = Physical substructure velocity
F_N = Numerical substructure force
V_N = Numerical substructure velocity
K = Physical substructure stiffness
x_P = Physical substructure position
F_D = Passivity controller damping force
C_D = Passivity controller damping coefficient
B = Passivity controller gain
$RtHT$ = Real-time hybrid test
PC = Passivity control

I. INTRODUCTION

Real-time hybrid testing is a means of analysing systems which cannot be reliably studied using purely experimental methods or simulations. This technique involves the separation of the system into two substructures, one as a physical experiment and one in a numerical simulation. The complete system is tested by running these two substructures in parallel with actuators and force sensors to couple the substructures in real-time. Large and/or complex structures which are too expensive to be setup in a laboratory environment or complicated systems which cannot be accurately modelled in a simulation are some examples which greatly benefit from this method. Hybrid testing also enables the user to easily update parameters of the numerical substructure and even enables systems to be analysed prior to realization of all components [1]. As such, in recent years, hybrid testing has seen rapid growth in a wide variety of engineering disciplines proving effective in applications such as seismic integrity testing of structures [2], testing of vehicle powertrain and active suspensions [3], wave energy harvesting devices and aerospace air-to-air refuelling systems [4], [5].

However, an issue of importance in this field is the presence of spurious dynamics introduced by the actuators required to transfer motion between the numerical and physical substructures. The responses of actuators are subject to delays in the time domain which result in tracking errors or instability.

Horiuchi et al. [6] propose a delay compensation scheme which predicts a future displacement of the actuator, based on an n^{th} order polynomial function fitted to the previous n displacements. The method can only be used to predict ahead of an integer multiple of the time step thereby posing a restriction on the delays that can be compensated for a given choice of time step [7]. Moreover, the higher order variations of the method introduce excess phase lead to the system and amplitude ratio magnification at high frequencies [8]. Wallace et al. [9] propose an adaptive forward prediction scheme based on a least squares polynomial curve fitting algorithm. Although more computationally complex, this method enables superior compensation with reduced amplitude ratio magnification and phase lead. Tang et al. [10] compare the effectiveness of a range of delay compensators in a hybrid test with a shaking table transfer system. Performance improvement is most notable within a narrow low frequency range whilst at higher frequencies accuracy and stability were seen to deteriorate. In these conditions, other methods may perform better.

Another model based technique used to mitigate transfer dynamics is lag compensation where a low order transfer function model is identified to emulate the behaviour of the actuator [11]. The model is then inverted and applied in series with the actuator so as to cancel the dynamic lag introduced in the transfer system. Avci and Christenson [12] apply this scheme to reduce the effective delay from 20ms to 5ms in a real-time hybrid test of an isolated building structure. However, it is often difficult to characterize actuation hardware using low order models and the difficulty in inverting models whilst maintaining causality introduces further limitations. du Bois et al. [13] explore compensation schemes which utilize a combination of a delay compensator and a transfer function inversion, and show that these out-perform either of the methods in isolation. However, all the aforementioned schemes

are based on linear analysis and therefore suffer in the presence of a nonlinear physical substructure or transfer system where the effective delay or transfer function varies during operation. They can also suffer where the transfer system cannot be characterized accurately. In this paper, a new method based on passivity control is explored to obviate the need for accurate models of the transfer system and physical substructure.

A brief review of passivity control is presented in section II highlighting its advantages for hybrid testing. Its application to hybrid testing is presented in section III. Sections IV and V explore its performance for linear systems, in terms of stability and tracking, using numerical simulations. Section VI examines a discontinuous system. In section VII harmonic distortion is investigated as a technique for analyzing the performance of the passivity controller, and conclusions are drawn in section VIII.

II. Passivity Control Theory

Passivity control aims to shape the energy in a system and to tune the flow of energy through the system [14, 15]. Adaptive damping forces based on energy differences between components in the system act to maintain stability under a range of operating conditions. According to the time-domain definition of passivity, the sum of the energy supplied to a passive system and the initial energy stored must always be greater than zero [16]. By ensuring that all components of a system are passive, the complete system can be made to behave passively [17]. This is achieved through a controller which adds damping to the system based on energy measurements at various ports in the system. Passivity control has seen notable success in the teleoperation industry where a human input is used in the interaction of a master and slave manipulator. Hybrid testing and teleoperation systems have analogous control requirements: they both require coupled interaction between subsystems with delays and/or lags in the transmission between the two. In particular, stability is an important requirement in each application. Unlike the conventional compensation schemes used in hybrid testing, passivity control does not require a model of the transfer system. This allows the use of complex nonlinear systems which are difficult to model.

Ryu et al. [17] propose a bilateral passivity control scheme which guarantees stability for a wide range of hard wall contact scenarios. Much like the hard wall contact of teleoperation systems, hybrid test systems too can be subject to discontinuous nonlinearities such as impacts and step changes in stiffness. In a more recent publication [18], the authors describe the effectiveness of using a variable energy threshold in passivity control as the excitation of high frequency modes are prevented whilst a more smooth response is achieved. Anderson and Spong [19] illustrate the effectiveness of passivity control in maintaining stable operation of a force reflecting bilateral teleoperation system with a large time delay. Results illustrate that stability was maintained in time delays as large as 2s. Thus it is likely that the application of passivity control would allow highly unstable systems to be stabilized which would be a property very beneficial to highly nonlinear hybrid systems where stability margins often vary substantially with the operating point.

A key limitation of passivity control in teleoperation systems is described in Hannaford and Ryu [16]. The authors describe that if the user moves to an active location after a long interaction in a dissipative location, the passivity controller may not act until a large amount of active behavior is observed which may require the threshold energy value set in the passivity observer to be heuristically reset. Thus, it may not be reasonable to expect the optimal parameters for a passivity controller to be universal for all operating conditions in a hybrid test. This observation is considered in section VII.

Unlike the work of the authors mentioned previously, Ye et al. [20] explore the effectiveness of power measurements rather than energy in the passivity control of a haptic interface system. The authors argue that the use of power over energy allows the passivity controller to activate more evenly in contrast to an energy based system where damping action is more suddenly triggered. The literature further describes that the use of power mitigates the need for integration thereby resulting in no energy calculation error.

III. Hybrid Test Implementation

The proposed system is based on the principle of minimizing the net energy added by the transfer system. The use of power based passivity control was initially considered here, as described by Ye et al. [20], however, simulations on a real-time hybrid test revealed that stable operation and better tracking performance could be achieved for a greater range of conditions with the use of energy.

A controller acting on the net energy input from the transfer system to the physical and numerical substructures is used to tune a virtual damper which augments the force acting on the numerical substructure. As the transfer system adds spurious energy to the hybrid system, this is removed by the damper.

The power flow is calculated by evaluating the product of the force and velocity at the substructure interfaces. Thus, the power at the numerical substructure P_N will be the product of the velocity demand to the actuator V_N and the force feeding back to the numerical substructure F_N. This force would be the sum of the physical substructure force and the corrective damping force introduced by the passivity controller. The physical substructure power P_P would simply be the measured velocity of the actuator V_P multiplied by the force measured at the physical substructure F_P. The fundamental test involves a linear physical substructure comprised of a stiffness K allowed to travel by displacement x_P. The controller with a gain of B, calculates a variable damper rate, C_D, resulting in a damping force, F_D, based on the net energy added at the transfer system, ΔE. A saturation limit is used to ensure that passivity damping is always positive so that stability margins are never eroded when transfer system net energy is negative. This can be expressed as follows for the linear hybrid system:

$$\Delta E = \int (P_P - P_N)\, dt$$

$$= \int (F_P V_P - F_N V_N)\, dt$$

$$= \int ((K x_P) V_P - (K x_P + F_D) V_N)\, dt$$

$$where\ F_D = C_D V_N$$

$$and\ C_D = \begin{cases} B\Delta E, & \Delta E > 0 \\ 0, & \Delta E \leq 0 \end{cases}$$

This technique does not require any identification procedures to characterise the coupled behaviour of the transfer system and physical substructure, and can be readily applied to a wide range of hardware, including highly nonlinear transfer systems and/or physical substructures.

Fig. 1 illustrates the block diagram of a simple passivity controlled real-time hybrid test. All components including the transfer system and physical substructure are simulated in the tests presented in this paper. The transfer system is modelled as a pure delay of 3ms. The numerical substructure describes a mass m on a spring and damper of stiffness k and rate c respectively whilst the physical substructure is a stiffness which will be setup differently in 3 experiments to study the performance of the system in the face of different levels of nonlinearity. For linear analysis, a constant stiffness will be used whilst a 3rd order stiffening characteristic will be chosen to instigate nonlinearity at large amplitudes. In the final test, the stiffness will be made discontinuous to emulate a contact scenario representing a severe nonlinearity. For the emulated system, the transfer dynamics are omitted to enable perfect coupling between substructures.

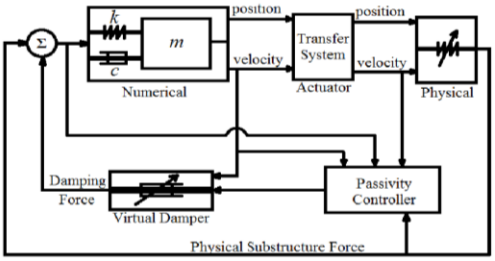

Fig. 1. Real-time hybrid simulation with passivity control

IV. Restoration of Stability

In order to assess the stability restoration properties of the passivity controller, the open loop transfer function of the hybrid test is used to compute delay margins (the phase margin divided by the angular frequency), shown in fig. 2, for a range of linear physical substructure stiffnesses. It can be seen that the delay margin in the system erodes as the physical substructure stiffness increases. Stable operation is only achievable for stiffness of 3.35 kN/m or less. For stiffnesses greater than this limiting value, a negative stability margin is seen, indicating an unstable closed loop system. For a stiffness of 20 kN/m, the delay margin is seen to be -2.5 ms (corresponding to a phase margin of -20.73^0) indicating a highly unstable closed loop system. Passivity control is applied to the linearized hybrid system at 3.35 kN/m and 20 kN/m to illustrate the restoration of stability in a marginally stable and a highly unstable hybrid system.

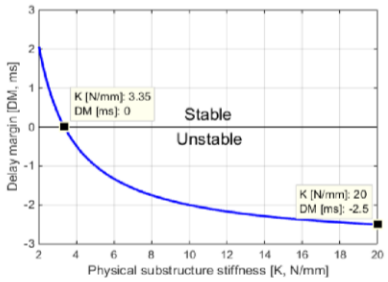

Fig. 2. Delay margin of linearized hybrid system (data cursors showing stiffnesses resulting in marginal stability and high instability)

Fig. 3 illustrates the frequency responses of these tests acquired using stepped sine inputs. The high stiffness hybrid test without passivity control is not shown as it is unstable. It is evident that stability has been restored in both systems with sensible amplitude ratio and phase responses at all frequencies tested.

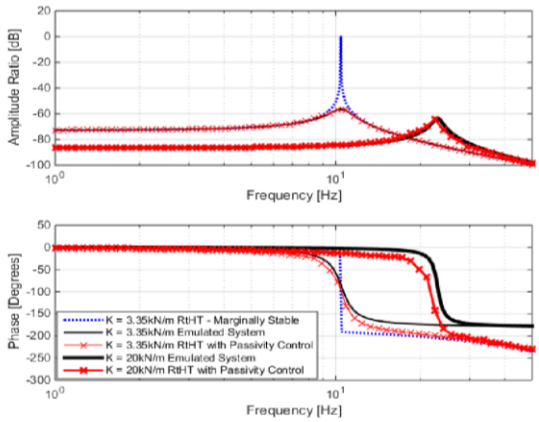

Fig. 3. Closed loop linear RtHT responses with passivity control

V. Tracking

With the restoration of stability, tracking improvements too can be seen. Fig. 4 shows the step response of the hybrid systems with both linear and cubic physical substructures, excited by a 50N force input. The amplitude ratios and settling times of the compensated systems match those of the emulated systems well, in contrast to the uncompensated systems.

There is a small phase delay in the responses however which cannot be completely eliminated. Referring again to fig. 3, it is seen that the phase of the compensated system shows noticeable improvement in the frequency range 5-20Hz. This is because the resonant frequency of the system lies in this range, and the passivity controller is able to mitigate the erosion of the stability margin caused by the delay and produce a phase response closer to that of the emulated system. The controller can only add damping, however, and

cannot compensate the delay itself, and this can be seen in the transfer function throughout the frequency spectrum.

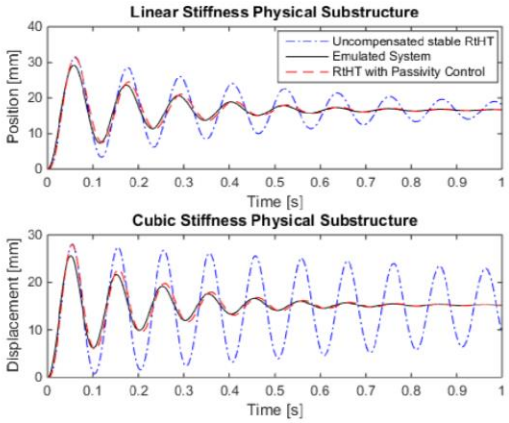

Fig. 4. Output position and net power response to step input

To further investigate the tracking performance improvements, the linear hybrid system is forced near the resonant frequency. The subspace plot of numerical and physical displacements is shown in fig. 5 for a range of passivity controller gains, *B*, where *B=0* is the uncompensated system. As expected, the emulated system representing a perfect actuator is seen as a diagonal line of angle 45^0 indicating that numerical and physical substructure displacements are always identical. However, the steady state responses of the hybrid tests with and without passivity control all manifest as ellipses due to the transfer system delay. Higher passivity controller gains result in smaller ellipses but the aspect ratios remain similar, confirming that the tracking delay cannot be mitigated. In fact, at high gains the controller produces an excess of damping which has a detrimental effect on the amplitude tracking performance.

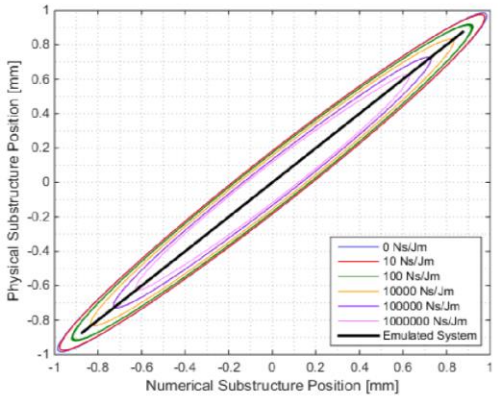

Fig. 5. Substructure position subspace plot near resonance

VI. Discontinuous Nonlinearity

In order to assess the effectiveness of passivity control in a more complex hybrid test, a discontinuous nonlinearity was set up as the physical substructure. The following tests simulate the hybrid system making contact with a surface of stiffness 10kN/m (high enough produce instability in a linear system) positioned at the centre of the motion.

Fig. 6 illustrates the contact scenario to a contact surface of stiffness 10kN/m positioned at 0mm on the positive displacement side. The system without passivity control is seen to exhibit large oscillations and injects large quantities of power into the hybrid system at the points of contact with the surface. However, with the application of passivity control, the oscillations follow those of the emulated system more closely as the spurious power injection into the system is rapidly reduced in subsequent contact cycles.

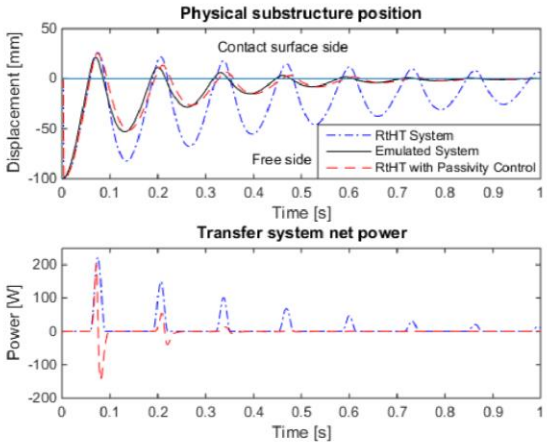

Fig. 6. Unforced response with 10kN/m contact surface at positive displacements

In the event of forced excitation with surface contact, the effectiveness of passivity control varies with the excitation frequency as seen in fig. 7. It is evident that at frequencies below resonance, passivity control works well, with the response being restored to that of the emulated system almost perfectly. Notable improvement in stability and tracking are also seen near resonance.

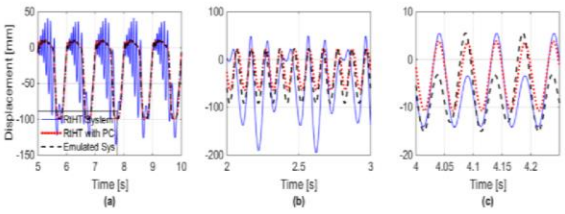

Fig. 7. Forced response with 10kN/m contact surface at positive displacements: (a) below resonance; (b) near resonance; (c) above resonance

However, the period doubling artefacts seen in the emulated system at frequencies above resonance are not evident when passivity control is applied. This nonlinear phenomenon can be sensitive to parametric changes and initial conditions, and at higher frequencies the uncompensated phase lag has nontrivial effects. It is seen that passivity control can be effective with discontinuous physical substructures, but may be unpredictable in some operating regimes.

VII. Performance Criteria and Nonlinear Distortion

Sections IV and V showed that amplitude and frequency response charateristics can be replicated well using passivity control. The first part of this section investigates in greater depth the performance with respect to these metrics. As the amount of virtual damping in the system is dependant on the transfer system net energy, a passivity controlled hybrid system can be expected to exhibit a dynamic natural frequency and damping ratio that vary with not only the controller gain, but also amplitude of the energy flow back and forth between the numerical and physical substructures. Here, step responses are used to determine the variation of these properties for different controller gains using a selection of input amplitudes. The properties shown in fig. 8 are normalised with respect to those of the emulated system.

The damping ratios illustrated in fig 8. have been calculated using the logarithmic decrement method applied to the 1st and 6th peaks of the responses. The natural frequencies were obtained by evaluating the power spectrum of the response signals and observing the frequency where the power is highest. It is evident that the effect of passivity control on the performance characteristics is dependant on the physical substructure displacement. This is as expected, since larger step inputs result in higher velocities and more energy flowing between substructures, which in turn affects the amount of passivity damping applied. Higher gains are seen to increase the hybrid system damping ratio initially until it matches that of the emulated system, after which a gradual decrease settling to approximately 80% of the emulated system damping ratio is evident. The natural frequency of the response is seen to decrease until a turning point is reached when the gain resulting in a matching damping ratio is applied. Further increases in gain result in excess damping in the system causing transfer system net energy to become negative. As this triggers the lower saturation on the passivity damper rate to prevent negative damping in the system, the excess energy dissipated is never returned to the system. Because the passivity control acts quickly to reduce the net energy difference, it only operates near the start of the response and does not act significantly over the majority of the response. The damping and frequency charactersitics therefore exhibit marked variation over the duration of the test, with only the aggregate response captured in fig. 8. Therefore, further increases in gain result in less passivity control causing the overall response to exhibit a natural frequency and damping ratio closer to that of the system without passivity control.

For all tests the first section of the curve, where the results have greatest validity, indicates that in general an increase in passivity controller gain leads to improvements in the damping characteristics along with deterioration of the frequency characteristics. There is a trade-off between matching these two characteristics.

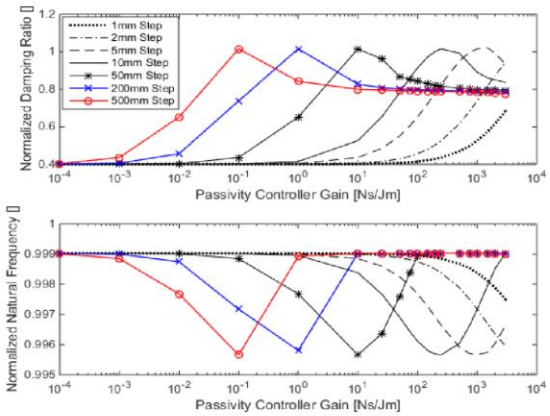

Fig. 8. Hybrid test performance parameters with passivity control

With the addition of a variable rate virtual damper, the passivity controller will tend to make any given hybrid system more nonlinear. High controller gains can result in rapid changes in damper rates which distort the system response. A highly distorted signal is indicative of poor tracking. To quantify this nonlinear disortion, the linear hybrid system was forced sinusoidally with different passivity controller gains at a range of vibration amplitudes. The total harmonic distortion of the output response is evaluated and plotted in fig. 9. It can be seen that nonlinear distortion is maximum when both the excitation amplitude and controller gain are high. For low amplitude tests, a greater range of controller gains can be used with less nonlinear distortion whilst high amplitude tests require the gains to be relatively low. This result agrees with the trend seen in fig. 8 which indicates the need for smaller gains in high energy hybrid tests in order to match the emulated system damping ratio.

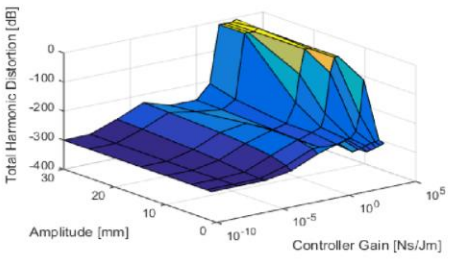

Fig. 9. Total harmonic distortion of hybrid test response

The optimal controller gain is seen to depend heavily on the test conditions. The optimal control gain would appear to lie where the damping ratio of the emulated system is matched with greatest accuracy; the change in natural frequency remains small at this point. But this requires prior knowledge of the expected behaviour of the emulated system: information that is not generally available. A general solution to this control gain selection remains an open research question.

Improvements in tracking with passivity control alone are limited when substructure energies are low at high frequency. The use of model based methods to complement passivity control is envisaged to lead to greater performance than purely passivity based or model based methods. Moreover, due to the variation of the optimal passivity controller gain with the magnitude of the energy flow, a hybrid test required to operate over a wide range of amplitudes will require various gains for maximum performance, and methods for tuning this gain, possibly using online methods, need to be established.

VIII. Conclusion

A novel technique to compensate for transfer system dynamics in real-time hybrid tests is presented, based on passivity control. Unlike conventional compensation schemes, this method does not require any information of the physical substructure or actuation hardware to be known in the implementation stage. Restoration of stability has been successfully demonstrated in marginally stable and highly unstable test cases with phase margins as low as -20.73^0. Tracking assessments in the time and frequency domains using step responses, stepped sine and contact scenarios indicate significant improvements in amplitude ratio tracking and marked improvements in phase over many frequencies. It is noted that passivity control alone cannot mitigate the delay in the transfer system itself, and this can lead to deterioration in the performance particularly at high frequencies and in complex nonlinear operating environments. Initial analysis shows the existence of an optimal controller gain which varies with response amplitude, and future work will address the idnetification of this point for general systems.

IX. References

[1] A. R. Plummer, “Model-in-the-Loop Testing,” *Proc. Inst. Mech. Eng. Part I J. Syst. Control Eng.*, vol. 220, no. 3, pp. 183–199, 2006.

[2] A. M. Reinhorn, M. V. Sivaselvan, Z. Liang, and X. Shao, “Real-time dynamic hybrid testing of structural systems,” *13th World Conf. Earthq. Eng.*, no. 1644, pp. 1–13, 2004.

[3] H. K. Fathy, Z. S. Filipi, J. Hagena, and J. L. Stein, “Review of hardware-in-the-loop simulation and its prospects in the automotive area,” vol. 6228, p. 62280E–62280E–20, 2006.

[4] T. Börner and M. Alam, “Real time hybrid modeling for ocean wave energy converters,” *Renew. Sustain. Energy Rev.*, vol. 43, pp. 784–795, 2015.

[5] M. Bolien, P. Iravani, and J. du Bois, “Robotic Pseudo-Dynamic Testing (RPsDT) of Contact-Impact Scenarios,” *Towar. Auton. Robot. Syst.*, vol. 9287, pp. 50–55, 2015.

[6] T. Horiuchi, M. Inoue, T. Konno and Y. Namita, "Real-time hybrid experimental system with actuator delay compensation and its application to a piping system with energy absorber", *Earthquake Engineering & Structural Dynamics*, vol. 28, no. 10, pp. 1121-1141, 1999.

[7] P. Bonnet, M. Williams and A. Blakeborough, "Compensation of actuator dynamics in real-time hybrid tests", *Proceedings of the Institution of Mechanical Engineers, Part I: Journal of Systems and Control Engineering*, vol. 221, no. 2, pp. 251-264, 2007.

[8] X. Weijie, G. Tong and C. Cheng, "Comparison of delay compensation methods for real-time hybrid simulation using frequency-domain evaluation index", *Earthquake Engineering and Engineering Vibration*, vol. 15, no. 1, pp. 129-143, 2016.

[9] M. Wallace, D. Wagg and S. Neild, "An adaptive polynomial based forward prediction algorithm for multi-actuator real-time dynamic substructuring", *Proceedings of the Royal Society A: Mathematical, Physical and Engineering Sciences*, vol. 461, no. 2064, pp. 3807-3826, 2005.

[10] Z. Tang, M. Dietz, Z. Li and C. Taylor, "The performance of delay compensation in real-time dynamic substructuring", Journal of Vibration and Control, p. 107754631774048, 2017.

[11] M. Wallace, D. Wagg, S. Neild, P. Bunniss, N. Lieven and A. Crewe, "Testing coupled rotor blade–lag damper vibration using real-time dynamic substructuring", *Journal of Sound and Vibration*, vol. 307, no. 3-5, pp. 737-754, 2007.

[12] M. Avci and R. Christenson, “Real-Time Hybrid Substructuring Shake Table Test of a Seismically Excited Base Isolated Building,” in Dynamics of Coupled Structures, Volume 4, 2018, pp. 71–78.

[13] J. du Bois, B. Titurus, and N. Lieven, “Transfer Dynamics Cancellation in Real-Time Dynamic Sub- structuring,” *Proc. ISMA 2010*, pp. 1891–1914, 2010.

[14] P. Falugi, "Model predictive control: a passive scheme", *IFAC Proceedings Volumes*, vol. 47, no. 3, pp. 1017-1022, 2014.

[15] C. Batlle, "Passive Control Theory 1", Bertinoro, Italy, 2005.

[16] B. Hannaford and J. Ryu, "Time-domain passivity control of haptic interfaces", *IEEE Transactions on Robotics and Automation*, vol. 18, no. 1, pp. 1-10, 2002.

[17] J. Ryu, D. Kwon and B. Hannaford, "Stable Teleoperation With Time-Domain Passivity Control", *IEEE Transactions on Robotics and Automation*, vol. 20, no. 2, pp. 365-373, 2004.

[18] J. Ryu, C. Preusche, B. Hannaford and G. Hirzinger, "Time domain passivity control with reference energy following", *IEEE Transactions on Control Systems \Technology*, vol. 13, no. 5, pp. 737-742, 2005.

[19] R. Anderson and M. Spong, "Bilateral control of teleoperators with time delay", *IEEE Transactions on Automatic Control*, vol. 34, no. 5, pp. 494-501, 1989.

[20] Y. Ye, Y. Pan, Y. Gupta and J. Ware, "A Power-Based Time Domain Passivity Control for Haptic Interfaces", *IEEE Transactions on Control Systems Technology*, vol. 19, no. 4, pp. 874-883, 2011.

3.2 Summary

The publication presented in this chapter illustrates that passivity control is a promising application in real-time hybrid testing having stabilized systems with linear, nonlinear and discontinuous physical substructures. The main findings are:

1) Stability of hybrid tests can be improved using passivity control
2) Tracking improvements are not inherently attainable although the controller can be tuned to achieve this if information of the emulated system is available.
3) Excess passivity control leads to nonlinear distortion of output

Preliminary analysis indicates that the scheme exhibits strong stabilizing properties and does not depend on predetermined assumptions about the actuator's behaviour. Although versatile, it does not eliminate the phase lag caused by the transfer system unlike existing model-based compensators. The immediate next steps are

1) To apply the passivity-based controller in an experimental real-time hybrid test setup and validate the findings of the simulations.
2) To investigate the performance of passivity control with model-based compensators.

These are explored in the following chapter in the next publication.

Chapter 4

Experimental Validation of Passivity Control in Nonlinear Real-time Hybrid Tests

4.1 Context

Having established the potency of passivity control in simulations of real-time hybrid tests, its performance in an experimental nonlinear real-time hybrid test with complex actuator dynamics was assessed. The methods first introduced in the publication presented in chapter 3 were utilized. Performance of the standalone passivity controller was assessed and compared with that of a state-of-the-art transfer dynamics mitigation scheme. The effectiveness of passivity control when used together with state-of-the-art techniques was also analysed to identify the capacity to alleviate some of the limitations incurred with standalone passivity control.

The hybrid test employed in the publication presented in this chapter consists of a linear single degree of freedom numerical substructure connected to a nonlinear stiffness actuated by an electromagnetic actuator running in position control mode. The nonlinear stiffness is approximately cubic in the range of displacements to be tested, like that of a Duffing oscillator. To prevent backlash, the springs are preloaded in the zero-deflection position. The non-zero tension in the preloaded springs result in a positive tangential stiffness around the initial zero-displacement state of the system, as described in [55].

The actuator has nonlinear friction acting on its shaft which was reduced using a state-of-the-art friction compensation scheme. A load cell was used to feedback the physical substructure force back to the numerical substructure. A CAD model of the test rig is shown in figure 2.

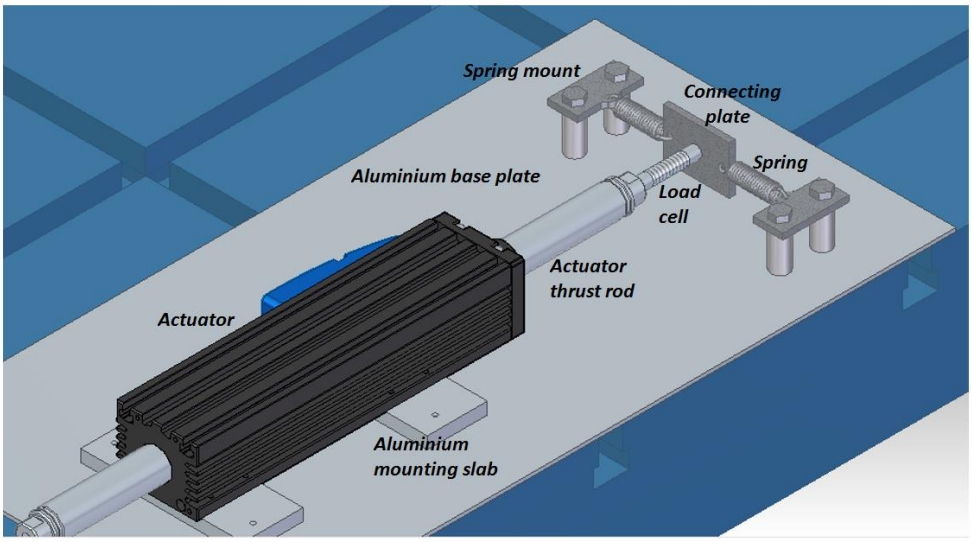

Figure 2: CAD model of test rig on reaction floor

The emulated system to be replicated using the hybrid test was setup as a simulation and used as a benchmark to assess the performance of the real-time hybrid test. Performance gains in the time and frequency domains were analysed by comparing the hybrid test response with and without passivity control against that of the emulated system simulation. The emulated system

represents the hybrid test with perfect actuator dynamics, i.e. instantaneous data transfer between the numerical and physical substructures.

This declaration concerns the article entitled:									
Passivity Control for Nonlinear Real-time Hybrid Tests									
Publication status (tick one)									
Draft manuscript		**Submitted**		**In review**	✓	**Accepted**		**Published**	
Publication details (reference)	L. D. H. Peiris, A. R. Plummer, and J. L. Du Bois, "Passivity Control for Nonlinear Real-time Hybrid Tests," *Proc. Inst. Mech. Eng. Part I J. Syst. Control Eng.*, 2020.								
Copyright status (tick the appropriate statement)									
I hold the copyright for this material	✓	Copyright is retained by the publisher, but I have been given permission to replicate the material here							
Candidate's contribution to the paper (provide details, and also indicate as a percentage)	**The candidate contributed to / considerably contributed to / predominantly executed the…** **Formulation of ideas:** Idea to write a paper which experimentally validates the results of preceding paper – supervisor Dr. Jonathan du Bois. Idea to compare results of new scheme with that of an existing scheme discussed with supervisor Dr. J. du Bois. Candidate's contribution (50%). Idea to include results of passivity control used together with an existing scheme solely by the candidate (100%). **Design of methodology:** Methodology designed with supervisors Dr. Jonathan du Bois and Prof. Andrew Plummer. Candidate's contribution (60%). **Experimental work:** • Design and manufacture of load cell for force sensing, by technician Mr. Steve Coombes. • Initial setup and configuration of actuator done with the help of technician Mr. Robin Harris. Candidate's contribution (70%). • Test rig set up solely by the candidate (100%). • All experiments implemented solely by the candidate (100%). **Presentation of data in journal format:** Paper written by candidate, reviewed and corrected by supervisors Prof. Andrew Plummer and Dr. Jonathan du Bois. Overall contribution of candidate (70%).								
Statement from Candidate	This paper reports on original research I conducted during the period of my Higher Degree by Research candidature.								
Signed				**Date**	24/09/2019				

Paper Two: Passivity Control for Nonlinear Real-time Hybrid Tests

Passivity Control for Nonlinear Real-time Hybrid Tests

L. D. Hashan Peiris[1], Andrew R. Plummer, Jonathan L. du Bois

Department of Mechanical Engineering, University of Bath, Claverton Down Rd. Bath, BA2 7AY

Abstract

In real-time hybrid testing, a system is separated into a numerically simulated substructure and a physically tested substructure, coupled in real time using actuators and force sensors. Actuators introduce spurious dynamics to the system which can result in inaccuracy or even instability. Conventional means of mitigating these dynamics can be ineffective in the presence of nonlinearity in the physical substructure or transfer system. This paper presents the first experimental tests of a novel passivity-based controller for hybrid testing. Passivity control was found to stabilize a real-time hybrid test which would otherwise exhibit instability due to the combination of actuator lag and a stiff physical substructure. Limit cycle behaviour caused by nonlinear friction in the actuator was also reduced by 95% with passivity control, compared to only 64% for contemporary methods. The combination of passivity control with conventional methods is shown to reduce actuator lag from 35.3degrees to 13.7degrees. A big advantage of passivity control is its simplicity compared with model-based compensators, making it an attractive choice in a wide range of contexts

Keywords: Real-time Hybrid Test; Passivity Control; Substructure.

Nomenclature

b – Passivity controller gain
c – Numerical substructure damper rate
c_D – Passivity controller damper rate
e_N – Numerical substructure energy
e_P – Physical substructure energy
f – Force input to numerical substructure
f_C – Coulomb friction force
f_D – Passivity damping force
f_F – Frictional force
f_N – Numerical substructure force
f_P – Physical substructure force
$G(s)$ – 2nd order transfer function to model actuator dynamics
$G^{-1}(z)$ – Discretized 2nd order transfer system model inversion
i_A – Actuator command current signal with friction compensation
i_C – Actuator command current signal without friction compensation
i_F – Friction compensatory current signal
k_P – Physical substructure stiffness
$k_P(0)$ – Physical substructure stiffness linearized about small displacements
k_F – Actuator force constant
K_L – Stiffness of a linear physical substructure
k – Numerical substructure stiffness
m – Numerical substructure mass
$N(s)$ – Numerical substructure transfer function
$P(s)$ – Physical substructure transfer function
RtHT – Real-time Hybrid Testing
s – Differential operator

[1] Corresponding author. Email address: L.D.H.Peiris@bath.ac.uk,
Conflict of interest - none declared

$T(s)$ – Actuator transfer function
x_N – Numerical substructure mass position
x_P – Physical substructure and actuator displacement
$\dot{x}_P$ – Physical substructure and actuator velocity
z – Backward shift operator
Δe – Net energy added to hybrid system by the actuator

1 Introduction

Real-time Hybrid Testing (RtHT) is a method of analysing complex systems utilising a combination of experimental and simulation based techniques. The complete system is split into numerical and physical components which are tested together, with actuators and sensors to couple the substructures in real-time. A number of advantages of this technique are detailed by Plummer [1]: the method not only enables cost savings by not having to set up a complete experimental system, but also enables testing of systems which are too complex for simulation or too large for conventional experimental testing. Moreover, RtHT also offers further advantages such as enabling systems to be tested prior to the design or realization of all physical components, and allows system parameters to be easily adjusted by the user [1]. Applications of RtHT include seismic integrity testing of building structures in the civil engineering industry [2], powertrain and suspension design in the automotive sector [3], air to air refuelling in the aerospace industry [4], and testing of wave energy harvesting devices in the marine energy sector [5]. The aerospace industry and automotive sectors have turnovers of £72 billion and £71.6 billion in the UK alone as of 2017 [6,7]. As an illustration of the time and cost savings that can be realised using hybrid test systems, National Instruments report field testing time reductions from 20 to 5 days for an aircraft arrestor system, at a cost saving of around $49,000 per day [8]. The benefits of analogous Hardware-in-the-Loop systems for electronic controllers have long since been established, with lead time reductions estimated at 15-50% [9].

A drawback of RtHT is the dynamics introduced to the system by the actuators. The delay and lag added to the closed loop system often leads to tracking errors and sometimes renders the system unstable. A number of authors propose delay compensation methods to minimize this effect. Horiuchi et al. [10] propose a delay compensation scheme which predicts forward by a fixed time based on a linear extrapolation of the past response of the system. A table of coefficients is available which enables the user to easily implement an n^{th} order forward predictive scheme to mitigate the delay of the actuator. However, this forward stepping algorithm can only compensate delays of integer multiples of the simulation time step. Wallace et al. [11] present a scheme which can compensate continuous delay times, and which adaptively tunes the time constant. However these schemes rely on the actuator behaving as a pure delay although the dynamics of real actuators are often more complex. Wallace et al. [12] utilize a compensation scheme where the actuator is modelled as a linear first order transfer function. The transfer function model is then inverted and applied as a discrete time feed-forward compensator to mitigate actuator dynamics. du Bois et al. [13] take this technique a step further by modelling actuator dynamics using combinations of first and second order transfer functions and delay.

Ou et al. [14] propose a feed-forward actuator control scheme based on H∞ optimization and linear quadratic estimation. A three story building with damping is emulated using a three degree of freedom hybrid system. The damper is setup as the physical substructure in this experiment and coupled to the numerical substructure of the building using a hydraulic actuator. The proposed algorithm applied to the hybrid test illustrates the effectiveness of the scheme in cancelling noise which is amplified by the size of the controller gain of the actuator. Real-time hybrid simulation results indicate good tracking of position and velocity, although excitation signals used are of low frequency where actuator lag is notably smaller than at higher frequencies.

Lag compensation technology to date is based on the identification of a linear model of the actuator which is used to design a feed-forward controller to mitigate the actuator's lag. Often, it is difficult to accurately model the actuator dynamics using a delay and/or linear transfer function especially when the dynamics of the actuator are affected by the physical substructure of the test. Moreover, nonlinearities such as Coulomb friction result in different behaviour depending on the operating conditions. While high-fidelity models of the physical system and test specimen can, in

principle, be used along with nonlinear control methods to mitigate these effects, the effort of implementation is high and the understanding of the physical specimen required undermines the purpose of the hybrid test. It is for this reason that such techniques are rarely employed, and the state of the art usually relies on simple linear theory. Therefore, there exists the need for a more robust scheme with less dependency on the transfer system behaviour.

In this paper, a passivity based approach is proposed where energy flow between the numerical and physical substructures and the transfer system is measured and used to set the damping coefficient of a virtual damper. This dissipates spurious energy added to the hybrid system by the actuation hardware. Excess transfer system energy can result in poor simulation accuracy and more critically, instability in the hybrid test. Even where high performance actuators and control techniques are incorporated to mitigate the addition of such spurious energy, passivity-based methods can supplement that control to extend the useful operational envelope of the equipment and improve upon the state of the art. The work presented here is the first experimental investigation of the methods initially explored in Peiris et al. [15].

Section 2 describes the structure and theory of the passivity controller proposed in this paper together with a description of some state of the art transfer dynamics compensators which are used to compare results. Section 3 presents the hybrid system used for testing the passivity controller and a description of the actuator used in the transfer system. In section 4 simulation results are discussed, and experimental results are presented and discussed in section 5.

2 Theory and Method

2.1 Passivity Control

A system which is dissipative with respect to the energy supplied to it is known as a passive system [16]. Passivity Control is widely applied in haptic interface systems in the teleoperation industry to maintain stable communication between master and slave manipulators. Zefran et al. [17] argue that passivity control can be used to guarantee stability in teleoperation systems provided that appropriate operating conditions are maintained throughout the tests. Real-time hybrid tests are analogous to haptic interface systems as the delay in the transfer system between the numerical and physical substructures is similar in nature to that between the master and slave manipulators.

Atashzar et al. [18] illustrate the effectiveness of passivity control in a human-robot interaction system where assistive and resistive therapy is delivered to a patient's limb. Results indicate that passivity control has enabled the system to prevent delay induced instability. The authors further acknowledge the fidelity of the proposed solution in the face of nonlinearity in the system such as variable time delays. As conventional model based compensation schemes in hybrid testing are often based on linear models, performance is compromised in the presence of nonlinearity in the system and passivity control offers a means to address this deficiency.

Sun et al. [19] apply a modified passivity control approach based on a wave variable to accommodate time delays in a teleoperation system. Results indicate good tracking between master and slave manipulators with a maximum error of less than 1 radian in response to low frequency inputs. Zhang et al. [20] utilize passivity control to stabilize a rehabilitation robot system used for motion recovery training in stroke patients. Passivity control has been utilized to enable a smooth transition of the system between different operating modes. This can be exploited in RtHT, particularly in nonlinear systems required to operate under several test conditions in a single experiment.

The passivity controller for hybrid testing proposed in this paper acts upon the energy flowing to the numerical and physical substructures. The energy error, i.e. additional energy introduced by the transfer system Δe, will be fed to the passivity controller which will control a variable rate virtual damper which acts on the numerical substructure. The energy error is obtained by integrating the net power flow from the transfer system. The numerical substructure and physical substructure powers are calculated by evaluating the product of force and velocity. The physical substructure force f_P, is measured using a load cell, whilst its velocity $\dot{x}_P$ is obtained by differentiating the position measurement of the actuator's built-in quadrature encoder. The force and velocity signals of the numerical substructure are acquired

from the model running in the Simulink real-time target controller. The passivity damping force f_D, at the numerical substructure can be expressed as [15]

$$f_D = c_D \dot{x}_N$$

where c_D and $\dot{x}_N$ are the passivity damper rate and numerical substructure velocity respectively. For a hybrid test with a physical substructure position x_P, the energy of the physical substructure e_P is given by

$$e_P = \int_0^t (f_P \ \dot{x}_P)\, dt$$

Similarly, the energy e_N, of the numerical substructure is given by

$$e_N = \int_0^t (f_N \dot{x}_N)\, dt$$

$$= \int_0^t \left((f_P + f_D)\dot{x}_N\right) dt$$

where f_N is the force at the numerical substructure. The net energy difference between the substructures is the energy added to the system by the actuator and is given by

$$\Delta e = e_P - e_N$$

This energy difference is used to calculate the damping rate at the virtual variable rate passivity damper. However, if the energy flowing from the numerical substructure to the actuator exceeds that flowing from the actuator to the physical substructure, it is desirable to turn off passivity control action. This is done to prevent adding negative damping to the system as this can make the closed loop hybrid test unstable. The passivity damper rate c_D can therefore be expressed as follows, if b is the passivity controller gain set by the user

$$c_D = \begin{cases} b\Delta e, & \Delta e > 0 \\ 0, & \Delta e \leq 0 \end{cases}$$

2.2 Friction compensation theory

The actuator used in these studies exhibits nontrivial levels of Coulomb friction; this is compensated as proposed by Eamcharoenying et al. [21] in order to minimize spurious effects caused by nonlinear friction on the actuator. This scheme for deterministic systems is based on applying a step in command current to the actuator so as to mitigate the expected Coulomb friction force. The friction force in the model, f_F, is approximated by the following equation

$$f_F = \begin{cases} f_C sign(\dot{x}_P), & if\ \dot{x}_P \neq 0 \\ -f_C \leq f_F \leq f_C, & if\ \dot{x}_P = 0 \end{cases}$$

where $\dot{x}_P$ is the actuator and physical substructure velocity and f_C is the Coulomb friction force acting on the actuator [21]. The step change in current required to cancel the Coulomb friction force is calculated using the force constant of the actuator using the following equation, where i_F and k_F are the compensatory current step signal and actuator force constant respectively.

$$i_F = \frac{f_F}{k_F}$$

The command current signal to the actuator is therefore augmented as follows in order to cancel the Coulomb friction force

$$i_A = i_C + i_F$$

where i_C and i_A respectively, are the command current signals before and after friction compensation is applied.

2.3 Model based compensation theory

In order to compare the performance of passivity control with a state-of-the-art compensation scheme, a second order lag compensator as utilized in du Bois et al. [13] is designed to mitigate the transfer dynamics of the actuator in the presence of the physical substructure. To design the lag compensator, a transfer function of the coupled dynamics of the actuator and physical substructure is required. To obtain this, the actuator with the physical substructure and friction compensation, was swept sinusoidally from 0.1Hz-50Hz over 50s at low amplitude (2mm) and the output position data was measured and used with the input demand for transfer function identification. The second order transfer function is fit to the data using the Gauss-Newton least squares search method.

$$G(s) = \frac{72590}{s^2 + 223.8s + 61660}$$

G(s) is the transfer function modelling the dynamics of the actuation hardware and is therefore expected to always have stable poles. The identified transfer function G(s) was then inverted by placing the identified poles as zeros. A pair of conjugate poles 10 times faster than the identified conjugate poles was placed in the denominator of the inversion so as to maintain causality. The inverted transfer function was then discretized at 10kHz using Tustin's approximation and subsequently implemented as a feedforward compensator to mitigate the actuator dynamics. The model-based compensator is given by the following discrete time transfer function.

$$G^{-1}(z) = \frac{76.2z^2 - 150.7z + 74.52}{z^2 - 1.747z + 0.8015}$$

3 Experimental System

3.1 Transfer system

The transfer system of the hybrid test consists of an actuator to apply the displacements calculated in the numerical substructure to the physical substructure, a load cell to feedback physical substructure force measurements to the numerical substructure, and the passivity controller. The actuator used for hybrid testing in the following experiments is a Copley STA2508S electromagnetic actuator.

The actuator is programmed to operate in force control mode using the proprietary Xenus XTL motor driver. The Xenus executes a current control loop serving as the inner loop controller driving the actuator. Nested outer control loops acting on position and velocity feedback are programmed in a Simulink real-time target controller to allow the actuator to track position in the hybrid tests. The structure of the actuator control system is shown in figure 1. The actuator has a built in quadrature encoder for position measurement and feedback. The position measurements are differentiated to obtain velocity feedback. The performance limits of the actuator are presented in Table 1. There is nonlinear sliding friction on the armature of the actuator. To minimize the effect of nonlinear friction in the system, a Coulomb friction compensator as proposed by Eamcharoenying et al. [21] is applied in the Simulink real-time target controller which also executes the position and velocity control loops of the actuator.

Table 1: Actuator performance limits

Peak force	$625\ N$
Continuous stall force	$75.1\ N$
Peak acceleration[2]	$542\ m/s^2$
Maximum speed	$4.7\ m/s$
Armature mass	*2kg*

[2] Based on peak force measurements/rating and an armature mass of 2 kg. Maximum acceleration in hybrid tests will be smaller due to armature friction and reaction forces from the physical substructure.

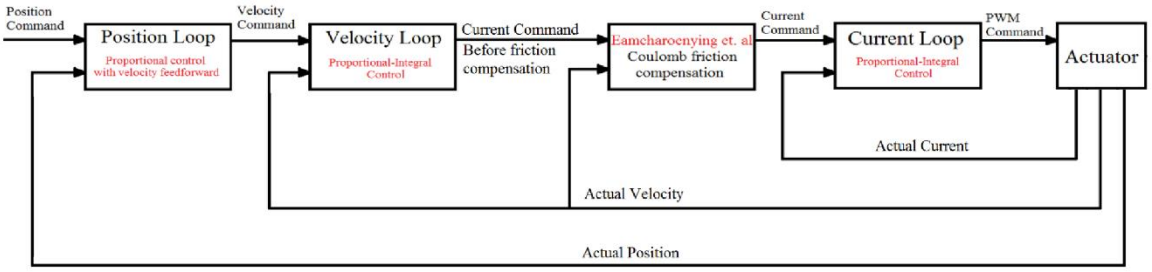

Figure 1: Actuator control system structure [22]

3.2 Hybrid Test

A single degree of freedom mass-spring system with a nonlinear stiffness, as shown in figure 2, is chosen as the emulated system, i.e. the system to be replicated using the hybrid test. The experimental system i.e. the actuator with the physical substructure is shown in figure 3(a). The physical substructure is set up with two linear extension springs positioned perpendicular to the direction of motion of the actuator as shown in figure 3(b) to result in a stiffness profile k_P which increases with displacement x_P , approximating a cubic stiffness. The numerical substructure is a linear system consisting of a mass connected to a linear spring and a viscous damper.

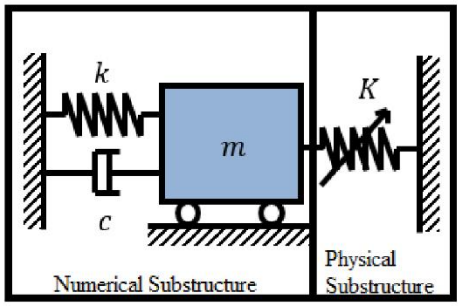

Figure 2: Diagrammatic representation of the emulated system

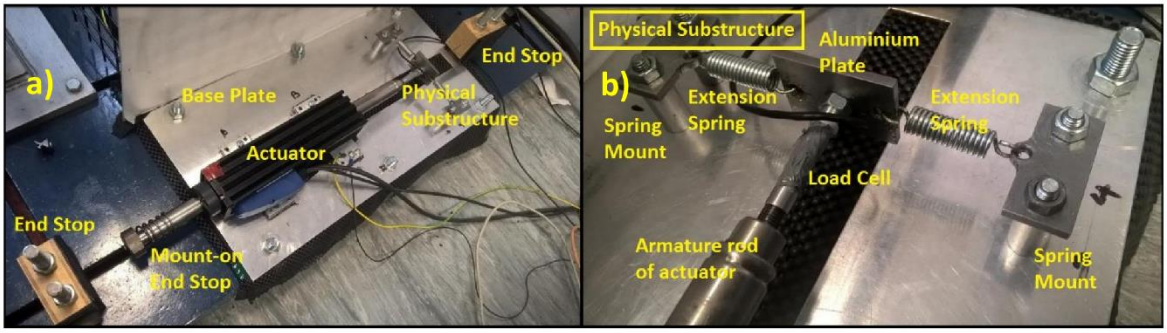

Figure 3: a) Actuator connected to Physical substructure through load cell, b) view zoomed into physical substructure

A block diagram of this hybrid test is illustrated in figure 4. The transfer functions of the numerical substructure, actuator and physical substructure are given by $N(s)$, $T(s)$ and $P(s)$ respectively, where s is the Laplace operator.

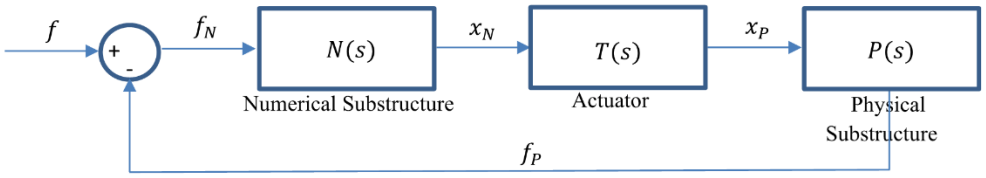

Figure 4: Hybrid test block diagram

The force acting on the numerical substructure f_N is determined by the excitation force f and the physical substructure force f_P. The transfer function of the numerical substructure can be expressed as

$$\frac{x_N}{f_N} = N(s) = \frac{1}{ms^2 + cs + k}$$

where m is the numerical substructure mass, k and c are the spring and damper rates respectively, and x_N is the displacement of the mass. Linearizing the physical substructure stiffness k_P, ($k_P(x_P) = k_P(0)$ for small actuator displacements x_P), the transfer function of the physical substructure relating the numerical substructure displacement x_m to the physical substructure force f_P can be expressed

$$\frac{f_P}{x_N} = P(s)T(s) = k_P(0)T(s)$$

where $T(s)$ is the transfer function of the actuator. The emulated system transfer function can be obtained by combining the numerical and physical substructure transfer functions and assuming a perfect actuator with no lag, i.e. setting $T(s) = 1$. This allows the closed loop transfer function of the emulated system linearized about small displacements relating the numerical substructure force input to the physical substructure force output to be expressed as

$$\frac{f_P}{f} = \frac{1}{\frac{1}{N(s)P(s)T(s)} + 1}$$

$$= \frac{k_P(0)}{ms^2 + cs + k + k_P(0)}$$

The transfer function relating the physical substructure displacement to the physical substructure force is given by

$$\frac{f_P}{x_P} = P(s) = k_P(0)$$

Hence the closed loop transfer function relating the excitation force to the physical substructure displacement, x_P, can be expressed as

$$\frac{x_P}{f} = \frac{1}{ms^2 + cs + k + k_P(0)}$$

The parameters of the emulated system transfer function are given in table 2.

Table 2: Emulated system parameters

Numerical substructure mass (m)	**$1\ kg$**
Numerical substructure damper rate (c)	$10\ Ns/m$
Numerical substructure stiffness (k)	$1\ kN/m$
Linearized physical substructure stiffness ($k_P(0)$)	$2.130\ kN/m$

In order to accurately identify the nonlinear stiffness of the physical substructure, the actuator connected to the springs was tested through full stroke sinusoidally at low frequency (0.1Hz). The measured force f_P is plotted against displacement x_P in figure 5(a). If f_P and x_P are vectors of load cell force in Newtons and physical substructure position in mm, a 3rd order polynomial function can be fitted using a least squares approximation. Only odd coefficients are included in the fitting process, under the assumption the geometry is symmetric, and noting that offset in the position is already accounted for. This results in the following expression relating the physical substructure force in Newtons, to the physical substructure displacement in mm. This equation is used to model the physical substructure in the emulated system. This equation is plotted against experimental data in figure 5(a).

$$f_P = 0.0014{x_P}^3 + 2.13x_P$$

Differentiating this expression enables the tangent stiffness of the physical substructure to be expressed as follows.

$$k_P = \frac{df_P}{dx_P} = 0.0042{x_P}^2 + 2.13$$

The nonlinear variation of the tangent stiffness of the physical substructure is shown in figure 5(b) and is seen to increase more than threefold from its zero-displacement value as amplitudes greater than 30mm are achieved. For small displacements, the stiffness of the physical substructure is approximately 2.13 N/mm.

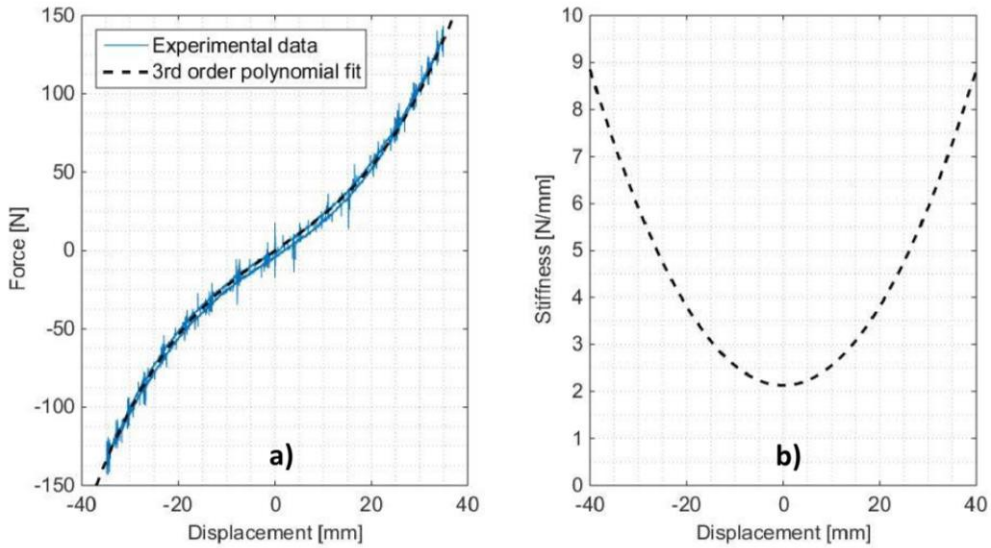

Figure 5: a) Physical substructure force profile, b) Physical substructure identified tangent stiffness

A diagram of the complete hybrid system is shown in figure 6. All components including the load cell, actuator, real-time controllers, substructures, passivity controller and virtual damper are shown.

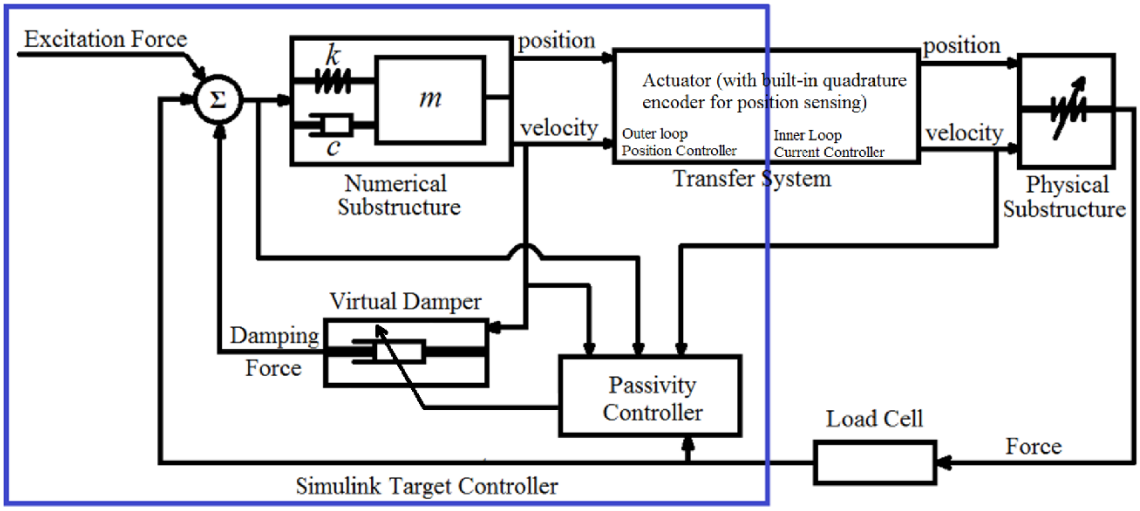

Figure 6: Diagram of passivity-controlled hybrid test system

3.3 Actuator Characterization

To identify the transfer dynamics of the hybrid test in the presence of the physical substructure, the actuator connected to the springs was swept from 0.1 Hz to 50 Hz over a period of 50 s at amplitudes 0.5 mm, 1 mm, 1.5 mm and 2 mm. A fifth order model of the actuator with nonlinear Coulomb friction was identified for preliminary simulation of the hybrid tests. Figure 7 illustrates the model and actuator responses obtained with and without the use of the friction compensator proposed by Eamcharoenying et al. [21].

It can be seen that without friction compensation, the actuator exhibits significant phase lag particularly in the frequency range 0.1-10Hz. This effect is more notable at low amplitudes such as 0.5mm, where the velocities are small and the actuation forces more comparable to the forces of friction. This phase lag is caused by the tendency of the actuator to stick when the driving force is less than the friction force. At high frequency this effect is less significant due to the high actuation forces needed to produce the required acceleration. In all amplitudes shown in figure 7, friction compensation is seen to reduce the actuator phase lag to a noticeable extent. However, complete linearity is not achievable as the phase lag of the actuator swept at 0.5mm is markedly higher than that seen at 2mm even with friction compensation. This is to be expected as real friction in the system is complex and cannot be modelled precisely using a simple Coulomb friction model. Therefore, complete eradication of the spurious effects of nonlinear friction in the following hybrid tests cannot be expected particularly at low amplitudes, although friction compensation is applied in all experiments unless otherwise stated, in order to minimize these effects.

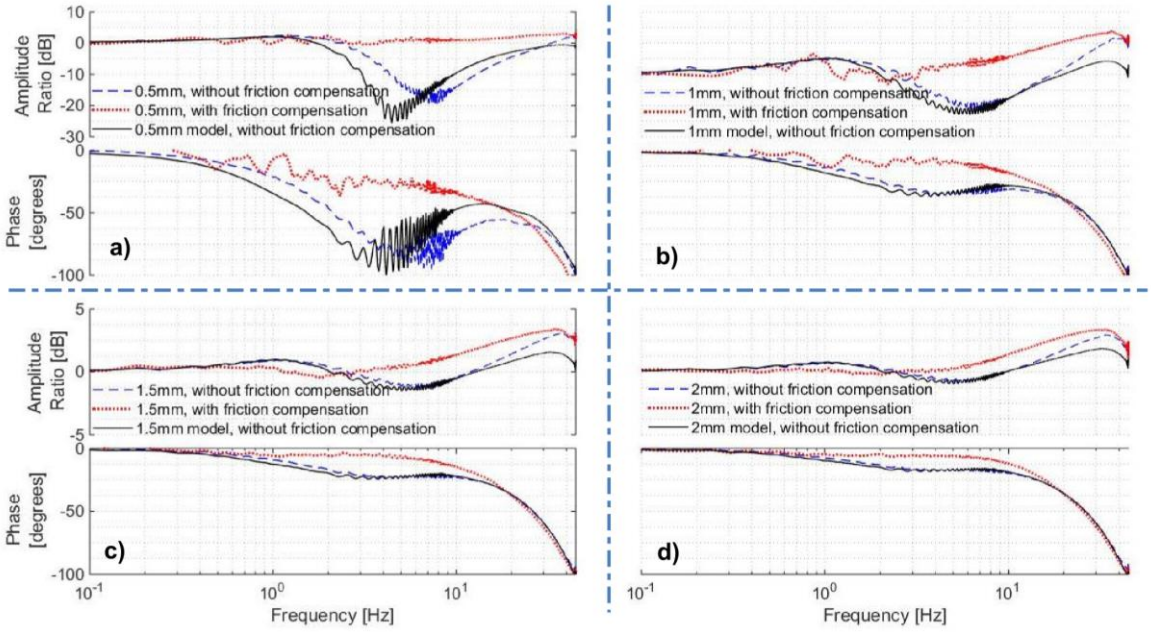

Figure 7: Model and experimental frequency responses of actuator with physical substructure with and without friction compensation at amplitudes: a) 0.5mm, b) 1mm, c) 1.5mm, d) 2mm

4 Simulation results and discussion

This section presents simulation results to show the expected findings of the application of passivity control. A simple delay of 3ms is used to model the transfer system dynamics, following the methods in Peiris et al. [15]. Two types of physical substructures are assessed; firstly, a linear stiffness is used as the physical substructure making the entire hybrid system without passivity control a linear system. Two different stiffness values are used to test how passivity control can affect (i) an otherwise stable system and (ii) an otherwise unstable system. Secondly, the nonlinear stiffening profile seen in Figure 5(a) is tested. The physical substructure stiffness for the linear hybrid tests is denoted as K_L.

Figure 8 shows the frequency response for the linear systems, with and without passivity control. The emulated systems are simulated without a delay and without passivity control. The hybrid system with the 20 kN/m physical substructure without passivity control is unstable and is therefore not shown. The results show how passivity control can both affect tracking and restore stability. At higher frequencies, however, it cannot compensate the delay itself and this is witnessed in the phase discrepancy between the emulated and hybrid system results [15].

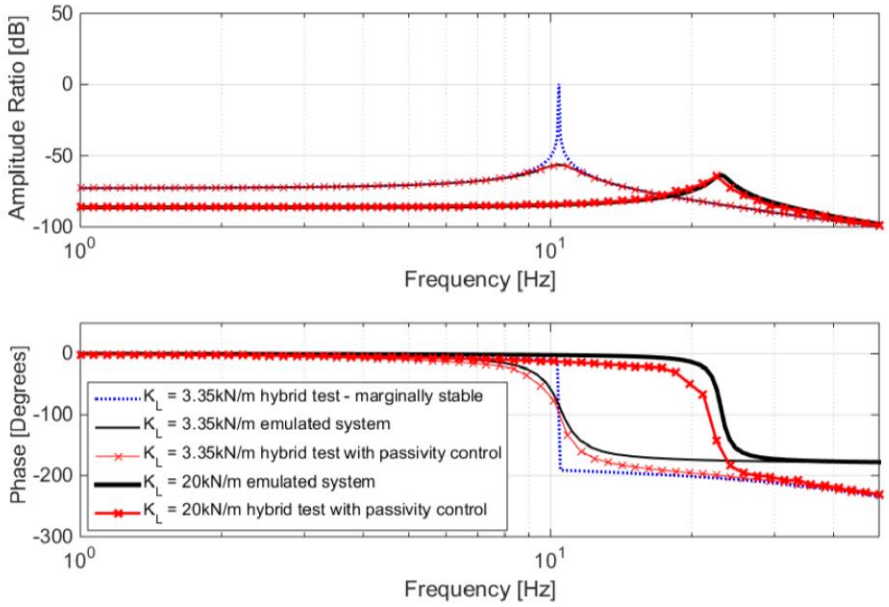

Figure 8: Linear hybrid test responses with passivity control [15]

Step responses for both linear and nonlinear systems are presented in figure 9, illustrating the effectiveness of passivity control in restoring the performance parameters of the hybrid test, most notably the damped response envelope. A phase delay in the compensated response is evident which corroborates the result seen in figure 8 indicating that passivity control does not eliminate the lag itself from a hybrid test, only the adverse effects of that lag on the damping properties [15].

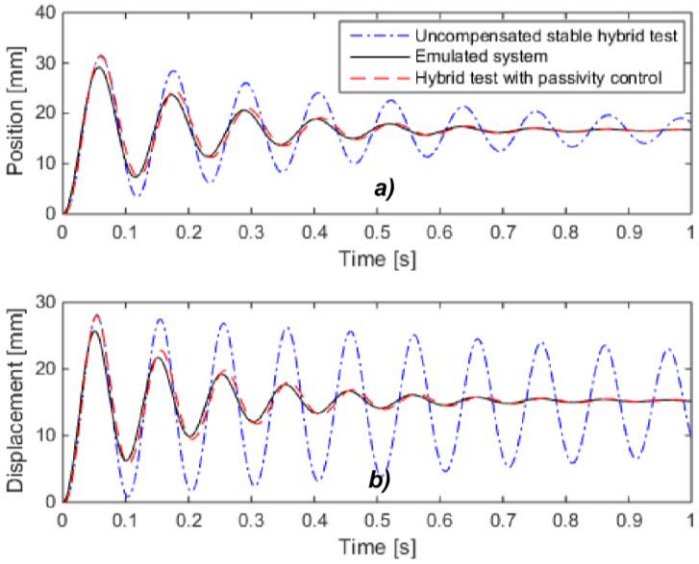

Figure 9: Step responses of hybrid test simulation with a) Linear physical substructure stiffness, b) Cubic physical substructure stiffness [15]

5 Experimental results and discussion

5.1 Stability

This section assesses the effectiveness of passivity control in restoring the stability in the nonlinear real-time hybrid test described in section 3.2. To understand the effect of the physical substructure in the stability of the hybrid test, the nonlinear physical substructure stiffness is linearized to enable the open loop transfer function of the hybrid test to be analysed. The open loop transfer function of the hybrid test is evaluated using the transfer functions of the numerical substructure, actuator and the physical substructure linearized for a range of physical substructure stiffnesses. The delay margin (phase margin divided by the angular frequency) is plotted against physical substructure stiffness as shown in figure 10. It is evident that the hybrid test will be unstable when stiffnesses greater than 2.4N/mm are achieved, as the delay margin becomes negative. Referring to figure 5(b), this corresponds to displacements of greater than 8mm in the cubic stiffening hybrid system presented in section 3.2.

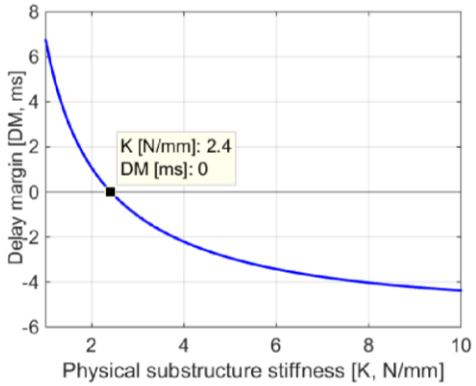

Figure 10: Stability margins of linearized hybrid test for a range of physical substructure stiffnesses

To instigate instability in the nonlinear hybrid test, a force input is required such that physical substructure displacements greater than 8mm are achieved. Figure 11 illustrates the frequency response of the emulated system and the hybrid test system with different passivity controller gains. The force input to the numerical substructure is measured in Newtons whilst the output displacement at the physical substructure is measured in m. The response is obtained by sweeping the system sinusoidally at the numerical substructure from 0.1Hz-50Hz in 50s with an input force amplitude of 15N. The amplitude ratio of the emulated system approaches -55dB near resonance which results in physical substructure displacements greater than 8mm. Hence the hybrid test without any passivity control is unstable and therefore could not be shown in the figure. The application of passivity control has enabled a stable hybrid test response to be achieved. The passivity controller gain can be tuned to vary the amount of virtual damping in the system. Low gains such as 1Ns/Jm are seen to result in the best match of resonant frequency, and hence phase, with respect to the emulated system whilst higher gains such as 25 Ns/Jm result in a better amplitude ratio response at the expense of a lower natural frequency. As before, the lag of the actuator cannot be eliminated using passivity control which only regulates the overall energy flowing in the system. At high frequency, all hybrid test results in figure 11 are seen to indicate similar levels of phase lag. This is because at high frequencies, vibration amplitudes are low due to the dynamics of the numerical substructure. Therefore, the passivity damping forces too will be low making the system behave similarly to that of a stable hybrid test with no other form of compensation.

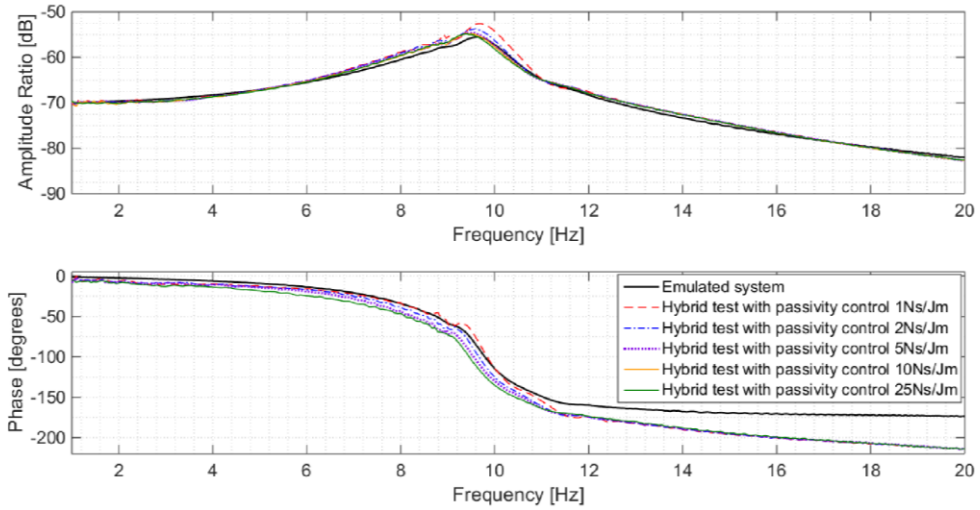

Figure 11: Comparison of the emulated system response with a nominally unstable hybrid test stabilised with passivity control

The excess energy added by the actuator to the hybrid test in this experiment is plotted against time in figure 12. Passivity control works to stabilize a system by enabling a means of eliminating the excess energy added by the actuator through virtual damping action. The emulated system represents a perfectly actuated hybrid test and appears in figure 12 as a line of 0 J.

Figure 12 indicates that the extra energy added by the actuator can be minimized by increasing the gain of the passivity controller, as higher gains result in greater energy dissipation and hence less excess transfer system energy throughout the test. Minimizing the net energy added at the transfer system will enable the closed loop hybrid test to remain stable. This is true regardless of the linearity of the hybrid test thereby making passivity control a good extension to a hybrid system required to operate under a range of stable and unstable conditions in a single experiment. Transitional instability between test conditions can be avoided using passivity control as net energy added is regulated. A higher controller gain will result in a more stable hybrid test. However, the controller gain selected must not be excessively high in order to prevent over damping as this may result in a large phase lag and subsequently high total harmonic distortion and poor tracking. Hence, the controller gain must be chosen adequately high so as to maintain stability but low enough to maintain acceptable tracking performance.

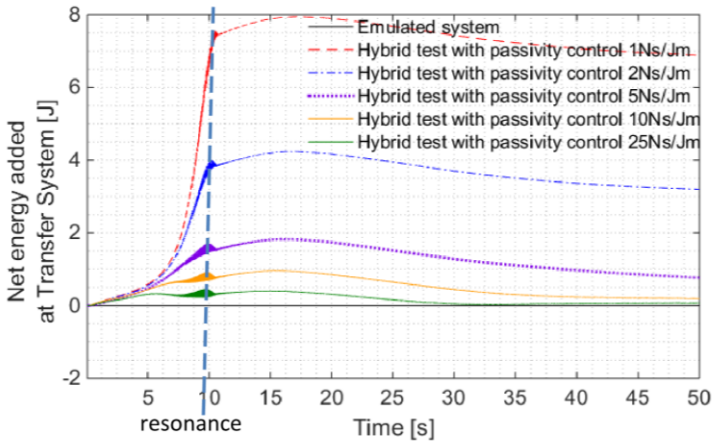

Figure 12: Net energy added to Hybrid test by actuator with different passivity controller gains

5.2 Time domain performance

The performance improvements enabled by passivity control in the time domain can be examined by perturbing the numerical substructure of the hybrid test by a step input in force. The force step is applied to the system such that a steady state change in displacement of 10mm is achieved. The displacement of the physical substructure with and without passivity control is plotted in figure 13 alongside the displacement of the emulated system simulation to the same step input. Without passivity control, the hybrid test results in sustained limit cycle oscillations. However, passivity control is seen to enable the 2% settling time of the hybrid test to be reduced to 0.674s which closely matches the expected settling time of 0.684s seen in the emulated system (error of 1.5%). A small steady state error of 0.2mm is also seen between the emulated system and compensated hybrid system response, attributed to the inaccuracy in modelling the physical substructure stiffness. As such, it is evident that passivity control can be used to adjust the settling time of a system.

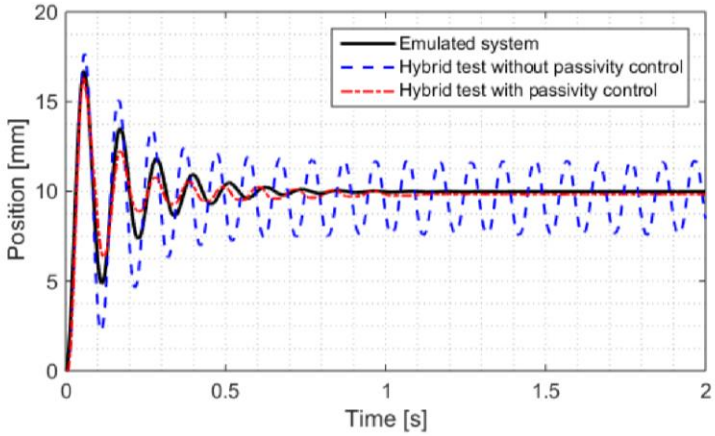

Figure 13: Step response of hybrid test with passivity control

It is important to note that various passivity controller gains lead to different levels of passivity damping which affect the natural frequency and damping ratio of the hybrid system. Figure 14 illustrates the variation in the impulse response of the hybrid test for a range of passivity controller gains. Friction compensation is not applied in the responses shown in order to ensure that the changes seen in the response are solely due to the action of varying amounts of passivity control. It can be seen that higher gains generally lead to a more damped response with oscillations decreasing in magnitude more quickly. However for gains above 1kNs/Jm, significant nonlinear distortion is seen in the output. This is to be expected as higher gains result in higher and more volatile virtual damper rates at the passivity controller. The period of the response is seen to elongate when higher gains are used. As before, stability of the closed loop hybrid test is improved through passivity control, while matching the damping properties requires careful tuning, and the frequency and distortion of the response are adversely affected. The optimal controller gain for a system will therefore need to be found on a case-by-case basis.

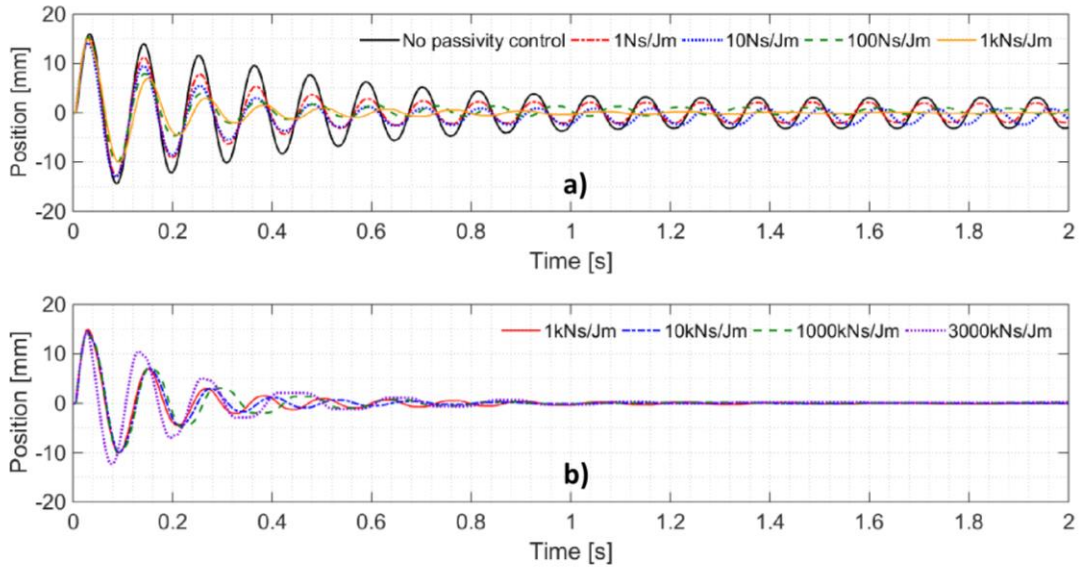

Figure 14: Hybrid test impulse response with different passivity controller gains (a) low-moderate gains, (b) moderate-excessive gains

5.3 Passivity control compared with model-based compensation

In this section the performance of a state-of-the-art model-based compensator in a hybrid test will be compared with that of passivity control at low and high frequency. The model-based compensator used is a 2nd order inverted actuator model, whose design is detailed in section 2.3.

Figure 15 illustrates the response of the identified linear transfer function model against that of the actuator's response with the physical substructure. The second order lag is seen to produce a good match with that of the actuator's amplitude ratio and phase response throughout the frequencies tested, with the largest amplitude and phase error being less than 2dB and 6 degrees respectively. The compensated hybrid system is tested with sine wave inputs to the numerical substructure at low and high frequency and the output of the physical substructure is measured and plotted in figure 16. The response of the emulated system is also shown for comparison. Three types of compensation are used; friction compensation, 2nd order lag compensation with friction compensation, and passivity control without friction compensation.

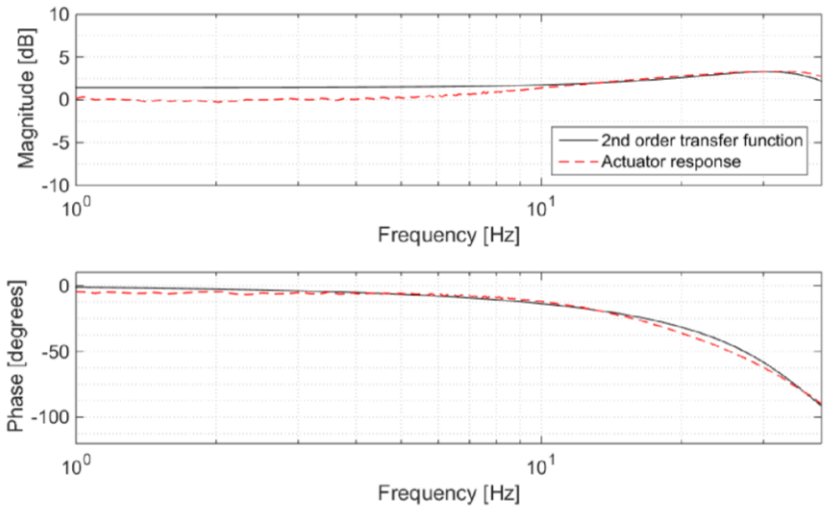

Figure 15: Actuator response plotted against that of the identified 2nd order transfer function model

Figure 16(a) illustrates that at 0.1Hz, the uncompensated hybrid test system produces limit cycles at its resonant frequency, away from the driving frequency. This is caused by the dominance of friction at low velocities. At low velocities, the forces of friction are comparable in size to the driving forces of the actuator which results in the actuator exhibiting a significant phase lag at low amplitude, seen in figure 7, eroding stability margins. At high frequency as shown in figure 16(b), this limit cycle is not seen due to the dominance of large actuation forces over friction.

Friction compensation is seen to result in a 24.5% reduction in the amplitude of the limit cycle compared with that of the uncompensated hybrid test in figure 16(a). Owing to its simplicity allowing for easy implementation, it is unable to accurately compensate the friction and completely restore linearity as described in section 3.3. The addition of the 2nd order model-based compensator is seen to improve the response further with the limit cycle amplitude reducing by 64% compared to the uncompensated case. This is achieved through reducing the lag to improve stability margins. Passivity control on the other hand is seen to almost completely cancel the spurious oscillation in the response with the limit cycle amplitude being reduced by 95%. This enables the physical substructure of the hybrid test to follow that of the emulated system with great precision. At high frequency in figure 16(b) however, the passivity-controlled response exhibits the anticipated phase lag with respect to the emulated system whilst the model-based compensator successfully mitigates the lag and results in a response which tracks that of the emulated system more accurately. A significant advantage of the passivity controller over the model-based compensator, however, lies in its simplicity and universal application, obviating the need for characterisation of the transfer system. The friction compensated response at high frequency in figure 16(b) is similar to that of the uncompensated system response at high frequency since actuation forces dominate over friction when velocities are high.

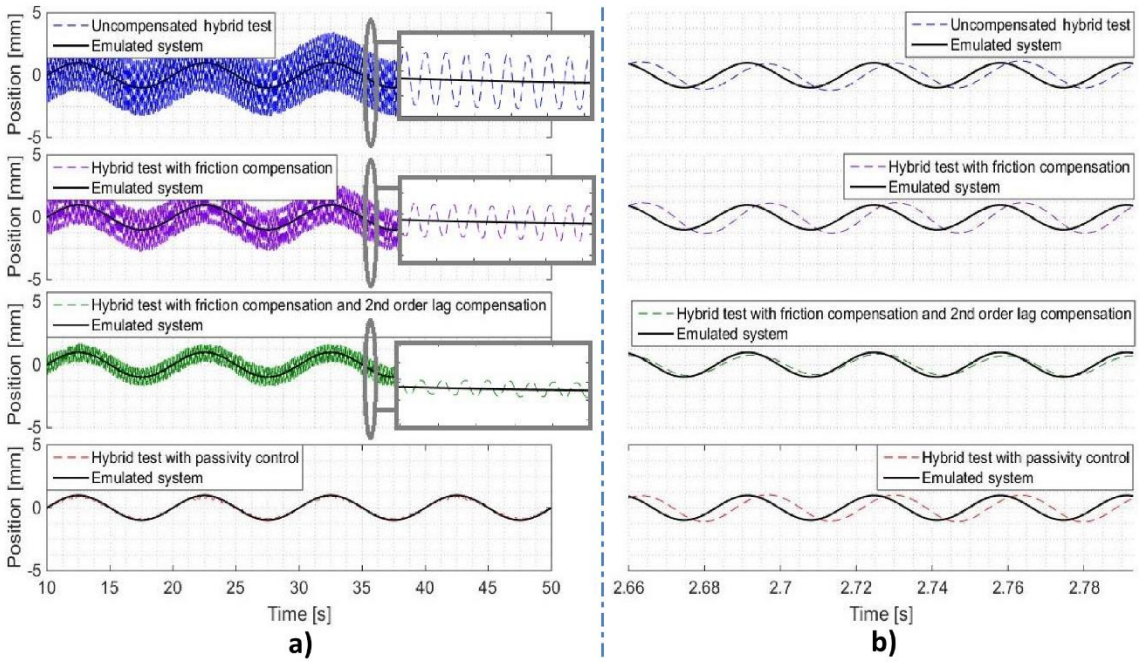

Figure 16: Hybrid test response with passivity control, friction compensation and model-based compensation at: a) Low frequency (0.1Hz), b) High frequency (30Hz)

Importantly, the model based compensation is effective at reducing phase lag between numerical and physical domains but struggles to adequately compensate for the limit cycles arising from the nonlinearity in the actuator, while the passivity controller is effective at suppressing the spurious limit cycles but cannot remove the inherent phase lag introduced by the transfer system. Thus, the two techniques are complimentary. Figure 17 illustrates the hybrid test responses obtained when combining the two methods. An excitation amplitude of 5mm is used and the responses are shown together with those of the emulated system. The response with passivity control and lag compensation applied together is seen to provide the benefits of both schemes; figures 17a and 17b illustrate the elimination of limit cycle oscillation due to passivity control whilst figure 17c indicates tracking improvements due to the lag compensation at high frequency. A phase lag of 35.3^0 is seen in the response without lag compensation, whilst the response with lag compensation and the response with passivity control and lag compensation exhibit reduced phase lags of 13.7^0 in figure 17c. As such, it is evident that the use of passivity control with more conventional model based compensation can provide the user with a system maintaining good stability and tracking simultaneously.

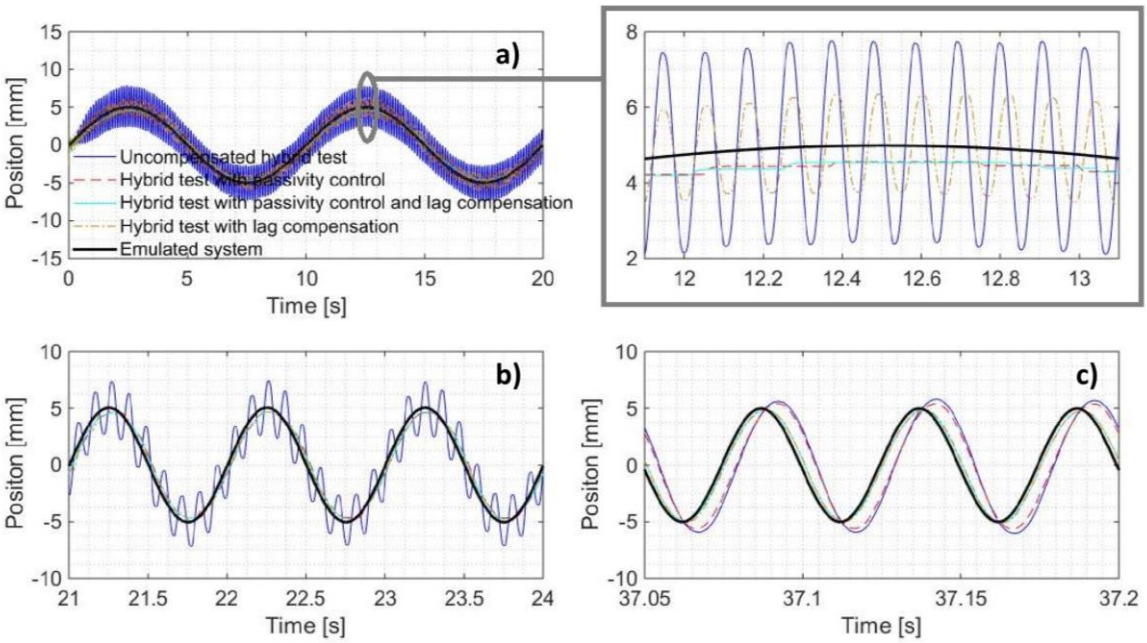

Figure 17: Hybrid test responses with model based compensation and passivity control at: a) 0.1Hz, b) 1Hz, c) 20Hz

6 Conclusion

This paper has demonstrated the first application of passivity control to the stabilisation of a real-time hybrid test. The method was found to successfully restore the stability of a hybrid test in the presence of two distinct types of destabilising nonlinearities: instability at high amplitudes due to stiffening of the physical substructure, and limit cycles at low amplitudes caused by friction in the actuator itself. In the latter case it was found that passivity control performed better than model-based methods or simple Coulomb friction compensation alone. Passivity control does not compensate lag directly and must be used to complement other methods where high-fidelity tracking is needed at high frequencies. However, it is extremely simple to implement, requiring no characterisation of the actuator dynamics and only tuning of a single gain parameter, so it is anticipated that it will find widespread application where the higher frequency dynamics are less critical to the test and stability is the main requirement. In addition, it has been shown to be valuable when used in conjunction with lag-compensation schemes, where it can compensate for model uncertainties and stabilise tests throughout transient events such as stiff impacts. This method is expected to play a key role in the development of the next generation of hybrid test equipment, in turn in facilitating rapid development cycles in industrial design.

Acknowledgements

This work has been supported through funding from the Engineering and Physical Sciences Research Council, grant reference EP/N032829/1.

References

[1] A. R. Plummer, “Model-in-the-Loop Testing,” *Proc. Inst. Mech. Eng. Part I J. Syst. Control Eng.*, vol. 220, no. 3, pp. 183–199, 2006.

[2] A. M. Reinhorn, M. V. Sivaselvan, Z. Liang, and X. Shao, “Real-time dynamic hybrid testing of structural systems,” *13th World Conference on Earthquake Engineering*, no. 1644, pp. 1–13, 2004.

[3] H. Fathy, Z. Filipi, J. Hagena and J. Stein, "Review of hardware-in-the-loop simulation and its prospects in the automotive area", *Proc. SPIE 6228, Modeling and Simulation for Military Applications*, vol. 62280, 2006. [Accessed 14 February 2019].

[4] M. Bolien, P. Iravani, and J. du Bois, “Robotic Pseudo-Dynamic Testing (RPsDT) of Contact-Impact Scenarios,” *Towards Autonomous Robotic Systems*, vol. 9287, pp. 50–55, 2015.

[5] T. Börner and M. Alam, “Real time hybrid modeling for ocean wave energy converters,” *Renew. Sustain. Energy Rev.*, vol. 43, pp. 784–795, 2015.

[6] "SMMT MOTOR INDUSTRY FACTS 2017", *Smmt.co.uk*, 2017. [Online]. Available: https://www.smmt.co.uk/wp-content/uploads/sites/2/SMMT-Motor-Industry-Facts-2017_online_May.pdf. [Accessed: 08- Jun- 2018].

[7] "INDUSTRY FACTS AND FIGURES: A GUIDE TO THE UK’S AEROSPACE, DEFENCE, SECURITY & SPACE SECTORS", *adsgroup.org.uk*, 2017. [Online]. Available: https://www.adsgroup.org.uk/wp-content/uploads/sites/21/2017/06/ADS-Annual-Facts-2017.pdf. [Accessed: 08- Jun- 2018].

[8] "HIL Testing Reduces CompactRIO Control System Development Cost", Instrumentation Newsletter, *National Instruments*, Q1, 2010. Published online 11 April 2011: http://www.ni.com/newsletter/51000/en/. [Accessed: 27- Nov- 2018].

[9] Ebert, C., Jones, C., Embedded Software: Facts, Figures, and Future, Computer, 2009, Vol. 42(4), pp. 42-52

[10] T. Horiuchi, M. Inoue, T. Konno and Y. Namita, "Real-time hybrid experimental system with actuator delay compensation and its application to a piping system with energy absorber", *Earthquake Engineering & Structural Dynamics*, vol. 28, no. 10, pp. 1121-1141, 1999.

[11] M. Wallace, D. Wagg and S. Neild, "An adaptive polynomial based forward prediction algorithm for multi-actuator real-time dynamic substructuring", *Proceedings of the Royal Society A: Mathematical, Physical and Engineering Sciences*, vol. 461, no. 2064, pp. 3807-3826, 2005.

[12] M. Wallace, D. Wagg, S. Neild, P. Bunniss, N. Lieven and A. Crewe, "Testing coupled rotor blade–lag damper vibration using real-time dynamic substructuring", *Journal of Sound and Vibration*, vol. 307, no. 3-5, pp. 737-754, 2007.

[13] J. du Bois, B. Titurus, and N. Lieven, “Transfer Dynamics Cancellation in Real-Time Dynamic Sub- structuring,” *Proc. ISMA 2010*, pp. 1891–1914, 2010.

[14] G. Ou, A. Ozdagli, S. Dyke and B. Wu, "Robust integrated actuator control: experimental verification and real-time hybrid-simulation implementation", *Earthquake Engineering & Structural Dynamics*, vol. 44, no. 3, pp. 441-460, 2014.

[15] L. D. H. Peiris, A. R. Plummer, and J. L. Du Bois, “Passivity Control in Real-Time Hybrid Testing,” in *2018 UKACC 12th International Conference on Control (CONTROL)*, 2018, pp. 317–322.

[16] W. Haddad and V. Chellaboina, *Nonlinear dynamical systems and control*. Princeton: Princeton University Press, 2008, p. 351.

[17] M. Zefran, F. Bullo, and M. Stein, “A notion of passivity for hybrid systems,” in *Proceedings of the 40th IEEE Conference on Decision and Control (Cat. No.01CH37228)*, 2001, vol. 1, pp. 768–773 vol.1.

[18] S. Atashzar, M. Shahbazi, M. Tavakoli and R. Patel, "A Passivity-Based Approach for Stable Patient–Robot Interaction in Haptics-Enabled Rehabilitation Systems: Modulated Time-Domain Passivity Control", *IEEE Transactions on Control Systems Technology*, vol. 25, no. 3, pp. 991-1006, 2017.

[19] D. Sun, F. Naghdy and H. Du, "Time domain passivity control of time-delayed bilateral telerobotics with prescribed performance", *Nonlinear Dynamics*, vol. 87, no. 2, pp. 1253-1270, 2016.

[20] J. Zhang and C. Cheah, "Passivity and Stability of Human–Robot Interaction Control for Upper-Limb Rehabilitation Robots", *IEEE Transactions on Robotics*, vol. 31, no. 2, pp. 233-245, 2015.

[21] P. Eamcharoenying, A. Hillis and J. Darling, "Friction compensation using Coulomb friction model with zero velocity crossing estimator for a force controlled model in the loop suspension test rig", *Proceedings of the Institution of Mechanical Engineers, Part C: Journal of Mechanical Engineering Science*, vol. 230, no. 12, pp. 2028-2045, 2015.

[22] *Xenus XTL™ User Guide*, 3rd ed. Copley Controls Corp, 2008.

4.2 Summary

Experimental results have been used to validate the usefulness of passivity control in nonlinear real-time hybrid tests. The following conclusions have been deduced.

1) Passivity control successfully maintains the stability of real-time hybrid tests by constraining the net energy added to the system by the actuator.
2) Passivity control alone is unable to alleviate the lag introduced by the actuator dynamics.
3) Nonlinear artefacts caused by the actuator are dealt with more effectively using passivity control than conventional linear model-based methods.
4) Passivity control used together with 2^{nd} order linear model-based lag compensation enables the benefits of both schemes to be acquired; the versatile stability of passivity control in the presence of actuator nonlinearity and the high frequency tracking improvements offered by lag compensation.
5) The amount of passivity control required for a test is dependent on the energy of the system and hence the operating conditions.
6) Excessive passivity controller gains tend to overdamp the response leading to unwanted nonlinear distortion.

Passivity control shines in its ability to achieve good stability of hybrid tests. Whilst this may lead to better tracking, targeted improvements in tracking cannot be achieved using passivity control alone unless design performance criteria of the system are available to aid the controller tuning process. However, used together with state-of-the-art compensation methods, passivity control has been seen to enable good stability and tracking to be achieved simultaneously. This makes passivity control a powerful tool in real-time hybrid tests that see highly nonlinear and/or discontinuous events such as impact scenarios which trigger a change in the system parameters that would generally cause linear model-based methods to fail. Most real-world applications of hybrid testing are bound to have a degree of nonlinearity that may not be replicable using linear model-based methods. Passivity control therefore acts to bridge the gap between hybrid testing and highly nonlinear systems which would encourage more nonlinear applications of hybrid testing, opening the door to a range of new test systems.

The key drawback of passivity control however, has been identified as the high dependency of the response on the operating conditions of the system and the possibility of introducing unwanted nonlinear distortion in the response. Moreover, there is no basis for selecting the passivity controller gain. A modified passivity control scheme is developed in the next chapter to address these limitations.

Chapter 5

Normalised Passivity Control

5.1 Context

Chapters 3 and 4 brought to light a key limitation of the passivity control scheme being the dependency of the response on the energy of the system. As the passivity damper rate was directly proportional to the energy error between substructures, high amplitude tests were inclined to have greater passivity damping than low amplitude tests for a fixed passivity controller gain. Moreover, with the passivity control scheme presented in chapters 3 and 4, the substructure energy error was calculated by integrating the substructure power error over time. As the controller acts on this variable to determine the damper rate required, it is intrinsically acting on the present and past response of the system since the commencement of the hybrid test.

However, it is more beneficial to have the controller be less sensitive to the history of the response and more sensitive to the current response. Moreover, some form of normalization of the controller error signal is required to ensure constancy over a range of operating conditions – the use of a single variable such as power or energy whose magnitude is dependent on the velocity of the system will result in low versatility. With these key requirements, the structure of the passivity controller was redefined to form a new and improved control scheme which is presented in the below publication. Simulation and experimental studies were carried out to validate its effectiveness whilst comparing its performance with that of the preceding passivity control scheme introduced above, where appropriate.

The damping properties of the new controller were assessed while observing the effect of passivity control on the total harmonic distortion of the response. The total harmonic distortion (THD) is a measure of the harmonic content of a waveform with respect to its fundamental [56]. The higher the THD of a signal, the more it deviates from that of a single frequency sinusoid. Thus, the THD of a response is a reliable measure of its nonlinearity. The THD is quantified by comparing the amplitude of the harmonics to that of the fundamental mode and can be expressed by the general expression in equation (1) (from [56]), where I_n is the amplitude of harmonic n.

$$THD = \frac{\sqrt{\sum_{n=2}^{\infty} {I_n}^2}}{I_1} \tag{1}$$

In this study, the total harmonic distortion was expressed in decibels and was evaluated using the fundamental frequency and the first five harmonics identified using a periodogram on the waveform as done in [57]. Thus, equation (1) is transformed into equation (2) depicted below.

$$THD_{dB} = 10 \log_{10} \left(\frac{\sqrt{{I_2}^2 + {I_3}^2 + {I_4}^2 + {I_5}^2 + {I_6}^2}}{I_1} \right) \tag{2}$$

This declaration concerns the article entitled:									
Normalised Passivity Control for Robust Tuning in Real-time Hybrid Tests									
Publication status (tick one)									
Draft manuscript		**Submitted**		**In review**	✓	**Accepted**		**Published**	
Publication details (reference)	L. D. H. Peiris, A. Plummer, and J. du Bois, "Normalised Passivity Control for Robust Tuning in Real-time Hybrid Tests," *Int. J. Robust Nonlinear Control*, 2020.								
Copyright status (tick the appropriate statement)									
I hold the copyright for this material	✓	Copyright is retained by the publisher, but I have been given permission to replicate the material here							
Candidate's contribution to the paper (provide details, and also indicate as a percentage)	**The candidate contributed to / considerably contributed to / predominantly executed the…** **Formulation of ideas:** Limitations of preceding passivity controller and motivation for new scheme discussed with supervisor Dr. Jonathan du Bois. Candidate's contribution (65%). Idea to assess controller response over a range of gains and natural frequencies by Dr. Jonathan du Bois. **Design of methodology:** Formulation of new passivity controller design based on discussions with supervisor. Candidate's contribution (65%). **Experimental work:** Selection of tests with supervisor Dr. Jonathan du Bois. Candidate's contribution (60%). Implementation of control scheme, modelling and simulation and all experimental work carried out solely by the candidate (100%). **Presentation of data in journal format:** Selection of results for presentation upon discussions with supervisor Dr. Jonathan du Bois. Candidate's contribution (60%). Paper written by candidate, reviewed and corrected by supervisors Prof. Andrew Plummer and Dr. Jonathan du Bois. Overall contribution of candidate (70%).								
Statement from Candidate	This paper reports on original research I conducted during the period of my Higher Degree by Research candidature.								
Signed	L DH Peiris					**Date**	24/09/2019		

Paper Three: Normalised Passivity Control for Robust Tuning in Real-time Hybrid Tests

Normalised Passivity Control for Robust Tuning in Real-time Hybrid Tests

L.D. Hashan Peiris[1], Andrew R. Plummer, Jonathan L. du Bois

Department of Mechanical Engineering, University of Bath, Claverton Down Rd. Bath, BA2 7AY

Abstract

Real-time hybrid testing involves the separation of a system into an experimental component and a numerically simulated substructure which are coupled and run together. The coupling between substructures is achieved using actuators and force sensors, comprising the transfer system. Close synchronisation is required between substructures for reliable hybrid testing. However, actuator lag may cause tracking errors or instability in hybrid tests. Existing lag compensation schemes require identification of the coupled dynamics of the transfer system and experimental component, and most struggle to effectively compensate highly nonlinear systems. Passivity control enables hybrid test stability to be maintained without system identification or assumptions about linearity. Yet, the tuning of existing passivity controllers is sensitive to both the system being tested and the amplitude and frequency range excited. This paper presents a new, normalized passivity controller which behaves well across a much broader range of operating conditions once tuned for a single test scenario. The proposed approach uses a virtual damping element on the numerical substructure to dissipate spurious power injected by the actuator into the system, based on the ratio of net power output to mean power throughput. The scheme has been shown to result in identical performance for a linear hybrid test with a range of step excitations from 0.5mm up to 500mm. Moreover, a single optimal gain is found for a hybrid test whose natural frequency varies systematically from 0.1Hz to 50Hz. The proposed method can be used to improve test stability and fidelity in isolation or alongside other compensation schemes to further improve performance. Given the guarantees it can provide on stability and therefore safety, and given its ease of implementation, and given that it can complement almost any other compensation scheme, it is not implausible that it will become the most widely used compensation scheme in practical applications.

Keywords: Mechanical Systems; Real-time Hybrid Test; Passivity; Vibration and Dynamics; Model-in-the-loop-testing.

Nomenclature

b – Passivity controller gain
c_D – Passivity damper rate
c_n – Numerical substructure damper rate
f – Hybrid test excitation force
f_N – Numerical substructure force
f_P – Physical substructure force
k – Physical substructure stiffness
K – Steady state gain
k_n – Numerical substructure stiffness
m_n – Numerical substructure mass

[1] Corresponding author. Email address: L.D.H.Peiris@bath.ac.uk, Address: Department of Mechanical Engineering, University of Bath, Claverton Down Rd. Bath, BA2 7AY

$N(s)$ – Numerical substructure transfer function
p_E – Transfer system spurious power injection
p_N – Numerical substructure power
p_P – Physical substructure power
p_S – Mean substructure power variable
p_T – Mean power flow through transfer system
$P(s)$ – Physical substructure transfer function
s – Laplace operator
t_E – Net power filter time constant
t_S – Mean power filter time constant
$T(s)$ – Actuator transfer function
$T_E(s)$ – Power output filter
$T_S(s)$ – Power throughput filter
x_P – Physical substructure/actuator displacement
$\dot{x}_P$ – Physical substructure/actuator velocity
$\dot{x}_N$ – Numerical substructure velocity
τ – Actuator delay
ω_n – Emulated system natural frequency
ζ – Emulated system damping ratio

1 Introduction

Real-time Hybrid Testing (RtHT) involves separating a system into a physical substructure to be tested experimentally, and a simulated numerical substructure. These two substructures are coupled and run in parallel using actuators and sensors to transfer forces and motion between substructures in real-time. This method aims to provide the benefits of both experimentation and computer simulations. Fathy et al. [1] review the technique in the context of automotive testing, describing a variety of benefits: There are significantly fewer hardware requirements with RtHT when compared to a full experimental test, as the complete system does not have to be set up. This leads to substantial cost savings whilst enabling rapid prototyping, and also allows for component testing at an early stage before the complete system has been manufactured. Destructive events can also be simulated using RtHT without damaging real hardware, which is particularly useful in the automotive sector to test scenarios such as vehicle accidents [1]. Furthermore, the scheme offers advantages over fully simulated tests by enabling the testing of physical components whose dynamics are not fully understood or modelled.

Further advantages of RtHT are detailed by Plummer [2]: Hybrid testing enables extreme environmental conditions to be simulated enabling systems to be tested under a range of operating conditions that cannot be physically emulated in a laboratory. Moreover, parameters of the numerical substructure are easily adjustable enabling several alternative configurations whilst test systems are made much less complex with the reduced complexity of physical test apparatus. Real-time hybrid testing is rapidly gaining recognition in a number of engineering disciplines such as testing of electric powertrains in the automotive sector [3], development of microgrid power management systems in the power distribution industry [4], testing of building structures in the field of civil engineering [5] and testing of rotorcraft vehicles in the aerospace sector [6].

However, a key limitation of real-time hybrid testing lies in the dynamics of the controllers and actuators used to synchronise the motion of the physical substructure with that of the numerical substructure. Actuator lag results in tracking errors, leading to an inaccurate emulation of the true system. In some cases the system can even become unstable. Conventional methods of mitigating actuator lag involve the identification of a linear model of actuator dynamics which is then inverted and applied as a feed-forward or open-loop outer controller in the real-time hybrid test. For example, Wallace et al. [7] identify actuator dynamics as a first order linear transfer function which is inverted to compensate lag in a real-time hybrid test of a rotor blade coupled to a lag damper. du Bois et al. [8] utilize 1st and 2nd order process models (i.e. polynomial transfer functions coupled with a delay) for inversion and compensator design, where it is shown that higher order process models can be more

effective in capturing the actuator dynamics accurately compared to lower order process models or pure transfer function or delay models. Another common scheme is to use forward predictive delay compensation techniques to predict the desired actuator response to mitigate delay. Forward predictive algorithms such as those proposed by Horiuchi et al. [9], Darby et al. [10] and Ahmadizadeh et al. [11] are used in real-time hybrid testing. Tang et al. [12] review the performance of these schemes in hybrid tests actuated by a shaker table, illustrating the development of delay compensation schemes in hybrid testing over the years. The authors of [12] conclude that performance gains through the use of delay compensation are confined to a narrow low frequency band where transfer system amplitude ratio deviations are small, with stability and accuracy experiencing deteriorations as frequencies rise.

In many hybrid tests, actuator dynamics may be difficult to characterise using a linear model. This could be due to the actuator behaviour being dependant on the physical substructure (whose dynamics are unknown), or due to inherent nonlinearity in the actuator due to effects such as stiction. In such cases, linear model-based methods would be unable to accurately compensate for actuator dynamics. In certain cases such as impacts, discontinuities or abrupt parametric changes in the physical system, drastic changes in actuator behaviour may result in the hybrid test becoming unstable. In such cases there exists the need for a compensation scheme that allows for both variability and nonlinearity in the combined actuator-physical substructure system. An approach that has been investigated by the present authors is the use of passivity control, to ensure stability and improve the fidelity of the simulations [13]. Passivity control is attractive because it does not require knowledge of the actuator dynamics, making it widely applicable.

In a passive system, the energy supplied always exceeds the energy output from the system, with the difference being accounted for by the energy dissipated in the system [14]. Passivity control is a scheme of regulating power and energy flow and is widely used in the teleoperation field to maintain stability between master and slave manipulators. In Coelho et al. [15], the passivity controller is described as measuring the energy flow in the system and adaptively dissipating energy by acting as a damper to ensure passivity. Chen et al. [16], apply passivity control to a multilateral teleoperation system consisting of two masters and slaves. The authors utilize a passivity observer which monitors the net energy flow into the system which activates the passivity controller, a time varying damping element, to dissipate excess energy when the energy flow becomes negative. The authors conclude that tracking performance on the slave side is not guaranteed, however, it is shown that the slave is able to follow the demands of the master manipulator even in the presence of delays as high as 0.8s. In real-time hybrid testing, the passivity control is applied to the transfer system (actuators, controllers and sensors) to ensure these remain passive and do not contribute spurious energy which can lead to instability. In real-time hybrid testing, passivity control can be used in isolation or to complement existing delay- and lag-mitigation strategies for even better performance.

One difficulty that has been identified when using passivity control with a wide range of forces and motion amplitudes is that the tuning of the controller is heavily dependent on the absolute magnitudes of the power flow between the substructures. A tuning that will work well at a low response amplitudes may produce overzealous damping at higher amplitudes, while one that works well at high amplitudes may allow the development of spurious limit cycles at lower amplitudes that mask the relevant system response. In this paper, the net power output is normalised with respect to the power throughput in an effort to broaden the useful test envelope of a given passivity controller tuning. Simulations and experiments are used to investigate the performance of this new configuration. Section 2 describes the structure of the passivity controller and the method of implementation. Section 3 presents simulated hybrid test results where the benefits of normalized passivity control over conventional passivity control for hybrid testing are highlighted. Experimental results are presented in section 4, where the effects of nonlinearity are examined, and conclusions are given in section 5.

2 Method

The three subsystems that make up a real-time hybrid test are the numerical and physical substructures and the transfer system. The numerical and physical substructures are representative of the true/emulated system and the transfer system is a foreign subsystem included only to link the numerical and physical parts of the test. The transfer system should be designed to influence the dynamics of the system as little as possible, in particular because spurious power contributed or dissipated by the actuators in this subsystem will result in deviations in dynamics from the true/emulated system and, critically, can result in instability. The passivity controller acts on the transfer system to dissipate surplus power in order to maintain stability. A passive transfer system will be one which does not output more energy into the physical substructure than the energy input to it from the numerical substructure or vice versa. Achieving this is the main purpose of the passivity controller. Figure 1 illustrates a generic hybrid test with the aforementioned subsystems and power flow illustrated. The passivity controller utilizing a variable rate virtual damper to dissipate energy in the hybrid test is also shown.

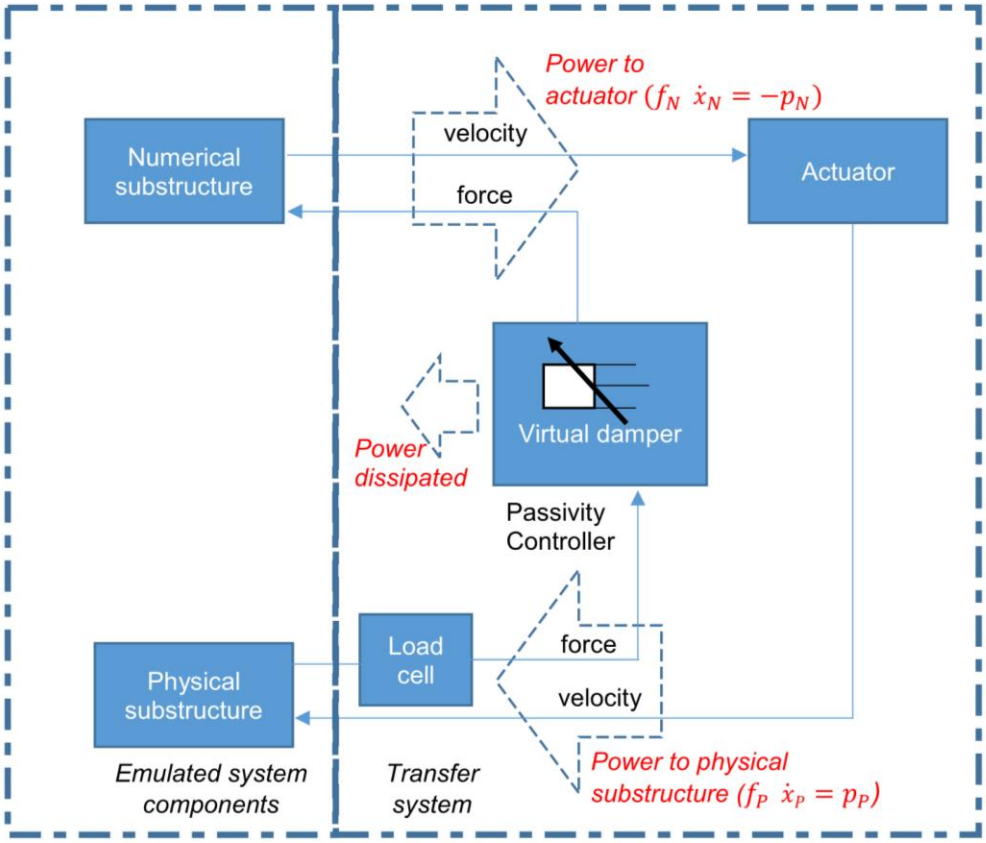

Figure 1: Structure of closed loop hybrid test with passivity control. The hollow arrows indicate the power flow within the system

Power in the hybrid test can be evaluated using the product of force and velocity. The power p_P flowing into the physical substructure from the transfer system can therefore be expressed as

$$p_P = f_P\ \dot{x}_P \tag{1}$$

where f_P and $\dot{x}_P$ are the measured physical substructure force and velocity respectively. The positive sign convention is used to indicate the power flow into a substructure from the transfer system whilst negative powers represent power outputs from the physical/numerical substructures and into the

transfer system. The power flow p_N flowing into the numerical substructure and out of the transfer system is thus

$$p_N = -f_N \, \dot{x}_N \tag{2}$$

where the numerical substructure force f_N is effectively the reaction force corresponding with f_P, acting in the opposite direction, and $\dot{x}_N$ is the velocity of the numerical substructure degree of freedom (DOF) with the same sign convention as the physical substructure. The net power flow from the transfer system into the emulated system, comprised of physical and numerical substructures, is then given by

$$p_E = p_P + p_N \tag{3}$$

This is the spurious power contributed by the transfer system to the hybrid test. In the emulated system, this quantity would be zero indicating a passive system. Any deviation from zero corresponds to a lack in test fidelity, but most importantly a positive value of p_E can erode stability margins leading to dangerous test conditions. A common passivity control configuration is to use the quantity p_E directly to determine the damping coefficient of the virtual damper. This arrangement has the disadvantage of being over-zealous at high response amplitudes and ineffective at low amplitudes. While both these scenarios are better than an unbounded instability, they cause unnecessary loss in fidelity in the form of over-damped response at high amplitude and spurious limit cycles at low amplitudes. To mitigate these effects, a normalized measure of power flow is proposed here, with respect to the mean power flowing through the transfer system:

$$p_T = \frac{|p_P - p_N|}{2}$$

To clean up the algorithm, the factor of 2 can be omitted to give

$$p_S = |p_P - p_N| \tag{4}$$

Using the instantaneous power output and power throughput of the transfer system to control the damper coefficient can lead to wild fluctuations, in particular where the normalising quantity p_S is close to zero. In any case, the desired normalising quantity is not the instantaneous power throughput but something more akin to the RMS value. To achieve this effect, the power measurements are subjected to low pass filtering:

$$T_E(s) = \frac{1}{t_E s + 1} \tag{5}$$

$$T_S(s) = \frac{1}{t_S s + 1} \tag{6}$$

where t_E and t_S are the time constants of the filters, the effects of which will be investigated in Section 3. The passivity controller gain, given by b, is a positive real number set by the user, which scales the filtered, normalized net power to output the passivity damper rate applied at the numerical substructure by the virtual damper. Thus, we can finally define the virtual damper rate in proportion to the normalised power output from the transfer system, as

$$c_D = \begin{cases} b\left(\dfrac{T_E(s)\, p_E}{T_S(s)\, p_S}\right), & p_E > 0 \\ 0, & p_E \leq 0 \end{cases} \tag{7}$$

A saturation limit is used to prevent negative virtual damper rates from being demanded so as to ensure net passivity of the transfer system.

3 Simulation

3.1 Normalized passivity control vs. conventional passivity control for hybrid tests.

In this section, the performance of the passivity controller in [13] is compared with that of the new, normalized passivity controller. The hybrid test simulation employed in this section consists of a linear, one DOF mass-spring-damper numerical substructure and a physical substructure modelled as a linear spring. The actuator is modelled as a pure delay. Table 1 illustrates the parameters of the hybrid test.

Table 1: Hybrid test parameters

Numerical Substructure	Physical Substructure	Actuator
1 degree of freedom lumped mass-spring-damper system: • Mass $m_n = 1$kg • Damper rate $c_n = 10$Ns/m • Stiffness $k_n = 1$kN/m	Stiffness $k = 2$kN/m	Pure delay of 3ms

Figure 2 illustrates the numerical and physical substructure components of the system and the excitation force given by f, whilst figure 3 presents a block diagram of the hybrid test.

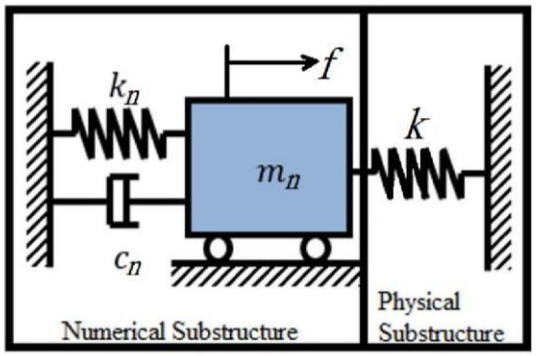

Figure 2: Diagrammatic representation of the emulated system

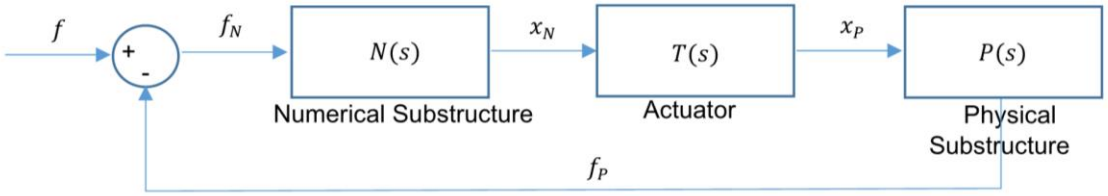

Figure 3: Hybrid test block diagram

The transfer functions relating the numerical substructure force f_N to the numerical substructure displacement x_N is described by the transfer function denoted $N(s)$ as follows

$$\frac{x_N}{f_N} = N(s) = \frac{1}{m_n s^2 + c_n s + k_n} \tag{8}$$

$T(s)$ denotes the transfer function of the actuator with delay τ and can be expressed as follows.

$$T(s) = \frac{x_p}{x_N} = e^{-\tau s} \tag{9}$$

The transfer function describing the physical substructure displacement x_p to the physical substructure force f_P is given by given by equation 10 as follows.

$$\frac{f_P}{x_P} = P(s) = k \tag{10}$$

Setting $T(s) = 1$, equations 8, 9 and 10 can be combined to describe the closed loop transfer function of the emulated system in equation as shown below.

$$\frac{f_P}{f} = \frac{1}{\frac{1}{N(s)P(s)T(s)} + 1}$$

$$= \frac{k}{m_n s^2 + c_n s + k_n + k} \tag{11}$$

If the physical substructure displacement is the measured output, the closed loop transfer function of the emulated system can be expressed as follows by combining equations 10 and 11

$$\frac{x_P}{f} = \frac{1}{m_n s^2 + c_n s + k_n + k} \tag{12}$$

This hybrid test is used to compare the performance of the normalized passivity controller with that of the passivity controller introduced in [13]. The system was given a step excitation force of magnitude 35N and the physical substructure output position response with normalized passivity control and then conventional passivity control are shown in figure 4. The passivity damper rates (given by equation 7 for the normalized controller) and the spurious power injection (given by equation 3) are also shown. Both the controllers are seen to dampen out oscillatory behaviour matching the position response of the emulated system with great accuracy. However, the normalized passivity controller achieves this using large damping rates over short time intervals whilst the conventional passivity controller relies on a smaller, more uniform damping rate. The advantage of the new controller in this instance is that it only acts when there is a discrepancy in synchronisation between the two systems and does not affect the system dynamics unnecessarily outside of these periods. The disadvantage is that it introduces a greater degree of distortion into the response.

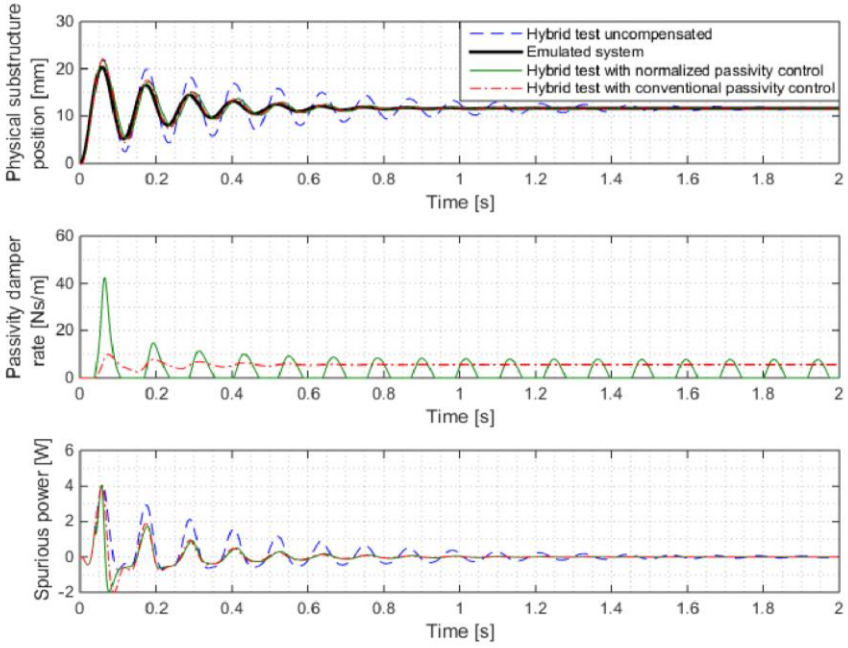

Figure 4: Hybrid test step responses

There are two key differences between the normalized controller, and the conventional controller from reference [13]. Firstly, the virtual damper rate of the conventional passivity controller is proportional to the integral of the substructure power error. As such, it acts on not only the present state of the system but also the response history. The new passivity controller designed in this publication on the other hand, acts on the low pass filtered power error so that the sensitivity to the response history can be tuned using the parameter T_E. The second, more significant change is that whilst the conventional controller acts on the absolute value of the integrated power error, the new controller acts on the normalised power error defined above.

Moreover, in hybrid testing a major disadvantage of passivity control without normalization as used in [13], is the dependency of the virtual damper rate on the absolute value of the substructure power error. With such a scheme, greater damping can be expected when larger excitation signals are used as this is associated with greater kinetic energy. This in turn would cause the response of the system to vary with the size and type of the excitation thereby requiring controller tunings unique to specific operating conditions. With the normalized control variable in the new passivity controller, the dependency of the virtual damper rate on the excitation signal is alleviated as shown in the following test.

In order to assess the response of the aforementioned hybrid test with passivity control over a range of frequencies and amplitudes, frequency responses will be employed. The system was excited by force sweeps from 0.1Hz to 25Hz over a period of 25s and the physical substructure position output was used to create frequency responses of amplitude ratio and phase using the ratio of the cross spectral density of the input and output to the power spectral density of the input. Figure 5 illustrates the frequency responses of the hybrid test with normalized passivity control and conventional passivity control, with fixed controller gains, swept over the above-mentioned frequency spectrum at different excitation force amplitudes. The response of the emulated system is also shown for comparison. The passivity controllers were tuned such that the amplitude ratio of the hybrid tests near resonance closely match that of the emulated system for the 50N force input. As such, the normalized passivity controller employed a gain of 1kNs/m whilst the conventional passivity controller used a gain of 100Ns/Jm for all tests shown.

From figure 5a, it is evident that the response of the hybrid test with passivity control from [13] varies depending on the amplitude of the excitation signals used. In figure 5b however, the normalized passivity controller hybrid test response is seen to be identical at all amplitudes with the single controller gain used. This saves considerable time and effort in controller tuning, alleviating the need to retune the controller each time operating conditions are changed. Furthermore, if validation is achieved at one operating condition it can provide confidence in results across a range of operating conditions, thus offering a route to meaningful validation against a full system while retaining many of the benefits of hybrid testing. As with conventional passivity control, the phase lag of the hybrid test at high frequency can be improved but not entirely eliminated, and the method will always benefit from supplementary control techniques to further improve phase response.

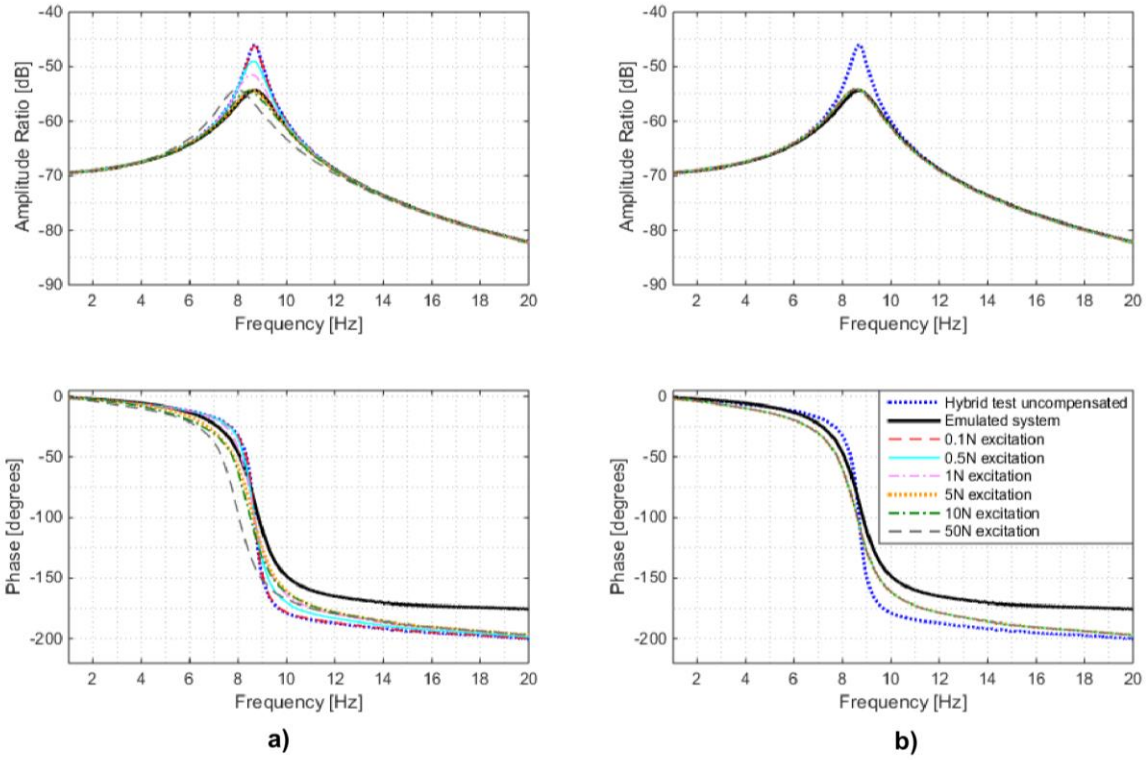

Figure 5: Frequency responses of hybrid test for a range of excitation amplitudes with a) conventional passivity control from [13]*, b) normalized passivity control*

3.2 Controller tuning

In this section, effects of changing the controller gain and power filter time constants will be assessed. To analyse the effects of the controller gain, step excitation signals are used and the natural frequency, damping ratio and total harmonic distortion of the physical substructure position output are estimated. These quantities allow comparison with the expected behaviour of the emulated system. The natural frequency and damping ratio should match the emulated system, while the total harmonic distortion measures the deviation from the expected single-frequency harmonic response of the linear emulated system: any harmonics measured are indicative of a distortion of the desired response. Due to the nonlinear damping nature of the passivity controller, the physical substructure position output will be a nonlinear response. The dominant natural frequency of the output is obtained by evaluating the periodogram of the response and measuring the frequency of the dominant mode. The damping ratio is obtained using the logarithmic decrement applied to the first four peaks of the response. These quantities are normalized with respect to the natural frequency and damping ratio of the emulated system which are obtained using the same methods applied to the emulated system simulated response. The normalized damping ratio and natural frequency of the hybrid test with passivity control has been evaluated for a range of controller gains and is plotted in figure 6 together with the total harmonic distortion of the output. The total harmonic distortion of the response in comparison to the fundamental mode is obtained using the method outlined in [18]. As such, a system with a normalized natural frequency and damping ratio of 1 represents a hybrid test with the same natural frequency and damping ratio as the emulated system. The net power filter time constant t_E is arbitrarily set to a tenth of the system period so as to allow quick adaption of the passivity damper rate whilst the mean power filter time constant t_S is set to match the period of the system to allow the history of a single cycle to be used in the normalization of the power error. Effects of varying filter time constants will be further investigated at the end of this section.

It is evident that as the controller gain is increased, the damping ratio of the system increases. It is interesting that even though the virtual damper only acts to correct for spurious excess energy in the system, with high enough gains it can evidently overcompensate and exceed the energy dissipation rates of the emulated system. The total harmonic distortion is also seen to increase with the passivity controller gain since higher gains lead to rapid corrections and more pronounced changes in the damper rate, thus leading to more pronounced departures from the linear response of the system. This distortion in the response is reflective of poor tracking. The natural frequency of the system is seen to decrease with increasing controller gain as a natural consequence of the increased damping in the system. Both the frequency response and the distortion of the response are seen to depart from the desired response of the emulated system as the controller gain increases. As such, there is a trade-off in terms of changes in the system's natural frequency, damping ratio and distortion with respect to the emulated system. For the hybrid system tested, figure 6 illustrates that a normalized damping ratio of 1, a natural frequency 2% lower than that of the emulated system and total harmonic distortion of -33.68dB is obtained when a gain of 544Ns/Jm. The most suitable trade-off will depend on specific test requirements. Moreover, the performance parameters are once again seen to be independent of the step excitation amplitude.

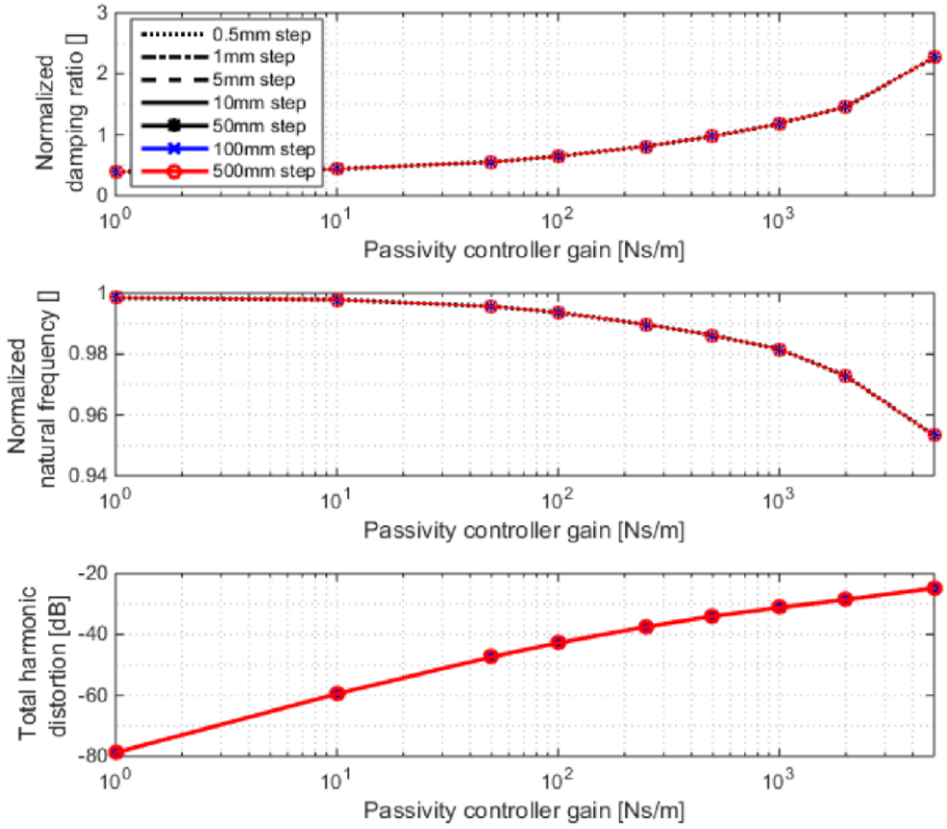

Figure 6: Performance metrics for hybrid test using the normalised passivity-controlled system with a step input. The performance is seen to be independent of the input amplitude: a significant benefit of the new control scheme proposed here.

Having investigated the effect of the controller gain on the hybrid test response, it is important to assess how the system response is affected by the power output and power throughout filters defined earlier as T_E and T_S. To do this, step responses will be used, and the position output of the physical substructure will be measured and observed over a range of filter time constants. To begin with, the effect of the power output filter time constant t_E will be studied. The aforementioned hybrid test was excited by a 50N force step at the numerical substructure. The power throughput filter time constant was arbitrarily set to match the period of the emulated system such that the history of a single past cycle will be used in power normalization. As earlier, the period of the emulated system was identified by applying a periodogram to its step response to measure the frequency of the dominant vibration

mode. The controller gain was set to 544Ns/Jm as this was found to result in a satisfactory response in figure 6 for a sensible choice of filter coefficients.

Figure 7 illustrates the hybrid test response against that of the emulated system for a range of different t_E values. The response without passivity control is seen in figure 7a to exhibit oscillations much larger than that of the emulated system. With passivity control active however, all tested t_E values result in an improved response largely following that of the emulated system. The response with t_E set to 1e-3s is seen to result in the best response for this system following that of the emulated system with greatest accuracy. Higher values of t_E such as 1e-2s are seen to result in greater phase lag. The reason for this is evident when observing figure 7b, as larger filter coefficients result in slower changes in the damper rate causing notable damper rates to be active for more time. However, a benefit of doing this is that the maximum damper rate required is small and thus distortion of the response will be low. On the other hand, although setting a small value of t_E such as 1e-3s was found to result in a good response in figure 7a, figure 7b indicates that it is achieved with damper rates as high as 418Ns/m which highlights a limitation of fast acting passivity controllers, that they may result in greater nonlinear distortion of the output due to the high and volatile damping. Thus, there is a trade off that must be made based on the requirement of the application. Solutions requiring low phase lag will benefit from rapid passivity controllers whilst those that prioritize low distortion over phase lag would be suitable with a slower power output filter. It is interesting to note that excessively large t_E values such as $t_E = 1s$ result in more oscillatory performance with less added phase lag as seen in figure 7a. This is due to the very low damper rates realized as seen in figure 7b which results in less passivity control action being applied when required. The damper rate curve is seen to grow overtime as the power error accumulates over the test, bringing the solution closer to that introduced in [13] where the power error is integrated to determine the passivity damper rate.

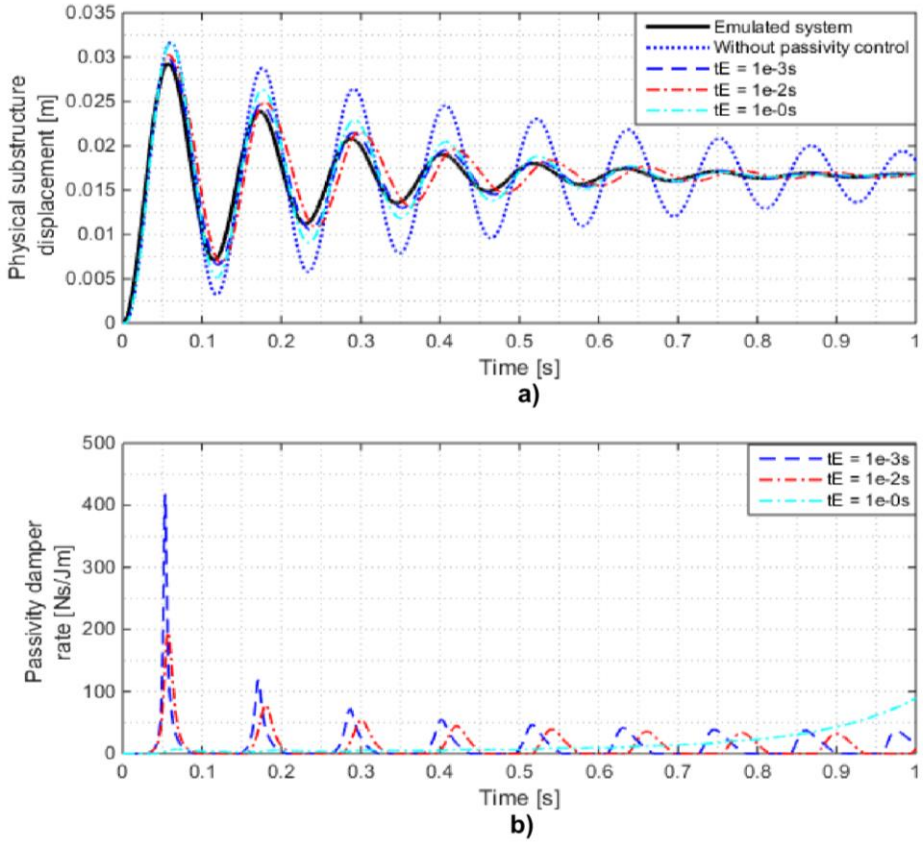

Figure 7: Hybrid test response to varying power output filter period t_E a) Physical substructure position, b) Passivity damper rate

In the next test, the effect of varying the power throughput filter time constant t_S on the hybrid test response will be analysed. As earlier, a 50N step excitation force at the numerical substructure was applied with the same controller gain of 544Ns/Jm as used in the previous test. The power output filter t_E was fixed to one tenth of the system period to allow for a reasonably fast acting controller. Figure 8 illustrates the response of the passivity-controlled hybrid test against that of the emulated system. The throughput filter time constant is set as multiples of the system period so that the normalisation can be quantified in terms of numbers of previous cycles.

Figure 8a indicates that excessive oscillation is present in the response without passivity control as seen earlier, whilst the application of passivity control leads to an improved response more representative of the emulated system. The response matching that of the emulated system most closely is seen when the t_S is set to match the period of the emulated system such that one preceding cycle is used for normalization. With the t_S value set too high or too low, the response is seen to exhibit greater phase lag and nonlinear distortion. The reason for this can be observed in figure 8b where it is seen that lower t_S values, such as a fiftieth of the system period, result in high and volatile damper rates. When t_S is small, $T_S(s)$ tends to 1 in equation 6, and thus the virtual damper rate is normalized over the mean power variable p_S in equation 7. In such a configuration, the virtual damper rate will be large when p_S is small giving rise to greater phase lag whilst rapid changes in p_S will give rise to notable nonlinear distortion in the response. Similarly, when larger t_S values are used, the values of $T_S(s)\ p_S$ in equation 7 will be smaller giving rise to greater, more volatile virtual damping as would be seen when the controller gain b is increased. As such, the most suitable setting for t_S will depend on the controller gain and the levels of distortion and extra phase lag that can be accepted for a given application.

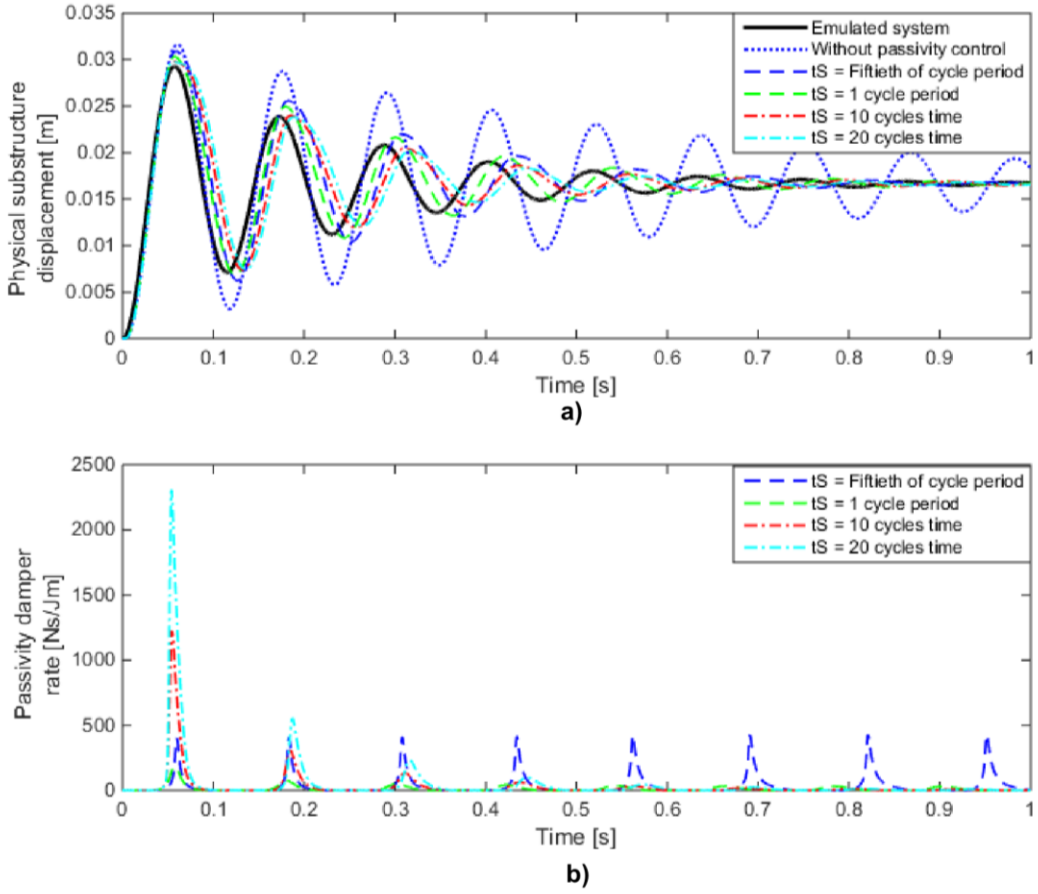

Figure 8: Hybrid test response to varying power throughput filter period t_S a) Physical substructure position, b) Passivity damper rate

The final set of test conducted in this section is to determine the sensitivity of the hybrid test performance to changes in the parameters of the numerical substructure, in the presence of a fixed passivity controller gain. To do this, the natural frequency of the emulated system is systematically increased while keeping the damping ratio and steady state gain constant. Equation 11 derived in section 3.1, can be rearranged to find expressions for numerical substructure mass, stiffness and damper rate.

$$\frac{f_P}{f} = \frac{k}{m_n s^2 + c_n s + k_n + k} \tag{11}$$

Rearranging equation 11 allows the emulated system transfer function to be expressed in the standard 2nd order lag form as shown below

$$\frac{k/m_n}{s^2 + \frac{c_n}{m_n} s + \frac{k_n + k}{m_n}} \equiv \frac{K{\omega_n}^2}{s^2 + 2\zeta\omega_n s + {\omega_n}^2}$$

Thus, expressions for numerical substructure mass, stiffness and damper rate can be written as follows

$$m_n = \frac{k}{K{\omega_n}^2} \tag{13}$$

$$c_n = 2\zeta\omega_n m_n \tag{14}$$

$$k_n = m_n{\omega_n}^2 - k \tag{15}$$

The physical substructure stiffness k was reduced to 1kN/m in order to allow a greater range of stability to be studied across the spectrum of natural frequencies tested. The steady state gain and damping ratio K and ζ were fixed at 0.5 $Ns^2/(kgmrad^2)$ and 0.1 respectively. The actuator is modelled as a pure delay of 3ms as earlier. To assess the versatility of a single controller gain in the face of changing system parameters, the normalized natural frequency, damping ratio and total harmonic distortion of the hybrid test response to a 300N force step in the numerical substructure is evaluated and plotted in figure 9 against the emulated system natural frequency. The power output filter time constant is set to a tenth of the emulated system period and the power throughput filter time constant is set to match the emulated system period for each frequency tested.

As the natural frequency of the system rises in the presence of a fixed actuator delay, the stability margins of the system erode. With a passivity control gain of zero, the damping ratios even become negative (unstable) at the top end of the frequency range tested. At these higher frequencies, the need for stability augmentation from the passivity control is evident, with the same trade-off observed previously between the natural frequency, damping ratio, and distortion. For the range of natural frequencies tested, a gain of 100Ns/m is seen to provide a good response at all frequencies, maintaining a normalized damping ratio close to 1. Thus, appears that a single control gain may be suitable across a broad range of system parameters, albeit with filter coefficients tuned to the specific choice of parameters.

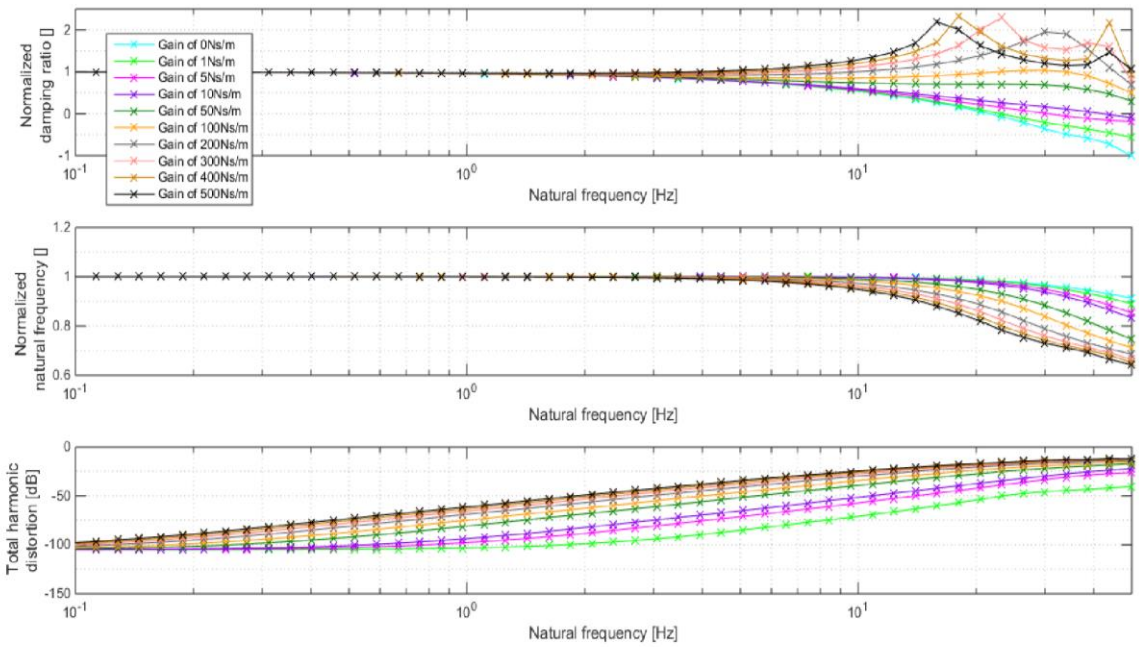

Figure 9: Hybrid test performance with fixed passivity controller gain over a range of emulated system natural frequencies

4 Experimentation

This section presents experimental hybrid test results using the normalized passivity controller. The numerical substructure of the hybrid test is the same as that described in table 1. The physical substructure is represented by an approximately cubic stiffness:

$$k = 0.0042{x_P}^2 + 2.13$$

Where x_P is the displacement of the physical substructure. This stiffness profile is realised by connecting two linear springs perpendicular to the direction of motion as shown in figure 10, which illustrates the test rig comprising the actuator and the physical substructure. The actuator used is a Copley STA2508S electromagnetic actuator running in position control mode via a proportional position controller with velocity feed forward nested outside cascaded velocity and current proportional integral controllers. The actuator response is third order in nature and its structure is shown in figure 11. Due to nontrivial friction acting on the armature, a Coulomb friction compensation scheme as proposed by Eamcharoenying et al. [19] is applied to the actuator in all tests.

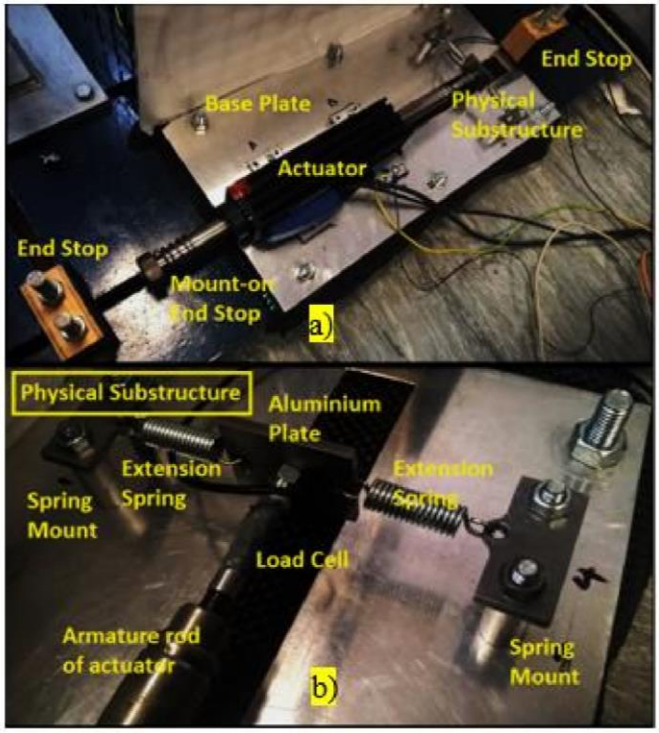

Figure 10: a) Actuator connected to physical substructure through load cell, b) view zoomed into physical substructure [17]

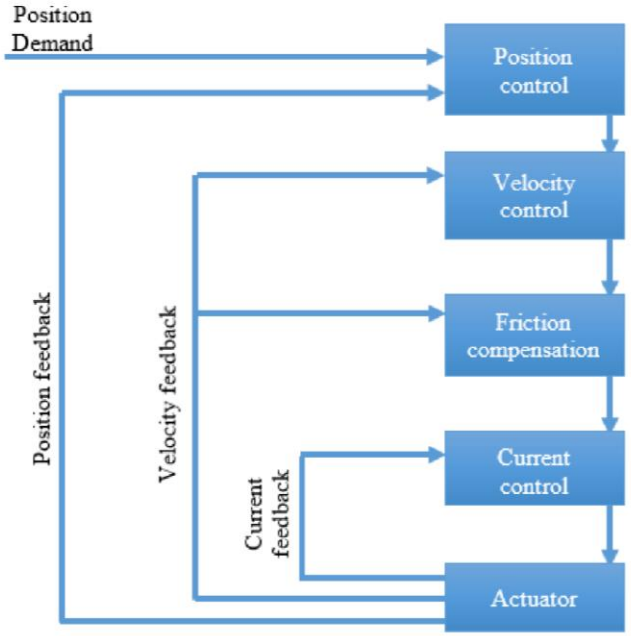

Figure 11: Actuator control system structure

The response of the numerical and physical substructure positions without passivity control are shown in figure 12a. The system is excited by a force input to the numerical substructure with amplitude 10N at a frequency of 10Hz. An unstable response is seen as oscillations grow in magnitude. The displacement of the physical substructure in this unstable test is limited by spatial constraints in the controller indicated by saturation limits in the plot. The saturation limits are programmed into the

actuator position controller with leeway to prevent damage due to overshoot. With the application of passivity control however, the response is seen to be stabilized and similar to that of the emulated system as seen in figure 12b. Figure 12c illustrates the damper rate for the virtual damper which indicates that most damping is required close to the turning points of the system which is in agreement with the simulation result seen in figure 4 described earlier.

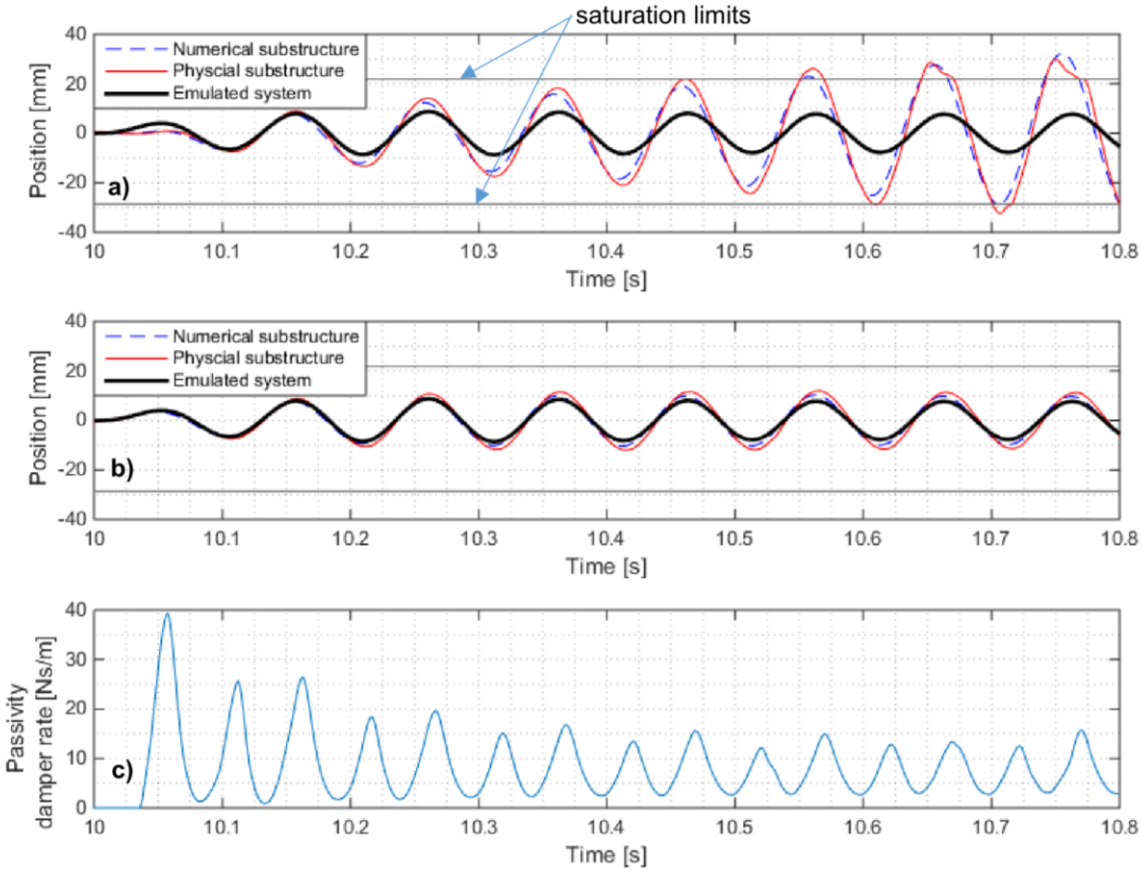

Figure 12: Hybrid test response a) without passivity control, b) with passivity control, c) passivity damper rates required for stabilization

Figure 13 illustrates experimental step responses of the nonlinear hybrid test with different passivity controller gains. The response without passivity control is seen to have far too little damping, with oscillations reaching a steady amplitude of 3.75mm in figure 13a. This limit cycle is caused by the increase in the actuator's phase lag at low velocities due to friction as described in [17]. The actuator exhibits greater phase lag at low velocities, making the controller unstable in this regime and preventing a stable equilibrium. Although friction compensation was shown to reduce this behaviour in [17], it is unable to fully compensate the effects. Passivity control is seen to bring the decay rate of the system back in line with that of the emulated system, but with clearly discerible changes to the natural frequency and harmonic distortion, increasing with the controller gain. Figure 13b illustrates that high damper rates are instigated even when the system settles, in order to supress the limit cycle oscillation. This is interesting because with a more conventional passivity controller, the passivity control would not operate in this low-amplitude regime. It is the innovation introduced in this paper, in normalising the power measurement, that improves the response here.

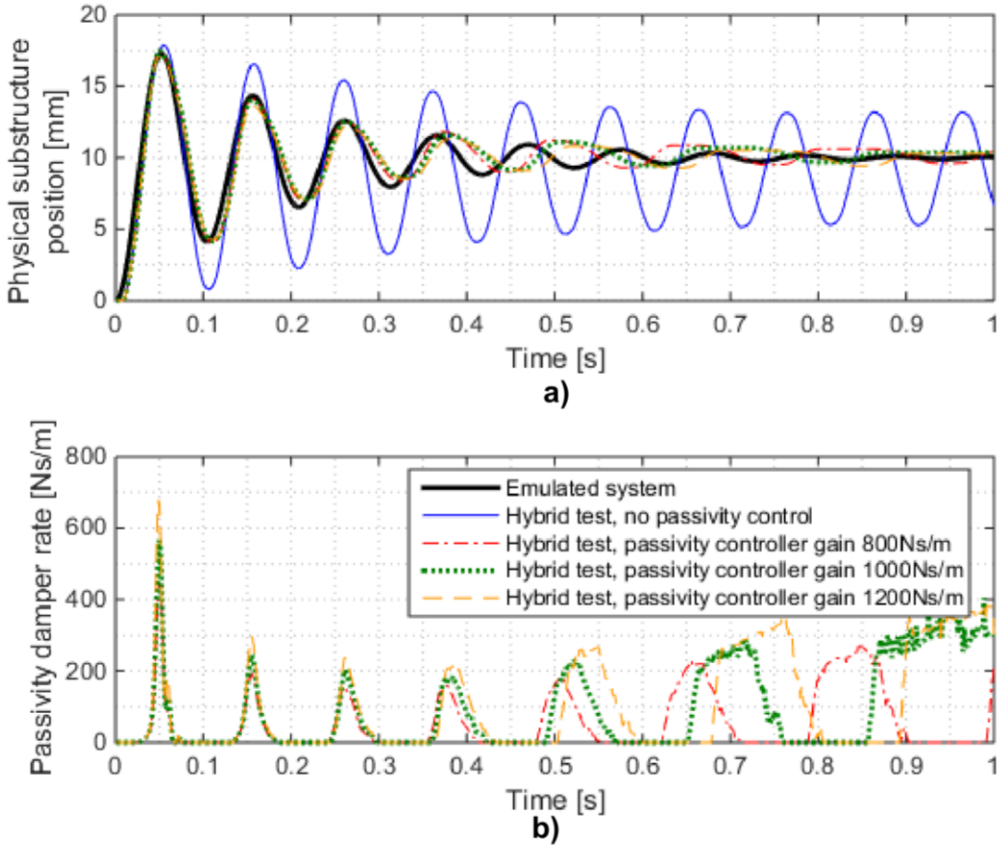

Figure 13: Hybrid test response with different passivity controller gains a) physical substructure position, b) passivity damper rate

5 Conclusion

A new algorithm for passivity control has been proposed, using normalised measures of power transfer in place of the conventional absolute power measurements. The result is a controller that is less sensitive to the amplitude of the system response. Whereas conventional controllers would need their gains tuning for a given range of response amplitudes, it is shown here that for a given system a single tuning may be adequate for a wide range of test conditions. The controller is used in real time hybrid test simulations and experiments, demonstrating its efficacy in this application. For real-time hybrid testing, the controller's insensitivity to the response amplitude is important because it offers the possibility of performing a full validation against a complete system for one test regime in order to provide confidence in the results of tests across a wide range of other test regimes. This tackles one of the most difficult questions in hybrid testing, that of validation, while still retaining many of the time and cost advantages of hybrid tests. In general, passivity controllers are easy to implement with little understanding of the dynamics of the system being tested, and only minimal tuning required. The new algorithm proposed further reduces the tuning burden, making the adoption of the technique in industrial applications even more straightforward, with nontrivial benefits. The studies herein have provided guidelines for the setup of the controller parameters and illustrated the sensitivity of the controller performance to variation of the tuning and test configuration.

Acknowledgements

This work has been supported through funding from the Engineering and Physical Sciences Research Council, grant reference EP/N032829/1. The authors have no competing interests to declare.

References

[1] H. K. Fathy, Z. S. Filipi, J. Hagena, and J. L. Stein, “Review of hardware-in-the-loop simulation and its prospects in the automotive area,” *Proc. SPIE 6228, Model. Simul. Mil. Appl.*, vol. 62280, 2006.

[2] A. R. Plummer, “Model-in-the-Loop Testing,” *Proc. Inst. Mech. Eng. Part I J. Syst. Control Eng.*, vol. 220, no. 3, pp. 183–199, 2006.

[3] A. S. Abdelrahman, K. S. Algarny, and M. Z. Youssef, “A Novel Platform for Powertrain Modeling of Electric Cars With Experimental Validation Using Real-Time Hardware in the Loop (HIL): A Case Study of GM Second Generation Chevrolet Volt,” *IEEE Trans. Power Electron.*, vol. 33, no. 11, pp. 9762–9771, Nov. 2018.

[4] A. Valibeygi *et al.*, “Microgrid Control Using Remote Controller Hardware-in-the-Loop Over the Internet,” *CoRR*, vol. abs/1804.0, 2018.

[5] T. T. Nguyen, T. N. Dao, S. Aaleti, J. W. van de Lindt, and K. J. Fridley, “Seismic assessment of a three-story wood building with an integrated CLT-lightframe system using RTHS,” *Eng. Struct.*, vol. 167, pp. 695–704, 2018.

[6] M. Hancer, R. Bitirgen, and I. Bayezit, “Designing 3-DOF Hardware-In-The-Loop Test Platform Controlling Multirotor Vehicles,” *IFAC-PapersOnLine*, vol. 51, no. 4, pp. 119–124, 2018.

[7] M. I. Wallace, D. J. Wagg, S. a. Neild, P. Bunniss, N. a. J. Lieven, and a. J. Crewe, “Testing coupled rotor blade–lag damper vibration using real-time dynamic substructuring,” *J. Sound Vib.*, vol. 307, no. 3–5, pp. 737–754, 2007.

[8] J. du Bois, B. Titurus, and N. Lieven, “Transfer Dynamics Cancellation in Real-Time Dynamic Sub- structuring,” *Proc. ISMA 2010*, pp. 1891–1914, 2010.

[9] T. Horiuchi, M. Inoue, T. Konno, and Y. Namita, “Real-time hybrid experimental system with actuator delay compensation and its application to a piping system with energy absorber,” *Earthq. Eng. Struct. Dyn.*, vol. 28, no. 10, pp. 1121–1141, Oct. 1999.

[10] A. Darby, A. Blakeborough, and M. S. Williams, *Improved Control Algorithm for Real-Time Substructure Testing*, vol. 30. 2001.

[11] M. Ahmadizadeh, G. Mosqueda, and A. M. Reinhorn, “Compensation of actuator delay and dynamics for real-time hybrid structural simulation,” *Earthq. Eng. Struct. Dyn.*, vol. 37, no. 1, pp. 21–42, Jan. 2008.

[12] Z. Tang, M. Dietz, Z. Li, and C. Taylor, “The performance of delay compensation in real-time dynamic substructuring,” *J. Vib. Control*, vol. 0, no. 0, p. 1077546317740488, 2017.

[13] L. D. H. Peiris, A. R. Plummer, and J. L. Du Bois, “Passivity Control in Real-Time Hybrid Testing,” in *UKACC 12th International Conference on Control (CONTROL)*, 2018, pp. 317–322.

[14] M. Becherif, “Passivity-based control of hybrid sources: fuel cell and battery,” *IFAC Proc. Vol.*, vol. 39, no. 12, pp. 585–590, 2006.

[15] A. Coelho, H. Singh, T. Muskardin, R. Balachandran, and K. Kondak, “Smoother Position-Drift Compensation for Time Domain Passivity Approach Based Teleoperation,” in *2018 IEEE/RSJ International Conference on Intelligent Robots and Systems (IROS)*, 2018, pp. 5525–5532.

[16] Z. Chen, Y.-J. Pan, J. Gu, and S. Forbrigger, “A novel multilateral teleoperation scheme with

power-based time-domain passivity control," *Trans. Inst. Meas. Control*, vol. 40, no. 11, pp. 3252–3262, Dec. 2016.

[17] L. D. H. Peiris, A. R. Plummer, and J. L. Du Bois, "Passivity Control for Nonlinear Real-time Hybrid Tests," *Proc. Inst. Mech. Eng. Part I J. Syst. Control Eng.*, 2020.

[18] D. Shmilovitz, "On the definition of total harmonic distortion and its effect on measurement interpretation," *IEEE Trans. Power Deliv.*, vol. 20, no. 1, pp. 526–528, 2005.

[19] P. Eamcharoenying, A. Hillis, and J. Darling, "Friction compensation using Coulomb friction model with zero velocity crossing estimator for a force controlled model in the loop suspension test rig," *Proc. Inst. Mech. Eng. Part C J. Mech. Eng. Sci.*, vol. 230, no. 12, pp. 2028–2045, Jun. 2015.

5.2 Summary

Passivity control using a normalised power variable has been evaluated and compared against the performance of energy-based passivity control in the above publication.

An experimental result not included in the above research paper was the performance of the new passivity controller in a hybrid test subject to a discontinuity applied in the numerical substructure. Hybrid tests may be susceptible to external events which cause changes in the parameters of the system. For example, an impact and subsequent linkage with a stiff surface may result in an increase in a stiffness in the system. Such events may erode stability of the hybrid test. This is studied in figure 3, where the hybrid test experiences a sudden increase in stiffness in the numerical substructure. The hybrid test responses before the parameteric change are represented by solid lines whilst the reponses after the discontinuity as dashed lines. The parameters of the emulated system are described in table 1, and the STA2508S electromagnetic actuator was once again selected for actuation. This discontinuous hybrid test is excited by a sinusoidal force input to the numerical substructure with amplitude 10N at a frequency of 10Hz throughout the test.

Table 1: Discontinous hybrid test parameters

Numerical Substructure	Physical Substructure
1 degree of freedom lumped mass-spring-damper system: • Mass of 1kg • Damper rate of 10Ns/m • Stiffness of 100Ns/m for t<25s stepping to 1000Ns/m for t>25s	Cubic stiffness described by $k = 0.0042{x_P}^2 + 2.13$

Figure 3a illustrates that without passivity control, the system before the impact at 25s is seen to be stable, however as the impact increases the stiffness of the numerical substructure, unstable behaviour is seen as oscillations begin to grow beyond 25s. As seen earlier in figure 12 in the journal paper of this chapter, the saturation limits on position are reached once again due to instability.The saturation limits placed due to space constraints restricts the unstable response. In figure 3b, it is evident that with passivity control in the system, growth of oscillations upon the discontinuity no longer take place. The system remains stable throughout the transition of stiffness in the system. A significant increase in passivity damper rate is not seen in figure 3c upon the discontinuity as the power error in the system is not allowed to grow substantially. However, a transient increase in the damper rate at 25s is seen after the step increase in numerical substructure stiffness. Thus, passivity control is able to maintain stability in a real-time hybrid test in the presence of discontinous events which cause changes in hybrid test parameters.

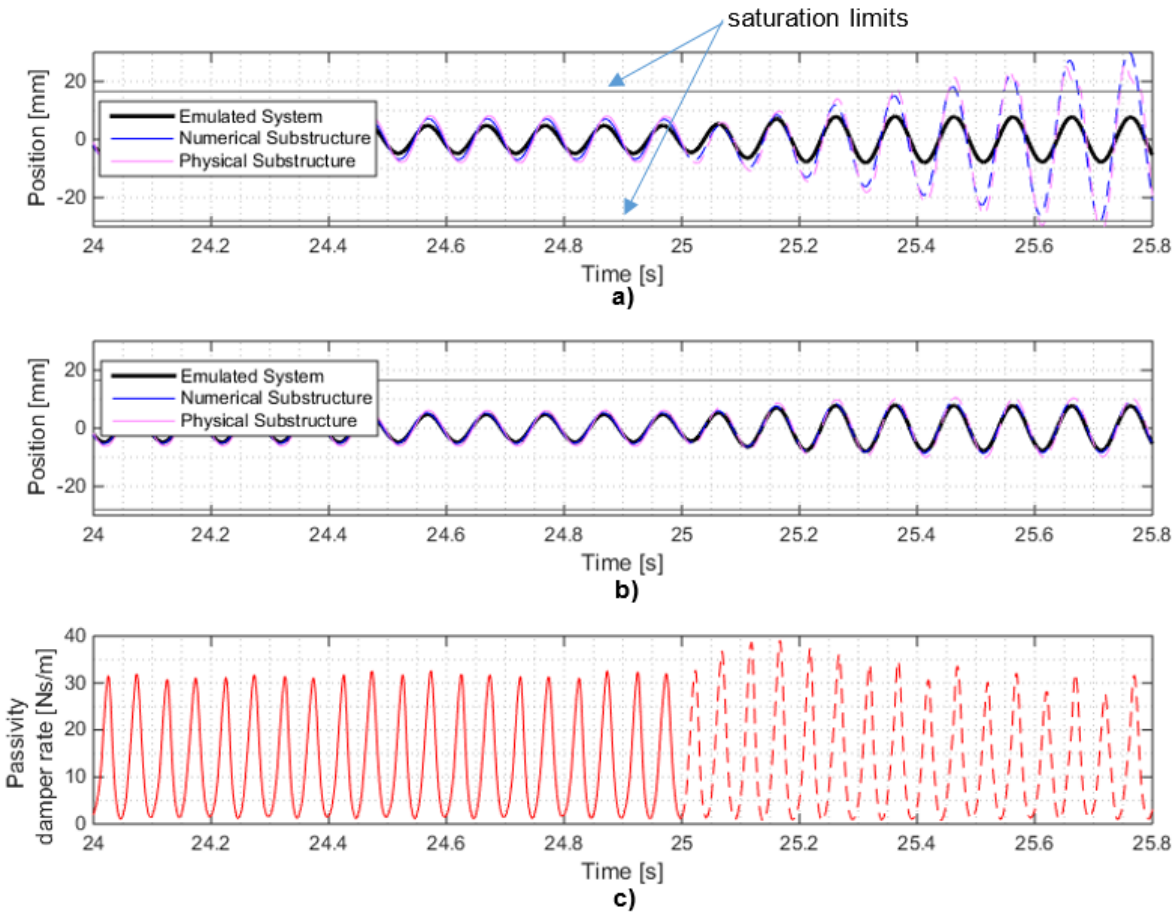

Figure 3: Hybrid test response a) substructure positions without passivity control, b) substructure positions with passivity control, c) passivity damper rate for response in figure 3b

From the journal paper and above result, the following key findings can be drawn

1) The new passivity control scheme improves real-time hybrid test stability as with the original passivity controller introduced earlier
2) The new controller applies passivity damping only when a notable substructure power error is present unlike energy-based passivity control where damping acts throughout the test.
3) A single controller tuning configuration was found to be suitable for a range of operating conditions unlike the previous energy-based design, thereby alleviating a key limitation of the original passivity controller.
4) The new passivity controller was seen to maintain stability in a nonlinear hybrid test subject to a stiff impact which would have caused instability had passivity control not been active.

Thus, it has been shown that the modified design of the passivity controller is able to achieve the same benefits as its predecessor whilst alleviating some of the key limitations. The passivity controller acts to stabilize the system regardless of the actuator dynamics making its application highly repeatable and useful for many different nonlinear hybrid tests. However, as with the original passivity controller, targeted improvements in tracking are still not achievable. The following chapter investigates a means of achieving good substructure position tracking performance as well, using passivity control combined with a novel adaptive transfer dynamics mitigation scheme.

Chapter 6

Normalised Passivity Control with Adaptive Feed-forward Filtering

6.1 Context

This chapter presents a publication where normalised passivity control was applied with a novel adaptive lag cancellation scheme designed to synchronise hybrid test substructure displacements in stable systems. The lag cancellation scheme known as adaptive feedforward filtering, acts on the substructure position error to augment the input to the actuator until synchronisation of numerical and physical substructure displacements are achieved. The motivation for using these two compensation strategies together lie in the ability of each scheme to function without prior information of actuator dynamics. Thus, a combined compensation scheme where passivity control and adaptive feed-forward filtering complement each other provides a solution that stabilizes and synchronizes hybrid tests. This ensures stability whilst also eliminating tracking errors in the hybrid test, all without any assumptions about linearity or transfer system dynamics, thereby providing a high-fidelity solution for a wide range of hybrid tests.

The structures of the passivity and adaptive feed-forward filtering controllers were discussed, and experimental tests were used to illustrate the effectiveness of both schemes used individually and together. Nonlinear hybrid tests were employed with a cubic stiffening physical substructure and the actuator utilized in chapters 4 and 5. The numerical substructure employed was a linear single degree of freedom mass-spring-damper system, although the response with a discontinuous change in numerical substructure stiffness was also tested.

The research presented in this publication was done with a colleague Dr. Andreas Bartl from the Technical University of Munich (TUM) in Germany, during his placement at the University of Bath as part of his PhD. The adaptive feed-forward filter was first introduced in one of his prior publications as detailed in the paper presented below. The methodology of the adaptive feed-forward filtering controller is attributed to Dr. Bartl. Formulation of ideas and experimental work were undertaken together.

In the following studies, the adaptive feed-forward filter as introduced in [58] is used to synchronise numerical and physical substructure displacements in the stable hybrid tests. The scheme closes the substructure gap error by applying a harmonic signal as the actuator input. The greater the number of harmonics used in the actuator input, the greater the synchronisation between substructures, at the expense of higher convergence times in the adaptive feed-forward filter. For the following experiments, a single harmonic was used to achieve synchronisation in hybrid tests in order to achieve acceptable convergence times. This was found to be sufficient to mitigate the phase lag between substructures. Although the use of more harmonics would enable greater synchronisation and thus better mitigation of nonlinear effects caused by the friction in the actuator, this would require a greater convergence time.

The adaptive feed-forward filtering scheme introduced in [58] is used in the publications of chapters 6 and 7. Table 1 provides an explanation of the main quantities and formulae of the scheme together with dimensions of each variable for general hybrid tests as well as for the specific system investigated in the following 2 publications.

Table 1: Parameters of the Adaptive Feed-forward filter

AFF Variable	Discussion	Dimensions (General case)	Dimensions (for system under study)
$\boldsymbol{u}(t)$	***Actuator input signal.*** This quantity is a scalar in our study, as a single degree of freedom hybrid test is used. Vectors are used instead, when multiple actuator inputs are required for multi degree of freedom hybrid tests.	$n \times 1$	1×1
$\boldsymbol{W}(t)$	***Basis function matrix for the actuator input.*** The number of harmonics, given by m, selected for our study is 1. Hence $\boldsymbol{W}(t)$ is a 1×2 vector, containing the cosine and sine components of the single frequency signal. Setting a greater number of harmonics will result in better synchronisation in nonlinear systems at the expense of greater convergence time.	$n \times 2mn$	1×2
$\boldsymbol{\theta}$	***Parameter vector.*** This vector describes the amplitude and phase of the input signal to the actuator. The elements of this vector are dynamic, and update as the gap error converges over time.	$2mn \times n$	2×1
$\boldsymbol{H}_u(\omega)$	Transfer function matrix between actuator input and gap error	$n \times n$	1×1
$\boldsymbol{H}_{ext}(\omega)$	Transfer function matrix between external forces and gap error	$n \times n$	1×1
$\boldsymbol{G}(\omega)$	***Interface gap in the frequency domain*** The gap error is a result of the actuator dynamics and the external forces $\boldsymbol{F}_{ext}(\omega)$. $\boldsymbol{G}(\omega) = \boldsymbol{H}_u(\omega)\boldsymbol{U}(\omega) + \boldsymbol{H}_{ext}(\omega)\boldsymbol{F}_{ext}(\omega)$ $\boldsymbol{U}(\omega)$ is the actuator input in the frequency domain.	$n \times 1$	1×1
$\boldsymbol{P}$	***Interface transfer matrix*** *(for parameter vector θ).*	$2nm \times 2nm$	2×2

	$\boldsymbol{P}$ encapsulates the transfer system response at each harmonic frequency. It applies a phase shift and gain to $\boldsymbol{\theta}$. As transfer dynamics are not known beforehand, $\widetilde{\boldsymbol{P}}$ an initial estimate of $\boldsymbol{P}$ is identified via measurement before the test.		
$\boldsymbol{g}(t)$	***Interface gap in the time domain.*** The interface gap can be expressed as function of above defined parameters as follows, where $\boldsymbol{g}_{ext}(t)$ is the contribution of the excitation. $$\boldsymbol{g}(t) = \boldsymbol{W}(t)\boldsymbol{P}\boldsymbol{\theta} + \boldsymbol{g}_{ext}(t)$$ $\boldsymbol{W}(t)\boldsymbol{P}\boldsymbol{\theta}$ is the contribution of the actuator to the interface gap. The objective of the adaption law is to identify a $\boldsymbol{\theta}$ which allows $\boldsymbol{g}(t) = 0$ via minimization of the cost function.	$n \times 1$	1×1
$\boldsymbol{J}$	***Cost function*** The cost function which is minimized to achieve desired specifications. In the publication of chapter 6, the cost function is defined with the sole purpose of minimizing the square of the gap error: $$J = \frac{1}{2}\boldsymbol{g}(t)\boldsymbol{g}^T(t)$$ In the publication of chapter 7, the cost function is defined as follows, to minimize the square of the gap error whilst also minimizing the regularisation term in order to reduce jumps in the parameter vector thus enabling smoother convergence. $$J = \boldsymbol{g}(t)\boldsymbol{g}^T(t) + \gamma\theta^T\theta$$ γ is referred to as the regularisation parameter in the publication of chapter 7.	1×1	1×1

The cost function of the adaptive feed-forward filter is a simple least means squares law defined to minimize the substructure gap error. The parameter vector theta which augments the actuator input is updated using the gradient descent optimization algorithm which uses only the last sample in the update law. Hence, each new sample is calculated using the preceding sample. However, more sophisticated developments in adaptive feed-forward filters have recognized the effectiveness of using windows of data which are prioritized using a forgetting factor to allow superior adaption to be achieved. Such a development is seen in [59] where a recursive least-squares adaption law is used instead and compared against the performance of the simple least mean squares law in real-time hybrid tests. The adaptive feed-forward filter begins adaption with an estimate of the interface transfer matrix P which is obtained using the method presented in [59].

The normalised passivity controller uses continuous time 1st order lag low pass filters on its power measurements which allow the user to intuitively select how much of the past response is used in the determination of the damper rate. The filter coefficients for the following experiments were selected as follows, based on the results found in the previous publication. For all following harmonic excitation tests unless otherwise stated, the power output filter cut-off period was set to a 10th of the excitation period to allow a rapid controller response to non-passive behaviour. In tandem, the power throughput filter cut-off period was set to match the period of excitation, in order to allow a single period of the past response to be used for damper rate normalisation, for a good balance between stability and low distortion.

The implementation of experiments of the following paper was done in 4 stages to allow the performance of both schemes in the hybrid tests to be analysed individually and collectively. Each stage of the experiment was run in parallel with a simulation of the emulated system while saving data. Hybrid tests were run in the following order with

1) Neither passivity control nor adaptive feed-forward filtering
2) Only passivity control active
3) Only adaptive feed-forward filtering active
4) Both passivity control and adaptive feed-forward filtering active.

Table 2 below describes the parameters used in the passivity controller and adaptive feed-forward filter in the experiments of the following publication.

Table 2: Parameters used in the experiments of paper 4

Parameter	Value
Adaptive feed-forward filter	
Adaption gain (μ)	0.0001
Number of harmonics (m)	1
Number of actuator inputs (n)	1
Standard deviation allowed for θ elements	0.0001
Interface transfer matrix Identification time	10s
Passivity controller	
Passivity controller gain (B)	200 Ns/m

Power output filter cut-off period (t_1) $$T_1(s) = \frac{1}{t_1 s + 1}$$ Power throughput filter cut-off period (t_2) $$T_2(s) = \frac{1}{t_2 s + 1}$$	0.01s, 0.005s, 0.003s (for 10Hz, 20Hz, 30Hz excitations respectively) 0.1s, 0.05s, 0.03s (for 10Hz, 20Hz, 30Hz excitations respectively)
Solver Sample time ODE solver	 0.0001 ODE4 Runge-Kutta (Fixed step)

This declaration concerns the article entitled:									
Passivity control with adaptive feed-forward filtering for real-time hybrid tests									
Publication status (tick one)									
Draft manuscript		**Submitted**		**In review**	✓	**Accepted**		**Published**	
Publication details (reference)	L. D. H. Peiris, A. Bartl, J. L. du Bois, and A. R. Plummer, "Passivity control with adaptive feed-forward filtering for real-time hybrid tests," *IFAC J. Syst. Control*, 2019.								
Copyright status (tick the appropriate statement)									
I hold the copyright for this material	✓	Copyright is retained by the publisher, but I have been given permission to replicate the material here							
Candidate's contribution to the paper (provide details, and also indicate as a percentage)	**The candidate contributed to / considerably contributed to / predominantly executed the…** **Formulation of ideas:** Idea to use passivity control together with adaptive feed-forward filtering discussed with colleague Dr. Andreas Bartl and supervisor Dr. Jonathan du Bois. Candidate's contribution (65%). Selection of results to present in paper jointly decided with colleague Dr. Andreas Bartl. Candidate's contribution (60%). **Design of methodology:** Passivity controller designed solely by the candidate (100%). Adaptive feed-forward controller designed solely by colleague Dr. Andreas Bartl. **Experimental work:** Selection of experiments based on discussions with Dr. Andreas Bartl. Candidate's contribution (50%). Programming of adaptive feed forward controller by Dr. Andreas Bartl, all other programming aspects (passivity control, emulated systems) by candidate – overall contribution of candidate (70%). **Presentation of data in journal format:** Paper written by candidate, reviewed and corrected by colleague Dr. Andreas Bartl, and supervisors Prof. Andrew Plummer and Dr. Jonathan du Bois. Overall contribution of candidate (70%).								
Statement from Candidate	This paper reports on original research I conducted during the period of my Higher Degree by Research candidature.								
Signed	L D H Peiris					**Date**	24/09/2019		

Paper Four: Passivity Control with Adaptive Feed-forward Filtering for Real-time Hybrid Tests

Passivity control with adaptive feed-forward filtering for real-time hybrid tests

L.D. Hashan Peiris[1], Andreas Bartl[2], Jonathan du Bois[3], Andrew Plummer[4]

Abstract

Real-time hybrid testing combines the reliability of experimental testing with the convenience of numerical simulation. The system to be tested is split into a physical substructure and a real-time numerical simulation which are coupled using actuators and sensors to transfer data at the interface in real-time. In order to achieve stable and accurate hybrid testing representative of the true system, high fidelity control is required at the substructure interface. However, actuators have a response lag which results in tracking errors and potential instability in hybrid tests. This paper investigates the effectiveness of a combined compensation strategy based on passivity control and adaptive feedforward filtering to improve stability, robustness and tracking performance in real-time hybrid testing. The combined strategy is adaptive and requires no prior information of the actuator dynamics unlike conventional transfer dynamics compensators in real-time hybrid testing. Moreover, the scheme requires no extra hardware making it inexpensive and applicable to a wide range of systems. Experimental results on a single degree of freedom nonlinear real-time hybrid test show the potency of the scheme in synchronising substructure displacements while improving stability. The scheme was also found to restore stability of hybrid tests inherently unstable due to actuator delay whilst phase lags of up to 58 degrees have been successfully mitigated in a lumped parameter mechanical oscillator system.

Keywords: Real-time hybrid test; Passivity control; Adaptive feed-forward filters; Mechanical systems; Vibration and dynamics; Model-in-the-loop testing

1 Introduction

Real-time hybrid testing involves the separation of a system into a numerically simulated subsystem and a physical subcomponent set up experimentally in a test rig. The physical and numerical substructures are coupled and run together in real-time to emulate the behaviour of the true system. The substructure coupling interface known as the transfer system, usually consists of actuators to apply the command displacements of the numerical substructure to the physical substructure and load cells to feedback force measurements of the physical substructure back to the numerical substructure. Hybrid testing provides many

[1] Corresponding author, Email: L.D.H.Peiris@bath.ac.uk, Dept. of Mechanical Engineering, University of Bath, Claverton Down, Bath BA2 7AY, United Kingdom
[2] Technical University of Munich, Boltzmannstr. 15, 85748 Garching, Germany
[3] Dept. of Mechanical Engineering, University of Bath, Claverton Down, Bath BA2 7AY, United Kingdom
[4] Centre for Power Transmission and Motion Control, University of Bath, Claverton Down, Bath BA2 7AY, United Kingdom

of the benefits of both experimentation and simulation making it an attractive solution for a wide range of systems. Hybrid testing enables significant cost savings as it alleviates the need to setup the complete system on a test rig [1]. This also leads to a simpler system to test with the reduction of hardware requirements [2]. Moreover, systems with complex components whose behaviour may be unknown or difficult to characterize mathematically will benefit from hybrid testing where the unknown component can be set up as a physical substructure [2]. Destructive events too can be tested safely without incurring damage to components whilst allowing the user a high degree of repeatability [1]. Alternative configurations can be implemented with ease in the numerical substructure compared to changing experimental components, and conditions which cannot be easily replicated in a lab environment can be emulated numerically [2].

Owing to its convenience and versatility, hybrid testing is rapidly becoming more popular in a number of fields. Some recent applications include power electronic conversion devices [3], electric vehicle powertrain testing [4], structural integrity testing of building structures [5] and air-to-air refueling in the aerospace sector [6]. The aerospace sector has benefited from hybrid testing of satellite docking in zero gravity, testing of flight components before spacecraft manufacture and testing aerospace equipment without the expense or danger of flight tests [7]. Moreover, National Instruments have documented reductions in field testing time for an aircraft arrestor system from 20 to 5 days [8]. Development of electronic controllers have been notably aided with real-time hybrid testing with estimated improvements in lead time of 15-50% [9].

However, an underlying limitation of real-time hybrid testing stems from the dynamics of the actuators which apply the displacement demands of the numerical substructure on to the physical substructure. The lag or delay in the actuator response results in tracking errors or instability of the hybrid test and often a transfer dynamics mitigation scheme is applied to address this issue. Conventional transfer dynamics cancellation schemes are based on the identification of a linear model of the actuator dynamics which is then inverted and used as a feedforward controller. For example, Wallace et al. [10] model actuator dynamics as a linear 1^{st} order transfer function which is inverted to cancel the transfer system lag in a hybrid test of a coupled rotor blade-lag damper system. du Bois et al. [11] on the other hand utilize 1^{st} and 2^{nd} order transfer functions and process models (transfer functions with an additional delay estimate) to compensate for actuator dynamics. The authors of [11] illustrate that higher order process models result in superior transfer dynamics mitigation than lower order models or pure transfer function models.

Another popular method of cancelling actuator dynamics is to use a delay compensator. The phase lag of the actuator is modelled as a delay which is then corrected by a forward predictive delay compensator which augments the input to the actuator based on the expected response ahead of the delay. A number of delay compensation schemes have been developed over the years. An early application of delay compensation in real-time hybrid testing can be seen in Horiuchi et al. [12] where an n^{th} order polynomial function is used to predict the response ahead of the actuator delay. The scheme is simple and can be implemented easily as a discrete time transfer function. A limitation of the method however is that the step sizes of the forward prediction are restricted to integer multiples of the timestep. A more accurate forward prediction scheme is proposed in Darby et al. [13] which utilizes more sophisticated interpolation. A delay compensation scheme proposed by Ahmadizadeh

et al. [14] identifies the actuator delay using the command and actual displacements obtained. Tang et al. [15] compare the performance of some conventional delay compensation schemes in terms of accuracy and stability in real-time hybrid tests. All delay compensation schemes however are based on the response of the actuator ahead of the delay being predictable. Therefore for systems with large delays or nonlinear/discontinuous responses, such schemes will result in a poor estimation of the response ahead of the delay.

Wallace et al. [16] propose an adaptive delay compensation strategy which minimizes the delay error in the system by adapting the extent of the forward stepping interpolation based on the position errors between the numerical and physical substructures. The delay identified is adapted until synchronisation between numerical and physical substructure displacements are achieved. However, the substructure position error is measured only when the system crosses zero and hence the number of iterations to converge to substructure synchronisation will manifest as an integer number of cycles of the response crossing zero. Depending on the frequency of the system this may result in large settling times. Moreover, the scheme requires cyclic demands to the system where multiple zero crossings are achieved, and activation of the scheme is not possible for step or ramp inputs.

Passivity Control is based on regulating the energy of a system to maintain its stability. It is widely applied in the teleoperation industry to guarantee good communication between master and slave manipulators. Examples of passivity control in teleoperation are seen in the work of Bianchini et al. [17] and Dong et al. [18]. Its application in real-time hybrid testing as a means of addressing transfer dynamics is novel and has been proven to be fruitful by Peiris et al. [19], [20], [21]. The scheme applied in hybrid testing regulates the flow of energy or power to the physical substructure and maintains stability in the system by dissipating the spurious energy added to the hybrid test through the actuation hardware. A variable rate virtual damper acting on the power difference between the numerical and physical substructures is used for energy dissipation. Simulation results from [19] illustrate the effectiveness of the scheme in stabilizing unstable hybrid tests with phase margins of up to -20.73 degrees and experimental results from [20] have validated its effectiveness in the presence of nonlinearity in the actuator. However, the scheme by itself is unable to achieve targeted improvements in tracking although it has been shown to complement the performance of state-of-the-art linear model based compensation schemes in [20], enabling stability and tracking improvements to be achieved simultaneously.

Most conventional transfer dynamics mitigation schemes are based on linear models. However, actuator behaviour is not always representable using a linear model, particularly in tests where the actuator behaviour is affected by a nonlinear physical substructure or in systems where actuator behaviour is inherently nonlinear due to effects like stiction. In such cases, a new scheme is required to deal with the actuator dynamics. This paper proposes the use of a normalized passivity control scheme to improve stability with adaptive feed-forward filtering (AFF) to improve tracking between the numerical and physical substructures.

2 Theory and Method

2.1 Hybrid Test system

The experimental system used in this paper to illustrate the control method is a one degree of freedom nonlinear mass-spring damper system as shown in figure 1.

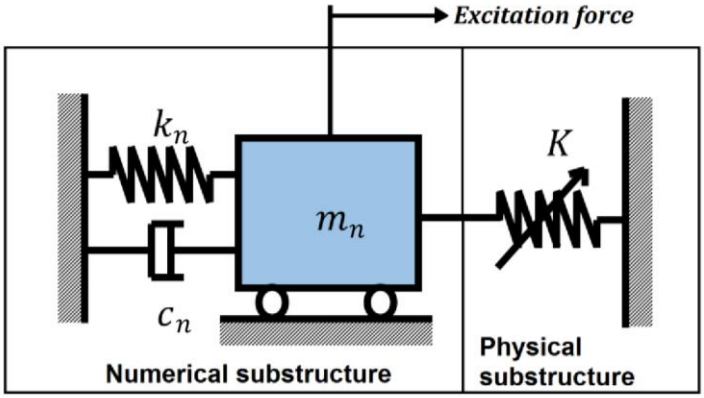

Figure 1: Schematic representation of the emulated system [20]

The numerical/virtual substructure consists of a mass m_n of 1kg attached to a spring of stiffness k_n = 1kN/m and a viscous damper of rate c_n = 10Ns/m. The transfer function relating the numerical substructure excitation force F to the numerical substructure position y_n is given by

$$\frac{y_n}{F} = \frac{1}{m_n s^2 + c_n s + k_n} \tag{1}$$

The experimental/physical substructure consists of a stiffening spring with a displacement dependent cubic stiffness. The force displacement profile of the cubic stiffening spring is plotted in figure 2a. A polynomial function is used to model the force-displacement characteristic. The parameters are identified using a least squares fitting procedure. The derivative of this polynomial function representing the tangent stiffness of the physical substructure is shown in figure 2b. There is nontrivial noise on the force measurements due to the high level of electromagnetic interference from the actuator. A 400Hz low pass filter is applied to the force measurements used by the controller.

If the displacement of the physical substructure and actuator is given by y_p, the mathematical function describing the tangent stiffness K (N/mm) of the physical substructure can be expressed as

$$K = 0.0042{y_p}^2 + 2.13 \tag{2}$$

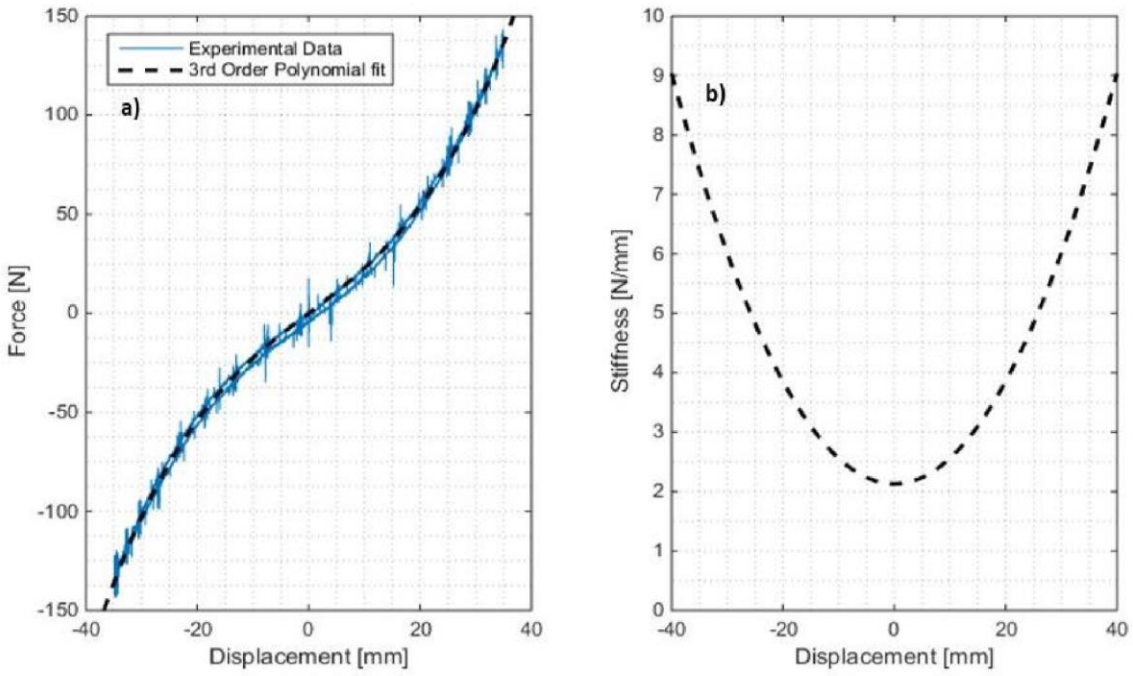

Figure 2: a) Physical substructure force profile, b) physical substructure tangent stiffness [20]

The actuator used is a Copley ST2508S electromagnetic linear actuator running in position control mode, with nested velocity and current control loops as shown in figure 3. The current and velocity loops utilize proportional-integral control schemes whilst the position control loop runs a proportional feedback controller with velocity feedforward. A simple deterministic Coulomb friction compensation scheme as detailed in [22] is applied to the actuator to reduce nonlinearity caused by the non-trivial friction acting on the armature rod. The actuator connected to the physical substructure is shown in figure 4 which illustrates the test rig used. The specifications of the actuator are given in table 1.

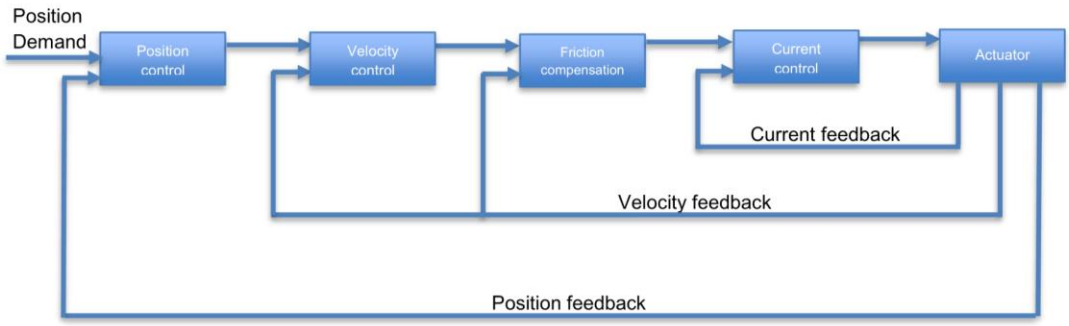

Figure 3: Actuator control system structure [20]

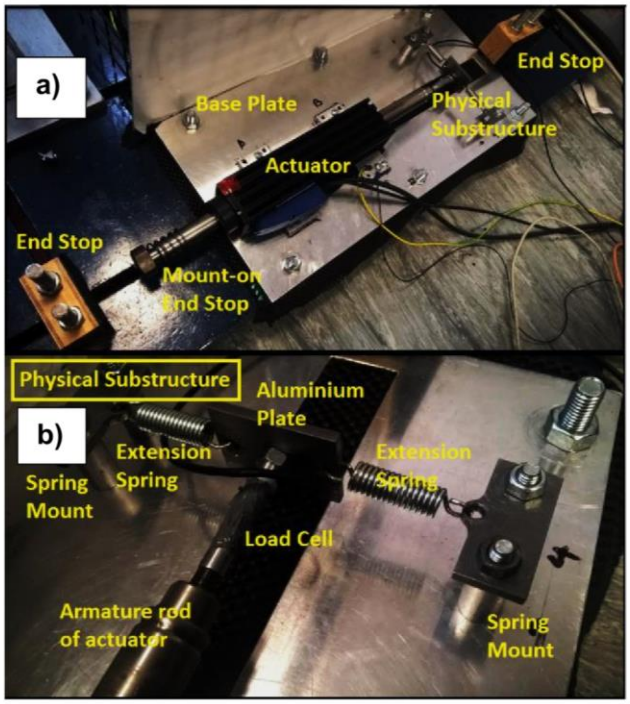

Figure 4: a) Actuator connected to physical substructure through load cell, b) view zoomed into physical substructure [20]

Table 1: Actuator performance limits [20]

Peak force	625 N
Continuous stall force	75.1 N
Armature mass	2 kg
Maximum speed	4.7 m/s

2.2 Passivity Control

The passivity controller utilized in this work was first presented in [21]. The scheme utilizes filtered measurements of the numerical and physical substructure powers which are then used to tune a variable rate virtual damper acting on the numerical substructure. Hybrid test instability is caused by the injection of spurious energy from the actuator into the system. This is detected by a surge in the power error between the numerical and physical substructure. Hence the passivity controller monitors the power error between substructures and the variable rate virtual damper is activated to dissipate the spurious power in the system so as to maintain stability of the overall hybrid test. A passive system is defined as one which outputs less energy than is supplied to it [23]. By maintaining the passivity of the transfer system, the passivity and thus stability of the overall hybrid test can be guaranteed as there are no other ports where energy enters the system besides the actuator.

The power of each substructure is identified using the product of its measured force and velocity. As such, the numerical substructure power p_n is given by the product of the numerical substructure force f_n and the numerical substructure velocity $\dot{y}_n$

$$p_n = f_n \dot{y}_n \tag{3}$$

Similarly, the physical substructure power p_p is given by the product of the physical substructure force f_p and the physical substructure velocity $\dot{y}_p$ as expressed below. The physical substructure force f_p is measured using a load cell whilst the velocity is obtained using the displacement measurements of the actuator.

$$p_p = f_p \dot{y}_p \tag{4}$$

The numerical substructure force consists of the force fed back from the physical substructure and the force applied by the passivity controller. If the passivity damping force is given by f_d, the numerical substructure force can be related to the physical substructure force as follows.

$$f_n = f_p + f_d \tag{5}$$

The actuator lag causes a discrepancy between the numerical and physical substructure displacements y_n and y_p. This in turn results in a power difference between substructures. The power error between substructures p_x is a measure of the spurious power injected into the hybrid test from the actuator, which results in poor stability. It can be expressed as

$$p_x = p_p - p_n \tag{6}$$

The total substructure power, i.e the sum of the numerical and physical substructure powers can be expressed as

$$p_s = p_p + p_n \tag{7}$$

The passivity damper rate acting on the numerical substructure is a function of the power error p_x and the magnitude of the total power p_s in the hybrid system and is given by

$$C_D = G_P \frac{T_1(s) p_x}{T_2(s)|p_s|} \tag{8}$$

where $T_1(s)$ and $T_2(s)$ are 1st order lag low pass filters with unity steady state gain whose cut off frequencies determine the rate of responsiveness of the passivity controller. G_P is the passivity controller gain. As described in [21], fast filters result in a rapidly changing damper rate which allows higher sensitivity to changes in power at the expense of more nonlinear distortion in the output. Slower filters result in less variation in the damper rates reducing the responsiveness to changes in the power flow of the system. When the power error in the system is negative, i.e. when the actuator is naturally passive, the passivity controller action is switched off and the output virtual damper rate is zero.

The passivity damping force on the numerical substructure is the product of the passivity damper rate C_D and the numerical substructure velocity $\dot{y}_n$ expressed as follows

$$f_d = C_D \dot{y}_n \tag{9}$$

By substituting the expressions of the physical substructure tangent stiffness and the passivity controller force from equations (2) and (9) the numerical substructure force described in equation (5) can be expanded as follows

$$f_n = f_p + f_d$$

$$f_n = Ky_p + C_D \dot{y}_n$$

$$f_n = \begin{cases} 0.0042{y_p}^3 + 2.13y_p + G_P \dfrac{T_1(s)p_x}{T_2(s)p_s} \dot{y}_n, & if\ p_x > 0 \\ 0.0042{y_p}^3 + 2.13y_p, & if\ p_x \leq 0 \end{cases} \quad (10)$$

2.3 Adaptive feedforward filtering

Coupling between the numerical and physical substructures requires that the interface forces are in equilibrium and the interface displacements match. The force equilibrium condition is inherently met due to the force feedback (see figure 5), if the stabilizing passivity controller is not active. The compatibility of the interface displacements, in turn, is not reached perfectly due to the actuator dynamics. To improve the compatibility between numerical and physical substructure displacements, an additional actuator input is applied. This actuator input is generated using the adaptive feed-forward filter. A control scheme for real-time hybrid testing based on adaptive feed forward filters is introduced in Bartl et al. [24]. The block diagram with the control structure including the use of an adaptive feedforward filter (abbreviated as AFF) is shown in figure 5.

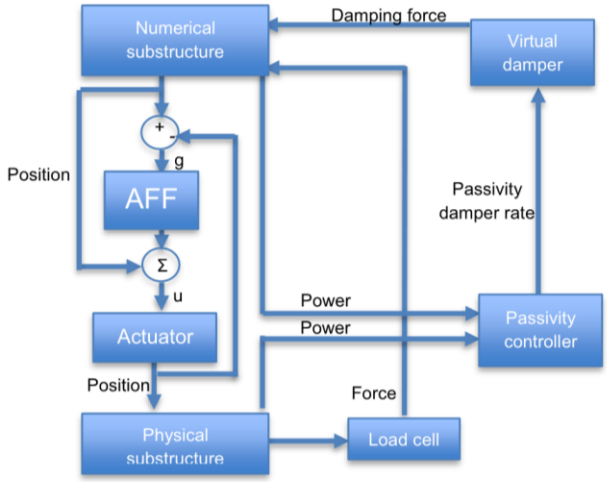

Figure 5: Hybrid test block diagram with passivity control and adaptive feedforward filtering

The state-space formulation of the test dynamics reads

$$\dot{\boldsymbol{x}} = \boldsymbol{A}\boldsymbol{x} + \boldsymbol{B}_u\boldsymbol{u} + \boldsymbol{B}_{ext}\boldsymbol{f}_{ext} \quad (11)$$

$$\boldsymbol{g} = \boldsymbol{C}\boldsymbol{x} \quad (12)$$

where $\boldsymbol{A}$ is the state-space matrix representing the dynamics of the real-time hybrid test, $\boldsymbol{x}$ is the associated state vector, $\boldsymbol{u}$ is an input vector which augments a signal to the actuator demand, $\boldsymbol{B}_u$ is the associated input matrix, $\boldsymbol{f}_{ext}$ is vector of external forces acting on the subcomponents of the test, $\boldsymbol{B}_{ext}$ is the associated input matrix, $\boldsymbol{g}$ is the residual interface gap and $\boldsymbol{C}$ is the output matrix.

If an external excitation is given by m harmonics and steady state is assumed, the additional actuator input signal $\boldsymbol{u}$ which yields perfect synchronization is a sum of harmonics and is generated as follows

$$\boldsymbol{u}(t) = \boldsymbol{W}(t)\boldsymbol{\theta} \tag{13}$$

The input signal $\boldsymbol{u}$ has n entries. $\boldsymbol{W}(t)$ is a matrix containing the sinusoidal functions

$$\boldsymbol{W}(t) = [\boldsymbol{I}\cos(\omega_1 t)\, \boldsymbol{I}\sin(\omega_1 t)\, \boldsymbol{I}\cos(\omega_2 t)\, \boldsymbol{I}\sin(\omega_2 t) \;\; \ldots \; \boldsymbol{I}\cos(\omega_m t)\, \boldsymbol{I}\sin(\omega_m t)\,] \tag{14}$$

$$\text{with } \boldsymbol{W}(t) \in \mathbb{R}^{n\times 2nm}$$

where ω_i are the frequencies of excitation, $\boldsymbol{\theta} \in \mathbb{R}^{2nm}$ is a vector of parameters which describes phase and amplitude of the input signal and $\boldsymbol{I} \in \mathbb{R}^{n\times n}$ is the identity matrix. The interface gap $\boldsymbol{g}$ can be transformed to the frequency domain and can be expressed as a function of the input signals

$$\boldsymbol{G}(\omega) = \boldsymbol{H}_u(\omega)\boldsymbol{U}(\omega) + \boldsymbol{H}_{ext}(\omega)\boldsymbol{F}_{ext}(\omega) \tag{15}$$

$\boldsymbol{H}_u(\omega)$ is the transfer function matrix between actuator input $\boldsymbol{U}(\omega)$ and interface gap $\boldsymbol{G}(\omega)$. $\boldsymbol{H}_{ext}(\omega)$ is the transfer function matrix between external forces $\boldsymbol{F}_{ext}(\omega)$ and interface gap $\boldsymbol{G}(\omega)$. Based on the transfer function of equation (15), the interface gap can be equivalently expressed in time domain as a sum of harmonics:

$$\boldsymbol{g}(t) = \boldsymbol{W}(t)\boldsymbol{P}\boldsymbol{\theta} + \boldsymbol{g}_{ext}(t) \tag{16}$$

$$\text{with } \boldsymbol{P} = \begin{bmatrix} \mathrm{Re}(\boldsymbol{H}_u(\omega_1)) & -\mathrm{Im}(\boldsymbol{H}_u(\omega_1)) & & \\ \mathrm{Im}(\boldsymbol{H}_u(\omega_1)) & \mathrm{Re}(\boldsymbol{H}_u(\omega_1)) & & \\ & & \ddots & \\ & & & \begin{matrix} \mathrm{Re}(\boldsymbol{H}_u(\omega_n)) & -\mathrm{Im}(\boldsymbol{H}_u(\omega_n)) \\ \mathrm{Im}(\boldsymbol{H}_u(\omega_n)) & \mathrm{Re}(\boldsymbol{H}_u(\omega_n)) \end{matrix} \end{bmatrix} \tag{17}$$

The matrix $\boldsymbol{P}$ applies a phase shift and gain to the parameter vector $\boldsymbol{\theta}$. The $\mathrm{Re}(\boldsymbol{H}_u(\omega_*))$ and $\mathrm{Im}(\boldsymbol{H}_u(\omega_*))$ denote the real and the imaginary part of the transfer matrix $\boldsymbol{H}_u(\omega_*)$. $\boldsymbol{g}_{ext}(t)$ is the contribution from the external forces. Proof of equations (16) and (17) is shown in [24].

The residual interface gap is closed by applying a suitable input signal $\boldsymbol{u}$ to the test setup. The input signal $\boldsymbol{u}$ is defined by the phase and amplitude vector $\boldsymbol{\theta}$ and $\boldsymbol{\theta}$ is identified using a gradient-descent adaptation law. Overtime, the algorithm converges such that numerical and physical substructure positions are synchronized and the gap error is eliminated. The objective of the adaption law is to minimize the squared interface gap. The cost function reads

$$J = \frac{1}{2}\boldsymbol{g}(t)\boldsymbol{g}^T(t) \tag{18}$$

The gradient of the cost function is $\nabla J = \boldsymbol{P}^T\boldsymbol{W}^T(t)\boldsymbol{g}(t)$. Hence the gradient-descent adaption law is given by

$$\dot{\boldsymbol{\theta}} = -\mu\nabla J = -\mu\widetilde{\boldsymbol{P}}^T\boldsymbol{W}^T(t)\boldsymbol{g} \tag{19}$$

where the unknown matrix $\boldsymbol{P}$ is replaced by an estimate $\widetilde{\boldsymbol{P}}$. The entries of $\widetilde{\boldsymbol{P}}$ can be identified by measurement before the test. A relatively rough identification of $\boldsymbol{P}$ is sufficient for stable operation of the adaptive feedforward filter. The positive adaption gain μ controls the performance of the adaption.

3 Results and Discussion

The hybrid system as described in section 2.1 was set up for testing. Initially, no compensation scheme was applied to the system. The mass spring damper system to be replicated using the hybrid test was created in simulation so that the hybrid test response could be compared against that of the emulated system. The hybrid test was given a sinusoidal force input of amplitude 10N and frequency 10Hz.

Figure 6a illustrates that the response without any form of compensation is unstable, as oscillation grows until the position saturation limits placed due to spatial constraints on the test rig are breached. Although the emulated system is inherently stable being a mass suspended between two springs, the delay in the actuator in eroding stability margins which are worsened by the stiffening of the physical substructure at high displacements. Figure 6b indicates the hybrid test response without passivity control but with adaptive feed-forward filtering. The response is still seen to be unstable as oscillations grow in magnitude. Although adaptive feed-forward filtering works to close the substructure displacement gap in hybrid tests and achieve behaviour representative of the emulated system, it is evidently unable to correct systems made unstable due to actuator lag. Hence, there is a clear need for passivity control to restore the stability of the system.

Normalized passivity control was then applied to the hybrid test without adaptive feed-forward filtering and the same experiment was run with the same initial conditions and input excitation to the numerical substructure. The response of the system is shown in figure 6c. It is evident that with the application of passivity control, the system is now stabilized and oscillations are of constant magnitude. There is however a tracking error in the response as the position output of the physical substructure does not match that of the emulated system.

Adaptive feedforward filtering was then applied to the hybrid test with passivity control and the response of this hybrid test is shown in figure 6d. It is now seen that the position responses of the numerical and physical substructures are not only synchronized, but also accurately match that of the emulated system.

This experiment indicates the individual strengths of passivity control and adaptive feedforward filtering and their compatibility to be used together in hybrid testing to obtain the unique benefits of both schemes. By regulating the power flow in to the hybrid test, passivity

control is able to achieve closed loop system stability although as envisaged in section 1, it is unable to lead to targeted improvements in tracking. Adaptive feedforward filtering on the other hand is a method applied to stable hybrid tests in order to achieve synchronisation of numerical substructure and physical substructure displacements. The combined scheme has been shown not only to restore stability of an unstable hybrid test, but to also lead to good tracking performance.

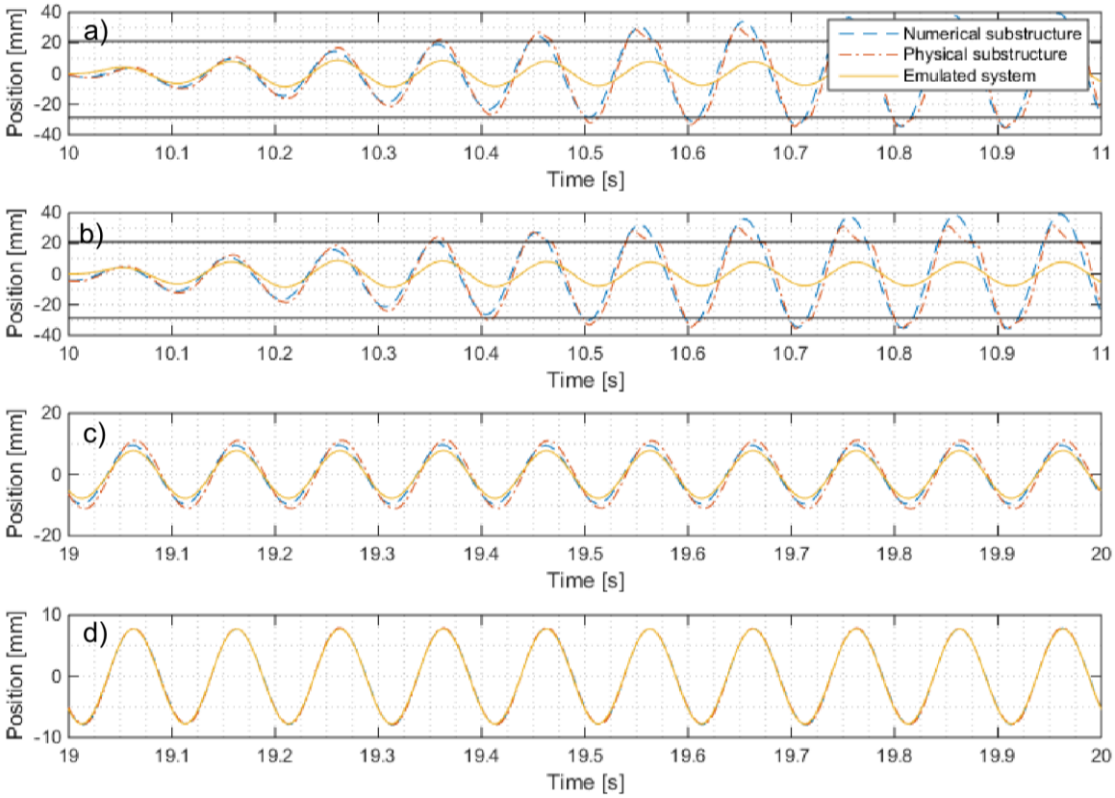

Figure 6: Hybrid test response at 10Hz with, a) no compensation, b) adaptive feedforward filtering only, c) passivity control only, d) passivity control and adaptive feedforward filtering

To further analyse the functionality of the compensation schemes, it is useful to observe the spurious power injection of the actuator to the hybrid test and the rate of passivity damping applied. This is measured and plotted in figure 7. The spurious power is obtained by evaluating the difference between the power of the physical substructure and the power of the numerical substructure. The power of each substructure is obtained by evaluating the product of the force and velocity of each substructure as described in section 2.1.

Figure 7a illustrates the spurious power injection of the hybrid test with passivity control and the test with both passivity control and adaptive feedforward filtering. Without adaptive feedforward filtering, the spurious power measurements are seen to fluctuate between -4W to 4W. The magnitude of the net power injection is non zero due to the synchronisation error between substructures caused by the delay of the actuator which cannot be eliminated using passivity control alone. However, the spurious power injection is seen to decay to a much smaller value with both passivity control and adaptive feedforward filtering applied. This is due to the improvements in tracking between the numerical and physical substructures, which leads to a smaller power error in the system.

The passivity damper rate required by the system is plotted in figure 7b. It is evident that without adaptive feedforward filtering, a passivity damper rate between 3-16Ns/m is required to maintain stability of the hybrid test. However, with adaptive feedforward filtering also applied, the required passivity damper rate decays to values between 0-3Ns/m. This indicates the non-intrusiveness of passivity control with adaptive feedforward filtering. Initially, the tracking error is relatively large which results in a sizable damper rate required to maintain closed loop stability. However, as adaptive feedforward filtering works to improve substructure synchronisation over time, the decaying spurious power allows the passivity controller to do less work overtime. This non-intrusiveness of normalized passivity control means that it will only act in the system when required. This is an advantage over conventional passivity control from [20] which outputs a damping rate depending on the history of the response since the start of the hybrid test [21].

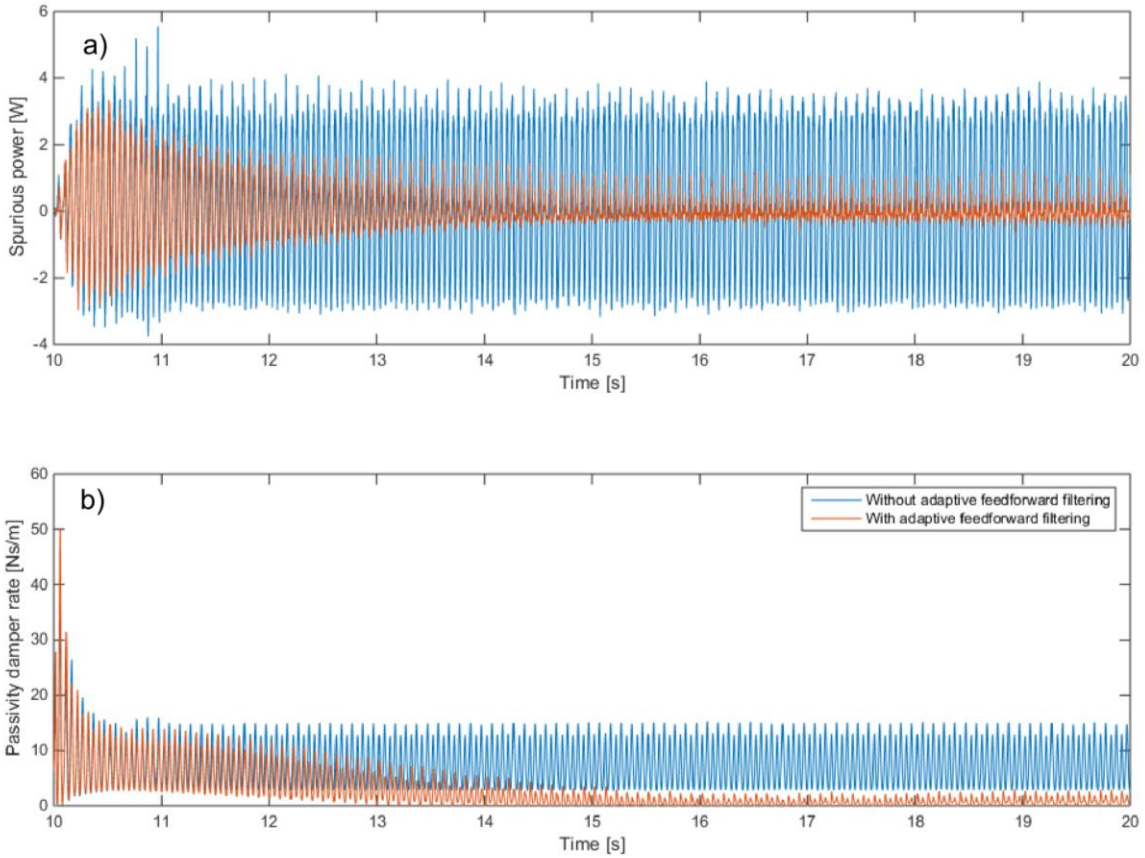

Figure 7: Hybrid test response at 10Hz with passivity control a) Actuator spurious power injection, b) Passivity damper rate

The responses of the hybrid test to excitations with frequencies of 20Hz and 30Hz are illustrated in figures 8 and 9. Passivity control is applied in all tests allowing stable responses to be achieved. However, without AFF, notable phase lags of 51^0 at 20Hz and 58^0 at 30Hz are seen in figures 8a and 8c. The application of AFF has enabled these phase lags to be eliminated as seen in figures 8b and 8d and also in figures 9a and 9b, which plot substructure positions against each other. However, period bifurcation is seen in figures 8a-8d with and without adaptive feedforward filtering as resonances of the hybrid test are

excited at 9.98Hz. This is due to nonlinear friction in the actuator shaft which excites the natural frequency of the system, a phenomenon also found in [20].

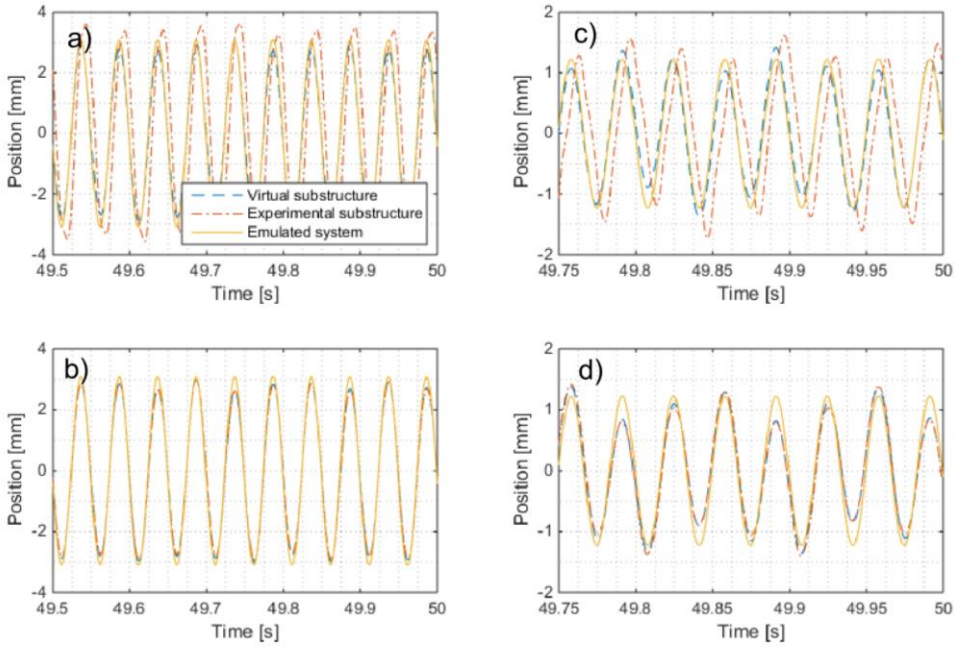

Figure 8: Position response of hybrid test with passivity control a) 20Hz, without AFF, b) 30Hz without AFF, c) 20Hz with AFF, d) 30Hz with AFF

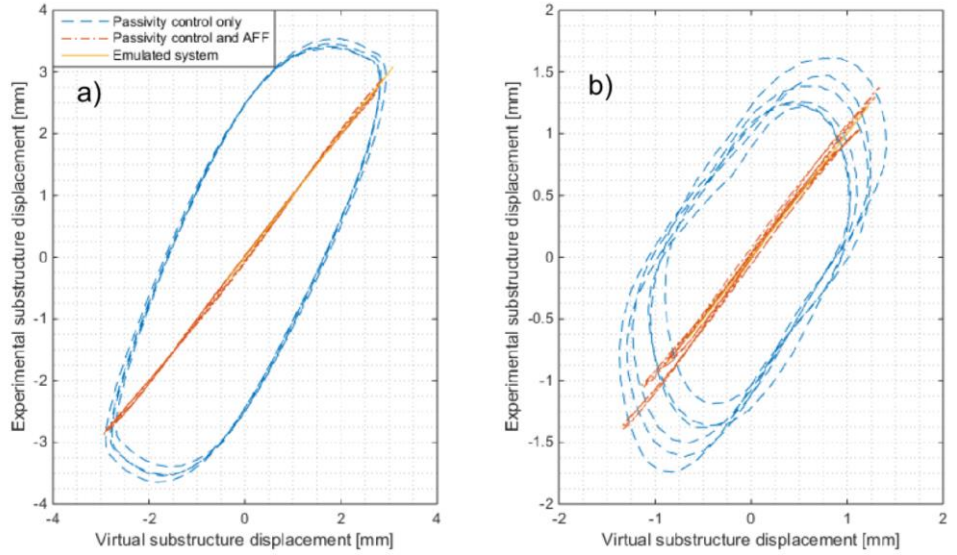

Figure 9: Hybrid test subspace plots with compensation applied a) 20Hz, b) 30Hz

So far, sinusoids have been used to excite the hybrid test in the aforementioned experiments. The following tests will assess the performance of the combined compensation strategy in the presence of discontinuous inputs. A sine wave between 0N and 10N and frequency 10Hz is superposed onto a square wave of amplitude 10N and frequency 0.05Hz. This signal is used to excite the numerical substructure of the hybrid test with passivity control. The square wave gives a change of operating point with respect to the nonlinear

spring. The response of the system without AFF is shown in figure 10 whilst the response with AFF is shown in figure 11. As seen earlier with the sinusoidal excitation, figures 10b and 10c indicate tracking errors of the hybrid test positions with respect to the emulated system in both halves of the square wave period. The application of AFF has enabled synchronisation between substructure displacements around both operating points enabling the response of the emulated system to be replicated.

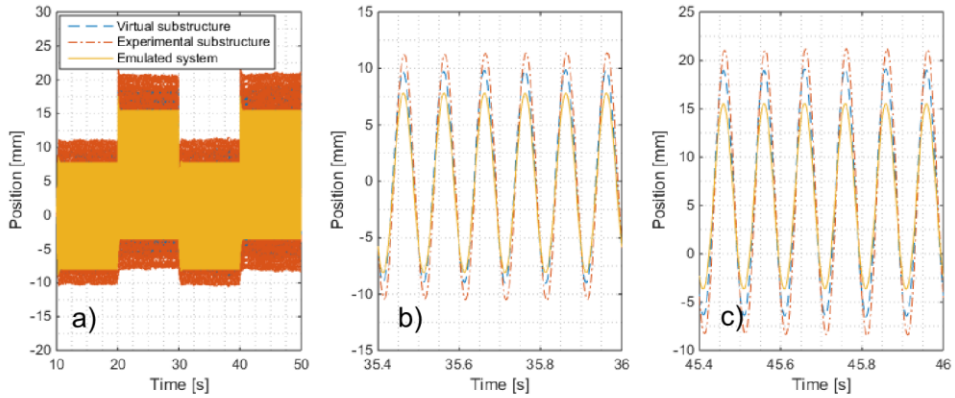

Figure 10: Passivity controlled hybrid test response (without AFF) to stepped sine excitation a) response envelope, b) response zoomed into low step, c) response zoomed into high step

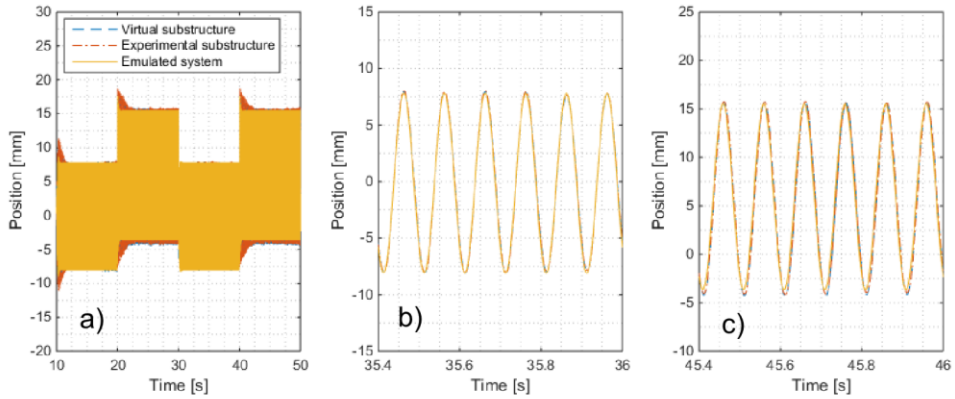

Figure 11: Passivity controlled hybrid test response (with AFF) to stepped sine excitation a) response envelope, b) response zoomed into low step, c) response zoomed into high step

The above experiments all involved a hybrid test with nonlinearity in the physical substructure but with a linear numerical substructure with constant parameters. In the following test, a change in the system parameters in the numerical substructure during the test is applied as well. Thus far, the stiffness of the numerical substructure has been chosen as a constant value of 1kN/m. This results in a hybrid test which is unstable without any form of compensation as shown previously in figure 6a. Now the numerical substructure is given a time dependent discontinuity in its stiffness. The stiffness of the numerical substructure is specified as 100N/m for a time period of 25s after which the stiffness experiences a step change to a final value of 1kN/m as before. The other parameters of the numerical substructure and hybrid test are unchanged. The hybrid test is excited by a sinusoidal input to the numerical substructure of amplitude 10N and frequency 10Hz. Figure 12 illustrates the hybrid test response with this discontinuous numerical substructure.

Figure 12a indicates that the hybrid test without any form of transfer dynamics compensation results in a stable response before 25s as oscillations are of constant magnitude, and an unstable response beyond 25s as oscillations begin to grow in magnitude until saturation limits the vibration amplitude of the system. The system is inherently stable in its low stiffness configuration but upon the step change in stiffness the system becomes unstable. Notable tracking errors in position are seen in the stable response before 25s due to the lag of the actuator.

Figure 12b indicates the response of the hybrid test with passivity control applied. It is seen now that the response after the step change in stiffness is stable resulting in the overall hybrid test exhibiting stable behaviour before, during and after the discontinuity in the numerical substructure. However, the tracking errors in position are still evident as expected.

Figure 12c illustrates the response of the system with both passivity control and adaptive feed-forward filtering applied. The response of the hybrid test is now not only stable but also achieves the displacement trajectory of the emulated system, as the tracking error between the numerical and physical substructures is small. Some transient tracking error between 25s and 26s is seen since the adaptive controller takes a finite time to adapt to the new boundary conditions of the hybrid test. However, steady state performance is seen to match that of the emulated system before and after the discontinuity is applied. As such it is found that the combination of passivity control and adaptive feed-forward filtering is suitable for transfer dynamics mitigation in highly discontinuous hybrid tests which are stable and also naturally unstable due to actuator lag.

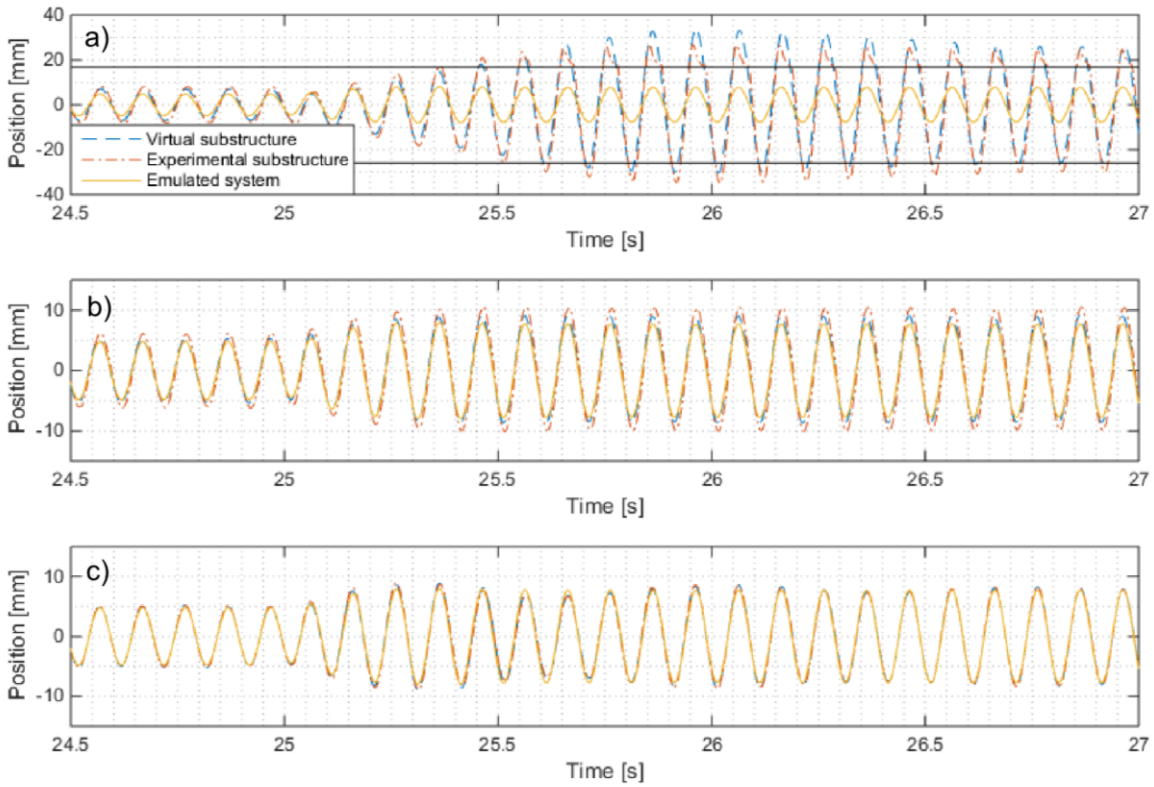

Figure 12: Hybrid test response with step change in numerical stiffness at 25s a) No compensation, b) passivity control applied, c) passivity control applied with adaptive feed-forward filtering

4 Conclusion

The performance of a combined control scheme based on normalized passivity control and adaptive feedforward filtering has been assessed in real-time hybrid testing. Passivity control was seen to maintain and restore stability in a single degree of freedom nonlinear real-time hybrid test by dissipating the spurious power injected to the system by the actuation hardware. The inability of passivity control to achieve good tracking is addressed through the application of adaptive feedforward filtering which synchronises numerical and physical substructure displacements in stable hybrid tests. The two schemes were seen to complement each other with passivity control demanding smaller virtual damper rates as the tracking error decreases overtime through the action of the adaptive feedforward filter. The scheme was found to be effective in hybrid tests with linear numerical substructures as well as those with discontinuities (a step change in stiffness), giving promise for a wide range of nonlinear systems to benefit from hybrid testing with the combined scheme used to mitigate actuator dynamics.

Future work will see the use of the combined compensation scheme in a multi degree of freedom hybrid test. Moreover, most work to date utilizes real-time hybrid testing with linear numerical substructures, whilst complex hybrid test systems are often tested on an extended time scale (pseudo-dynamic testing). The experiments presented in this paper illustrate the effectiveness of the combined control scheme in hybrid tests with numerical substructure discontinuity, which may encourage further applications of hybrid testing with nonlinear numerical substructures in the future.

Acknowledgements

This work has been supported through funding from the Engineering and Physical Sciences Research Council, grant reference EP/N032829/1. We the authors have no conflicts of interest to declare.

References

[1] H. K. Fathy, Z. S. Filipi, J. Hagena, and J. L. Stein, “Review of hardware-in-the-loop simulation and its prospects in the automotive area,” vol. 6228, p. 62280E–62280E–20, 2006.

[2] A. R. Plummer, “Model-in-the-Loop Testing,” *Proc. Inst. Mech. Eng. Part I J. Syst. Control Eng.*, vol. 220, no. 3, pp. 183–199, 2006.

[3] G. Lauss and K. Strunz, “Multirate Partitioning Interface for Enhanced Stability of Power Hardware-in-the-Loop Real-Time Simulation,” *IEEE Trans. Ind. Electron.*, vol. 66, no. 1, pp. 595–605, 2019.

[4] A. S. Abdelrahman, K. S. Algarny, and M. Z. Youssef, “A Novel Platform for Powertrain Modeling of Electric Cars With Experimental Validation Using Real-Time Hardware in the Loop (HIL): A Case Study of GM Second Generation Chevrolet Volt,” *IEEE Trans. Power Electron.*, vol. 33, no. 11, pp. 9762–9771, Nov. 2018.

[5] T. T. Nguyen, T. N. Dao, S. Aaleti, J. W. van de Lindt, and K. J. Fridley, “Seismic assessment of a three-story wood building with an integrated CLT-lightframe system using RTHS,” *Eng. Struct.*, vol. 167, pp. 695–704, 2018.

[6] M. Bolien, P. Iravani, J. L. du Bois, T. Richardson, and A. Robertsson, “Hybrid Tests

of Contact Events in Air-to-Air Refueling," *J. Aircr.*, vol. 55, no. 5, pp. 2092–2103, May 2018.
[7] J. L. du Bois, "Techniques for Nonlinear Real-time Hybrid Testing." Engineering and Physical Sciences Research Council, Bath, 2016.
[8] "HIL Testing Reduces CompactRIO Control System Development Cost," *National Insruments*, 2011. [Online]. Available: http://www.ni.com/newsletter/51000/en/.
[9] C. Ebert and C. Jones, "Embedded Software: Facts, Figures, and Future," *Computer (Long. Beach. Calif).*, vol. 42, no. 4, pp. 42–52, 2009.
[10] M. I. Wallace, D. J. Wagg, S. a. Neild, P. Bunniss, N. a. J. Lieven, and a. J. Crewe, "Testing coupled rotor blade–lag damper vibration using real-time dynamic substructuring," *J. Sound Vib.*, vol. 307, no. 3–5, pp. 737–754, 2007.
[11] J. du Bois, B. Titurus, and N. Lieven, "Transfer Dynamics Cancellation in Real-Time Dynamic Sub- structuring," *Proc. ISMA 2010*, pp. 1891–1914, 2010.
[12] T. Horiuchi, M. Inoue, T. Konno, and Y. Namita, "Real-time hybrid experimental system with actuator delay compensation and its application to a piping system with energy absorber," *Earthq. Eng. Struct. Dyn.*, vol. 28, no. 10, pp. 1121–1141, Oct. 1999.
[13] A. Darby, A. Blakeborough, and M. S. Williams, *Improved Control Algorithm for Real-Time Substructure Testing*, vol. 30. 2001.
[14] M. Ahmadizadeh, G. Mosqueda, and A. M. Reinhorn, "Compensation of actuator delay and dynamics for real-time hybrid structural simulation," *Earthq. Eng. Struct. Dyn.*, vol. 37, no. 1, pp. 21–42, Jan. 2008.
[15] Z. Tang, M. Dietz, Z. Li, and C. Taylor, "The performance of delay compensation in real-time dynamic substructuring," *J. Vib. Control*, vol. 0, no. 0, p. 1077546317740488, 2017.
[16] M. I. Wallace, D. J. Wagg, and S. a. Neild, "An adaptive polynomial based forward prediction algorithm for multi-actuator real-time dynamic substructuring," *Proc. R. Soc. A Math. Phys. Eng. Sci.*, vol. 461, no. May 2004, pp. 3807–3826, 2005.
[17] G. Bianchini, J. Bimbo, C. Pacchierotti, D. Prattichizzo, and O. A. Moreno, "Transparency-oriented passivity control design for haptic-enabled teleoperation systems with multiple degrees of freedom," in *2018 IEEE Conference on Decision and Control (CDC)*, 2018, pp. 2011–2016.
[18] Y. Dong and N. Chopra, "Passivity-Based Bilateral Tele-Driving System With Parametric Uncertainty and Communication Delays," *IEEE Control Syst. Lett.*, vol. 3, no. 2, pp. 350–355, 2019.
[19] L. D. H. Peiris, A. R. Plummer, and J. L. Du Bois, "Passivity Control in Real-Time Hybrid Testing," in *UKACC 12th International Conference on Control (CONTROL)*, 2018, pp. 317–322.
[20] L. D. H. Peiris, A. R. Plummer, and J. L. Du Bois, "Passivity Control for Nonlinear Real-time Hybrid Tests," *Proc. Inst. Mech. Eng. Part I J. Syst. Control Eng.*, 2020.
[21] L. D. H. Peiris, A. Plummer, and J. du Bois, "Normalised Passivity Control for Robust Tuning in Real-time Hybrid Tests," *Int. J. Robust Nonlinear Control*, 2020.
[22] P. Eamcharoenying, A. Hillis, and J. Darling, "Friction compensation using Coulomb friction model with zero velocity crossing estimator for a force controlled model in the loop suspension test rig," *Proc. Inst. Mech. Eng. Part C J. Mech. Eng. Sci.*, vol. 230, no. 12, pp. 2028–2045, Jun. 2015.
[23] M. Becherif, "Passivity-based control of hybrid sources: fuel cell and battery," *IFAC Proc. Vol.*, vol. 39, no. 12, pp. 585–590, 2006.
[24] A. Bartl, J. Mayet, and D. J. Rixen, "Adaptive feedforward compensation for real time hybrid testing with harmonic exciation," in *Proceedings of the 11th International Conference on Engineering Vibration*, 2015.

6.2 Summary

Passivity control based on a normalised power variable was used together with adaptive feed-forward filtering in a nonlinear real-time hybrid test. The main findings were as follows.

1) Used individually, passivity control was able to restore or maintain the stability of a real-time hybrid test.
2) Adaptive feed-forward filtering was designed to close the synchronisation error between the hybrid test substructures in stable systems.
3) Passivity control when used together with adaptive feed-forward filtering enabled the benefits of both schemes to be achieved – passivity control ensured stability whilst adaptive feedforward filtering closed the substructure position error overtime.
4) The combined scheme was found to be effective in improving stability and tracking of systems without information of the hybrid test system or actuator dynamics.
5) The combined scheme was seen to function as expected in a highly nonlinear hybrid test with cubic stiffening behaviour in the physical substructure, nonlinear friction in the actuator and a discontinuous parameter change in the numerical substructure.

Passivity control and adaptive feed-forward filtering have been found to be highly compatible with one another, each providing unique benefits to the hybrid test in terms of stability and tracking. With no information of the test system available prior to the commencement of the hybrid test, the combined scheme is greatly beneficial ensuring stability and good tracking in the presence of high nonlinearity and/or parametric changes. Thus far, most applications of hybrid testing have utilized linear numerical substructures and linear model-based compensation schemes. However, the results of this publication are expected to encourage more applications of nonlinear real-time hybrid testing with the use of this novel combined scheme of addressing actuator dynamics.

Chapter 7

The use of Passivity in stabilizing Adaptive Feed-forward Filters for Real-time Hybrid Tests

7.1 Context

One of the limitations of the adaptive feed-forward filtering control scheme is its instability when subject to high gains. Much like the controller gain of the energy-based passivity controller presented in chapters 3 and 4, the adaption gains of adaptive feed-forward controllers for optimal performance is dependent on the test conditions. Selection of a gain too low results in slow convergence whilst a gain too high results in instability. Moreover, the user is unable to raise the adaption gain in large increments without risking system instability. This chapter presents a journal paper which introduces a passivity-based scheme integrated into the design of the adaptive feed-forward filter in order to mitigate these limitations.

Power-based passivity control theory is utilized to schedule the parameters of the adaptive feed-forward controller such that the adaption gain is automatically decreased until the hybrid test is stable whenever excessive adaption gains are applied by the user. This enables high adaption gains to be used without resulting in an unstable system and is especially useful when fast convergence times are required. Stable nonlinear real-time hybrid tests are employed for this study. This work is another joint project undertaken with Dr. Andreas Bartl.

The passivity observer monitors the power flow from the numerical substructure to the actuator and the power flow from the physical substructure to the numerical substructure. When the actuator power outflow exceeds its inflow, the combined system of the actuator and the feed-forward filter adds power into the hybrid test which tends to cause instability. When an excess transfer system power surge is detected, the adaption gain steps down and the regularization parameter is increased to correct the feed-forward filter coefficients until passivity of the transfer system is restored.

The adaptive feed-forward filter in the following publication operates on a sample-wise basis, using only the last sample in the parameter vector update law, as with the implementation in chapter 6. Similarly, adaption begins with an estimate of the interface transfer matrix P which is obtained using the procedure presented in [59]. However, the power observing passivity controller no longer uses filters in its implementation, as stepping down the filter gains in the presence of unstable behaviour must be rapidly achieved. Moreover, the passivity controller triggers gain reduction when a specified passivity threshold is breached, thus alleviating the need for power flow normalisation. As such, the passivity-based gain monitoring scheme in the following publication depends only on state of passivity in the system at the present time step.

In order to assess the stability of the adaptive feed-forward filter, the hybrid tests of the following publication were implemented in open loop, i.e. the direct signal line from the numerical substructure to the actuator input is removed. The hybrid tests are run with initially unstable adaption gains and the passivity observer is then allowed to reduce this gain automatically until stable behaviour is seen when passivity of the transfer system is restored. Table 3 shows the controller parameters used in the hybrid tests.

Table 3: Adaptive feed-forward filter and passivity controller parameters

Parameter	Value
Passivity observer and adaptive feed-forward filter	
Initial adaption gain (μ_{init})	10
Passivity breach power generation limit	-1W
b_μ exponent	10
b_γ exponent	2
Initial regularisation parameter (γ_{max})	1
Number of harmonics (m)	1 (unless otherwise stated)
Number of actuator inputs (n)	1
Standard deviation allowed for θ elements	0.0005
Interface transfer matrix Identification time	10s
Solver	
Sample time	0.0001
ODE solver	ODE4 Runge-Kutta (Fixed step)

This declaration concerns the article entitled:									
Power-flow-based Stabilization for Adaptive Feed-Forward Filters in Hybrid Testing									
Publication status (tick one)									
Draft manuscript		**Submitted**		**In review**	✓	**Accepted**		**Published**	
Publication details (reference)	Andreas Bartl, L.D. Hashan Peiris, Jonathan L. du Bois, Daniel Rixen & Andrew Plummer "Power-flow-based Stabilization for Adaptive Feedforward Filters in Hybrid Testing", *Experimental Techniques*, 2019.								
Copyright status (tick the appropriate statement)									
I hold the copyright for this material	✓	Copyright is retained by the publisher, but I have been given permission to replicate the material here							
Candidate's contribution to the paper (provide details, and also indicate as a percentage)	**The candidate contributed to / considerably contributed to / predominantly executed the…** **Formulation of ideas:** • Idea to use passivity to adjust the parameters of the adaptive feed-forward filter, by colleague Dr. Andreas Bartl. • Selection of plots for presentation solely by Dr. Andreas Bartl. **Design of methodology:** Design of passivity control algorithm most suitable for use in adaptive feed-forward filtering controller, joint contribution with Dr. Andreas Bartl. Candidate's contribution (60%) Adaptive feed-forward filtering algorithm – solely by colleague Dr. A. Bartl. **Simulation work:** Solely by colleague Dr. Andreas Bartl. **Experimental work:** Experimental work carried out with Dr. Andreas Bartl. Breakdown of work as follows: • Setup and calibration of test rig, solely by the candidate (100%) • Conversion of simulation models to experiment files for real-time execution in controller hardware, candidate's contribution (80%) • Experiments done with Dr. Andreas Bartl. Candidate's contribution (50%) • Acquisition of data, solely by the candidate (100%) • Postprocessing of data for generation of plots by Dr. Andreas Bartl. **Presentation of data in journal format:** Solely by colleague Dr. Andreas Bartl.								
Statement from Candidate	This paper reports on original research I conducted during the period of my Higher Degree by Research candidature.								
Signed	L DH Peiris			**Date**	24/09/2019				

Paper Five: Power-flow-based Stabilization for Adaptive Feedforward Filters in Hybrid Testing

Power-flow-based Stabilization for Adaptive Feedforward Filters in Hybrid Testing

Andreas Bartl[1], L.D. Hashan Peiris[2], Jonathan L. du Bois[2], Daniel Rixen[1], Andrew Plummer[2*]

Tuesday 28th May, 2019

Abstract

Real-time hybrid testing is a technology which allows the coupling of simulations and component tests in order to simulate complex system dynamics. Delays and time lags caused by actuator dynamics and signal processing deteriorate the stability of the tests in many cases. The application of adaptive feedforward filters to hybrid testing enables circumventing this problem. The stability of the filter itself, however, can be affected by the choice of the algorithm parameters or changes in dynamics of the system being tested. Test safety requirements and practical considerations require a failsafe implementation. In this paper, we propose a method for adjusting the parameters of the adaptive feedforward filter based on power-flows in the test setup. The objective is to maintain a passive behavior of the actuation and control system. The stabilization acts on the leakage factor and the adaptation gain of a least-mean-squares adaptation law. A simple numerical system is used to investigate the effect of the algorithm parameters on the stabilization. The method was applied to an experimental setup including a nonlinear stiffness. Several originally unstable configurations were stabilized, the adaptation process could be continued and interface synchronization was achieved in all test cases.

1 Introduction

Real-time hybrid testing—also referred to as real-time dynamic substructuring—is a method for implementing realistic dynamical tests of components of complex systems. The system is split into a virtual system—which is simulated in real time—and an experimental component which is physically present in the test. Applications of the method have been reported in various fields as in aerospace, automotive, civil and mechanical engineering. In literature, a large number of use cases have been described. To name only a few examples: Satellite tests using hybrid approaches are proposed in [1], [2] describes air-to-air refilling scenarios and [3] proposes the tests on chassis dynamics of cars in combination with aerodynamic simulations. The objective of any Real-time hybrid testing technology is to test the experimental component under realistic boundary conditions. To do so, the dynamics of the virtual component are coupled to the test rig during the test, using an actuation system. Actuators apply forces to the interface of the experimental component, while sensors measure interface forces and interface displacements. Most test setups make time lags and delays inevitable. Frequency-dependent time lags are caused by the dynamics of the actuators. Delays are caused by the computational and communication processes as well as by signal-processing procedures. Time lags and delays can cause instability or inaccuracies if occurring in a test without a further compensation technique. To overcome these stability problems, a number of methods have been proposed in hybrid-testing literature. [4] suggests using a polynomial forward prediction scheme which compensates for delay and amplitude errors. Based on this work, [5] introduces an additional adaptation scheme which tunes phase shifts and amplitude corrections according to errors at the zero crossings. Other methods for delay compensation and interface synchronization include the application of model reference adaptive control by [6], inverted models of the actuation system by [7] and model predictive control by [8]. [9] applies a passivity based control method to real-time hybrid testing.

Fig. 1 gives an example of an application of hybrid tests to a structural dynamic system: The objective of the test is to analyze the influence of different designs of drive trains and transmission cross beams on the vibration behavior of a car. The body in white is a complex structure which is hard to model, while the transmission cross beam and the drive train are only available as models and their design frequently changes during the design process. A hybrid testing approach allows to couple the physical body in white to the model of the transmission system. Applications where structural systems are coupled often exhibit high model density and low damping. This fact makes the application of feedback-based methodology using low-order

*Authors are with the Chair of Applied Mechanics, Technical University of Munich, Boltzmannstr. 15, 85748 Garching, Germany[1] and the Centre for Power Transmission and Motion Control, University of Bath, Claverton Down, Bath BA2 7AY, United Kingdom[2] andreas.bartl@tum.de

models challenging. Adaptive feedforward filters offer an alternative in this field. Instead of closing the control loop directly, feedforward filters generate the actuator input using the external excitation forces as an input signal. Since the structure of the filter is not known beforehand, information on the interface gap is used in an update law to adapt the filter coefficient such that virtual and experimental component are coupled. An approach based on feedforward filters has been applied to the testing of piezoelectric actuators in [10]. The application to problems with multiple degree-of-freedom interfaces has been addressed in [11].

The work in this paper is based on least-mean-square filters as it is described in [12]. Adaptation gains are parameters which define the aggressiveness of the adaptation. Despite the fact that adaptive feedforward-filter-based methods show more robust stability properties than their feedback counterparts, adaptation gains have to be selected with care. High adaptation gains, insufficient plant identification or changes in the system dynamics during the test can lead to unstable filter dynamics. We address the problem with an approach inspired by passivity-based techniques from the fields of teleoperation, force reflection, robotic impedance control, and haptic interfaces. These cases relate to hybrid testing, since in all problem settings physical systems are coupled via an actuation and sensing system, and delay and time lag frequently degenerate system performance. In teleoperation, the environment exhibits unknown dynamics and the communication link can show significant delays. Many works in this field employ passivity-based methods. The reason is that passivity is a sufficient condition for stability. The system stability can be concluded from assessing the subsystem separately. Additionally, passivity theory is not limited to linear systems but applies to non-linear systems as well. A system is passive if the energy inflow is higher than the energy outflow for all the time. The work of [13] and [14] introduce methods based passivity which utilize wave variables to make the

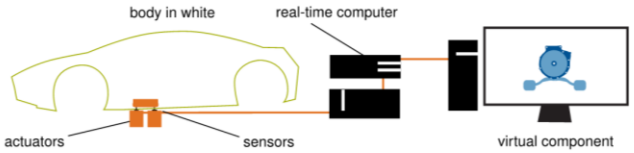

Figure 1: Application case: The virtual component can be optimized with respect to its effect on the body in white's vibrations.

communication line passive. Passivity-based methods have been applied to robotic impedance control such as e.g. in [15]. [16] proposes a control scheme for haptic interfaces which uses adaptive dissipative elements to ensure passivity. The technique presented in [9] is a passivity-based approach to hybrid testing. The method implements a variable rate virtual damping element to the numerical substructure to ensure the passivity of the transfer system. The damping-coefficient is controlled by the excess energy added to the hybrid system by the actuator. In this paper, we propose a method which uses the power flow as a measure to update the adaptation parameters in the case of unstable behavior caused by a large adaptation gain set by the user. The technique restores filter stability and subsequently enables adaptation with accurate synchronization in all investigated test cases. The paper is organized as follows: Section II introduces a hybrid-testing method based on adaptive feedforward filters. The power flow supervision approach is presented in section III. Section IV gives an overview of the influence of the algorithm parameters using an exemplary numerical simulation. In section V, the experimental results of tests with a physical duffing oscillator are analyzed.

2 Coupling Problem and Adaptive Feedforward Filters

Coupling between virtual and experimental components is achieved if the interface displacements of the virtual and the experimental component match and if the interface forces are in equilibrium. In order to apply adaptive feedforward filters to the problem, we make use of the control structure depicted in Fig. 2. The equilibrium is imposed by applying the measured interface forces of the experimental component onto the virtual component. Using a controller, the interface compatibility constraint is then enforced by providing appropriate input to the actuation system. It is noteworthy that control strategies other than adaptive feedforward filtering can be applied in this framework. Eqs. (1) describe the virtual component's dynamics in

state-space form using the symbols $\boldsymbol{M}^{VIR}$ $\boldsymbol{D}^{VIR}$ and $\boldsymbol{K}^{VIR}$ for mass, damping and stiffness matrices and the state vector $\boldsymbol{x}^{VIR}$.

$$\begin{aligned}\dot{\boldsymbol{x}}^{VIR} &= \underbrace{\begin{bmatrix}\boldsymbol{0} & \boldsymbol{I}\\ -\boldsymbol{M}^{VIR-1}\boldsymbol{K}^{VIR} & -\boldsymbol{M}^{VIR-1}\boldsymbol{D}^{VIR}\end{bmatrix}}_{\boldsymbol{A}^{VIR}}\boldsymbol{x}^{VIR} + \underbrace{\begin{bmatrix}\boldsymbol{0}\\ \boldsymbol{M}^{VIR-1}\boldsymbol{G}^{VIR\,T}\end{bmatrix}}_{\boldsymbol{B}_{\lambda}^{VIR}}\boldsymbol{f}_b^{VIR} + \underbrace{\begin{bmatrix}\boldsymbol{0}\\ \boldsymbol{M}^{VIR-1}\end{bmatrix}}_{\boldsymbol{B}_{ext}^{VIR}}\boldsymbol{f}_{ext}^{VIR}\\ \boldsymbol{y}^{VIR} &= \boldsymbol{C}_y^{VIR}\boldsymbol{x}^{VIR}\end{aligned} \tag{1}$$

The interface forces are denoted by $\boldsymbol{f}_b^{VIR}$. $\boldsymbol{G}^{VIR}$ is the matrix mapping the interface forces onto the system coordinates. The

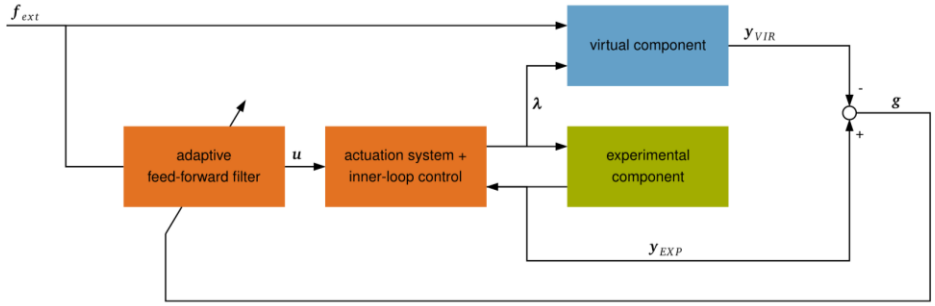

Figure 2: General control structure: Interface equilibrium is enforced by imposing the measured interface forces on the virtual component. A feedback controller reduces the interface gap $\boldsymbol{g}$ such that the system meets the compatibility constraints.

external excitation forces are denoted by $\boldsymbol{f}^{ext}$ and the output matrix for the interface displacements is denoted by $\boldsymbol{C}_y^{VIR}$. Being assembled in the test rig, the experimental component may influence the dynamics of the actuation system. Using the coupled dynamics of the actuation system and the experimental component in the following section accounts for this feedback. Note that the actuation system may contain an inner-loop control with actuator-specific features such as friction compensation. Eqs. (2) describe the dynamics of the actuation system and the experimental component in state-space form:

$$\begin{aligned}\dot{\boldsymbol{x}}^{EXP} &= \boldsymbol{A}^{EXP}\boldsymbol{x}^{EXP} + \boldsymbol{B}_u^{EXP}\boldsymbol{u} + \boldsymbol{B}_{ext}^{EXP}\boldsymbol{f}_{ext}^{EXP}\\ \boldsymbol{y}^{EXP} &= \boldsymbol{C}_y^{EXP}\boldsymbol{x}^{EXP}\\ \boldsymbol{\lambda} = \boldsymbol{f}_b^{EXP} &= \boldsymbol{C}_{\lambda}^{EXP}\boldsymbol{x}^{EXP} + \boldsymbol{D}_u^{EXP}\boldsymbol{u} + \boldsymbol{D}_{ext}^{EXP}\boldsymbol{f}_{ext}^{EXP}\end{aligned} \tag{2}$$

Here $\boldsymbol{A}^{EXP}$, $\boldsymbol{B}_u^{EXP}$, $\boldsymbol{B}_{ext}^{EXP}$, $\boldsymbol{C}_y^{EXP}$ and $\boldsymbol{C}_{\lambda}^{EXP}$ are the the state-space matrices, and $\boldsymbol{x}^{EXP}$ is the state vector. The inputs to the system are the actuator demand signal $\boldsymbol{u}$ and the external forces acting on the experimental component. The interface displacement of the experimental component $\boldsymbol{y}^{EXP}$ and the interface forces $\boldsymbol{f}_b^{EXP}$, namely the inner forces between the virtual and experimental substructures, are defined as the outputs of the system. The open-loop dynamics—which are later controlled such that the compatibility constraint is met—are given by Eq. (3). The interface force vector $\boldsymbol{f}_b^{VIR}$ is eliminated by applying the output of the actuation system to the virtual component. In practice, this involves measuring the interface forces between the actuator system and the experimental component. We refer to the equilibrium interface forces as $\boldsymbol{\lambda}$.

$$\boldsymbol{\lambda} = \boldsymbol{f}_b^{EXP} = -\boldsymbol{f}_b^{VIR} \tag{3}$$

Actuator demand and external forces on both subcomponents are defined as system inputs, and the interface gap $\boldsymbol{g}$ is defined as system output. The interface gap $\boldsymbol{g}$ is the difference between the virtual component's and the experimental component's interface displacements.

$$\begin{aligned}\dot{\boldsymbol{x}} &= \underbrace{\begin{bmatrix}\boldsymbol{A}^{VIR} & \boldsymbol{B}_{\lambda}^{VIR}\boldsymbol{C}_{\lambda}^{EXP}\\ \boldsymbol{0} & \boldsymbol{A}^{EXP}\end{bmatrix}}_{\boldsymbol{A}}\boldsymbol{x} + \underbrace{\begin{bmatrix}\boldsymbol{B}_{\lambda}^{VIR}\boldsymbol{D}_u^{EXP}\\ \boldsymbol{B}_u^{EXP}\end{bmatrix}}_{\boldsymbol{B}_u}\boldsymbol{u} + \underbrace{\begin{bmatrix}\boldsymbol{B}_{ext}^{VIR} & \boldsymbol{B}_{\lambda}^{VIR}\boldsymbol{D}_{ext}^{EXP}\\ \boldsymbol{0} & \boldsymbol{B}_{ext}^{EXP}\end{bmatrix}}_{\boldsymbol{B}_{ext}}\boldsymbol{f}_{ext}\\ \boldsymbol{g} &= \underbrace{\begin{bmatrix}\boldsymbol{C}_y^{VIR} & -\boldsymbol{C}_y^{EXP}\end{bmatrix}}_{\boldsymbol{C}}\boldsymbol{x} \quad \text{with} \quad \boldsymbol{x} = \begin{bmatrix}\boldsymbol{x}^{VIR^T} & \boldsymbol{x}^{EXP^T}\end{bmatrix}^T \quad \text{and} \quad \boldsymbol{f}_{ext} = \begin{bmatrix}\boldsymbol{f}_{ext}^{VIR^T}\boldsymbol{f}_{ext}^{EXP^T}\end{bmatrix}^T\end{aligned} \tag{4}$$

Eqs. (5) shows the time-domain solution of interface gap $\boldsymbol{g}$. The solution is a combination of contributions from actuator input, external forces and initial conditions. The contributions from the actuator input and the external forces can be expressed as convolutions between the impulse responses $\boldsymbol{h}_u$ and $\boldsymbol{h}_{exp}$ and the inputs.

$$\boldsymbol{g}(t) = \int_{t_0}^{t} \underbrace{\boldsymbol{C}\mathrm{e}^{\boldsymbol{A}(t-\tau)}\boldsymbol{B}_u}_{\boldsymbol{h}_u(t-\tau)} \boldsymbol{u}(\tau)\mathrm{d}\tau + \int_{t_0}^{t} \underbrace{\boldsymbol{C}\mathrm{e}^{\boldsymbol{A}(t-\tau)}\boldsymbol{B}_{ext}}_{\boldsymbol{h}_{ext}(t-\tau)} \boldsymbol{f}_{ext}(\tau)\mathrm{d}\tau + \boldsymbol{C}\mathrm{e}^{\boldsymbol{A}t}\boldsymbol{x}(t_0) \tag{5}$$

The objective of any controller is to close the interface gap. In many applications, harmonic excitation occurs. The harmonic excitation force $\boldsymbol{f}_{ext}(t)$ with the excitation frequencies Ω_i and $i \in [1 \dots n_{exc}]$ is given in Eq. (6).

$$\boldsymbol{f}_{ext}(t) = \sum_{i=1}^{n_{exc}} \boldsymbol{a}_i \cos(\Omega_i t) + \boldsymbol{b}_i \cos(\Omega_i t) \tag{6}$$

Assuming steady-state and harmonic excitation, the interface gap can be closed by applying a harmonic signal as the actuator input. The actuator input in Eq. (7) is constructed by the multiplication of a harmonic basis function matrix $\boldsymbol{W}(t)$ and the parameter vector $\boldsymbol{\theta}$. The matrix $\boldsymbol{W}(t)$ contains sinusoidal functions using the excitation frequencies and their multiples. The total number of frequencies contained in the basis function matrix $\boldsymbol{W}(t)$ is n_Ω. Using multiples of the excitation frequencies in the basis functions higher harmonics in slightly nonlinear systems can be compensated for. The parameter vector controls amplitude and phase of the actuator input signal $\boldsymbol{u}$. Note that we use the time-discrete form of the signals which can be retrieved by setting in $t = k\Delta t$ with time instance k and time-step width Δt. The number of the time instance is indicated with square brackets.

$$\boldsymbol{u}[k] = \underbrace{\begin{bmatrix} \boldsymbol{I}\cos\Omega_1 k\Delta t \\ -\boldsymbol{I}\sin\Omega_1 k\Delta t \\ \vdots \\ \boldsymbol{I}\cos\Omega_{n_\Omega} k\Delta t \\ -\boldsymbol{I}\sin\Omega_{n_\Omega} k\Delta t \end{bmatrix}^T}_{\boldsymbol{W}[k]} \boldsymbol{\theta}[k] \tag{7}$$

Using the Fourier transform $\mathfrak{F}(\boldsymbol{h}_u(t)) = \boldsymbol{H}_u(\omega)$ of the impulse response $\boldsymbol{h}_u(t)$ and neglecting the transient terms, the interface gap $\boldsymbol{g}(t)$ can be written in the matrix-vector form of Eq. (8). A proof is shown in [11]. The expression contains the basis function matrix $\boldsymbol{W}(t)$, the transfer function matrix $\boldsymbol{P}_{gu}$ and the parameter vector $\boldsymbol{\theta}$ as well as the contribution of the external excitations $\boldsymbol{g}_{ext}$. The objective of the adaptation law is now to find a parameter vector $\boldsymbol{\theta}$ such that $\boldsymbol{g}(t) = \boldsymbol{0}$ holds.

$$\boldsymbol{g}[k] = \boldsymbol{W}[k] \underbrace{\begin{bmatrix} \mathrm{Re}(\boldsymbol{H}_u(\Omega_1)) & -\mathrm{Im}(\boldsymbol{H}_u(\Omega_1)) & & & \\ \mathrm{Im}(\boldsymbol{H}_u(\Omega_1)) & \mathrm{Re}(\boldsymbol{H}_u(\Omega_1)) & & & \\ & & \ddots & & \\ & & & \mathrm{Re}(\boldsymbol{H}_u(\Omega_{n_\Omega})) & -\mathrm{Im}(\boldsymbol{H}_u(\Omega_{n_\Omega})) \\ & & & \mathrm{Im}(\boldsymbol{H}_u(\Omega_{n_\Omega})) & \mathrm{Re}(\boldsymbol{H}_u(\Omega_{n_\Omega})) \end{bmatrix}}_{\boldsymbol{P}_{g,u}} \boldsymbol{\theta}[k] + \boldsymbol{g}_{ext}[k] \tag{8}$$

Eq. (9) gives the objective function for the adaptation law which is the sum of the squared interface gap and a regularization term. The regularization term contains the squared parameter vector $\boldsymbol{\theta}$ and the regularization parameter γ.

$$J[k] = \boldsymbol{g}^T[k]\boldsymbol{g}[k] + \gamma\boldsymbol{\theta}^T\boldsymbol{\theta} \tag{9}$$

The least least-mean-squares (LMS) update law for the parameter vector $\boldsymbol{\theta}$ given in Eq. (10) is basically a gradient descent algorithm. The gradient of the objective function can be calculated using the transfer matrix $\boldsymbol{P}_{gu}$, the basis function matrix $\boldsymbol{W}(t)$ and the interface gap $\boldsymbol{g}$. The adaptation gain $\bar{\mu}$ controls the convergence speed of the adaptation process. High values of $\bar{\mu}$ may result in an unstable adaptation process. The leakage factor ν stems from the regularization term in the objective function. In this paper, the leakage factor is used to reduce the filter coefficient in the case of an unstable behavior. Besides a choice of $\bar{\mu}$ the matrix $\boldsymbol{P}_{gu}$ is critical to the stability and the quality of the adaptation process. Since the actual values of matrix $\boldsymbol{P}_{gu}$ are not known beforehand, the matrix has to be estimated. Usually $\boldsymbol{P}_{gu}$ is identified in an identification phase which precedes the

adaptation phase. Errors in the identification or changes in the system dynamics can lead to the instability of the adaptation process.

$$\boldsymbol{\theta}[k+1] := \nu\boldsymbol{\theta}[k] - \bar{\mu}\boldsymbol{P}_{g,u}^{T}\boldsymbol{W}[k]^{T}\boldsymbol{g}[k] \qquad \text{with} \qquad \nu = 1 - \bar{\mu}\gamma \tag{10}$$

In order to make the choice of the adaptation gain more practicable, we use a normalized adaptation gain μ according to Eq. (11). The normalization makes use of the maximum eigenvalue λ_{max} of the matrix $\boldsymbol{P}_{g,u}^{T}\boldsymbol{P}_{g,u}$. See e.g. [17] for a derivation of the expressions. In theory, a normalized adaptation gain of $\mu = 1$ results in the fastest possible convergence. Changes in the system dynamics and inaccuracy in the identification process may bring the maximum adaptation gain down to a lower value.

$$\bar{\mu} = \mu \frac{1}{\lambda_{max} + \gamma} \tag{11}$$

3 Power-flow Supervision

In order to overcome the aforementioned stability issues, we propose the use of a supervisor which reduces the adaptation gain μ whenever necessary. To do so, we analyze the power-flows between the subcomponents. Those power-flows are closely linked to passivity properties of the hybrid test. Passive systems are defined as systems which consume energy but do not produce energy. Coupling two arbitrary passive systems results in a passive overall system. One can think of the control system and actuation system of a hybrid test as an interconnection device between the virtual and the experimental component. We refer to this combination of the control system and the actuation system as the "transfer system" in this section. If the transfer system and the subcomponents are passive, the test setup is guaranteed to be passive. This implies that energy is only injected through external forcing on the virtual or the experimental component but not through the transfer system. Fig. 3 shows the power-flows in a hybrid test using adaptive feedforward filters. The transfer system is referred to as "passive" if the power-inflow into the system is always larger than the power-outflow. The power-inflow P_{in}^{ACT} to the transfer system is the sum of the power-inflow from the experimental component and the power-inflow from the virtual component. Both are the product of collocated interface forces and interface velocities. As a result, the power-inflow to the transfer system in Eq. (12) is the product of interface forces and the time derivative of the interface gap.

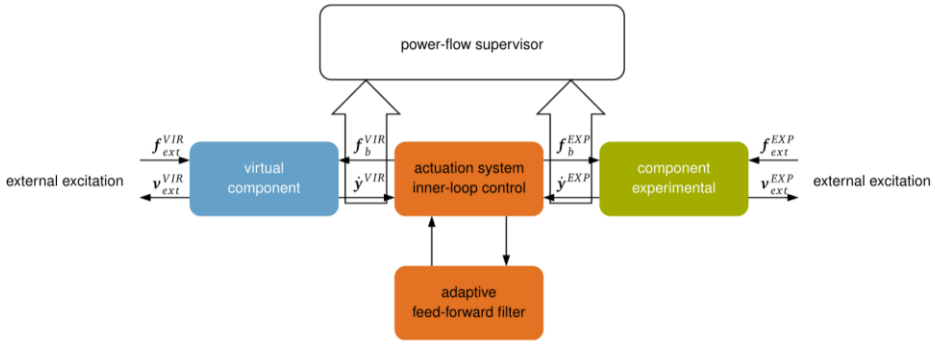

Figure 3: Power-flow diagram and power-flow supervisor

$$P_{in}^{ACT} = \boldsymbol{f}_{b}^{VIR}\dot{\boldsymbol{y}}_{VIR} + \boldsymbol{f}_{b}^{EXP}\dot{\boldsymbol{y}}_{EXP} = -\boldsymbol{\lambda}\dot{\boldsymbol{y}}_{VIR} + \boldsymbol{\lambda}\dot{\boldsymbol{y}}_{EXP} = \boldsymbol{\lambda}\dot{\boldsymbol{g}} \tag{12}$$

A negative power-inflow into the transfer system—or in other words a power-outflow from the transfer system—implies undesirable energy injection into the hybrid test. In order constrain the power-outflow of the transfer system which deteriorates its passive nature, we introduce a limit to the power-outflow P_{lim}. The limit $P_{lim} < 0$ is a negative value specific to the required power-outflow limit of the test. The objective of the power-flow supervision is to constrain the power-flow according to Eq. (13).

$$\lim_{t\to\infty} P_{in}^{ACT} \geq P_{lim} \tag{13}$$

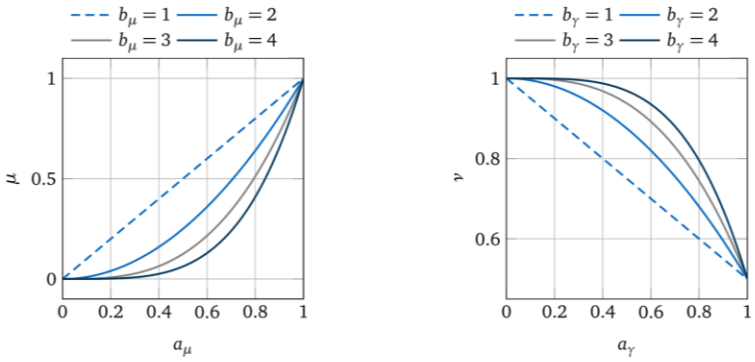

Figure 4: Parameter adjustment functions

Note that the energy inflow is defined as the time integral of the power-inflow:

$$E_{in}^{ACT} = \int_0^t P_{in}^{ACT}(\tau)\mathrm{d}\tau$$

Following a simple heuristic approach, as a result of the violation of the passivity constraint, the two parameters μ and γ of the adaptation algorithm are adjusted. The objective is to reduce the actuator amplitudes, to restore passivity and to enable fast adaptation. Approaches such as [18] where the leakage factor is adjusted according to the algorithm's performance have been proposed in literature. The stability and the convergence of the least-mean-squares algorithm is controlled by the adaptation gain μ: A high adaptation gain μ leads to a fast convergence of the filter coefficients, but high values can lead to the unstable behavior of the algorithm. In contrast, lower values of μ cause a slower convergence but stability is ensured if the value falls below the stability threshold. As a consequence, the adaptation gain μ is reduced using the exponential function in Eq. (14) with the initial adaptation gain μ_{init}, the variable a_μ and the user-defined exponent $b_\mu \geq 1$. The reasons for using an exponential function are to enable a faster drop of the adaptation gain μ in the initial phase, to ensure a fast restoration of passivity and a slower change in μ if it is closer to its optimal value. Fig. 4 shows the functions for some exemplary values b_μ.

$$\mu = \mu_{init} \cdot a_\mu^{b_\mu} \qquad \text{with} \qquad \mu \in [0,\ \mu_{init}] \quad \forall \quad a_\mu \in [0,\ 1] \tag{14}$$

The initial value is $a_\mu = 1$. If the power-inflow to the actuation system falls below the threshold P_{lim}—meaning that the system is not passive—the variable a_μ is reduced by the user-defined step-size parameter $\Delta_\downarrow a_\mu$. The lower bound for the variable a_μ is zero. As a result, the adaptation gain is bound by zero and the initial adaptation gain μ_{init}. The leakage factor ν results from the regularization factor γ according to Eq. (10). A low leakage factor—or equivalently, a high regularization factor—enforces lower filter coefficients. It is desirable to reduce the filter coefficients after a violation of the passivity constraint is detected. After the passive state is restored by the drop in the adaptation gain μ, the regularization should be reduced to ensure that the filter coefficients are adapted accurately to their optimal values. The regularization parameter γ is calculated using the exponential function in Eq. (15) with the user-defined maximum regularization factor γ_{max}, the variable a_γ and the user-defined exponent $b_\gamma \geq 1$. Fig. 4 shows the functions for some exemplary values b_γ. The nature of the exponential function leads to a progressive behavior of the leakage: In cases of severe power-outflow, the filter coefficients fall faster.

$$\gamma = \gamma_{max} \cdot a_\gamma^{b_\gamma} \qquad \text{with} \qquad \nu = 1 - \bar{\mu}\gamma \qquad \text{and} \qquad \nu \in [1 - \bar{\mu}\gamma_{max},\ 1] \quad \forall \quad a_\gamma \in [0,\ 1] \tag{15}$$

The initial value is $a_\gamma = 0$. If the power-inflow to the actuation system P_{in}^{ACT} falls below the threshold P_{lim}—meaning that the system is not passive—the variable a_γ is increased by the user-defined step-size parameter $\Delta_\uparrow a_\gamma$. If the power-inflow to the actuation system P_{in}^{ACT} rises above the threshold P_{lim}—meaning that the system is assumed to be passive—the variable a_γ is reduced by the user-defined step-size parameter $\Delta_\downarrow a_\gamma$. The lower bound for the variable a_γ is zero and the upper bound is 1. As a result, the adaptation gain is bound by one and $1 - \bar{\mu}\gamma_{max}$. The complete procedure including the adaptation of μ and ν is summarized in the pseudo-code of Alg. 1.

Algorithm 1 Power supervision for adaptive feedforward filters in hybrid testing

Initialize $a_\gamma := 0$ and $a_\mu := 1$
while adaptation is running **do**
  if $P_{in}^{ACT} < P_{lim}$ **then**
    Set $a_\gamma := \min(a_\gamma + \Delta_\uparrow a_\gamma, 1)$
    Set $a_\mu := \max(a_\mu - \Delta_\downarrow a_\mu, 0)$
  end if
  if $P_{in}^{ACT} > P_{lim}$ **then**
    $a_\gamma := \max(a_\gamma - \Delta_\downarrow a_\gamma, 0)$
  end if
  Set $\gamma := \gamma_{max} \cdot a_\gamma^{b_\gamma}$
  Set $\mu := \mu_{init} \cdot a_\mu^{b_\mu}$
end while

Virtual Component (VIR)	
m^{VIR}	$0.1\,\mathrm{kg}$
d^{VIR}	$0.05\,\frac{\mathrm{N\cdot s}}{\mathrm{m}}$
k^{VIR}	$1000\,\frac{\mathrm{N}}{\mathrm{m}}$

Experimental Component (EXP)	
m^{EXP}	$0.02\,\mathrm{kg}$
d^{EXP}	$0.05\,\frac{\mathrm{N\cdot s}}{\mathrm{m}}$
k^{EXP}	$1000\,\frac{\mathrm{N}}{\mathrm{m}}$

Actuator (ACT)	
m^{ACT}	$0.1\,\mathrm{kg}$
d^{ACT}	$1\,\frac{\mathrm{N\cdot s}}{\mathrm{m}}$
k^{ACT}	$100\,\frac{\mathrm{N}}{\mathrm{m}}$

Table 1: System parameters used in the numerical case study

4 Numerical Example of Choice of the Algorithm's Parameters

In order to demonstrate the effects of changes in the adaptation parameters a_μ and b_μ as well as the power-inflow limit P_{lim}, we make use of a simple numerical test case. The overall system emulated in the test is a lumped mass-spring-damper system as shown in Fig. 5. The system is split into a virtual component and an experimental component. In Fig. 5 the virtual component is depicted in blue and the experimental component is depicted in green. The experimental component is controlled via an actuation system, which is depicted in orange in Fig. 5. Since the adaptive feedforward filter exactly at the excitation frequencies measurement noise can cause a drift of the interface gap. A peak filter using the excitation frequency was applied at the actuator input in order to prevent those drift effects. The properties of the subsystems are listed in Tab. 1.

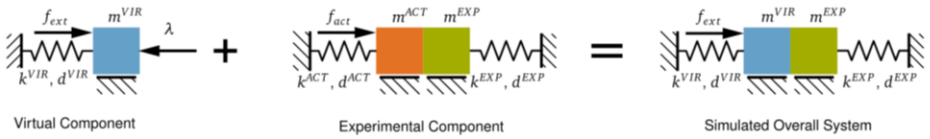

Figure 5: Lumped mass system used for the numerical experiment

4.1 Adaptation gain step-size $\Delta_\downarrow a_\mu$

The objective of the first numerical experiment is to investigate the influence of the changes in $\Delta_\downarrow a_\mu$. To do so, we varied the parameter $\Delta_\downarrow a_\mu$ while keeping the step-sizes $\Delta_\uparrow a_\gamma$ and $\Delta_\downarrow a_\gamma$, the exponents b_γ and b_μ, the initial adaptation-gain μ_{init}, the power-outflow P_{lim}, the excitation amplitude A_{ext} as well as the excitation frequency f_{ext} constant. Tab. 2 gives an overview of the parameters. Note that the initial adaptation-gain $\mu_{init} = 10$ is a high value, which causes an unstable system behavior without the passivity-preserving mechanism. As mentioned earlier, such instabilities can be caused in exactly the same way by an insufficient system identification process as well as as by changes in the system parameters. The values of the power-inflow P_{in}^{ACT}, the energy inflow E_{in}^{ACT}, the leakage-factor ν, the adaptation-gain μ, and the interface gap $\boldsymbol{g}$ are recorded during the simulation. The simulation includes a 50 s identification phase. The identification was performed according to the

Variable		Values			
step-size	$\Delta_{\downarrow} a_{\mu}$	0.0001	0.0004	0.0007	0.001
initial adaptation-gain	μ_{init}	10			
exponent	b_{μ}	10			
step-size	$\Delta_{\downarrow} a_{\gamma}$	0.001			
step-size	$\Delta_{\uparrow} a_{\gamma}$	0.01			
initial regularization factor	γ_{max}	1			
exponent	b_{γ}	2			
power-generation limit	P_{lim}	$-1\,\mathrm{W}$			
excitation amplitude	A_{ext}	$10\,\mathrm{N}$			
excitation frequency	f_{ext}	$50\,\mathrm{Hz}$			

Table 2: Parameters for the numerical experiment different adaptation-gain step-sizes $\Delta_{\downarrow} a_{\mu}$

procedure which is described in [11]. The long duration of the identification phase is chosen to rule out all possible influences of identification errors on the simulation. Fig. 8 shows the development of the adaptation-gain μ and the leakage-factor ν during the simulation. As expected, the decay rate of the adaptation-gain is higher for higher step-sizes $\Delta_{\downarrow} a_{\mu}$. The adaptation-gain reduction is activated when the passivity constraint is violated. Depending on the reduction step-size $\Delta_{\downarrow} a_{\mu}$, the adaptation-gain may overstep the optimal adaptation-gain or reach it gradually. The resulting adaptation-gains for the passive state vary: Higher step-sizes $\Delta_{\downarrow} a_{\mu}$ result in a lower end value. Lower step-sizes $\Delta_{\downarrow} a_{\mu}$ exhibit a slower decay of the adaptation-gain but result in μ being closer to the optimal value. The behavior of the leakage-factor ν with respect to the step-size $\Delta_{\downarrow} a_{\mu}$ follows the development of the adaptation-gain μ: For a fast decaying adaptation-gain μ, the drop in the leakage-factor is lower since passivity is restored faster. On the other hand, a slow decay in μ makes a larger drop in ν necessary.
Fig. 7 shows the power-inflow P_{in}^{ACT} to the actuator system, the energy inflow E_{in}^{ACT} to the actuator system and the envelope of the interface gap $\boldsymbol{g}$. Note that the power-inflow is normalized with the peak values of the power-inflow into the reference system $P_{in,max}^{REF}$, the energy-inflow is normalized with the peak values of the energy in the reference system E_{max}^{REF} and the interface gap is normalized with the amplitude of displacement of the reference system y_{amp}^{REF} The duration of the power-outflow of the actuator system is longer for lower step-size values $\Delta_{\downarrow} a_{\mu}$. For higher step-size values $\Delta_{\downarrow} a_{\mu}$ the duration gradually decreases. Accordingly, further energy injection is stopped after the settling of the algorithm. This fact can be seen in the diagram as the curves flatten after the settling time of the algorithm. It is noteworthy that the total energy outflow is highest for the lowest step-size values $\Delta_{\downarrow} a_{\mu}$. The interface gap is a measure for the synchronization of the interface between the virtual component and the experimental component. The step-size $\Delta_{\downarrow} a_{\mu} = 0.0001$ shows a high peak value of the interface gap, while with increasing values of the step-size $\Delta_{\downarrow} a_{\mu}$ the peak gradually decrease. The duration which is needed to reach synchronization improves in the same way for higher step-size values. The reason is that lower choices for the step-size $\Delta_{\downarrow} a_{\mu}$ result in higher amplitudes at the start of the adaptation phase. The higher resulting adaptation-gain μ, however, may result in a faster convergence later in the test. To conclude, there is a trade-off between the higher adaptation-gain and a longer duration of the passivity violation on the one hand, and lower adaptation-gains and shorter durations of the passivity violation on the other. Choosing $\Delta_{\downarrow} a_{\mu}$ determines the quality of the resulting adaptation-gain and the duration of passivity violations.

4.2 Leakage-factor step-size $\Delta_{\uparrow} a_{\gamma}$

The objective of the second numerical experiment is to investigate the influence of the changes to $\Delta_{\uparrow} a_{\gamma}$. The parameter $\Delta_{\uparrow} a_{\gamma}$ was varied while the step-sizes $\Delta_{\downarrow} a_{\mu}$ and $\Delta_{\downarrow} a_{\gamma}$, the exponents b_{γ} and b_{μ}, the initial adaptation-gain μ_{init}, power-outflow limit P_{lim}, the excitation amplitude A_{ext} as well as the excitation frequency f_{ext} remained constant. Tab. 3 gives an overview of the parameters. The values of the power-inflow P_{in}^{ACT}, the energy inflow E_{in}^{ACT}, the leakage-factor ν, the adaptation-gain μ, and the interface gap $\boldsymbol{g}$ are recorded during the simulation. As in the simulation described earlier in the text, a 50 s identification phase was applied. Fig. 8 shows the effects of changes in the leakage-factor step-size $\Delta_{\uparrow} a_{\gamma}$, on the leakage-factor and the

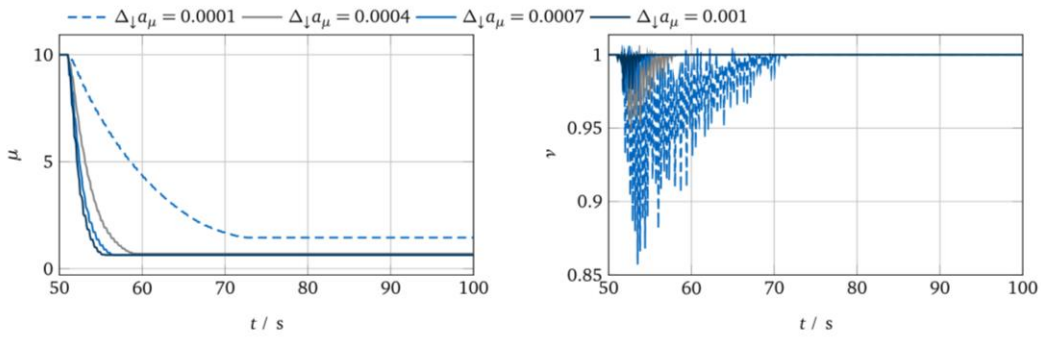

Figure 6: adaptation gain and leakage-factor for different adaptation-gain step-sizes $\Delta_\downarrow a_\mu$

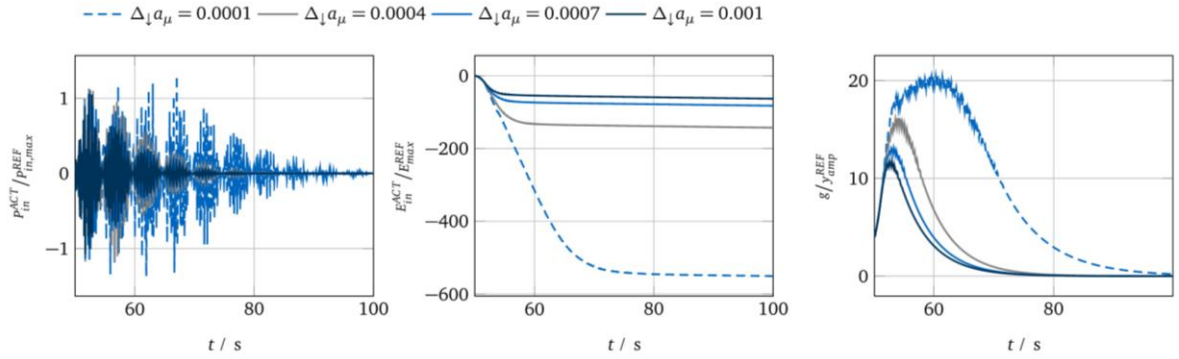

Figure 7: Power/energy inflow to actuator system and learning curve for varying adaptation-gain step-sizes $\Delta_\downarrow a_\mu$

adaptation-gain. As expected, higher step-sizes result in a larger drop in the leakage-factor. Since the lower leakage-factors reduce further power-outflow, the drop in the adaptation-gain μ is steeper and it settles faster for lower step-sizes $\Delta_\uparrow a_\gamma$. As a consequence, the duration of the reduction in the leakage-factor is higher for high values of $\Delta_\uparrow a_\gamma$.
Fig. 9 shows the power and energy inflow P_{in}^{ACT} and E_{in}^{ACT} as well as the envelope of the interface gap. The maximum power-outflows are close to the trigger value P_{lim} for higher step-size values $\Delta_\uparrow a_\gamma$. The reason is that lower leakage-factors allow the filter coefficient—and as a consequence the amplitudes—to drop faster. However, the increasing settling time prolongs the duration of the power-outflow. Equivalently, the curves for the energy inflow flatten later using higher values of $\Delta_\uparrow a_\gamma$. The total energy outflow is lowest for low values of $\Delta_\uparrow a_\gamma$. Similar effects can be observed for the interface gap: High values of $\Delta_\uparrow a_\gamma$ help to reduce the peak values of the interface gap but prolong the settling time to full synchronization.
To conclude, high values of $\Delta_\uparrow a_\gamma$ reduce the peak values of the power-outflow and of the interface gap but increase the settling-time. Consequently, a trade-off between settling time peak values has to be made.

4.3 Power-outflow limit P_{lim}

The objective of the third numerical experiment is to investigate the influence of the changes in the power-inflow limit P_{lim} which triggers the algorithm. As the trigger value P_{lim} is applied to the power-inflow values, it takes on negative values. During the numerical experiment, the step-sizes $\Delta_\downarrow a_\mu$, $\Delta_\uparrow a_\gamma$ and $\Delta_\downarrow a_\gamma$, the exponents b_γ and b_μ, the initial adaptation-gain μ_{init}, the excitation amplitude A_{ext} as well as the excitation frequency f_{ext} remained constant. Tab. 4 gives an overview of the parameters. The values of the power-inflow P_{in}^{ACT}, the energy inflow E_{in}^{ACT}, the leakage-factor ν, the adaptation-gain μ, and the interface gap g are recorded during the simulation. As in the simulation described earlier in the text, a 50 s identification phase was applied.
Fig. 10 shows the development of the adaptation-gain μ and the leakage-factors ν for a range of values of P_{lim}. The curves

Variable		Values			
step-size	$\Delta_{\downarrow} a_{\mu}$	0.0001			
initial adaptation-gain	μ_{init}	10			
exponent	b_{μ}	10			
step-size	$\Delta_{\downarrow} a_{\gamma}$	0.001			
step-size	$\Delta_{\uparrow} a_{\gamma}$	0.001	0.004	0.007	0.01
initial regularization factor	γ_{max}	1			
exponent	b_{γ}	2			
power-generation limit	P_{lim}	$-1\,\mathrm{W}$			
excitation amplitude	A_{ext}	$10\,\mathrm{N}$			
excitation frequency	f_{ext}	$50\,\mathrm{Hz}$			

Table 3: Parameters for the numerical experiment different leakage-factor step-sizes $\Delta_{\uparrow} a_{\gamma}$

Variable		Values			
step-size	$\Delta_{\downarrow} a_{\mu}$	0.0001			
initial adaptation-gain	μ_{init}	10			
exponent	b_{μ}	10			
step-size	$\Delta_{\downarrow} a_{\gamma}$	0.001			
step-size	$\Delta_{\uparrow} a_{\gamma}$	0.01			
initial regularization factor	γ_{max}	1			
exponent	b_{γ}	2			
power-generation limit	P_{lim}	$-0.1\,\mathrm{W}$	$-0.4\,\mathrm{W}$	$-0.7\,\mathrm{W}$	$-1\,\mathrm{W}$
excitation amplitude	A_{ext}	$10\,\mathrm{N}$			
excitation frequency	f_{ext}	$50\,\mathrm{Hz}$			

Table 4: Parameters for the numerical experiment varying power-outflow limit P_{lim}

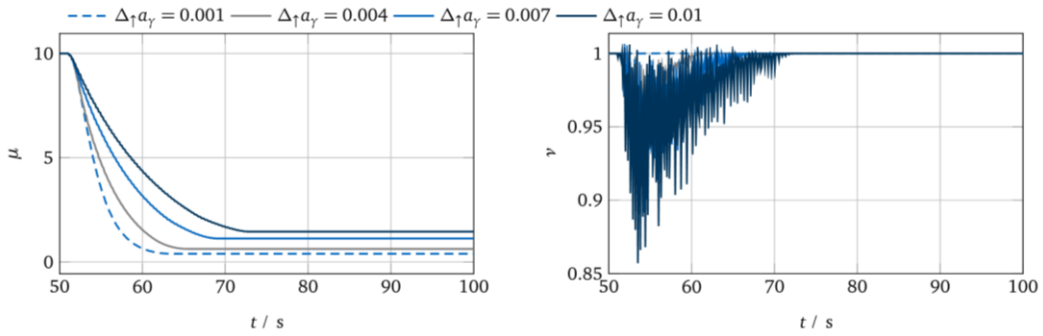

Figure 8: adaptation gain and leakage-factor for varying leakage-factor step-sizes $\Delta_\uparrow a_\gamma$

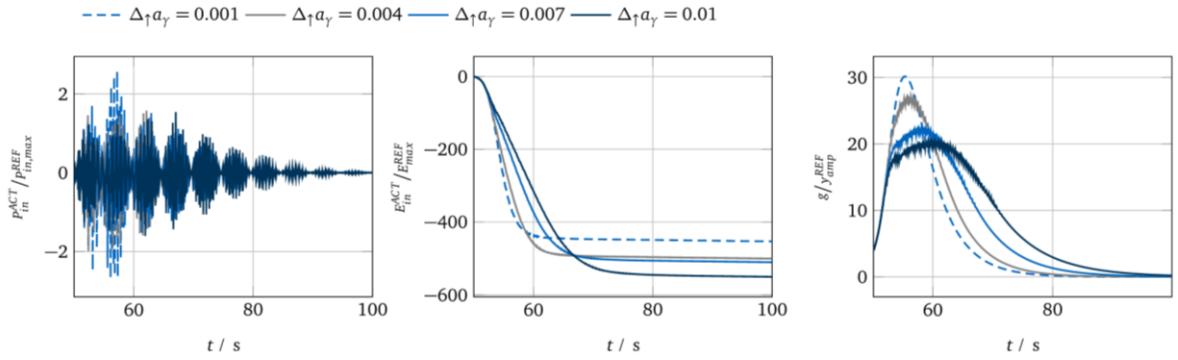

Figure 9: Power/energy inflow to actuator system and learning curve for varying leakage-factor step-sizes $\Delta_\uparrow a_\gamma$

for μ are shifted in time since the different values of P_{lim} trigger the reduction of the adaptation-gain at different points in time. Slopes and final values of μ are not affected significantly by the choice of P_{lim}. The duration of the drops in the leakage-factor ν are similar for all tested values of P_{lim}. However, the initial drop of ν is largest for the lowest trigger level $P_{lim} = 0.1$ W. The reason is that the initial drop is triggered by transient dynamics with amplitudes in the ranges of the trigger level $P_{lim} = 0.1$ W. Fig. 11 shows the power-inflow, energy inflow and interface gap over time. As expected, different trigger values of P_{lim} result in different maximum power-outflow values. The duration of the outflow is similar for all values. As a consequence, the peak values of the interface gap gradually decrease for tighter power-outflow limits. In summary, the power-outflow limit—even though it has only a minor influence on the final value of the adaptation-gain—influences the expected peak amplitudes of the test.

5 Experimental Validation

For the experimental validation of the approach, we use a cubic spring as a physical subcomponent and a linear lumped-mass system as a virtual subcomponent. The test setup is depicted in Fig. 12. The cubic spring, which performs as the experimental component, is achieved using two linear springs with all forces acting perpendicular to the spring axis. The expression for the spring force is given by Eq. (16). The spring constants k_3^{EXP} and k^{EXP} were identified using a least-mean-squares fit. They are given in Tab. 5.

$$f^{EXP} = k_3^{EXP} x^3 + k^{EXP} x \tag{16}$$

The virtual component is a mass-spring-damper system and receives the external forces. A linear actuator—a Copley

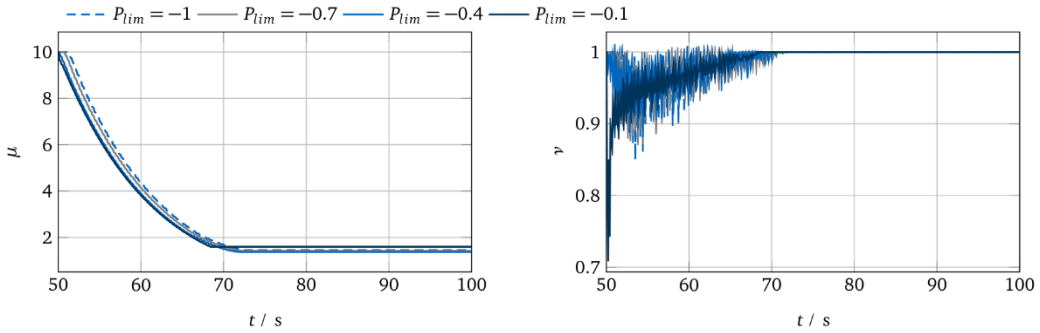

Figure 10: adaptation gain and leakage-factor for varying power-outflow limits P_{lim}

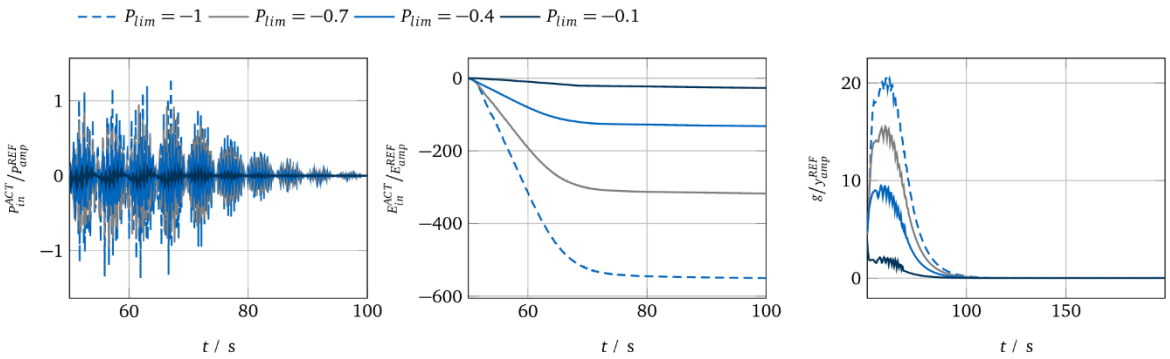

Figure 11: Power/energy inflow to actuator system and learning curve for varying power-outflow limits P_{lim}

Virtual Component (VIR)	
m^{VIR}	$1\,\mathrm{kg}$
d^{VIR}	$10\,\frac{\mathrm{N\cdot s}}{\mathrm{m}}$
k^{VIR}	$1000\,\frac{\mathrm{N}}{\mathrm{m}}$

Experimental Component (EXP)	
k^{EXP}	$1.95\,\frac{\mathrm{N}}{\mathrm{m}}$
k_3^{EXP}	$0.0014\,\frac{\mathrm{N}}{\mathrm{m}^3}$

Table 5: System parameters of the experimental setup

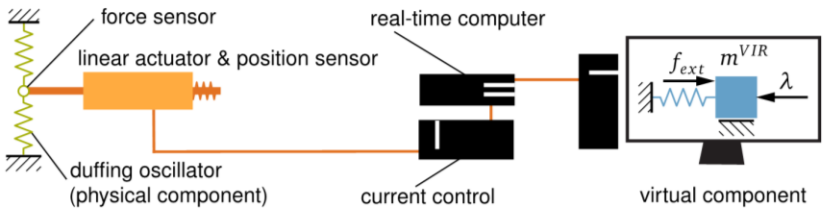

Figure 12: Test setup for the experimental validation of the approach

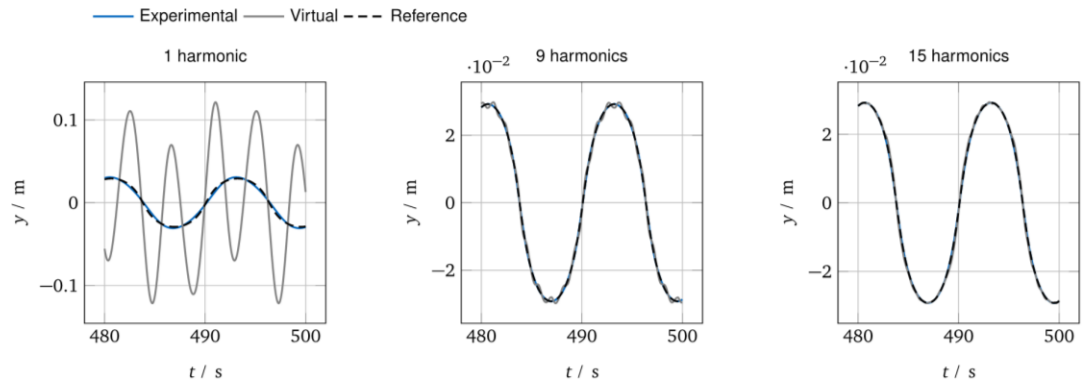

Figure 13: Exemplary interface displacements for excitation frequency 0.5 Hz and varying number of harmonics in basis function space. The excitation frequency was chosen such that the nonlinear behavior can be observed. In the first plot with one harmonic, the higher harmonic in the virtual component are excited through the interface forces but the higher harmonic interface displacement are not synchronized.

ST2508S electromagnetic linear actuator—applies the coupling forces to the experimental component. The actuator is controlled using a cascaded control scheme acting with a proportional term on the position demand, and with a proportional and integral term on the velocity demand. Friction has a significant effect on the actuator dynamics and, due to its non-linear nature the performance of hybrid-testing control schemes deteriorates. For that reason, a friction compensation scheme is implemented which acts on the input to the current control loop. The actuator operates with a position saturation at $2.5 \cdot 10^{-2}$ m around the initial position for safety reasons. The interface forces are measured using a custom-made force sensor. Since the adaptive feedforward filter exactly at the excitation frequencies measurement noise can cause a drift of the interface gap. A peak filter using the excitation frequency was applied at the actuator input in order to prevent those drift effects. The position is measured using the internal sensor of the linear actuator. The coupled system exhibits nonlinear dynamics due to the nature of the spring assembly. If this setup is excited with one harmonic component, the response will contain higher harmonics. The presence of these higher harmonics, in general, requires the enrichment of the basis function space with higher harmonics. This means that the frequencies Ω_k of the harmonics in the basis function matrix $\boldsymbol{W}(t)$ are defined as multiples of the periodic excitation basis frequency Ω_0:

$$\Omega_k = k\Omega_0 \qquad \text{with} \qquad k \in [1, 2, ..., n_\Omega]$$

Fig. 13 shows the effect of the additional harmonics in the basis function matrix of the simulated system. However, for the excitation frequencies and amplitudes described in this section, one harmonic basis function is sufficient to couple the virtual and the experimental component satisfactorily. Note that the proposed approach is applicable to any number of harmonics in the basis function matrix. The test is performed keeping the parameters $\Delta_\downarrow a_\mu$, $\Delta_\downarrow a_\gamma$, $\Delta_\uparrow a_\gamma$, b_μ, b_γ, γ_{max} and P_{lim} constant. As mentioned above, one harmonic was used in the basis function matrix $\boldsymbol{W}(t)$. The excitation frequencies Ω_0 are varied. The excitation amplitudes were adjusted to the excitation frequencies because the resulting response amplitudes had to remain

Variable		Values		
step size	$\Delta_{\downarrow} a_{\mu}$		0.001	
initial adaptation-gain	μ_{init}		0.1	
exponent	b_{μ}		2	
step size	$\Delta_{\downarrow} a_{\gamma}$		0.001	
step size	$\Delta_{\uparrow} a_{\gamma}$		0.01	
initial regularization factor	γ_{max}		1	
exponent	b_{γ}		2	
power-generation limit	P_{lim}		−0.3 W	
excitation amplitude	A_{ext}	10 N	40 N	40 N
excitation frequency	f_{ext}	10 Hz	20 Hz	30 Hz

Table 6: Parameters used in the experiment

within the actuator workspace. The initial adaptation-gain μ_{init} was selected such that the resulting adaptation process is unstable without the proposed algorithm. Since we want to validate the performance of the power-flow supervision, the test for each frequency was performed in two modes: one using power-flow supervision and one using the pure adaptive feedforward control law without power-flow supervision. In the first experiment the adaptive feedforward filter approach is applied without power-flow-based stabilization. As a result, the adaptation-gain μ and the leakage factor ν stay constant throughout the test. Due to the selection of the adaptation-gain μ, the dynamics of the filter are expected to be unstable. Fig. 14 shows the interface gap as well as the time-domain synchronization plots for all excitation frequencies. In all cases, unstable filter dynamics can be observed. The actuator operates in a state of saturation and the responses show undefined peaks. Fig. 15 exhibits the high power- and energy-outflow from the actuator system caused by the instability. The power-flow-based stabilization algorithm

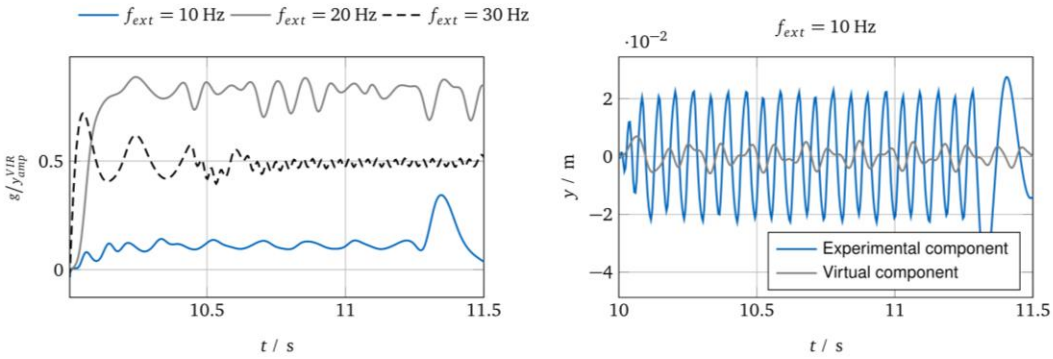

Figure 14: Unstable power and energy inflow to actuator system without power-flow supervision.

is activated in the second experiment. The adaptation-gains μ in Fig. 16 correspondingly drop to a value which allows the stable operation of the filter. The leakage factor ν also drops to values of 0 in the phases where the power-flow constraint is violated. Fig. 17 shows the power and energy outflow due to the initially unstable behavior. The maximum power-outflow is constrained to approximately 3 W. In the energy-outflow plot, a slight energy outflow can be observed after the stabilization of the test. The reason for this effect is stick-slip friction effects which are not compensated for by the actuator control. The remaining interface gap may cause the energy outflow which does not result in a unstable behavior. Finally, learning curve and time-domain synchronization plots in Fig. 18 show the stabilization effect of the proposed algorithm: Despite the fact that displacement peaks initially occur, the system is stabilized after a timespan of less than 0.5 s. After the stabilization, the adaptation continues and results in a synchronization between the virtual and the experimental component. Note that

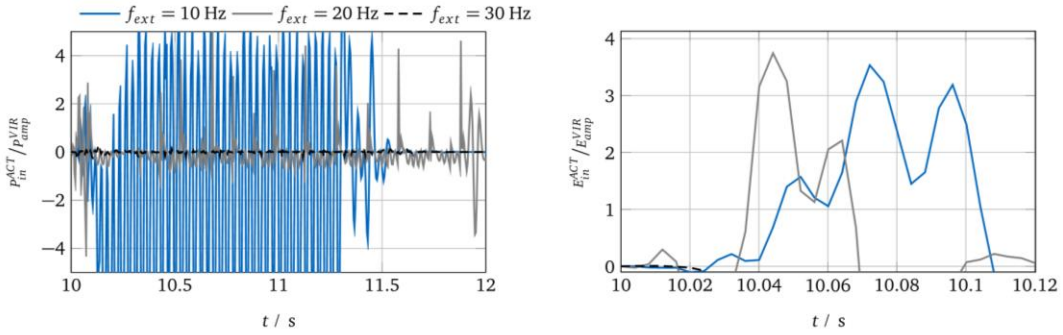

Figure 15: Unstable learning curve and interface synchronization without power-flow supervision.

the displacement peaks can be prevented in a practical application by the application of a peak or comb filter to the actuator input. To summarize, the proposed approach enables the stabilization of an initially unstable test with a nonlinear spring. After stabilization, the adaptation-gain settles and the system finally reaches interface synchronization.

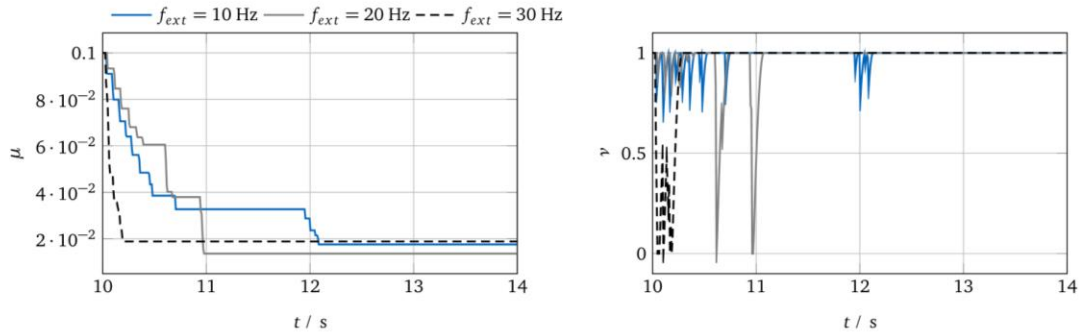

Figure 16: adaptation gain and leakage factor with activated power-flow supervision

6 Conclusion

In this paper, we propose a method to update the parameters of an adaptive feedforward filter in a hybrid test based on the power-outflow from the actuator and control system. In order to investigate the influence of the algorithm's parameters, we make use of a simple purely numerical case. The study leads to the following conclusions:

- Step size $\Delta_{\downarrow} a_{\mu}$ defines the convergence speed of the adaptation gain μ. High values can lead to lower values of μ.
- Step size $\Delta_{\uparrow} a_{\gamma}$ defines the convergence speed of the leakage factor ν. Higher values can reduce the peak values of power-outflow but increase the settling time.
- The power-outflow limit P_{lim} has only a slight influence on the final value of the adaptation gain but higher values reduce the peak interface gap.

The method has been applied to an experimental test case which coupled a physical cubic spring with a virtual mass-spring-damper system. The results showed that the proposed method helped to stabilize the filter with initially unstable filter behavior. The instability is caused by the high adaptation gain. The adaptation gain is updated as a reaction to the power-outflow from the actuator system and settles to a positive value. This allows the filter coefficient to converge such that the interface is synchronized. In other cases where adaptation with the chosen filter parameters is impossible such as for a high phase error of P_{gu}, the passivity constraint is maintained and the adaptation gain μ is taken down to zero. This means that the adaptation has failed but possibly damaging behavior is prevented.

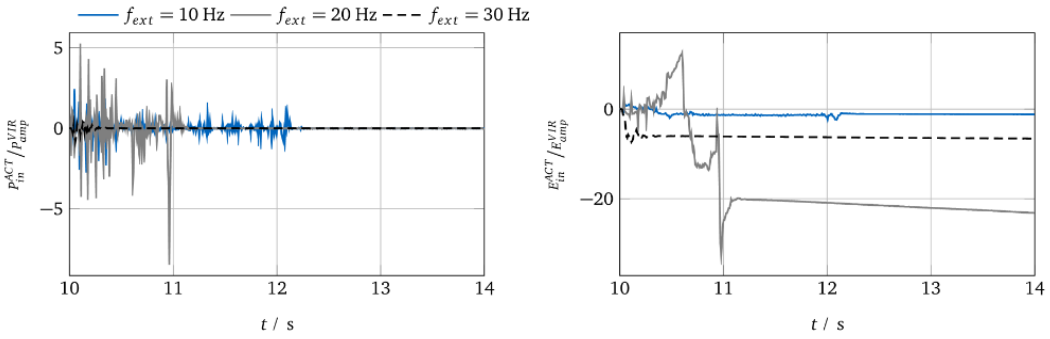

Figure 17: Power and energy inflow to actuator system with activated power-flow supervision.

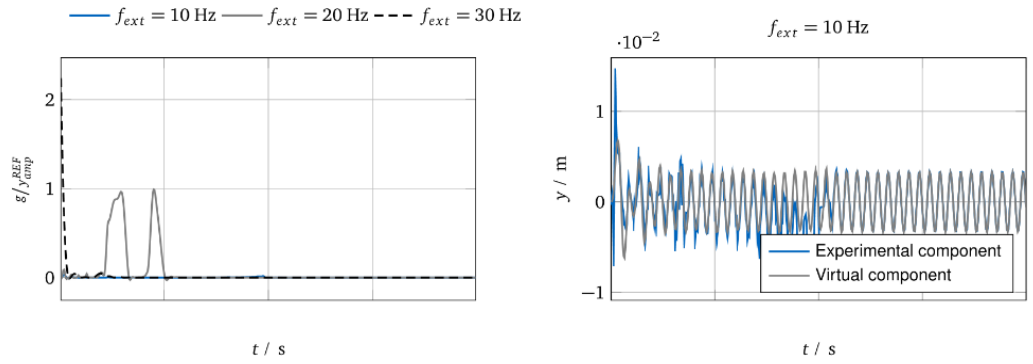

Figure 18: Learning curve and interface synchronization with activated power-flow supervision.

References

[1] V. Bayer et al. “On real-time pseudo-dynamic sub-structure testing: algorithm, numerical and experimental results”. In: *Aerospace Science and Technology* 9.3 (2005), pp. 223–232. ISSN: 12709638. DOI: 10.1016/j.ast.2005.01.009.

[2] M. Bolien, P. Iravani, and J. du Bois. “Toward Robotic Pseudodynamic Testing for Hybrid Simulations of Air-to-Air Refueling”. In: *IEEE/ASME Transactions on Mechatronics* 22.2 (2017), pp. 1004–1013.

[3] A. Plummer. “Model-in-the-Loop Testing”. In: *Proceedings of the Institution of Mechanical Engineers, Part I: Journal of Systems and Control Engineering* 220.3 (Jan. 2006), pp. 183–199. DOI: 10.1243/09596518JSCE207.

[4] T. Horiuchi et al. “Real-time Hybrid Experimental System with Actuator Delay Compensation and its Application to a Piping System with Energy Absorber.” In: *Earthquake Engineering and Structural Dynamics* 28.10 (1999), pp. 1121–1141.

[5] M.I. Wallace, D.J. Wagg, and S. Neild. “An adaptive polynomial based forward prediction algorithm for multi-actuator real-time dynamic substructuring”. In: *Proceedings of the Royal Society A: Mathematical, Physical and Engineering Sciences* 461.2064 (Dec. 2005), pp. 3807–3826. DOI: 10.1098/rspa.2005.1532.

[6] D. J. Wagg and D. P. Stoten. “Substructuring of dynamical systems via the adaptive minimal control synthesis algorithm”. In: *Earthquake Engineering & Structural Dynamics* 30.6 (2001), pp. 865–877.

[7] J. du Bois, B. Titurus, and N. Lieven. “Transfer Dynamics Cancellation in Real-Time Dynamic Sub- structuring”. In: *Proceedings of ISMA 2010*. 2010, pp. 1891–1914.

[8] D. Stoten, G. Li, and J. Tu. “Model predictive control of dynamically substructured systems with application to a servo-hydraulically actuated mechanical plant”. In: *IET Control Theory & Applications* 4.2 (2010), pp. 253–264.

[9] H. Peiris, A. Plummer, and J. du Bois. “Passivity Control in Real-time Hybrid Testing”. In: *2018 UKACC 12th International Conference on Control (CONTROL)* (2018), pp. 317–322.

[10] J.-M. Bras. “Development of a Standardized Method for Actuator Characterization using Active Control of Impedance”. Dissertation. Virginia Polytechnic Institute and State University, 1999.

[11] A. Bartl, J. Mayet, and D. Rixen. “An adaptive approach to coupling vibration tests and simulation models with harmonic excitation”. In: *IEEE/ASME International Conference on Advanced Intelligent Mechatronics, AIM* 2018-July (2018), pp. 262–267. DOI: 10.1109/AIM.2018.8452358.

[12] A. Bartl, J. Mayet, and D.J. Rixen. “Adaptive Feedforward Compensation for Real Time Hybrid Testing with Harmonic Exciation.” In: *Proceedings of the 11th International Conference on Engineering Vibration* September (2015), pp. 7–10.

[13] R. Anderson and M. Spong. “Anderson - 1989 - Bilateral Control of Teleoperators.pdf”. In: *IEEE Transactions on Automatic Control* 34.2 (1989).

[14] G. Niemeyer and J. Slotine. “Stable Adaptive Teleoperation”. In: *IEEE Journal of Oceanic Engineering* 16.I (1991).

[15] A. Albu-Schäffer and C. Ott. “A Unified Passivity- based Control Framework for Position , Torque and Impedance Control of Flexible Joint”. In: *The International Journal of Robotics Research* 26.1 (2007), pp. 23–29. DOI: 10.1177/0278364907073776.

[16] B. Hannaford and J. Ryu. “Time-Domain Passivity Control of Haptic Interfaces”. In: *IEEE Transactions on Robotics and Automation* 18.1 (2002), pp. 1–10.

[17] S. Kuo and D. Morgan. *Active Noise Control Systems*. John Wileys & Sons, 1996.

[18] M. Kamenetsky and B. Widrow. “A Variable Leaky LMS Adaptive Algorithm”. In: *Conference Record of the Thirty-Eighth Asilomar Conference on Signals, Systems and Computers, 2004.* Vol. 1. 650. 2004, pp. 125–128. ISBN: 0780386221.

7.2 Summary

The publication presents an improved adaptive feed-forward filtering algorithm that utilizes substructure power measurements to schedule the adaption gain and regularization parameter of the controller. The following conclusions can be inferred

1) Adaptive feed-forward filtering with passivity-based gain scheduling mitigates instability caused by excessive adaption gains
2) The adaption gain steps down in discrete decrements and the size of the decrement determines how quickly the stability of the system will be restored.

The passivity observer is unobtrusive to the function of the adaptive feed-forward filter. Hence, there are no disadvantages of superposing the passivity observer on to the adaptive feed-forward filter for any given system. When acceptable adaption gains are used, passivity-based gain scheduling will not trigger. Future work will investigate more sophisticated adaptive feed-forward filters incorporating passivity observers to move the adaption gain in both directions thereby allowing the gain to be raised when possible, for faster convergence.

Chapter 8

Passivity based Adaptive Delay Compensation for Real-time Hybrid Testing

8.1 Context

This chapter presents a technical article introducing a novel passivity based adaptive delay compensation scheme to mitigate actuator delay in real-time hybrid tests. Experimental results on a nonlinear real-time hybrid test system are used to validate its effectiveness whilst comparing the performance obtained with that of a state-of-the-art adaptive delay compensation scheme, identifying the unique advantages offered by the new scheme.

The state-of-the-art compensation scheme (discussed in detail in the paper), is based on using the substructure position error at the zero crossings to quantify the effective delay in the transfer system. However, the novel passivity-based scheme utilizes the substructure energy error to quantify the actuator delay. Both schemes employ a least squares 2^{nd} order polynomial extrapolation scheme to predict the actuator response ahead of the identified delay.

A positive energy error indicates lag introduced at the transfer system of the hybrid test. As the energy error in the system feeds the delay compensator, larger energy errors will lead to greater identified delays, which when compensated, eliminate some lag in the hybrid test. This in turn leads to smaller energy errors and thus smaller identified delays until the energy error is sufficiently small resulting in little to no lag in the actuator response. In this steady state configuration, the net energy added to the hybrid test by the actuator will be minimal, as will be the transfer system effective delay.

This declaration concerns the article entitled:									
Passivity based Adaptive Delay Compensation for Real-time Hybrid Tests									
Publication status (tick one)									
Draft manuscript		**Submitted**		**In review**	✓	**Accepted**		**Published**	
Publication details (reference)	L. D. Hashan Peiris, Jonathan L. du Bois & Andrew R. Plummer, "Passivity based Adaptive Delay Compensation for Real-time Hybrid Tests", *Proc. of the Inst. of Mech. Eng., Part I: J. of Sys. and Cont. Eng.,* 2019.								
Copyright status (tick the appropriate statement)									
I hold the copyright for this material	✓	Copyright is retained by the publisher, but I have been given permission to replicate the material here							
Candidate's contribution to the paper (provide details, and also indicate as a percentage)	**The candidate contributed to / considerably contributed to / predominantly executed the…** **Formulation of ideas:** Idea to apply energy-based passivity control with a polynomial forward predictive delay compensator based on discussions with supervisors Dr. Jonathan du Bois and Prof. Andrew Plummer. Candidate's contribution (50%). **Design of methodology:** Methodology designed with supervisors Dr. Jonathan du Bois and Prof. Andrew Plummer. Candidate's contribution (70%). **Experimental work:** Solely by the candidate (100%) **Presentation of data in journal format:** Paper written by candidate, reviewed and corrected by supervisors Prof. Andrew Plummer and Dr. Jonathan du Bois. Overall contribution of candidate (75%).								
Statement from Candidate	This paper reports on original research I conducted during the period of my Higher Degree by Research candidature.								
Signed	L DH Peiris					**Date**	24/09/2019		

Paper Six: Passivity based Adaptive Delay Compensation for Real-time Hybrid Tests

Passivity based Adaptive Delay Compensation for Real-time Hybrid Tests

L. D. Hashan Peiris
Department of Mechanical Engineering, University of Bath
Bath, United Kingdom
ldhp20@bath.ac.uk

Jonathan L. du Bois
Department of Mechanical Engineering, University of Bath
Bath, United Kingdom

Andrew R. Plummer
Department of Mechanical Engineering, University of Bath
Bath, United Kingdom

***Summary*—This paper presents a novel passivity based adaptive delay compensation (PBADC) scheme for cancelling actuator dynamics in real-time hybrid testing. This scheme uses the energy added to the system by actuation hardware, to quantify a variable delay, which is subsequently used for delay compensation. It offers the advantage of correcting for tracking errors and instability in hybrid tests and can be implemented without any information of the actuator's dynamics. Thus, it offers an advantage over most conventional actuator dynamics mitigation schemes which require an accurate model of the actuator prior to testing. Experimental results compare the performance of PBADC with that of a state-of-the-art adaptive delay compensation scheme based on position. It was found that PBADC continuously updates the delay estimate whilst the position based scheme only updates the delay when the system crosses zero. The performance of both schemes were found to be similar for sinusoidal inputs, mitigating phase lags of up to 35.6 degrees at 10Hz in the hybrid system tested. PBADC requires no extra hardware as it can be run on the same hardware used to drive the actuator, enabling an affordable solution applicable to a wide range of hybrid tests.**

I. Nomenclature

ΔE = Net energy added at the transfer system
P_P = Physical substructure power
P_N = Numerical substructure power
F_P = Physical substructure force
V_P = Physical substructure velocity
F_N = Numerical substructure force
V_N = Numerical substructure velocity
$PBADC$ = Passivity based adaptive delay compensation
B = Passivity controller gain
τ = Identified delay
x_i = y-coordinate of data point
y_i = y-coordinate of data point
X = matrix of polynomials of x_i
y = Polynomial function used in delay compensation
a_i = Polynomial coefficients for delay compensator
N = Order of polynomial function in delay compensator
n = Number of data points for delay compensation

II. Introduction

Real-time hybrid testing involves separating systems into numerical and physical substructures which are tested in parallel with actuators and force sensors used for real-time data transfer. Actuator lag is a notable problem in hybrid testing as it results in tracking errors and can lead to instability. Conventional schemes of addressing this issue are based on the identification of an accurate model of the actuator, which is then inverted and applied as a feed-forward controller to mitigate actuator lag. However, fixed models are often inaccurate, particularly in hybrid tests where actuator behaviour is nonlinear and/or affected by the physical substructure. PBADC offers a compensation strategy where the actuator delay estimate is online and dynamic, enabling adaptive compensation for nonlinear hybrid tests, as well as linear hybrid tests experiencing variable delays in the actuator. The scheme requires no information of the hybrid system or actuation hardware prior to testing and can therefore be easily implemented.

III. Methodology

In a hybrid test excited at the numerical substructure, displacements calculates in the virtual subsystem of the hybrid test are applied to the physical substructure via actuators. Load cells are often used to measure forces at the physical substructure which are fed back to the numerical substructure to close the loop of the hybrid test. There is a calculated energy flow from the numerical substructure to the physical substructure, and an actual energy flow from the actuator to the physical substructure, and these are in general different due to actuator tracking errors. The energy flowing from the actuator may exceed that intended by the numerical substructure. This surplus of energy leads to tracking errors and potential instability in hybrid tests.

The proposed passivity based adaptive delay compensation (PBADC) scheme is based on regulating the energy flow in the hybrid test. The existence of a delay in the actuator's response can cause its energy output to exceed the correct magnitude. Hence, the difference between the real energy imparted to the physical substructure and the virtual energy calculated by the numerical substructure, is used as a control signal in the passivity controller which outputs a delay estimate subsequently used for delay compensation. The passivity controller used is a simple proportional controller acting on the

substructure energy error. A delay compensation scheme as utilized in Wallace *et al.* [1] is used with the identified delay to compensate for actuator dynamics. The delay estimate grows as long as there is positive spurious energy injection by the actuator into the hybrid test. As delay compensation mitigates phase lag in the actuator, the spurious energy injection will tend to decrease. As the energy error reaches zero, so does the identified delay and the delay compensation will in turn lead to synchronization between substructure responses.

The real (physical) and virtual powers are evaluated by taking the product of force and velocity. For the numerical substructure, these quantities are easily accessible from the real-time model of the virtual subsystem. For the physical substructure these quantities are obtained using sensor measurements. The load cell measures physical substructure force whilst physical substructure velocity can be obtained using actuator displacement information. The passivity based delay compensator can be run on the same hardware used to drive the actuator resulting in low implementation costs.

The power flow calculated by the numerical substructure P_N is given by

$$P_N = F_N V_N$$

where F_N and V_N are the numerical substructure force and velocity respectively. Similarly, the physical substructure power P_P is given by

$$P_P = F_P V_P$$

where F_P and V_P are the physical substructure force and velocity respectively. The delay τ identified by the passivity controller is given by the following equation where B is the passivity controller gain. By integrating the spurious power injected by the actuator, the net energy can be obtained.

$$\tau = B \int_0^t (P_P - P_N)\, dt$$

The delay compensator used with this adaptive scheme is the polynomial forward predictive scheme presented in [1]. The delay compensator fits a polynomial function to the past response of the numerical substructure based on a least squares approximation as detailed in [2] and subsequently in [1]. This polynomial function is used to predict the response of the substructure time τ ahead so the delay of the actuator can be cancelled by using this predicted signal as the actuator demand. As described in [1], a polynomial function in x of order N with coefficients a_i (where $i = 0, \ldots . N$) can be expressed as

$$y = a_0 + a_1 x + \ldots + a_N x^N$$

Given n input-output data points $(x_0, y_0), \ldots . . (x_{n-1}, y_{n-1})$ with polynomial coefficients $a_0, \ldots . . a_N$, the equation of the curve is given by

$$\begin{bmatrix} y_0 \\ y_1 \\ \vdots \\ y_{n-1} \end{bmatrix} = \begin{bmatrix} 1 & x_0 & {x_0}^2 & \ldots & x_0^N \\ 1 & x_1 & {x_1}^2 & \ldots & x_1^N \\ \vdots & \vdots & \ddots & & \vdots \\ 1 & x_{n-1} & x_{n-1}^2 & \ldots & x_{n-1}^N \end{bmatrix} \begin{bmatrix} a_0 \\ a_1 \\ \vdots \\ a_N \end{bmatrix}$$

Hence, in matrix form, the equation for a polynomial fit can be expressed as

$$y = Xa$$

This is solvable by premultiplying by the matrix transpose such that $X^T y = X^T X a$. The matrix can then be inverted directly to obtain the following solution

$$a = (X^T X)^{-1} X^T y$$

The hybrid test block diagram with the delay compensator and passivity controller are illustrated in fig. 1.

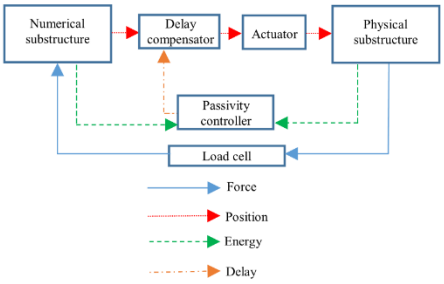

Fig. 1. Controlled hybrid test block diagram

IV. Experimental Setup

In order to demonstrate the passivity based adaptive delay compensation scheme, a single degree of freedom nonlinear real-time hybrid test system was set up. The numerical substructure consisted of a lumped parameter mechanical system of a mass suspended on a linear spring and viscous damper whilst the physical substructure consisted of a stiffening spring. A diagrammatic view of the system is shown in fig. 2.

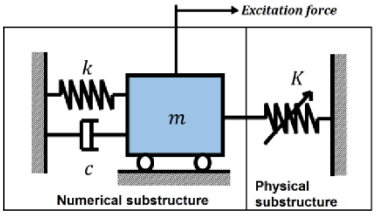

Fig. 2. Mechanical system to be emulated by hybrid test

The stiffening behavior of the physical substructure was achieved by connecting two linear springs perpendicularly to the actuator such that displacement dependent stiffening is achieved much like a Duffing oscillator. Fig 3a shows the experimental system consisting of the actuator connected to the physical substructure. A zoomed in view of the physical substructure is given in fig 3b.

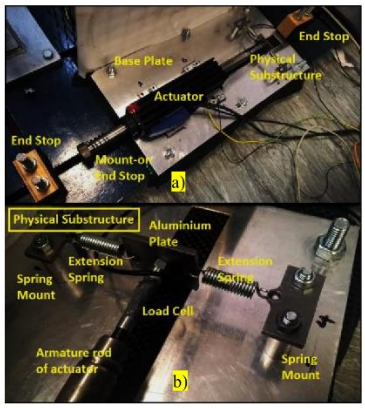

Fig. 3. a) Actuator connected to physical substructure through load cell, b) view zoomed into physical substructure [3]

For actuation, a Copley STA2508S electromagnetic linear actuator is used which runs in position control mode, with cascaded current and velocity control loops as shown in fig. 4. For real-time control, a Simulink Real-time Target is used to execute the position and velocity loops whilst the current loop runs in the Xenus XTL motor driver. Due to nontrivial friction acting on the actuator shaft, a simple Coulomb friction compensator as proposed by Eamcharoenying et al. [4] is utilized, although due to the complex nature of the friction, complete elimination of friction is not achieved albeit it is reduced to a notable extent.

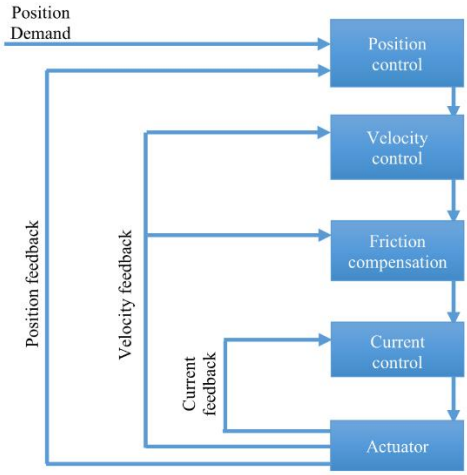

Fig. 4. Actuator control system structure [5]

Table 1 presents the parameters of the hybrid test. The results presented in section IV compare the output of the hybrid tests with that of the emulated system, i.e. the true system to be replicated. The emulated system was created in simulation after identification of the physical substructure force profile using the load cell.

TABLE I. HYBRID TEST PARAMETERS

Numerical substructure	Physical substructure	Copley STA2508S actuator
Mass: 1kg Damper rate: 10Ns/m Stiffness: 1kN/m	Force profile (displacement dependent) given by; $F_P = 0.0014x^3 + 2.13x$	Peak force 625N Continuous stall force 75.1N Peak acceleration 542m/s^2 Maximum speed 4.7m/s

V. EXPERIMENTAL RESULTS

The aforementioned hybrid test and its emulated system simulation were excited at the numerical substructure using a stepped sine force input from 0-40s. Frequencies of 0.1, 1, 5, 10, 20Hz were applied at times 0, 20, 25, 30, 35s. The amplitude of the force input for each step was chosen such that the physical substructure vibration amplitude would be 5mm, to maintain consistency among tests given the displacement dependent stiffness of the physical substructure. The hybrid test position response of the physical substructure with and without passivity based delay compensation is plotted against the response of the emulated system in fig. 5a-5f. The response of the hybrid test with the application of an adaptive delay compensation scheme by Wallace et al. [1] is also shown for comparison. The passivity based compensator monitors the energy flow of the system throughout the hybrid test to identify the delay in the transfer system whilst the scheme by Wallace et al. [1] identifies the delay in the system based on the substructure position gap measured at the zero crossings.

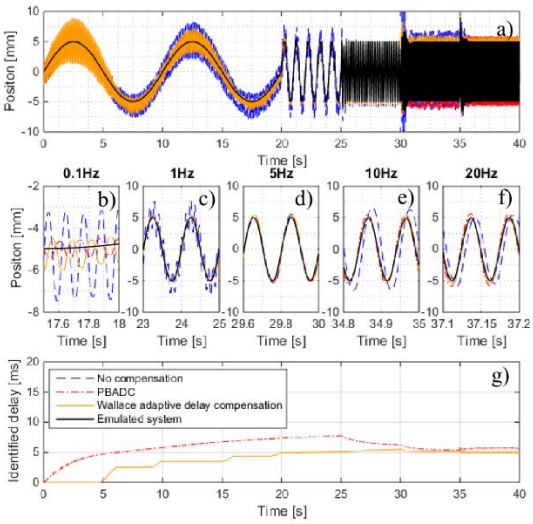

Fig. 5. Compensated hybrid test responses a) physical substructure position envelope, b-f) zoomed in views of physical substructure position at frequencies of 0.1, 1, 5, 10, 20Hz, g) identified delay

Fig. 5b illustrates that the hybrid test response at 0.1Hz is very oscillatory. Whilst following the 0.1Hz demand, the system also exhibits a limit cycle at 8.3Hz. This is an artefact caused by the nonlinear friction of the actuator as described in [3]. At low velocities, the actuator phase lag due to friction is high resulting in an unstable system. As velocity grows due to the instability, the actuation forces dominate over the forces of friction and the system becomes stable once again, manifesting as a limit cycle at the natural frequency of the system [3].

It can be seen that the oscillatory nature of the response at 0.1Hz is greatly reduced with the application of passivity based delay compensation. The delay compensation alleviates some of the phase lag of the actuator which enables the stability of the system to be restored at lower velocities thereby leading to a smaller limit cycle. The delay compensation by Wallace's adaptive scheme too exhibits a reduction in the amplitude of the limit cycle, however to a smaller extent. Particularly, as seen in fig. 5a, Wallace's compensation scheme does not show an improvement in the response until after 5s. This is due to the nature of adaption as seen in fig. 5g, which plots the delay identification of both compensators in the hybrid test.

The passivity based delay compensator updates the delay identification in real-time as the transfer system net energy is continuously monitored. However, Wallace's method which only updates the delay identification at the zero crossing is seen to respond much slower with the delay being updated only at 5, 10, and 15s for the 0.1Hz response. This means that a finite number of cycles will be required to allow Wallace's adaptive delay compensator to converge and for low frequency signals, this may lead to large settling times. Moreover, as the method only updates the delay when the measured position crosses zero, the scheme will not be directly applicable when the system response has no zero crossings (eg: when excited by step or ramp inputs). In such cases, passivity based delay compensation poses a unique advantage.

At 1Hz as shown in fig. 5c, both compensators successfully mitigate the limit cycle oscillation seen in the hybrid test response without compensation. At 1Hz, the time at which the system is at low velocities is smaller resulting in a less significant limit cycle. At 5Hz, the response without compensation is seen to be similar to that of the emulated system in fig. 5d. In fig. 5e, the amplitude of oscillation of the uncompensated hybrid test exceeds that of the emulated system. This phenomenon takes place because the excitation frequency of 10Hz is near the resonant frequency of the system (8.3Hz as seen from the limit cycle). Both compensation schemes are seen to mitigate this effect. There is notable phase lag in the uncompensated hybrid test responses at 10Hz and 20Hz as seen in fig. 5e and 5f. A phase lag of 35.6degrees is seen at 10Hz and 35.3degrees at 20Hz in fig. 5e and fig. 5f respectively. As earlier, both compensation schemes are seen to effectively mitigate this phase lag although Wallace's method achieves this with greater accuracy to that of the emulated system than the passivity based method.

In fig. 5g, it is evident that the delay estimates of both schemes are similar after 30s (10Hz and 20Hz tests). However from 0-30s the Wallace delay compensation scheme takes longer to identify the transfer system delay due to its discrete operation at the zero crossings compared to the continuous operation of the passivity based method.

VI. Conclusion

The performance of a novel passivity based adaptive delay compensator for real-time hybrid tests have been assessed. The scheme has been shown to improve stability and tracking in a single degree of freedom nonlinear real-time hybrid test. Performance of the scheme has been compared with that of a state-of-the-art adaptive delay compensation strategy and in performance was seen to be largely similar. However, the novel passivity based approach enables the advantage of continuous monitoring of the actuator delay unlike the state-of-the-art method. This enables faster convergence whilst also being applicable to systems that do not cross zero. Therefore, PBADC is envisaged to be particularly useful with non-sinusoidal drive signals such as steps or unidirectional inputs where the system does not return to its original position. Future work will see further investigations in this regard whilst testing the scheme in multi-degree of freedom systems with nonlinearities in the numerical substructure as well.

Acknowledgment

This work has been supported through funding from the Engineering and Physical Sciences Research Council, grant reference EP/N032829/1.

References

[1] M. I. Wallace, D. J. Wagg, and S. a. Neild, "An adaptive polynomial based forward prediction algorithm for multi-actuator real-time dynamic substructuring," *Proc. R. Soc. A Math. Phys. Eng. Sci.*, vol. 461, no. May 2004, pp. 3807–3826, 2005.

[2] E. Kreyszig, *Advanced engineering mathematics*, 8th ed. New York: Wiley, 1999.

[3] L. D. H. Peiris, A. R. Plummer, and J. L. Du Bois, "Passivity Control for Nonlinear Real-time Hybrid Tests," *Proc. Inst. Mech. Eng. Part I J. Syst. Control Eng.*, 2020.

[4] P. Eamcharoenying, A. Hillis, and J. Darling, "Friction compensation using Coulomb friction model with zero velocity crossing estimator for a force controlled model in the loop suspension test rig," *Proc. Inst. Mech. Eng. Part C J. Mech. Eng. Sci.*, vol. 230, no. 12, pp. 2028–2045, Jun. 2015.

[5] L. D. H. Peiris, A. Plummer, and J. du Bois, "Normalised Passivity Control for Robust Tuning in Real-time Hybrid Tests," *Int. J. Robust Nonlinear Control*, 2020.

8.2 Summary

A novel passivity based adaptive delay compensation scheme has been developed and tested on an experimental nonlinear real-time hybrid test system. The following conclusions were inferred.

1) Passivity based adaptive delay compensation allows the effective delay of the actuator in real-time hybrid tests to be mitigated, resulting in similar performance to that of the tested state-of-the-art adaptive delay compensation scheme.
2) Unlike the tested state-of-the-art scheme which activates at the zero crossings, passivity based adaptive delay compensation is continuously active thus enabling compensation even for tests where the system does not return to the zero position.

For such adaptive delay compensation schemes, the process of identifying the effective delay in the transfer system is of paramount importance. Both the passivity based adaptive delay compensation scheme and the state-of-the-art adaptive delay compensation scheme have unique means of identifying this delay as detailed below. The effective delay is represented by τ and plotted in the publication in figure 5g.

For the passivity based adaptive delay compensator, the effective delay is identified as a proportion of the spurious energy injection. The existence of a non-zero effective delay will manifest as positive net energy injections into the hybrid test. Thus, the effective delay variable fed to the delay compensator is given by equation (3), where B, E_P and E_N are the user specified passivity controller gain, the total energy injected into the hybrid test by the actuator, and the energy leaving the numerical substructure, respectively.

$$\tau = B\,(E_P - E_N) \tag{3}$$

The energy leaving the numerical substructure is readily available from the numerical component of the hybrid test. This is the integral of the product of the numerical substructure force and velocity. The energy injected by the actuator into the hybrid test is obtained by integrating the product of the actuator velocity (obtained using encoder measurements) and the physical substructure force (measured using the load cell in the test rig).

As the delay identification is fed into the adaptive delay compensator, the effective delay in the system is reduced which results in a more passive system, i.e. smaller net power injections from the actuator. When the system is passive, i.e. the actuator injects zero net power into the hybrid test, the delay identification reaches an equilibrium. As such, passivity-based delay compensation is continuously active throughout the test.

The delay identification scheme for the state-of-the-art adaptive delay compensation as outlined in [29] is given by the following algorithm. The numerical substructure displacement is given by x_N.

If x_N changes sign from negative to positive (rising edge) or positive to negative (falling edge),
Calculate the adaptive forward prediction parameter ρ:

$$\rho_{n+1} = \rho_n \pm \alpha e^{\gamma} \quad (4)$$

Where e is the substructure gap error, and α and γ are user specified parameters. α is known as the adaption gain parameter and γ sets the rate of convergence which must be greater than or equal to 1.

Note: The $\pm$ relates to whether the signal is rising edge (+) or falling edge (-).

Next, the delay is identified using the following equation:

$$\tau = \Delta t \, (P + \rho) \quad (5)$$

End

Where Δt is the sample timestep size, and P is the fixed initial number of timesteps to be forward predicted. P is set at zero to allow delay compensation to be fully adaptive.

The above delay identification procedures are implemented in the numerical environment of the real-time hybrid test so as to augment the input to the actuation hardware.

Table 4 indicates the parameters of the compensation schemes used in the above study.

Table 4: Parameters used in the passivity based and state-of-the-art adaptive delay compensation schemes

Parameter	Value
Passivity Based Adaptive Delay Compensation:	
Passivity controller gain (B)	$1.3\ s/J$
State-of-the-art Adaptive Delay Compensation [29]:	
Adaption gain parameter (α)	120
Convergence exponent (γ)	1
Fixed initial number of timesteps (P)	0
Polynomial Delay Compensator Parameters:	
Order of least squares fitting scheme (N)	2
Number of data points used for curve fitting (n)	3
Stepped sine excitation force at the numerical substructure	• 15.8N at 0.1Hz, for 20s • 17.8N at 1Hz, for 5s • 11.0N at 5Hz, for 5s • 4.8N at 10Hz, for 5s • 162N at 20Hz, for 5s
Solver:	
Program execution sample time	0.001s
Numerical solver	ODE4 Runge-Kutta (Fixed step)

The passivity-based scheme offers a new means of achieving actuator delay cancellation in real-time hybrid tests. For most cases, its usage is equally feasible to that of the position-based adaptive delay compensation scheme used as a benchmark to compare performance gains in the paper. However, unlike with the state-of-the-art scheme which updates the delay at the zero crossings, continuous delay adaption is expected to enable faster convergence particularly for low frequency excitations where fewer zero crossings are seen per given period. Moreover, for specific tests where zero crossings are not seen, passivity-based delay compensation will still function, enabling continuous mitigation of actuator dynamics.

Chapter 9

Conclusions and Future work

9.1 Conclusions

A number of passivity-based schemes for real-time hybrid testing have been developed, tested and analysed in this thesis. To begin with, a simple proportional passivity controller acting on the net energy of the transfer system was designed and tested in simulation. Preliminary analysis indicated the effectiveness of the simple control scheme in improving performance of stable systems by reducing oscillation and restoring stability of inherently unstable hybrid test simulations. Unlike most transfer dynamics compensation strategies, passivity control required no information of the actuator dynamics.

In the second publication presented in this thesis, passivity control was applied to a real-time hybrid test of a nonlinear system actuated by an electromagnetic actuator with nonlinear friction. It serves as an experimental validation of the simulation results. As expected, following the simulations in the first publication, passivity control stabilized the hybrid test made unstable due to a stiff physical substructure whilst improving performance by suppressing unwanted oscillations caused by friction in the actuator. Performance at low frequency was seen to surpass that of a linear 2^{nd} order model-based compensator which was unable to accurately capture the nonlinearities in the actuator response. At high frequency the dynamics of the actuator was seen to result in a notable phase lag in the hybrid test which could not be eliminated with passivity control alone. However, it was shown that passivity control and model-based compensation used together enabled high stability as well as good demand tracking to be simultaneously achieved. The modularity and unobtrusiveness of passivity control was thus demonstrated making it suitable for a range of hybrid tests as a standalone application or a scheme to complement existing linear lag compensation strategies in the presence of model error or transient nonlinearities.

However, three main limitations were found with the simple energy based proportional passivity control scheme.

1) The output of the passivity controller was sensitive to the magnitude of the energy flowing in the system – this resulted in the amount of passivity damping applied being dependant on the amplitude, frequency and type of the excitation signal. To counter this effect, the controller needs to be retuned each time operating conditions are changed.

2) By acting on the integral of the power error, the passivity controller not only responds to the present state of the hybrid test but also to the response history since the start of the test. As such, it tends to act continuously even when stabilizing damping action is no longer required.

3) High levels of harmonic distortion are seen in the output when large controller gains are used – High controller gains resulting in volatile damper rates were seen to induce high levels of total harmonic distortion. The user of passivity control therefore needs to identify an acceptable trade off between overall stability and tracking.

4) Targeted improvements in tracking could not be achieved – as the scheme was based on damping the numerical substructure, it was unable to result in targeted tracking improvements although it could be tuned to achieve specified design criteria if such information was available. Information of the emulated system performance is often unavailable however in the testing phase. Nevertheless, simplified reduced order simulations of the emulated systems may be used to identify approximate performance criteria which can be used to tune the passivity controller.

Passivity control with a normalised power variable enabled limitation 1) mentioned above to be alleviated and the results presented in publication 3 of chapter 5 illustrated the independence of the scheme on the magnitude of the excitation signal. Moreover, the normalised passivity controller was seen to enable more damping to be applied near the turning points of the response where stability is low, and less damping when good stability and tracking are seen. Thus, limitation 2) posed by the initial controller design was alleviated. Low pass filters were also incorporated in the design to enable more sophisticated forms of control over the simple proportional control scheme employed in the initial passivity controller design. The effects of tuning the filter coefficients and controller gains were assessed and tuning configurations to achieve good stability with acceptable nonlinear distortion have been identified.

Nonetheless, as passivity control is based on damping out instabilities in the system, it is unable to improve tracking performance in hybrid tests. Results in publication 2 have shown scope for lag cancellation when used with linear model-based compensation strategies, however this requires the actuator response to be predictable and pre-determined by a mathematical model. Such models are not always available for compensator design particularly in systems where actuator behaviour is affected by the physical substructure or in systems where actuator behaviour is inherently nonlinear. Therefore, in publication 4, the improved passivity controller was used together with an adaptive lag compensator for hybrid tests in order to alleviate limitation 4).

Results in publication 4 illustrated the effectiveness of passivity control and adaptive feedforward filtering in real-time hybrid tests where unstable systems were seen to be first stabilized by passivity control and then synchronized with respect to the emulated system with adaptive feedforward filtering. The damping action of the passivity controller was seen to slowly decrease overtime as the adaptive feedforward filter converged the substructure gap error towards zero thereby indicating high compatibility between schemes. The combined strategy was also tested in a discontinuous hybrid test with a step change in numerical substructure parameters which resulted in instability without passivity control. It was found that passivity control enabled stability in the system to be maintained in the presence of the discontinuity allowing the adaptive feedforward filter to adapt to the new gap error and achieve substructure synchronisation in the steady state. In publication 5, another use of passivity control in hybrid testing was highlighted, as it was employed to schedule the parameters of the adaptive feedforward filter. The passivity-based scheme successfully prevented the instability triggered due to inappropriate controller gains, by adjusting the adaption gain and regularisation parameter of the adaptive feed-forward filter thereby suppressing the net power injection by the actuator.

The final publication in this thesis explores a different concept of using passivity in real-time hybrid tests. A novel adaptive delay compensation scheme was explored where the net energy surplus added to the hybrid test by the actuator was used to quantify a delay variable. The identified delay was used to compensate for the actuator dynamics with a least square based 2nd order delay compensation scheme. The hybrid system response with passivity-based adaptive delay compensation was compared with the response of the system compensated by a state-of-

the-art adaptive delay compensation scheme, and similar performance was found. Despite the comparable performance, the passivity-based scheme offers unique advantages over the state-of-the-art scheme such as its continuous monitoring of the delay. This allows for more rapid and smoother adaption as opposed to the benchmark scheme which only measures and adapts the delay estimation at the zero crossings of the system. Thus, the new scheme offers a niche in hybrid tests required to operate in unidirectional tests or for systems excited by step inputs where zero crossings do not take place. This novel scheme also alleviates limitation 4) described above.

As such, four novel passivity-based compensation strategies for real-time hybrid tests have been developed with successive methods overcoming the limitations and improving the functionality of preceding schemes. The simple energy based proportional passivity controller is a quick and easy solution that offers stability, whilst the normalised scheme brings a more versatile approach which maintains the modularity and compatibility with other transfer dynamics compensation schemes. The passivity based adaptive delay compensator was seen to enable actuator lag to be eliminated from the hybrid test. It resulted in similar performance to that of a state-of-the-art method while at the same time offering special benefits due to its unique means of quantifying the delay in the transfer system.

The enablement of the use of passivity control in real-time hybrid testing has a multitude of implications to engineering systems in areas such as automotive, aerospace, mechanical and energy. The prime feature that makes passivity control attractive is its simplicity and ability to alleviate the problem of instability in any hybrid test. All measurements and signals required to run the passivity controller are obtainable from the sensors already in use, and the passivity controller itself can be run in the same hardware driving the actuator. This makes passivity control in hybrid testing an inexpensive and therefore attractive solution for use in industry.

With its ease of use, unobtrusiveness and modularity, passivity control shines not only as a standalone solution, but also as a tool to complement other transfer dynamics compensation schemes as a buffer to maintain stability. For example, a hybrid test compensated with a linear transfer dynamics cancellation scheme would be susceptible to instability in the face of a stiff impact, without passivity control in the system. Further, if used with an adaptive scheme like adaptive feed-forward filtering, passivity control will hold the system in a stable state until the filtering scheme converges to resynchronise substructure displacements after the impact.

Moreover, many industrial applications of hybrid testing such as the testing of automotive active suspensions, wave energy conversion devices and flight testing involve setting up a crucial component of the system as the physical substructure. Such components are likely to be prototypes which cannot be readily replaced if damaged or are expensive to manufacture. With product development deadlines and other limited resources to manage, it is expected that many industries will find passivity control an attractive solution for hybrid tests, predominantly as a safety feature to prevent damage to crucial components by maintaining stability.

Moreover, with instability no longer a risk with passivity control in real-time hybrid testing, a whole new range of hybrid test applications are envisaged. For example, more tests incorporating human operators in the loop may emerge resulting in the possibility of new research in areas such as space exploration. The development of improved biomimetic prosthetics with greater user integration in the testing stage is also envisaged given the guarantee of safety provided by passivity control.

9.2 Contributions

The major contributions made by the author through this thesis are summarized below.

1) The development of an energy-based passivity control scheme for real-time hybrid tests.
2) The experimental validation of the passivity control scheme in a real-time hybrid test with nonlinearity in the physical substructure and actuation hardware.
3) Demonstration of the use of passivity control with a state-of-the-art model-based compensation strategy to illustrate the complementation of both schemes.
4) The development of a revised (normalised) passivity controller algorithm with performance insensitive to excitation amplitude.
5) Application of the normalised passivity controller with a recently developed adaptive lag compensation scheme to enable stability and synchronised substructure displacements to be achieved without prior information of actuator dynamics.
6) The application of passivity control as a gain scheduling tool in an adaptive lag compensation scheme to prevent instability caused by inappropriate control parameters.
7) The development of a novel passivity based adaptive delay compensation scheme to mitigate phase lag in real-time hybrid test systems.

9.3 Future work and Closing remarks

The growth of knowledge through research is powered by the development and flow of ideas. With the manifestation of every new solution from every novel idea, there will always be direction for further improvement. The flow of research connecting new and preceding ideas together, form an iterative process of advancement resulting in the creation of further enhanced solutions and new technology, as time progresses. Such is the case for the work presented through this thesis as well. With the development and implementation of a number of passivity-based schemes for real-time hybrid tests, the following areas for improvement remain free to explore to further strengthen the integration of passivity control in real-time hybrid test systems of the future.

Although parametric changes in the normalised passivity controller have been linked to changes in performance and qualitative guidelines for filter tuning are provided, there is scope for the development of a heuristic method of tuning passivity controllers for real-time hybrid tests. Much like the Ziegler-Nichols method for tuning PID controllers, a similar scheme for tuning passivity controllers is expected to be a very useful tool to complement the work developed herein.

Another promising area of future work lies in the use of passivity control with hybrid tests of multiple degrees of freedom, where two or more actuators would be used to displace the physical substructure. Such tests would monitor the passivity of several actuators and thus possibilities for research in this regard may begin with the adaptation of the single actuator passivity control schemes proposed through this thesis, to such systems. The use of a single passivity controller acting on a weighted mean of the spurious power injections of each actuator may or may not be a solution superior to having several passivity controllers monitoring each actuator independently. Alternatively, passivity control schemes embedded into the control loop of the actuator may enable higher gains to be used in the control of the actuator resulting in high performance which would otherwise have caused an unstable control system. Such areas are yet to be explored and

future work in this direction is expected to be highly beneficial to the field of real-time hybrid testing.

To conclude with, it is worth mentioning that the above suggested research ideas and scope for improvement do not dwarf the contributions made through this thesis. The identification of a scheme that maintains stability in real-time hybrid tests is highly beneficial and forms a major milestone in the chronological growth of hybrid testing. In a world where computing technology sees rapid growth and simulation capabilities rise at strong rates, there is a global shift towards the use of more hybrid and simulation-based techniques over conventional full-scale experimentation. With passivity control and hybrid testing, the scope for such future developments are immensely increased through a safe and cost-effective solution attractive to researchers and industry alike.

References

[1] P. Benson Shing, "Modern Testing Techniques for Structural Systems: Dynamics and Control," O. S. Bursi and D. Wagg, Eds. Vienna: Springer Vienna, 2008, pp. 259–292.

[2] J. E. Carrion and B. F. Spencer, "Model-based Strategies for Real-time Hybrid Testing," no. December, p. 211, 2007.

[3] M. Bolien, P. Iravani, and J. du Bois, "Robotic Pseudo-Dynamic Testing (RPsDT) of Contact-Impact Scenarios," *Towar. Auton. Robot. Syst.*, vol. 9287, pp. 50–55, 2015, doi: 10.1007/978-3-662-43645-5.

[4] M. J. Hochrainer, "Real-Time Hybrid Testing: Challenges and Experiences from a Teaching Point of View," in *Topics in Modal Analysis {&} Testing, Volume 9*, 2019, pp. 175–186.

[5] H. K. Fathy, Z. S. Filipi, J. Hagena, and J. L. Stein, "Review of hardware-in-the-loop simulation and its prospects in the automotive area," *Proc. SPIE 6228, Model. Simul. Mil. Appl.*, vol. 62280, 2006, doi: 10.1117/12.667794.

[6] A. R. Plummer, "Model-in-the-Loop Testing," *Proc. Inst. Mech. Eng. Part I J. Syst. Control Eng.*, vol. 220, no. 3, pp. 183–199, 2006, doi: 10.1243/09596518JSCE207.

[7] T. T. Nguyen, T. N. Dao, S. Aaleti, J. W. van de Lindt, and K. J. Fridley, "Seismic assessment of a three-story wood building with an integrated CLT-lightframe system using RTHS," *Eng. Struct.*, vol. 167, pp. 695–704, 2018, doi: https://doi.org/10.1016/j.engstruct.2018.01.025.

[8] O. Flodén, G. Sandberg, and K. Persson, "Reduced order modelling of elastomeric vibration isolators in dynamic substructuring," *Eng. Struct.*, vol. 155, pp. 102–114, 2018, doi: https://doi.org/10.1016/j.engstruct.2017.11.001.

[9] X.-Q. Wang, L.-Y. Xu, and M.-X. Tao, "Influence of slab spatial composite effect on dynamic behaviour of composite frame structures under earthquake excitation," *Bull. Earthq. Eng.*, 2019, doi: 10.1007/s10518-019-00568-6.

[10] S. Borjigin, C.-W. Kim, K.-C. Chang, and K. Sugiura, "Nonlinear dynamic response analysis of vehicle–bridge interactive system under strong earthquakes," *Eng. Struct.*, vol. 176, pp. 500–521, 2018, doi: https://doi.org/10.1016/j.engstruct.2018.09.014.

[11] L. Qi and J. Xue, "Pseudo Dynamic Test and Time-History Analyses of Traditional-Style Steel Frame Structures," *Int. J. Steel Struct.*, vol. 18, no. 2, pp. 402–416, 2018, doi: 10.1007/s13296-018-0007-0.

[12] R. Yadav, B. Chen, H. Yuan, and Z. Lian, *PSEUDO-DYNAMIC TEST OF CFST BRIDGE PIER UNDER DIFFERENT GROUND EXCITATIONS*. 2018.

[13] F. Melo, A. Pereira, A. B. Morais, and P. Authors, *The Simulation of an Automotive Air Spring Suspension Using a Pseudo-Dynamic Procedure*, vol. 8. 2012.

[14] A. M. Reinhorn, M. V. Sivaselvan, Z. Liang, and X. Shao, "Real-time dynamic hybrid testing of structural systems," *13th World Conf. Earthq. Eng.*, no. 1644, pp. 1–13, 2004.

[15] J. Dimig, C. Shield, C. French, F. Bailey, and A. Clark, "Effective force testing: A method of seismic simulation for structural testing.," *J. Struct. Eng.*, pp. 1028–1037, 1999.

[16] N. D. Marks, W. Y. Kong, and D. S. Birt, "Stability of a Switched Mode Power Amplifier Interface for Power Hardware-in-the-Loop," *IEEE Trans. Ind. Electron.*, vol. 65, no. 11, pp. 8445–8454, 2018, doi: 10.1109/TIE.2018.2814011.

[17] D. Thönnessen, S. Rakel, N. Reinker, and S. Kowalewski, "Matching Discrete Signals for Hardware-in-the-Loop-Testing of PLCs," *IFAC-PapersOnLine*, vol. 51, no. 10, pp. 229–234, 2018, doi: https://doi.org/10.1016/j.ifacol.2018.06.267.

[18] G. De Carne, G. Buticchi, and M. Liserre, "Current-type Power Hardware in the Loop (PHIL) evaluation for smart transformer application," in *2018 IEEE International Conference on Industrial Electronics for Sustainable Energy Systems (IESES)*, 2018, pp. 529–533, doi: 10.1109/IESES.2018.8349933.

[19] P. Kotsampopoulos *et al.*, "A Benchmark System for Hardware-in-the-Loop Testing of Distributed Energy Resources," *IEEE Power Energy Technol. Syst. J.*, vol. 5, no. 3, pp. 94–103, 2018, doi: 10.1109/JPETS.2018.2861559.

[20] C. s. Yoo, Y. s. Kang, and B. j. Park, "Hardware-In-the-Loop simulation test for actuator control system of Smart UAV," in *Control Automation and Systems (ICCAS), 2010 International Conference on*, 2010, pp. 1729–1732.

[21] M. Montazeri-Gh, M. Nasiri, M. Rajabi, and M. Jamshidfard, "Actuator-based hardware-in-the-loop testing of a jet engine fuel control unit in flight conditions," *Simul. Model. Pract. Theory*, vol. 21, no. 1, pp. 65–77, Feb. 2012, doi: 10.1016/j.simpat.2011.09.006.

[22] T. Börner and M. Alam, "Real time hybrid modeling for ocean wave energy converters," *Renew. Sustain. Energy Rev.*, vol. 43, pp. 784–795, 2015, doi: 10.1016/j.rser.2014.11.063.

[23] "Computer Image." Fulltechtricks Online, available from URL: http://www.fulltechtricks.com/wp-content/uploads/2016/02/best-computer-brands-2016.jpg.

[24] "MODELS STA2504-2510 SERVOTUBE ACTUATOR Datasheet." Copley Controls Corp. available from URL: http://www.scsautomation.co.uk/SCSControls/Downloads/STA25Datasheet.pdf, doi: DS01088/J.

[25] "Load Cell Image." Forsentek Online, available from URL: http://www.forsensor.com/photo/pl1800924-load_cell_sensor_3kg_4kg_5kg_10kg_20kg_30kg_50kg.jpg.

[26] "Physical Substructure Image." Neeshub Online, available from URL: https://nees.org/resources/6642/download/Quanser.jpg.

[27] R. M. Botelho and R. E. Christenson, "Robust Stability and Performance Analysis for Multi-actuator Real-Time Hybrid Substructuring," *Dyn. Coupled Struct.*, vol. 4, pp. 1–7, 2015, doi:

10.1007/978-3-319-15209-7.

[28] M. I. Wallace, J. Sieber, S. A. Neild, D. J. Wagg, and B. Krauskopf, “Stability analysis of real-time dynamic substructuring using delay differential equation models,” *Earthq. Eng. Struct. Dyn.*, vol. 34, no. 15, pp. 1817–1832, 2005, doi: 10.1002/eqe.513.

[29] M. I. Wallace, D. J. Wagg, and S. a. Neild, “An adaptive polynomial based forward prediction algorithm for multi-actuator real-time dynamic substructuring,” *Proc. R. Soc. A Math. Phys. Eng. Sci.*, vol. 461, no. May 2004, pp. 3807–3826, 2005, doi: 10.1098/rspa.2005.1532.

[30] M. I. Wallace, D. J. Wagg, S. a. Neild, P. Bunniss, N. a. J. Lieven, and a. J. Crewe, “Testing coupled rotor blade–lag damper vibration using real-time dynamic substructuring,” *J. Sound Vib.*, vol. 307, no. 3–5, pp. 737–754, 2007, doi: 10.1016/j.jsv.2007.07.004.

[31] P. J. Gawthrop, M. I. Wallace, S. A. Neild, and D. J. Wagg, “Robust real-time substructuring techniques for under-damped systems,” *Struct. Control Heal. Monit.*, vol. 14, no. 4, pp. 591–608, 2007, doi: 10.1002/stc.174.

[32] J. du Bois, B. Titurus, and N. Lieven, “Transfer Dynamics Cancellation in Real-Time Dynamic Sub- structuring,” *Proc. ISMA 2010*, pp. 1891–1914, 2010.

[33] G. Ou, A. Prakash, and S. Dyke, “Modified Runge-Kutta Integration Algorithm for Improved Stability and Accuracy in Real Time Hybrid Simulation,” *J. Earthq. Eng.*, vol. 19, no. 7, pp. 1112–1139, 2015, doi: 10.1080/13632469.2015.1027018.

[34] K. Nikzad, J. Ghaboussi, and S. L. Paul, “Actuator Dynamics and Delay Compensation using Neurocontrollers,” *J. Eng. Mech.*, vol. 122, no. 1967, pp. 966–975, 1996.

[35] G. Ou, A. I. Ozdagli, S. J. Dyke, and B. Wu, “Robust integrated actuator control: experimental verification and real-time hybrid-simulation implementation,” *Earthq. Eng. Struct. Dyn.*, vol. 44, no. 3, pp. 441–460, 2015, doi: 10.1002/eqe.2479.

[36] A. M. El-Nagar and M. El-Bardini, “Hardware-in-the-loop simulation of interval type-2 fuzzy PD controller for uncertain nonlinear system using low cost microcontroller,” *Appl. Math. Model.*, vol. 40, no. 3, pp. 2346–2355, 2016, doi: 10.1016/j.apm.2015.09.005.

[37] B. G. B. Hunnekens, N. v. d. Wouw, and D. Nešić, “Overcoming a fundamental time-domain performance limitation by nonlinear control,” *Automatica*, vol. 67, pp. 277–281, May 2016, doi: 10.1016/j.automatica.2016.01.021.

[38] A. P. Darby, A. Blakeborough, and M. S. Williams, “Real-Time Substructure Tests Using Hydraulic Actuator,” *J. Eng. Mech.*, vol. 125, no. 10, pp. 1133–1139, 1999, doi: 10.1061/(ASCE)0733-9399(1999)125:10(1133).

[39] T. Hu and Z. Lin, *Control Systems with Actuator Saturation*, 1st ed. Birkhäuser Basel, 2001.

[40] A. Visioli, “Modified anti-windup scheme for PID controllers,” *IEE Proc. - Control Theory Appl.*, vol. 150, no. 1, pp. 49–54, Jan. 2003, doi: 10.1049/ip-cta:20030142.

[41] A. Bemporad, “Model Predictive Control: Basic Concepts,” *IMT School for Advanced Studies Lucca*. 2009.

[42] Y. C. Zhao, “Generalized Model Predictive Control,” in *Control Engineering and Information Systems*, 2014, pp. 47–52.

[43] D. Stoten, G. Li, and J. Tu, “Model predictive control of dynamically substructured systems with application to a servohydraulically actuated mechanical plant,” *IET Control Theory*

Appl., vol. 4, no. 2, pp. 253–264, 2010, doi: 10.1049/iet-cta.2009.0011.

[44] G. Li, G. Herrmann, D. P. Stoten, J. Tu, and M. C. Turner, "Application of Robust Antiwindup Techniques to Dynamically Substructured Systems," *IEEE/ASME Trans. Mechatronics*, vol. 18, no. 1, pp. 263–272, Feb. 2013, doi: 10.1109/TMECH.2011.2167237.

[45] C. A. Desoer and M. Vidyasagar, *Feedback systems: input-output properties*, vol. 55. Siam, 1975.

[46] Z. Chen, Y.-J. Pan, J. Gu, and S. Forbrigger, "A novel multilateral teleoperation scheme with power-based time-domain passivity control," *Trans. Inst. Meas. Control*, vol. 40, no. 11, pp. 3252–3262, 2018, doi: 10.1177/0142331216679500.

[47] B. Hannaford and Jee-Hwan Ryu, "Time-domain passivity control of haptic interfaces," *IEEE Trans. Robot. Autom.*, vol. 18, no. 1, pp. 1–10, Feb. 2002, doi: 10.1109/70.988969.

[48] Jee-Hwan Ryu, Dong-Soo Kwon, and B. Hannaford, "Stability guaranteed control: time domain passivity approach," *IEEE Trans. Control Syst. Technol.*, vol. 12, no. 6, pp. 860–868, Nov. 2004, doi: 10.1109/TCST.2004.833648.

[49] A. M. Dissanayake and N. C. Ekneligoda, "Adaptive Passivity Based Control of DC-DC Power Electronic Converters," in *2019 IEEE Applied Power Electronics Conference and Exposition (APEC)*, 2019, pp. 2984–2988, doi: 10.1109/APEC.2019.8722041.

[50] B. Henze, R. Balachandran, M. A. Roa-Garzón, C. Ott, and A. Albu-Schäffer, "Passivity Analysis and Control of Humanoid Robots on Movable Ground," *IEEE Robot. Autom. Lett.*, vol. 3, no. 4, pp. 3457–3464, Oct. 2018, doi: 10.1109/LRA.2018.2853266.

[51] Y. Gui, B. Wei, M. Li, J. M. Guerrero, and J. C. Vasquez, "Passivity-based coordinated control for islanded AC microgrid," *Appl. Energy*, vol. 229, pp. 551–561, 2018, doi: https://doi.org/10.1016/j.apenergy.2018.07.115.

[52] Y. Zhang, S. Li, J. Zou, and A. H. Khan, "A Passivity-Based Approach for Kinematic Control of Redundant Manipulators with Constraints," *IEEE Trans. Ind. Informatics*, p. 1, 2019, doi: 10.1109/TII.2019.2908442.

[53] M. J. Kim *et al.*, "A Passivity-based Nonlinear Admittance Control with Application to Powered Upper-limb Control under Unknown Environmental Interactions," *IEEE/ASME Trans. Mechatronics*, p. 1, 2019, doi: 10.1109/TMECH.2019.2912488.

[54] J.-H. Ryu, D.-S. Kwon, and B. Hannaford, "Stable Teleoperation With Time-Domain Passivity Control," *Robot. Autom. IEEE Trans.*, vol. 3, pp. 365–373, 2004, doi: 10.1109/TRA.2004.824689.

[55] N. Johnston, "Vibration of Nonlinear Systems," in *ME30033: Mechanical Vibrations and Noise*, University of Bath, p. 16.

[56] D. Shmilovitz, "On the definition of total harmonic distortion and its effect on measurement interpretation," *IEEE Trans. Power Deliv.*, vol. 20, no. 1, pp. 526–528, 2005, doi: 10.1109/TPWRD.2004.839744.

[57] "THD Total Harmonic Distortion MATLAB R2019b," *Mathworks*. [Online]. Available: https://uk.mathworks.com/help/signal/ref/thd.html. [Accessed: 02-Feb-2020].

[58] A. Bartl, J. Mayet, and D. J. Rixen, "Adaptive feedforward compensation for real time hybrid testing with harmonic exciation," in *Proceedings of the 11th International Conference on Engineering Vibration*, 2015.

[59] A. Bartl, M. K. Mahdiabadi, C. Insam, J. Mayet, and D. J. Rixen, “A hybrid testing method based on adaptive feed-forward filters,” *Mech. Syst. Signal Process.*, vol. 139, p. 106586, 2020, doi: https://doi.org/10.1016/j.ymssp.2019.106586.